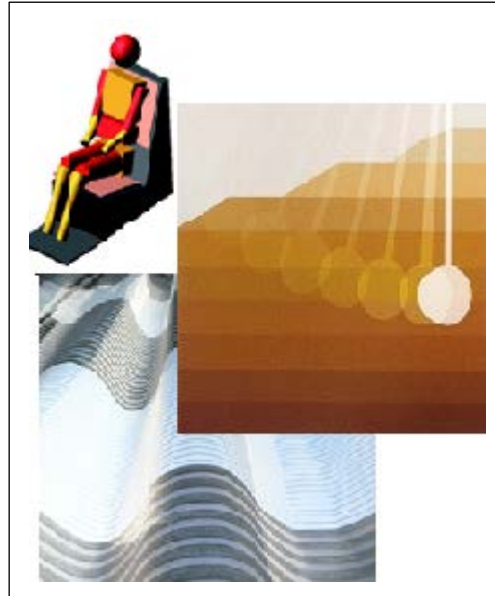




The 26th Japan Conference on Human Response to Vibration Proceedings

(JCHRV2018)



Osaka, Japan
August 22 – 24, 2018



SECRETARIAT OF JCHRV2018

Setsuo Maeda
Faculty of Applied Sociology
Kindai University

6-D, G-Bld., E-Campus,
228-3, Shinkamikosaka, Higashi-Osaka City, Osaka 577-0813, Japan
Tel: +81 - (6) 6721 - 2332 ext:3263 or 5001
Fax: +81 - (6) 6721 - 2512

Email: maeda@socio.kindai.ac.jp

Program of JCHRV2018



Day 1: 22nd August 2018

13:00 – 14:45 Registration (G-6D)

Teas/Coffee and Networking Break (G603)

Welcome and Introduction (G602)

14:45 – 14:50 Introduction and Domestic

14:50 – 15:00 Welcome

Session 1: WBV (G602)

CP: Junya Tatsuno

15:00 – 15:30 P1 - **Kazushige Ebe and Kenji Kumagai**
Introduction of seat comfort evaluation and ride comfort improvement

15:30 – 16:00 P2 - **Kousuke Suzuki**
Improvement of ride comfort through the reduction of occupants' low-frequency motion

16:00 – 16:30 P3 - **Yasuo Higurashi**
Accelerations at the upper limb and the head during motocross riding

16:30 – 17:00 *Teas/Coffee and Networking Break (G603)*

CP: Kazushige Ebe

17:00 – 17:30 P4 - **Kazuma Ishimatsu**
Cognition and performance during whole-body vibration

17:30 – 18:00 P5 - **Junya Tatsuno**
Comparison of Detection Methods of Seat Fidgets and Movements in Vehicle Seat

18:00 – 18:30 P6 - **Mutsuhiro Yoshizawa**
Modeling the effect of building shaking caused by earthquakes on human body

18:30 – 20:30 **Welcome Party at THE LOUNGE (4-3F)**

Day 2: 23rd August 2018

8:30 – 9:00: *Teas/Coffee and Networking Break (G603)*

Key Note Speech (G602)

CP: Setsuo Maeda

- 9:00 - 9:30: P7 - **Kazuhisa Miyashita & Shigeki Takemura**
New strategies to prevent hand-arm vibration syndrome with work practice management

Session 2: HAV (G602)

CPs: Kazuhisa Miyashita & Shigeki Takemura

- 9:30 - 10:00: P8 - **Thomas Jetzer**
Shock and Vibration Issues in Professional Sports
- 10:00 - 10:30: P9 - **Nobuyuki Shibata**
Vibration attenuation performance of gloves under tri-axial hand-arm vibration
- 10:30 - 11:00: P10 - **Shigeki Takemura**
How much does cold-water immersion contribute to detecting peripheral neuropathy and vasculopathy among industrial vibrating tool
- 11:00 - 11:30: P11 - **Leif Anderson**
ASSESSING THE RELATIONSHIP BETWEEN THE HUMAN RESPONSE TO VIBRATION IN THE VIBROTACTILE THRESHOLD SHIFT WITH HAV EXPOSURE DETERMINED ON THE SUBJECT
- 11:30 - 12:00: P12 - **Setsuo Maeda**
Is it effective to prevent HAVS by using tool vibration declaration values?
- 12:00 - 13:30: **Lunch at THE LOUNGE (4-3F)**
- 13:30 - 14:00: **Move to JR Osaka Castle Station by TAXI**
- 14:00 - 18:00: **Sightseeing Tour of Osaka Castle**
- 18:30 - 20:30: **Banquet at Crossfield with TERRACE LOUNGE of the LANDMARK SQUARE Osaka of MIRAIZA OSAKA-JO 2F**

Day 3: 24th August 2018

Session 3: WBV (G602)

CP: Peter Johnson

- 9:00 - 9:30: P13 - **Mohd Amzar Azizan**
Effects of whole-body vibrations on lane keeping performance
- 9:30 - 10:00: P14 - **Mohammed Hedayet Ullah Bhuiyan**
Effect of vehicle vibration magnitude on driver drowsiness

10:00 – 10:30: P15 - Koki SUGIMOTO
Experimental examination for vibration masking on human perception

10:30 – 11:00 *Teas/Coffee* (G603)

CP: Mohd Amzar Azizan

11:00 – 11:30 P16 - Peter Johnson
A New Paradigm for Evaluating and Designing Seat Suspensions

11:30 – 12:00: P17 - Mitsuaki KANOU
Vibration characteristics of human body on a rigid seat

12:00 – 12:30: P18 - Subashi De Siva G.H.M.J
Investigation on characteristics of Whole Body Vibration exposures of Roller Compactors and effect of Waste Rubber on reducing the vibration

Session 4: Conference close

12:30 – 12:45: Close of conference

12:45 – 14:00 **Lunch at THE LOUNGE (4-3F)**

CONFERENCE CLOSE

P1

The 26th Japan Conference on Human Response to Vibration (JCHRV2018)

Kindai University, Osaka, Japan

August 22-24, 2018

**Introduction of seat comfort evaluation and ride comfort
improvement activities**

Kazushige Ebe, Kenji Kumagai

Bridgestone Corporation

1, Kashio-Cho, Totsuka-Ku,

Yokohama 244-8510

Japan

The 26th Japan Conference on Human Response to Vibration (JCHRV2018)

Kindai University, Osaka, Japan

August 22-24, 2018

**Improvement of ride comfort through the reduction of occupants'
low-frequency motion**

Kousuke SUZUKI, Kazuhito KATO, Chikanori HONDA and Masashi OHYAMA

NHK Spring Co., LTD.

kou.suzuki@nhkspg.co.jp

3-10 Fukuura, Kanazawa-ku, Yokohama, 236-0004, Japan

Abstract

Human body instability and lateral human body shaking are ride comfort phenomena relating to low frequency motion and there is a trade-off between them. This paper considers the causes of those phenomena and their methods of reduction. As a result, we have realized exceptional, simultaneous reduction of both human body instability and lateral human body shakes using the same specifications in the driver and passenger seats.

1. Introduction

Human body instability and lateral human body shaking are the two major ride comfort phenomena manifested by motor vehicle occupants during driving (Fig.1), and correspond to the primary and secondary lateral vibration modes for occupant bodies [1]. "Human body instability" means the leaning of the pelvis and torso to one side during vehicle cornering or lane changing operation, which often causes physical fatigue to the occupants due to necessary muscular effort to keep their postures upright and also mental fatigue of having to maneuver a difficult driving situation safely. To moderate human body instability, vehicles are fitted with cushion bolsters and backrest bolsters on the front seats [2]. On the other hand "lateral human body shaking" means the phenomenon of the occupant body shaken by the roll vibrations of the vehicle body responding to road surface roughness, and is accompanied by a feeling of ride discomfort due mainly to the lateral swaying of the head and the pressing of thorax against the backrest and may also be accompanied by mental fatigue of having to pass the oncoming vehicles safely on rough-surface roads. As an approach to the reduction of lateral human body shakes being the shielding of occupants against excitation force from the seats, it is regarded important not to excessively restrain the occupants in the seats [3]. So human body instability and lateral human body shaking are ride comfort phenomena having a trade-off relationship.

Employed as test vehicles in the present study were SUVs which are known to generate greater lateral human body shakes. Using these vehicles, occupant body behavior mechanisms were examined in relation to human body instability and lateral human body shaking so as to optimize occupant support by the seat and resolve the trade-off problem of the two ride comfort phenomena.

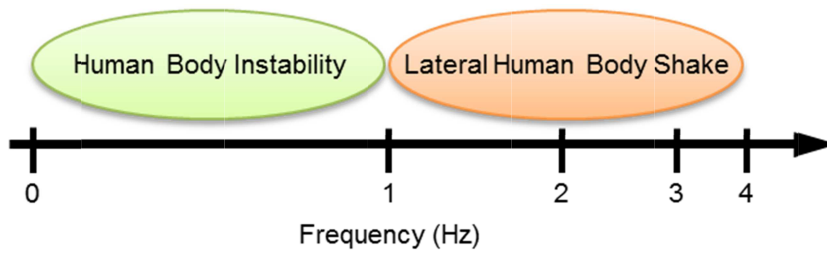


Fig.1 Ride comfort phenomena in low-frequency

2. Low-Frequency Behavioral Mechanisms of Occupants

2.1. Human body instability mechanism

Earlier studies have indicated difference in human body instability behavior between driver and passenger[4] as illustrated in Figure 2. The driver exhibits active posture control whereby, while pelvis rolls outward, upper body is bent inward by mobilizing flank and thigh muscles [5]. This is considered to be a series of posture-correcting behaviors for realigning the center of upper thorax with the center of steering wheel in order to continue an accurate steering. In contrast to the driver, the passenger normally exhibits passive posture control whereby, as pelvis rolls outward, upper body also rolls outward while leaning on the backrest, and the head is let projected farther outward. Only when the human body instability is excessively severe or when the support from the seat is insufficient does the passenger tries to hold up posture by reflective muscular responses.

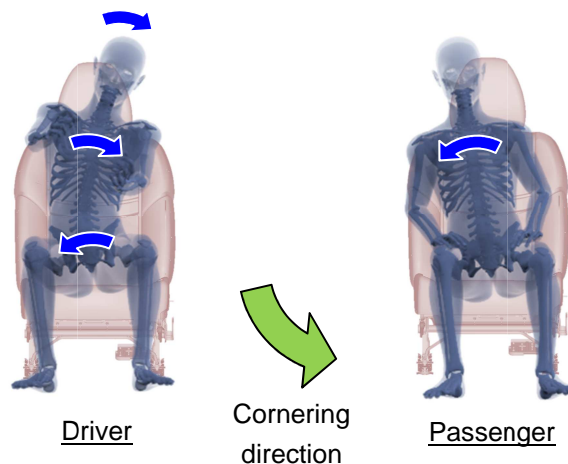


Fig.2 Difference in human body instability behavior between driver and passenger

2.2. Lateral Human body shake mechanism

Unlike human body instability, lateral human body shaking involves body motion too quick for the occupant to control his/her posture[6] so that both driver and passenger exhibit practically the same lateral body shaking behaviors (Fig.3). In continuous lateral body shaking, accelerations in antiphase are generated to head and thorax.

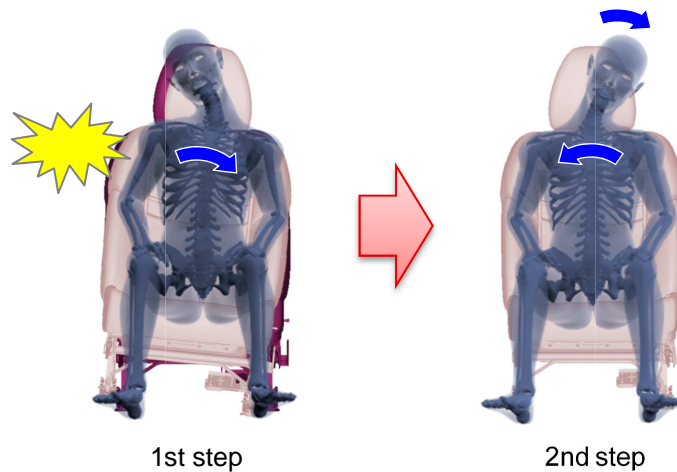


Fig.3 Passenger's behavior in lateral human body shaking

3. Measures to Reduce Human Body Instability and Lateral Human Body Shaking

3.1. Measures to reduce lateral human body shaking (common to driver and passenger)

For lateral human body shaking whereby both driver and passenger exhibit the same behaviors, it is considered necessary to minimize the transmission of excitation force from the seat to occupant upper body. Assuming that backrest bolster position affects the transmission of excitation force, relations between backrest bolster height/width and excitation force transmission were examined in the present study. It was found that higher backrest bolster position increased the transmission of excitation force to the upper thorax, resulting in a greater swaying of the head; lower backrest bolster position resulted in a lateral bending of the thorax and concomitant instabilities in upper-body behavior. As for separation between the pair of backrest bolsters, wider separation caused time lags between thorax shaking and seat shaking, resulting in a hitting of thorax with the backrest bolsters. Narrower separation indicated a direct shaking of the upper body by the seat and a greater swaying of head as the thorax was braced more rigidly by the two side bolsters. It was confirmed that a proper height and separation of backrest bolsters reduced the transmission of excitation force from the seat and moderated head swaying, thus suggesting that optimizing backrest bolster height and separation is an effective way of reducing lateral human body shaking.

3.2. Measures to reduce driver body instability

Since during cornering the driver controls posture by bending torso sideways with the help of flank and thigh muscles (Fig.4), it is considered necessary to hold the upper body upright with the minimum muscular load. In this regard the thigh muscles having a greater force generation capacity can perform body control with a minimum feeling of muscular effort; therefore, it is more advantageous to utilize thigh muscles for the control of driver posture during cornering. So more effective thigh support was explored to enable a greater contribution of the thighs to driver body control during cornering. It was found that the front part of the thigh--region farther away from the hip joint--was easily pushed back by the cushion bolster while the rear part of the thigh failed to apply sufficient muscular force to the cushion bolster due to the small amount of its displacement. At certain midway points, however, it proved easier for the thigh to keep pressing the cushion bolster and to contribute its muscular force for reducing body instability. Thus, it was confirmed that driver posture can be held as upright as possible during cornering by optimizing cushion bolster shape/rigidity so as to enable thigh to exert greater muscular force.

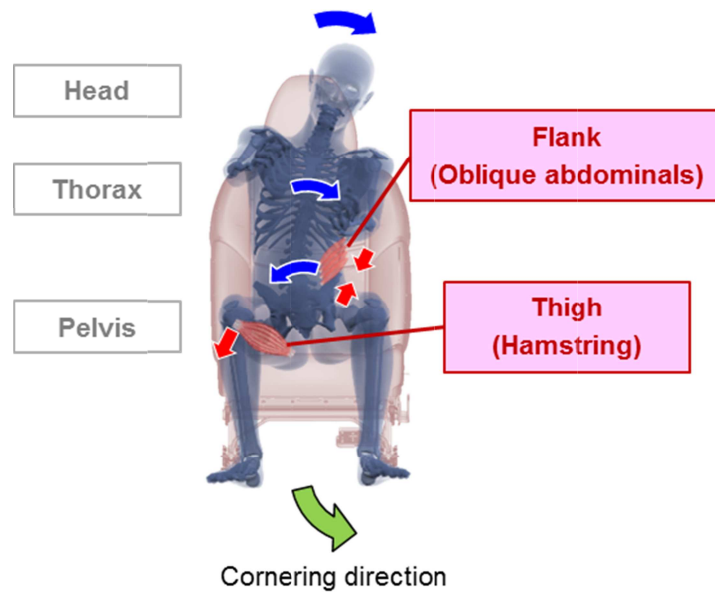


Fig.4 Driver body instability dynamics during cornering

3.3. Measures to reduce the passenger's body instability

For passengers it is not necessary that posture is corrected by reflexional muscular responses, which suggests a need for cushion bolsters capable of moderating the roll motion of pelvis and providing greater support to thorax for the reduction of passenger body instability. Optimizing the cushion bolster shape and cushion pad rigidity/attenuation was considered to moderate the rolling of pelvis. While thorax support against the passenger's body instability should be provided at the upper part of the backrest bolster, it would be necessary that this support be compatible with the aforementioned support for the reduction of lateral human body shaking. Consequently it was decided that the passenger seat be optimized in such a way that excitation force from the seat would be dampened to reduce body shaking of a large acceleration and a small amplitude and that thorax motion would be restrained at the backrest bolster upper part for body shaking of a small acceleration and a large amplitude.

4. Experimental Method

In the present study, both laboratory and field tests were conducted to evaluate human body instability and lateral human body shaking in quantitative terms. Used in the laboratory tests were the pairs of front seats taken from a Japanese-brand small SUV for sale ("Car A"), from a European-brand small SUV with a rated top-class ride comfort ("Car B"), and a pair of developmental seats incorporating the aforementioned improvement measures ("Prototype"). The Car A and Prototype seats were employed in the field tests. The subjects in driver seats were instructed to keep natural or normal posture for steering. The subjects in passenger seats were instructed to be seated and lean fully on the seatback but with some separation between head and headrest. Two male adults of standard body size were employed as subjects and both of them gave their informed consent to participate in the experiment.

4.1. Laboratory tests on human body instability

For the quantitative evaluation of human body instability in a laboratory environment, an experimental apparatus was devised to quasi-statically simulate lateral accelerations in cornering based on the component forces of gravitational accelerations of a seat inclined in the direction of rolling. Each subject

was instructed to sit on the experimental seat and wear range-limiting glass to observe closely only a display monitor attached to a jig but not things around the monitor. Shown in the monitor were stationary photo images of a bending road taken from a driver's sitting position. The subject, instructed to simulate actual cornering behavior, performed steering in keeping with the photo images as the seat was inclined. A seat inclination angle of 23.5 degrees to right and left was applied, assuming a component force of 0.4G to the seat and a cornering vehicle speed of 40 km/h. The subjects' behaviors were recorded by a motion capture system. From the results of preliminary tests, the body behaviors of the subjects were evaluated in terms of pelvis roll angle and upper-thorax displacement which were the two parameters indicating a notable correlation with the subjects' sensory evaluations of their body instabilities. These measured values were evaluated in relation to seat inclination. Upper-thorax displacement values nearing zero were considered to indicate that the subject held up his thorax as close as possible to the center of the steering wheel.

4.2. Field tests on human body instability

In the field tests, human body instability was quantitatively evaluated from the measurements of occupants' behaviors and sEMG (surface electromyogram) responses during cornering on an in-plant road, using Car A fitted with Prototype driver and passenger seats. In driver seat the subject actually drove the test vehicle, while merely seated in the passenger seat. As in the laboratory tests, the subjects' behaviors were recorded by a motion capture system, and their pelvis roll angles and upper-thorax displacements were evaluated quantitatively. Normalized integrated sEMG measurement was also carried out to evaluate the activation of flank (abdominal oblique on inward side) and of thigh (hamstring on outward side) as shown in Figure 5.

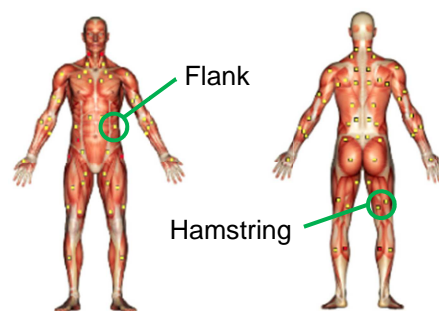


Fig.5 Body locations of sEMGs measurement

4.3. Laboratory tests on lateral human body shaking

A test seat and a footrest jig were fixed on the 1.8m x 1.8m oscillation table of an electric vibration machine with six degrees of freedom (Fig.6). Each subject was seated on the test seat and exposed to artificial vibrations simulating the actual seat vibrations on an uneven road. His body behaviors were recorded by a motion capture system. Since lateral body shaking behaviors had proved identical between driver and passenger, only passenger tests were conducted. As the preliminary tests had found a good correlation between head sway discomfort and head acceleration and between thorax discomfort and upper-thorax acceleration, effective values of head and upper-thorax accelerations were measured.



Fig.6 Laboratory apparatus for lateral human body shaking evaluation

5. Experimental Results

5.1. Results of quantitative evaluation of human body instability

Figure 7 compares the measured values of pelvis roll angle and upper-thorax displacement for the 3 types of seats. Since the measurements obtained from the 2 subjects proved highly similar, data from only one subject were used hereafter in this paper. For pelvis roll angle in both driver and passenger seats, Car B and Prototype proved equally excellent and both clearly better than Car A. For upper-thorax displacement in driver seats, Prototype recorded a 31% reduction against Car A and a 12% reduction against Car B. Similarly in passenger seats, Prototype showed a 22% cut against Car A and a sharp 33% cut against Car B.

Figure 8(a) compares the field test results of Car A and Prototype with respect to pelvis roll angle and upper-thorax displacement. For pelvis roll angle, Prototype recorded a 29% reduction against Car A in driver seats and a 21% reduction in passenger seats. For upper-thorax displacement, Prototype failed to show a notable cut against Car A in driver seats; however, Prototype achieved a 21% cut against Car A in passenger seats. Thus the results of both laboratory and field tests indicated greater reductions of pelvis roll angle and upper-thorax displacement by the Prototype seats than by the seats installed in the commercially available vehicles.

Figure 8(b) compares sEMG measurements in driver seats between Car A and Prototype. Prototype indicated a notable 30% reduction in flank muscle effort but a 14% increase in thigh muscle (hamstring) effort against Car A. This is in accord with the general observation that driver posture during cornering is maintained primarily by thigh muscles characterized by a large force generation capacity.

The test results on occupant behaviors and sEMG responses suggest that driver posture during cornering can be best maintained if the seat cushion bolsters are optimized to facilitate thigh muscular effort, which will reduce upper-thorax displacement while also reducing flank muscular load. As for the support of passenger posture, it was confirmed that the improvement of cushion pad rigidity and attenuation proved effective in reducing pelvis roll angle for both drivers and passengers. Furthermore, it is also confirmed that Prototype's optimization of backrest bolster upper part is effective in moderating human body instability as well as lateral human body shaking.

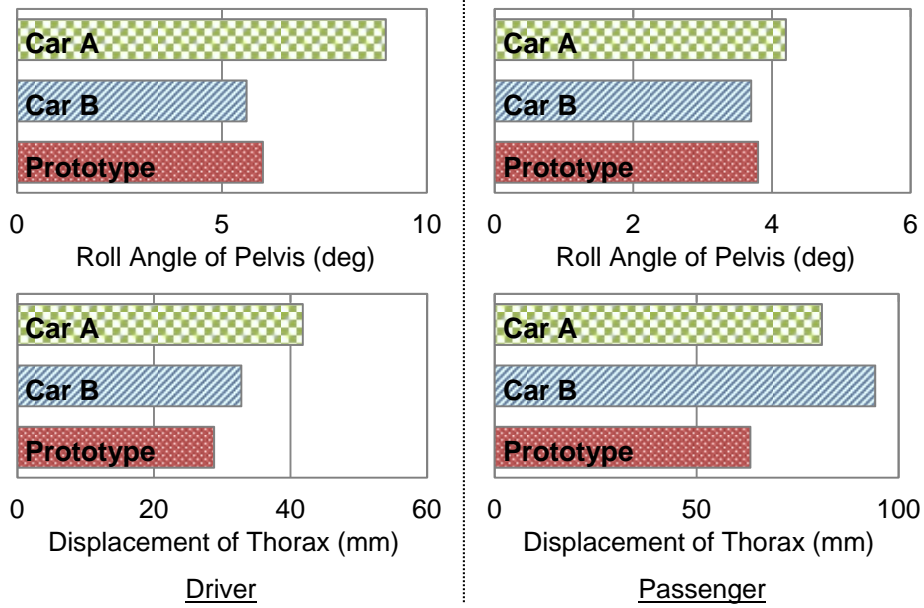
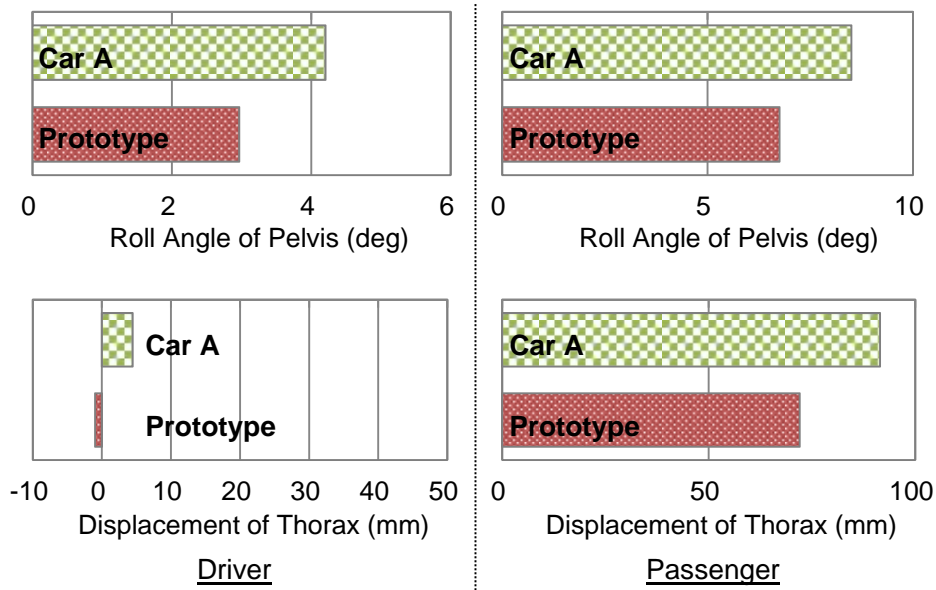
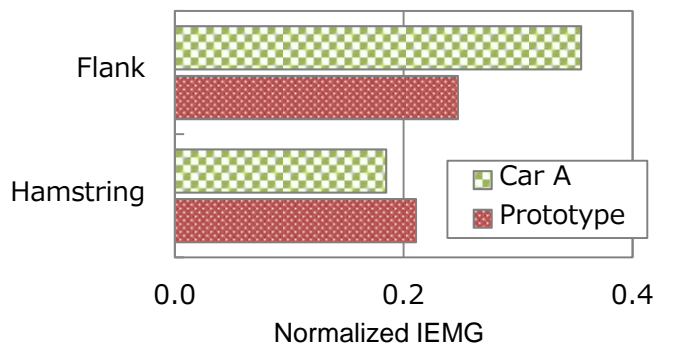


Fig.7 Laboratory test results of human body instability behavior



(a) Occupant motion during cornering



(b) sEMGs measurements of muscle force in driver seats

Fig.8 Field test results of human body instability behavior

5.2. Results of quantitative evaluation of lateral human body shaking

Figure 9 compares the measured values of human body acceleration for the 3 types of seats. For head acceleration in both driver and passenger seats, Car B and Prototype were equally excellent and clearly better than Car A. For thorax acceleration, Prototype recorded the smallest value--22% less than Car A and 14% less than Car B. Since Prototype indicated smaller head and thorax accelerations, which had proved significantly correlative with the subjects' sensory evaluations of their body conditions, Prototype was considered capable of reducing discomfort of head and thorax caused by lateral human body shaking, as its optimized backrest bolsters effectively dampened the transmission of excitation force from the seat.

Quantitative evaluation results indicated that the Prototype exceeded commercially available vehicles in reducing both human body instability and lateral human body shaking. Thus Prototype proved to be a seat capable of dissolving the trade-off relationship between human body instability and lateral human body shaking and also capable of moderating both phenomena simultaneously at high ride comfort levels.

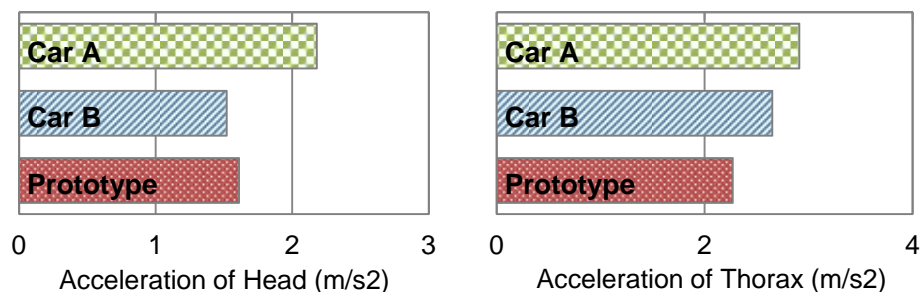


Fig.9 Measured accelerations in laboratory tests on lateral human body shaking

6. Discussion

Focused here is the difference in the measured values of driver upper-thorax displacement between laboratory and field tests in the present study. In the laboratory tests the subjects, instructed to perform steering in a simulated setup, tried to maintain their postures during cornering but their thorax center lost alignment with the steering wheel center. On the other hand in the field tests, the subjects aligned their thorax center with the steering wheel center more accurately.

Two influencing factors may be considered to explain this difference. One is different physical conditions between laboratory and field tests. Because in the laboratory tests the seat was inclined sideways to quasi-statically simulate only the vehicle's lateral accelerations during cornering, the vertical accelerations on the occupant in a seat local coordinate system were smaller in laboratory than field tests. Additionally, test environments were such that the subjects were more strongly prompted to make preparatory behaviors for transition from straight-ahead driving to cornering operation in field tests than in laboratory tests. These differences in vertical acceleration and preparatory driving behavior may have brought difference in the overall behaviors of occupants between laboratory and field tests.

The other influencing factor is different mental conditions induced by laboratory and field tests. While steering error in laboratory tests would not lead to an actual accident in laboratory tests, in field tests steering error may cause an excessive vehicle turning or an actual accident. Due to the above differences in physical and mental conditions, it is likely that subjects become motivated to hold up the upper-thorax center over the steering wheel center more strongly in field tests than in laboratory tests.

7. Conclusions

The present study was intended to dissolve the trade-off relationship existing between human body instability and lateral human body shaking. For the reduction of human body instability, it was found effective to hold up occupant posture by minimizing pelvis roll motion and by improving support to thorax and thigh. For the reduction of lateral human body shaking, it proved effective to minimize the transmission of excitation force from the seat to the occupant by optimizing backrest bolster shape. As a result the roles of cushion bolsters and backrest bolsters were defined more clearly, and their shapes and characteristics were optimized, achieving the reduction of body instability and lateral body shaking for both drivers and passengers. Hence, the trade-off relationship was dissolved and the two phenomena were moderated at high ride comfort levels.

References

- [1] Kanke T., Yoshimura T., Tamaoki G., Kato K. and Kitazaki S. (2007) Modeling of vehicle passenger for comfort evaluation, Proceedings of Annual Congress of the Society of Automotive Engineers of Japan, No.138-07, p23-28 (in Japanese).
- [2] Yamada K., Motojima H., Kitagawa Y. and Yasuki T. (2016) Investigation of relations between occupant kinematics and supporting by the seat in lane change maneuvers, Proceedings of Annual Congress of the Society of Automotive Engineers of Japan, No.38-16, p941-946 (in Japanese).
- [3] Kawano K., Taguchi T., Motohata K., Yasuda E. and Kubota A. (2017) Motion analysis of a passenger in reaction to vehicle sway by varying seat side support, Proceedings of Annual Congress of the Society of Automotive Engineers of Japan, No.174-17, p1644-1650 (in Japanese).
- [4] Koike T., Yoshimura T., Tamaoki G. and Kato K. (2013) Vibration behavior of seated human body (Difference between driver and passenger), JSME Dynamics and Design Conference 2013 USB Proceedings, p447-453 (in Japanese).
- [5] Kato K., Suzuki K. and Ohyama M. (2014) Stability of vehicle occupant's body during cornering, Proceedings of the 49th United Kingdom Conference on Human Responses to Vibration, USB proceedings.
- [6] Griffin M.J. (1990) Handbook of Human Vibration, Academic press, London.

The 26th Japan Conference on Human Response to Vibration (JCHRV2018)

Kindai University, Osaka, Japan

August 22-24, 2018

Accelerations at the upper limb and the head during motocross riding**Yasuo Higurashi¹, Yuki Hattori¹, Eitaro Namazue², Toshiya Taguchi², Yuji Komiyama², Hidetaka Kamiya², Jinpei Yoshimura², You Tuchihashi², Ryo Okada², Naomi Wada¹**

¹ Joint Faculty of Veterinary Medicine, Yamaguchi University
1677-1 Yoshida
Yamaguchi, Yamaguchi 753-8515, Japan

² SHOWA CORPORATION
2601 Matsubara
Fukuroi, Shizuoka 437-1194

Abstract

Motocross is a motorcycle racing sport held on a track with a rough terrain. Vibration is transmitted from the track terrain to the whole-body of riders. Head stabilization is important for navigating an environment, but is not investigated for motocross riding. To clarify how the upper limb is used to attenuate vibration transmitted to the head, we measured three-dimensional accelerations at the left hand, left elbow, left shoulder, and head during motocross ridings. Four professional motocross athletes participated in this study. We found the root mean square (RMS) of resultant accelerations (α_{xyz}) and the peak α_{xyz} at the head were lower than those at the other accelerometer locations. The differences in the RMS of α_{xyz} between the two adjacent accelerometer locations are largest for the left elbow-left shoulder pair. These results suggest that the forelimb, particularly the elbow, contributes to head stabilization during motocross riding.

1. Introduction

Motocross is a motorcycle racing sport held on a track with a rough terrain. A motocross track has different sections, including the whoops, which cause continuous up and down movements, the sharp turns, which requires significant slowing and technical aptitude, and the jumps, where riders experience large landing impact. Vibration is transmitted from the track terrain to the whole-body of riders. Motocross riding is such a physically demanding sport, and highly trained motocross athletes have higher anaerobic power, higher anaerobic peak power, and extended arm hang duration compared with age-matched physically active persons [1].

Head stabilization is important for navigating an environment. The head has the visual and vestibular apparatus. During walking, accelerations at the head are lower than those at the trunk [2-4]. During cross country mountain biking, accelerations at the head are lower than those at the arm and

leg [5,6]. These studies suggest that the limbs and trunk act as shock absorbers. Head stabilization during motocross riding, where riders experience larger vibrations than during walking and cross country mountain biking, is not investigated. We hypothesized that vibration transmitted to the head during motocross riding is attenuated by the upper limb, as observed during cross country mountain biking. Therefore, we predicted that accelerations at the head are lower than those at the upper limb.

The aim of this study was to clarify how the upper limb is used to attenuate vibration transmitted to the head during motocross riding. To this end, we measured three-dimensional accelerations at the upper limb and the head using accelerometers when professional motocross athletes rode on a motocross track. We calculated the root mean square (RMS) of resultant accelerations (α_{xyz}) and the peak α_{xyz} to quantify vibration transmitted to the upper limb and the head.

2. Materials and Methods

2.1. Participants

Four professional motocross athletes (riders A–D, height 169–175 cm, body mass 60–77 kg) participated in this study. All participants provided informed consent in accordance with the Declaration of Helsinki.

2.2. Protocol

Three-dimensional accelerations were measured at the back of the left hand, the left elbow, the left shoulder, and the top of the head using tri-axial accelerometers (measurement range ± 200 g for riders A, C, and D and ± 16 g for rider B) at a sampling frequency of 200 Hz to calculate α_{xyz} (Figure 1). The accelerometers were placed on the body and a motocross helmet using an adhesive tape. The accelerometers were connected to an amplifier and a recorder, both of which were housed in a backpack. The mass of the entire apparatus was ~ 3.5 kg and equivalent to $\sim 5\%$ of the participant's body mass. A handheld CASIO EX-F1 was used to film participants riding the motocross bike at 300 frames-per-second and at 512×384 resolution.

The participants were required to ride at a motocross circuit. The circuit included eight corners, 10 ramps, and one whoops. Each participant performed 10 laps of the circuit.

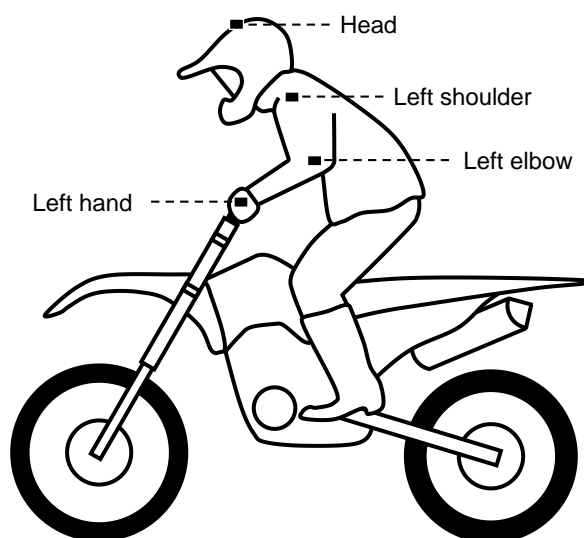


Figure 1. Accelerometer locations.

2.3. Data analysis

Three-dimensional accelerations were combined using the root sum of squares to calculate α_{xyz} (Figure 2). This was expressed as:

$$\alpha_{xyz} = \sqrt{a_x^2 + a_y^2 + a_z^2}$$

where α_x , α_y , and α_z are the accelerations in the x-axis, y-axis, and z-axis, respectively.

For each lap of the circuit, the RMS and peak values of α_{xyz} were calculated. The accelerometers used for rider B (± 16 g) did not have sufficient measurement range to record the peak acceleration during motocross riding (Figure 2), and we did not report it here. The RMS and peak acceleration were averaged over 10 laps within an individual.

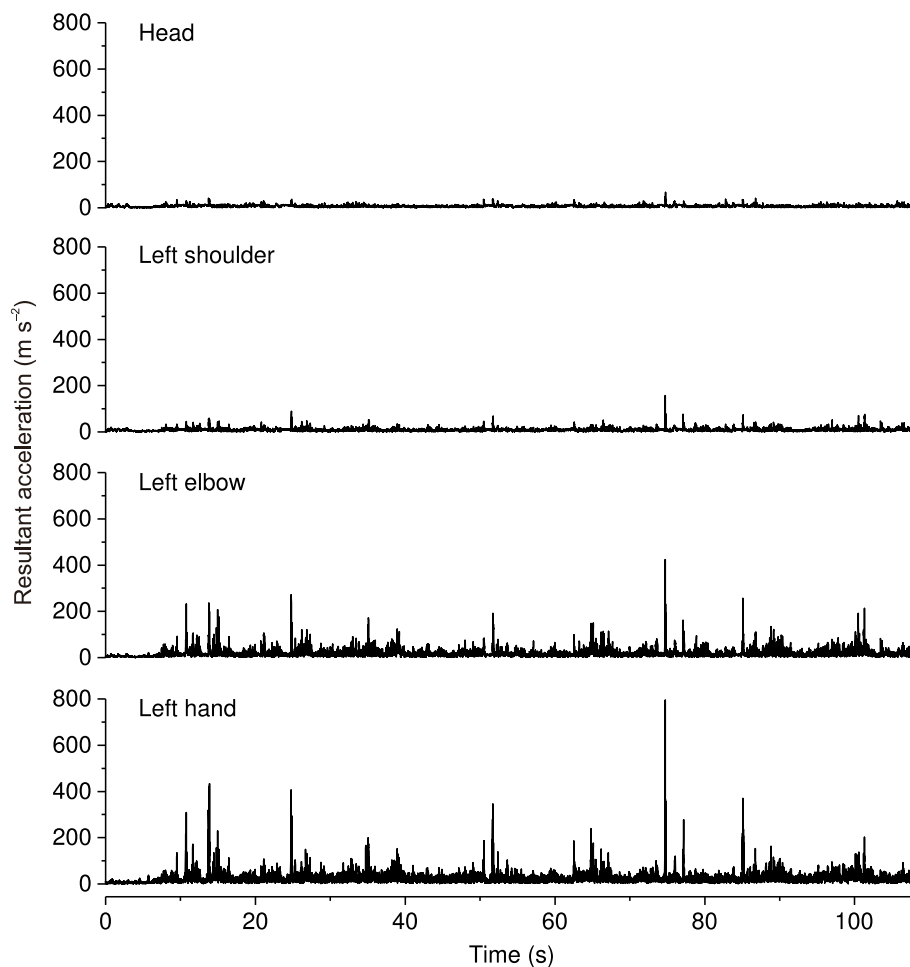


Figure 2. An example of resultant accelerations at each accelerometer location during one lap.

2.4. Statistical analysis

All statistical tests were performed using BellCurve for Excel (Social Survey Research Information, Tokyo, Japan). A one-way repeated measures analysis of variance (ANOVA) was used to evaluate differences among accelerometer locations (left hand, left elbow, left shoulder, head) within an individual. Post hoc multiple comparisons were performed using the Holm's test. The level of significance was set at $\alpha = 0.05$.

3. Results

3.1. RMS

For all participants, the RMS of α_{xyz} significantly differed among accelerometer locations (Figure 3 and Table 1). The RMS of α_{xyz} at the left hand was significantly greater than that at the other three accelerometer locations (left elbow, left shoulder, and head). The RMS of α_{xyz} at the left elbow was significantly greater than that at the left shoulder and head. The RMS of α_{xyz} at the left shoulder was significantly greater than that at the head. The RMS of α_{xyz} at the head was lowest among accelerometer locations.

The differences in the RMS of α_{xyz} between the two adjacent accelerometer locations are largest for the left elbow-left shoulder pair in all participants.

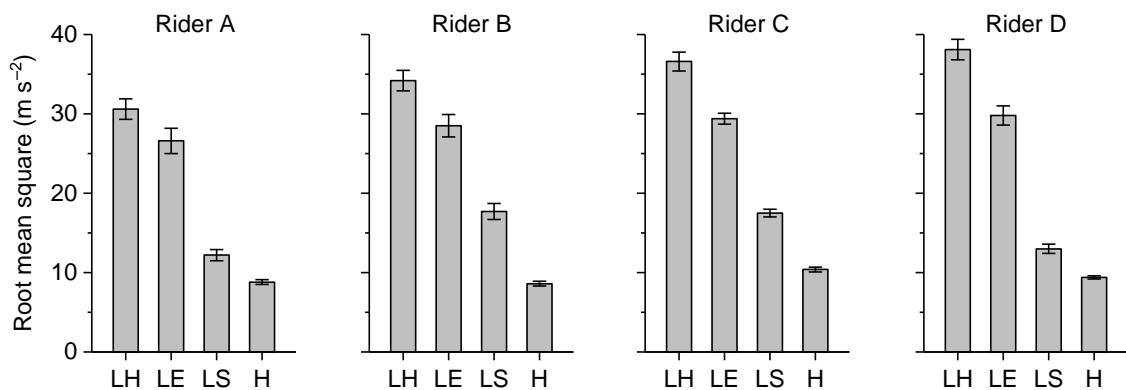


Figure 3. Mean RMS of resultant accelerations for each participant. The values were averaged over 10 laps of the circuit. LH = left hand, LE = left elbow, LS = left shoulder, H = head.

Table 1. Results of ANOVA and post hoc tests comparing the RMS of resultant accelerations among accelerometer locations.

Participant	ANOVA	Holm's <i>P</i> -value			
Rider A	$F_3 = 3060.9$ < 0.001	Left hand	Left elbow	Left shoulder	Head
		< 0.001	< 0.001	< 0.001	< 0.001
		Left elbow		< 0.001	< 0.001
		Left shoulder			< 0.001
		Head			
Rider B	$F_3 = 4285.0$ < 0.001	Left hand	Left elbow	Left shoulder	Head
		< 0.001	< 0.001	< 0.001	< 0.001
		Left elbow		< 0.001	< 0.001
		Left shoulder			< 0.001
		Head			
Rider C	$F_3 = 4638.8$ < 0.001	Left hand	Left elbow	Left shoulder	Head
		< 0.001	< 0.001	< 0.001	< 0.001
		Left elbow		< 0.001	< 0.001
		Left shoulder			< 0.001
		Head			
Rider D	$F_3 = 5521.5$ < 0.001	Left hand	Left elbow	Left shoulder	Head
		< 0.001	< 0.001	< 0.001	< 0.001
		Left elbow		< 0.001	< 0.001
		Left shoulder			< 0.001
		Head			

3.2. Peak acceleration

For all participants, the peak α_{xyz} significantly differed among accelerometer locations (Figure 4 and Table 2). The peak α_{xyz} at the left hand was greater than that at the other three accelerometer locations, but the difference between the left hand and left elbow was not significant for rider A. The peak α_{xyz} at the left elbow was significantly greater than that at the left shoulder and head. The peak α_{xyz} at the left shoulder was greater than that at the head, but this difference was not significant for rider A.

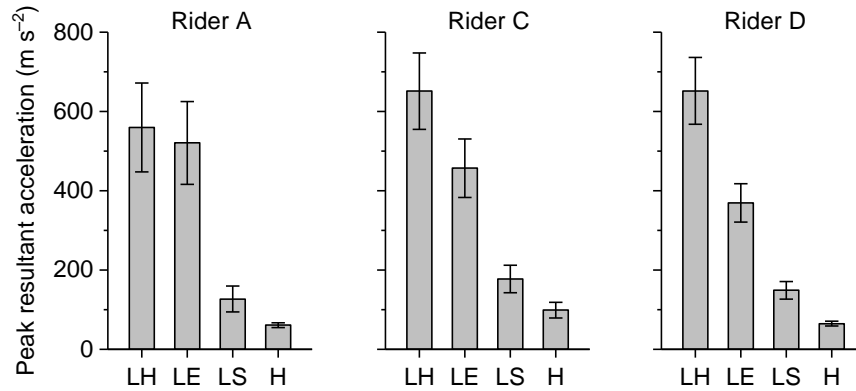


Figure 4. Mean peak resultant acceleration for each participant. The values were averaged over 10 laps of the circuit. The data on rider B were excluded because of the narrow measurement range of the accelerometers used. LH = left hand, LE = left elbow, LS = left shoulder, H = head.

Table 2. Results of ANOVA and post hoc tests comparing the peak resultant acceleration among accelerometer locations.

Participant	ANOVA	Holm's <i>P</i> -value			
Rider A	$F_3 = 148.6$ < 0.001	Left hand	Left elbow	Left shoulder	Head
		Left hand	0.205	< 0.001	< 0.001
		Left elbow		< 0.001	< 0.001
		Left shoulder			0.075
		Head			
Rider C	$F_3 = 189.2$ < 0.001	Left hand	Left elbow	Left shoulder	Head
		Left hand	< 0.001	< 0.001	< 0.001
		Left elbow		< 0.001	< 0.001
		Left shoulder			< 0.001
		Head			
Rider D	$F_3 = 364.4$ < 0.001	Left hand	Left elbow	Left shoulder	Head
		Left hand	< 0.001	< 0.001	< 0.001
		Left elbow		< 0.001	< 0.001
		Left shoulder			0.006
		Head			

The data on rider B were excluded because of the narrow measurement range of the accelerometers used.

4. Discussion

This study reports α_{xyz} at the left hand, left elbow, left shoulder, and head during motocross riding to clarify how the upper limb contributes to head stabilization. As predicted, the RMS of α_{xyz} and the peak α_{xyz} at the head were lower than those at the other accelerometer locations. The differences in the RMS of α_{xyz} between the two adjacent accelerometer locations are largest for the left elbow-left shoulder pair.

These results suggest that the forelimb, particularly the voluntary movements of the elbow, contributes to head stabilization during motocross riding.

We did not measure accelerations at the lower limb. During motocross riding, vibration is transmitted from the track terrain through both upper and lower limbs to the head. Further studies are needed to clarify how the lower limb contributes to head stabilization.

5. References

- [1] Bach CW, Brown AF, Kinsey AW, Ormsbee MJ (2015) Anthropometric characteristics and performance capabilities of highly trained motocross athletes compared with physically active men. *The Journal of Strength and Conditioning Research*, 29, 3392-3398.
- [2] Menz HB, Lord SR, Fitzpatrick RC (2003) Acceleration patterns of the head and pelvis when walking on level and irregular surfaces. *Gait and Posture* 18, 35-46.
- [3] Kavanagh JJ, Morrison S, Barrett S (2005) Coordination of head and trunk accelerations during walking. *European Journal of Applied Physiology* 94, 468-475.
- [4] Mazzà C, Iosa M, Pecoraro F, Cappozzo A (2008) Control of the upper body accelerations in young and elderly women during level walking. *Journal of NeuroEngineering and Rehabilitation*, 5, 30.
- [5] Macdermid PW, Fink PW, Stannard SR (2014) Transference of 3D accelerations during cross country mountain biking. *Journal of Biomechanics*, 47, 1829-1837.
- [6] Macdermid PW, Fink PW, Stannard SR (2014) The effects of vibrations experienced during road vs. off-road cycling. *International Journal of Sports Medicine*, 36, 783-788.

The 26th Japan Conference on Human Response to Vibration (JCHRV2018)

Kindai University, Osaka, Japan

August 22-24, 2018

Cognition and performance during whole-body vibration:**Whole-body vibration influences target detectability****Kazuma Ishimatsu**

Graduate School of Health Care Sciences, Jikei Institute

1-2-8 Miyahara, Yodogawa-ku,

Osaka, 532-0003, JAPAN

Abstract

Helicopter aircrew members engage in highly demanding cognitive tasks in an environment subject to whole-body vibration (WBV). This study used a Sustained Attention to Response Task (SART) to examine whether action slips were more frequent during exposure to WBV. Nineteen participants performed the SART in two blocks. In the WBV block participants were exposed to 17 Hz vertical WBV, which is typical of larger helicopter working environments. In the No-WBV block there was no WBV. There were more responses to the rare no-go digit 3 (i.e. action slips) in the WBV block, and participants responded faster in the WBV block. Target detectability (measured by A' , a sensitivity index) was also lower in the WBV block. These results suggest that WBV may increase the likelihood of action slips, mainly due to failure of response inhibition and reduction in target detectability.

1. Introduction

Reason and Mycielska (1982) summarized information on private aircraft accidents in which an error committed by a pilot was implicated, and concluded that the errors displayed many of the characteristics of absent-minded slips in that they involved apparently unintentional execution of well-established control actions, or omission of such actions [1]. Specialists such as aircraft pilots will easily be able to imagine circumstances in which omitting to execute particular actions in the event of engine failure would have catastrophic consequences. The resemblance between these pilot errors and everyday absent-minded slips does not in itself constitute an explanation for these accidents but the underlying mechanism may be similar. As Reason and Mycielska (1982) put it, '*the resemblance between these pilot errors and everyday absent-minded slips does suggest we could learn a good deal more about catastrophic errors from a closer scrutiny of action slips of our daily life*' [1]. In addition, action slips provide important clues about the organization of human performance and the role of conscious attention in the guidance of action especially when sustained attention to action is required to execute a task successfully.

According to an analysis of all European helicopter accidents between 2000 and 2005, pilot judgement and actions was the most common causative factor, and was involved in almost 70% of the accidents

[2]. Undesired Aircraft States (UAS) are flight-crew induced aircraft position or speed deviations, misapplication of flight controls or incorrect system configurations associated with a reduction in margins of safety. An inappropriately managed UAS may lead to an incident/accident [3].

Whole-body vibration (WBV) is one of the more distinctive features of the helicopter working environment. The frequency and intensity of vibration to which the helicopter aircrew is subjected depend on the aircraft type, weather and flight profile [4]. In every helicopter, peak WBV is related to the blade pass frequency, which varies normally between 15 and 24 Hz according to rotor velocity (3-7 revolutions per second) and number of rotor-blades [4].

WBV has an impact on performance of various tasks involving vision, motor activity and information processing [5, 6, 7, 8, 9, 10]. The effects of WBV may be attributable to the direct effects of WBV on input processes (such as the collection of information via the various senses, particularly vision) and output processes (such as task-related responses in various modalities, usually manual responses). Conway et al. (2007) conducted a meta-analysis of empirical studies assessing the influence of WBV on human performance; they showed that WBV generally caused a decrement in performance [5]. The disruptive effects of WBV were related to the type of task being performed. The impact was greatest on perceptual tasks such as vigilance or target detection tasks. There was also a negative impact on continuous and discrete fine motor tasks (such as tracking and switching tasks) and on cognitive performance. The impact of WBV was also related to the type of outcome investigated; accuracy of response was degraded more than speed of response. Although previous research has examined whether or how performance is degraded, it is not clear why this happens.

Ishimatsu, Meland, Hansen, Kåsin and Wagstaff (2016) used a Sustained Attention to Response Task (SART) to examine whether action slips were more frequent during exposure to WBV [8]. In their study, 19 participants performed the SART in two blocks. In the WBV block participants were exposed to 17 Hz vertical WBV, which is typical of larger helicopter working environments. In the No-WBV block there was no WBV. There were more responses to the rare no-go digit 3 (i.e. action slips) in the WBV block, and participants responded faster in the WBV block. These results suggest that WBV influences response inhibition, and can induce impulsive responding. They showed that WBV may increase the likelihood of action slips, mainly due to failure of response inhibition. These findings provoked a new question of why response inhibition failure happened during WBV. One may argue that the sensitivity of signal detection (i.e., target detectability) could become worse during WBV. Thus, we tried to resolve this question by reanalyzing Ishimatsu et al.'s data.

The purpose of this study was to examine whether WBV at frequencies likely to be experienced in helicopter working environments influenced sustained attention, response inhibition and target detectability (measured by Aprime).

2. Methods

2.1. Participants

Nineteen healthy volunteers with a mean age of 22.8 years ($SD = 4.4$) participated in this study. All participants had normal or corrected-to-normal vision. All participants gave written informed consent before taking part and the study was approved by the Regional Committee for Medical and Health Research Ethics, Oslo, Norway.

All participants were elite orienteering runners. In order to reduce the effects of workload, we capitalized on a close cooperation with Norwegian elite athlete organizations and gained access to 19 elite runners in orienteering competing at a national level. The athletes were recruited via the national

coaches. Orienteering is a highly cognitive sport and these athletes were highly trained in carrying out information processing tasks under environmental stress and could be expected to adapt readily to environmental changes, similar to helicopter pilots.

2.2. Apparatus

The experiment was carried out in a hypobaric chamber (Aeroform, Poole Dorset, UK) set to “sea level” air pressure (941 hPa).

The stimuli were presented on a 27-inch LCD display (Samsung SyncMaster SA350) located at eye level, keeping the distance to the required 64cm from participants in order to get the correct visual angle of stimuli. The timing of the events, generation of stimuli and recording of reaction times were controlled by a laptop computer connected to the LCD running SuperLab 4.0 software (Cedrus Corporation, San Pedro, California, U.S.).

Vibration was generated using an electrodynamic vibrator (LDS Model 725 LIN-E-AIR, Ling Dynamic System Ltd., Royston, Herts., UK); a chair with a high backrest and a footrest was mounted on the vibrator [11]. The vibrator was powered by a solid state Modular Power Amplifier (LDS MPA 1, Ling Dynamic Systems Ltd.) situated outside the hypobaric chamber. Vibration frequency and acceleration were monitored using a seat pad with accelerometers placed along three axes (Endevco type 2560, Brüel & Kjær, Nærum, Denmark). The pad was connected to a front end (type 3560C, Brüel & Kjær, Denmark). Vibration data were processed and monitored in real time using specialized software (Pulse Labshop 12.1, Brüel & Kjær). WBV in the vertical axis (z-axis) was 17 Hz with an unweighted magnitude of 1.0m/s^2 RMS throughout the experiment.

2.3. Task

The SART was used in this experiment. Single digits (1 to 9) were presented centrally on a 27-inch LCD; each digit was presented 25 times giving a total of 225 stimulus presentations during a 4.3 min period. Each stimulus presentation consisted of a 250ms presentation of the digit followed by a 900ms presentation of the mask (an encircled X). Digit presentation was regularly paced, with an onset-to-onset interval of 1150ms. Both digits and mask were white against a black background. Participants responded to the go digits (i.e. 1, 2, and 4-9) with a key press on a handheld response device; when the no-go digit (3) was presented they were required to withhold this response. The 25 no-go trials were randomly distributed among the 225 trials. The 225 trials were presented in a single continuous block. Participants responded by pressing the key on the response device with the thumb of their dominant hand. Digits were presented in one of five randomly assigned font sizes (48-, 72-, 94-, 100- and 120-point size; Symbol font) following the procedure described by Robertson et al. (1997) [12]. Participants were instructed that speed and accuracy were equally important.

2.4. Procedure

Participants were tested individually. After completing a practice session consisting of 18 trials, two of which were no-go trials (i.e. digit 3) participants walked into the experimental chamber and sat in the chair mounted on the vibrator. Participants used noise canceling headphones (Bose A20, Bose Corporation, Massachusetts, U.S.) throughout the experiment in order to avoid confounding noise effects. Participants performed two SART blocks, one without WBV (No-WBV) and one with WBV. Before the WBV block participants were exposed to the WBV for one minute to allow them to adapt to the situation. Ten participants performed the No-WBV block first; the remaining 9 started with the WBV block. Block presentation order was pseudo-randomly determined.

At the end of each block participants reported the mental demand (How do you rate the mental demand required to complete the task?) and effort (How do you rate the effort required to complete the task?)

using subscales of the NASA-TLX which is a multi-dimensional scale designed to obtain estimates of workload [13]. Responses were given on a twenty-point scale. At the end of the WBV block participants also reported perceived discomfort associated with exposure to WBV using a five-point scale (1, not uncomfortable; 2, a little uncomfortable; 3, fairly uncomfortable; 4, uncomfortable; 5, very uncomfortable).

2.5. Data analysis

Four scores were derived from the SART data: Aprime (A' , a nonparametric index of sensitivity), number of errors of commission (responses to the rare no-go digit), number of errors of omission (failures to respond to go digits) and mean reaction time (RT) [14, 15]. A' was calculated from “hit” (accuracy in response to digit 3 in the no-go trials) and “false alarm” (errors in response to digits in the go trials) to account and correct for unequal weighting of the trial types [15, 16]. Mean RTs were calculated from the number of go-trials on which the RT was over 100ms.

To examine the primary hypotheses, A' , errors of commission, errors of omission and RT in the WBV block were compared with those of No-WBV. Second, the relationships among the SART variables were investigated to understand the mechanism underlying errors of commission.

Statistical analyses were performed using SPSS (SPSS version 22.0 for Windows, IBM Corporation). Considering the sample size of the current research, we statistically tested the differences in the SART variables between the WBV block and the No-WBV block by using Wilcoxon signed-rank test. In line with the previous studies [14, 17], Pearson product-moment correlations were used to assess relationships between variables.

3. Results

Aprime (A'), errors of commission, errors of omission and RT in each block are shown in Table 1.

A' score was lower in the WBV block than in the No-WBV block ($Z = -2.42$, $p = .016$). Errors of commission were found more frequently in the WBV block than in the No-WBV block ($Z = -2.08$, $p = .037$). The number of errors of omission in the WBV block was similar with that of the No-WBV block ($Z = -1.22$, $p = .223$). Mean RT was shorter in the WBV block than in the No-WBV block ($Z = -2.13$, $p = .033$).

Table 1 The SART performance.

SART variables: M (SD)	Block	
	No-WBV	WBV
A'	0.82 (0.06)	0.76 (0.15)
Errors of commission	16.9 (5.2)	19.0 (3.5)
Errors of omission	1.9 (2.4)	2.7 (3.3)
RT [ms]	330 (40)	316 (43)

Pearson product-moment correlations among the SART variables are shown in Table 2.

In the No-WBV block, A' score was highly correlated with errors of commission ($r = -.950$, $p < .01$), errors of omission ($r = -.459$, $p < .05$) and RT ($r = .908$, $p < .01$). Errors of commission were highly correlated with RT ($r = -.875$, $p < .01$). In the WBV block, A' score was highly correlated with errors of

commission ($r = -.726, p < .01$) and RT ($r = .840, p < .01$). Errors of commission was highly correlated with RT ($r = -.721, p < .01$).

Table 2 Correlation coefficients (r) between variables in the No-WBV block and the WBV block.

	A'	Errors of commission	Errors of omission	RT
No-WBV block				
A'	-	-.950**	-.459*	.908**
Errors of commission		-	.185	-.875**
Errors of omission			-	-.428
RT				-
WBV block				
A'	-	-.726**	-.387	.840**
Errors of commission		-	.110	-.721**
Errors of omission			-	-.301
RT				-

Note: * $p < .05$, ** $p < .01$.

4. Discussion

This study was investigated sustained attention, response inhibition and target detectability (measured by Aprime) during WBV using the SART. A', errors of commission, errors of omission and mean RT were compared across two experimental blocks (the No-WBV block vs. the WBV block). The results revealed significant effects of WBV on SART performance.

Errors of commission on the SART increased during exposure to WBV. Errors of commission are usually considered analogous to real-world action slips [14] suggesting that WBV with the parameters used in this experiment may cause an increase in the frequency of action slips. Given that there were more errors of commission under WBV, one might expect that responses would be faster (indicating a speed-accuracy trade off). Speed-accuracy trade-offs on the SART have been reported previously [12, 14, 17]. We found that mean RT was shorter in the WBV block than the No-WBV block. However, errors of omission in the WBV block did not significantly differ from those of the No-WBV block, supporting the notion that WBV decreases response inhibition, rather than sustained attention.

In this study, errors of commission were negatively correlated with RT in both the No-WBV and the WBV blocks, suggesting a speed-accuracy trade-off. It is interesting to note that after controlling for RT, errors of commission in the WBV block were not correlated with other SART measures [8]. This implies that RT mediates the relationship between errors of commission and the other SART variables. In short, there were more action slips (i.e. errors of commission in the SART) under WBV primarily due to the shortening of mean RT. However, there are some possible explanations as to why RT became shorter during WBV. One possible explanation was based on failure of response inhibition rather than failure of sustained attention [8, 17]. Inhibitory control is an important executive function, allowing us to suppress, interrupt or delay an activated action. The SART is sensitive to impulsive responding [18] and the higher error rates in the WBV block may reflect more impulsive responding during WBV.

Another possible explanation was based on the effect of WBV on target detectability, which was the primary interest of the current study. Target detectability was lower in the WBV block than in the

No-WBV block. The reduction in target detectability coupled with the reduction in response latencies to incoming stimuli under WBV may be the main cause the increase in the frequencies of action slips.

5. Conclusion

Our findings suggest that exposure to WBV at a frequency which is common in helicopter working environments increases the probability of committing errors of commission on the SART (i.e. action slips). The reduction in target detectability coupled with the reduction in response latencies to incoming stimuli under WBV could be the main cause the increase in the frequencies of action slips.

6. References

- [1] Reason JT, Mycielska K (1982) *Absent-minded? The psychology of mental lapses and everyday errors*. Englewood Cliffs, NJ: Prentice Hall.
- [2] European Helicopter Safety Team (EHEST) (2010) *EHEST analysis of 2000-2005 European Helicopter Accidents*. European Aviation Safety Agency (EASA) Safety Analysis and Research Department. Retrieved from The European Helicopter Safety Team (EHEST) website: <http://easa.europa.eu/essi/ehest/category/publication-type/reports-and-analysis/>
- [3] European Helicopter Safety Team (EHEST) (2014) *The principles of threat and error management for helicopter pilots, instructors and training organisations*. European Aviation Safety Agency (EASA). Retrieved from The European Helicopter Safety Team (EHEST) website: <http://easa.europa.eu/essi/ehest/2014/12/he-8-the-principles-of-threat-and-error-management-tem-for-helicopter-pilots-instructors-and-training-organisations/>
- [4] Kåsin JI, Mansfield NJ, Wagstaff AS (2011) Whole body vibration in helicopters: risk assessment in relation to low back pain. *Aviation, Space, and Environmental Medicine*, 82(8), 790-796.
- [5] Conway GE, Szalma JL, Hancock PA (2007) A quantitative meta-analytic examination of whole-body vibration effects on human performance. *Ergonomics*, 50 (2), 228-245.
- [6] Griffin MJ (1990) *Handbook of human vibration*. London: Academic Press.
- [7] Hopcroft R, Skinner M (2005) *C-130J Human Vibration*. DSTO-TR-1756. Australian Government Department of Defence, Defence Science and Technology Organisation.
- [8] Ishimatsu K, Meland A, Hansen TA, Kasin JI, Wagstaff AS (2016) Action slips during whole-body vibration. *Applied Ergonomics*, 55, 241-247.
- [9] Mansfield NJ (2005) *Human response to vibration*. Boca Raton, FL: CRC Press.
- [10] Newell GS, Mansfield NJ (2008) Evaluation of reaction time performance and subjective workload during whole-body vibration exposure while seated in upright and twisted postures with and without armrests. *International Journal of Industrial Ergonomics*, 38(5-6), 499-508.
- [11] Hansen TA, Kåsin JI, Edvardsen A, Christensen CC, Wagstaff AS (2012) Arterial oxygen pressure following whole-body vibration at altitude. *Aviation, Space, and Environmental Medicine* 83(4), 431-435.
- [12] Robertson IH, Manly T, Andrade J, Baddeley BT, Yiend J (1997) 'Oops!': Performance correlates of everyday attentional failures in traumatic brain injured and normal subjects. *Neuropsychologia* 35(6), 747-758.
- [13] Hart SG, Staveland LE (1988) Development of NASA-TLX (Task Load Index): Results of empirical and theoretical research, In P. A. Hancock and N. Meshkati (Eds), *Human Mental Workload*. Amsterdam: North-Holland Press.

- [14] Cheyne JA, Solman GJF, Carriere JSA., Smilek D (2009) Anatomy of an error: a bidirectional state model of task engagement/disengagement and attention-related errors. *Cognition* 111(1), 98-113.
- [15] Jha AP, Morrison AB, Dainer-Best J, Parker S, Rostrup N, Stanley EA (2015) Minds "at attention": mindfulness training curbs attentional lapses in military cohorts. *PLoS One*, 10(2), e0116889.
- [16] Stanislaw H, Todorov N (1999). Calculation of signal detection theory measures. *Behavior Research Methods, Instruments, & Computers*, 31(1), 137-149.
- [17] Wilson KM, Russell PN, Helton WS (2015) Spider stimuli improve response inhibition. *Consciousness and Cognition*, 33, 406-413.
- [18] Sakai H, Uchiyama Y, Shin D, Hayashi MJ, Sadato N. (2013) Neural activity changes associated with impulsive responding in the sustained attention to response task. *PLoS One* 8(6), e67391.

The 26th Japan Conference on Human Response to Vibration (JCHRV2018)

Kindai University, Osaka, Japan

August 22-24, 2018

**Comparison of Detection Methods of
Seat Fidgets and Movements in Vehicle Seat****Junya Tatsuno**Faculty of Engineering,
Kindai University1 Takaya-umenobe, Higashihiroshima,
Hiroshima, 739-2116, Japan**Hitomi Nakamura**Faculty of Engineering,
Kindai University1 Takaya-umenobe, Higashihiroshima,
Hiroshima, 739-2116, Japan**Koki Suyama**Graduate School of Systems Engineering,
Kindai University1 Takaya-umenobe, Higashihiroshima,
Hiroshima, 739-2116, Japan**Setsuno Maeda**Faculty of Applied Sociology,
Kindai University3-4-1 Kowakae, Higashiosaka,
Osaka, 577-8502, Japan**Abstract**

To evaluate human discomfort in a vehicle seat, we have focused on the seat fidgets and movements (SFMs) of participants. In our previous studies, we carried out the driving simulator experiment to investigate a change in human discomfort during 60 minutes traveling. In the experiment, we video-recorded the participant's movements and checked all video off-line to obtain the SFMs frequencies of participants. Consequently, we could discuss the relationship between the subjective ratings of participants and the SFMs frequencies. However, we recognized that it was too heavy for us to obtain more experimental data with the visual judgment. Thus, we have studied the applicability of SFMs detection with other methods. In this paper, we show trials flex sensor, body pressure measurement system and motion capture system.

1. Introduction

Automobile occupants are exposed to whole-body vibration during traveling. Since the whole body vibration results in human discomfort and health effect, many technologies such as suspension system, seat, and tire have been developed to decrease whole-body vibration exposure. Here, it is important for the automotive manufacturer and supplier to evaluate human discomfort during traveling by any method. In general, human discomfort evaluations are classified into subjective and objective methods. There are many studies on the subjective evaluation of personal discomfort caused by the whole-body vibration. For example, Huang et al. verified the differences between absolute magnitude estimation and relative magnitude estimation when participants judged the intensity of noise and vibration subjectively [1]. It is well-known that more sample size required when we adopt such a subjective evaluation method. Meanwhile, various objective measures have been utilized to evaluate human discomfort. Recently, because of the sensing technology advancement, the use of cutting-edge technology such as near-

infrared spectroscopy (NIRS) has been studied for the evaluation of human discomfort [2]. We have focused on discomfort evaluation with seat fidgets and movements (SFMs) that Sammonds et al. proposed [3]. The thinking way of the SFMs is as follows. Through our daily life, we can understand that people move unconsciously to relieve the pressure of compressed body parts when we sit on chairs. Some researchers have focused on this phenomena to evaluate human discomfort, and for example, Fenety et al. [4] reported In-Chair Movements (ICM) to determine the effect of sitting chairs on the body. Sammonds et al. applied the concept to the discomfort evaluation of seated occupants in a vehicle and showed that there was a high correlation between subjective discomfort and frequency of SFMs. Also, we reported the driving simulator experiment in which the SFMs concept was applied to the evaluation of automotive seat [5]. In these previous studies, we video-recorded the participant's movements during all experiment and checked all video off-line to derive the SFMs frequencies of participants. Through the analysis, we strongly felt that such work was too heavy to do. Thus, we have discussed other detection method of SFMs. In this paper, we will report several trials for SFMs detection methods.

2. Seat fidgets and movements

First, we would like to explain the seat fidgets and movements (SFMs). As mentioned above, people move unconsciously when seated with the purpose of relieving pressure on compressed body parts with impeded blood flow and joint pressure. We found that participants likely move their leg or torso during driving simulator experiment of one hour long. Figure 1 to 3 are frame shots of three kinds of typical



(a) before movement (b) during movement (c) after movement

Figure 1: Frame shots when participant moved right leg



(a) before movement (b) during movement (c) after movement

Figure 2: Frame shots when participant moved left leg



(a) before movement (b) during movement (c) after movement

Figure 3: Frame shots when participant moved torso

SFMs. In the previous research, we focused on ride comfort evaluation and improvement of passenger or autonomous vehicle driver [6]. Since our interesting is discomfort when occupants do not drive, we gave participants reading task instead of driving task. In Figure 1, the participant moved his right leg unconsciously while riding the driving simulator. Conversely, the participant's left leg was moved in Figure 2. In case of this camera angle, there is a possibility that we overlook this movement because the left leg was covered with the right leg. We reported that the visual judgment method has problems of oversight as well as heavy workload [7]. Meanwhile, the SFMs include torso movement as shown in Figure 3. In the following discussion, we asked the participant to produce these types of the SFMs consciously instead of waiting for the unconscious movements of the participant.

3. Detection of SFMs

The overall objective of this study is to develop a system in which we can measure participant movement when they sit automotive seat in a car or driving simulator. In this section, we investigated several methods through measurement experiments.

3.1 Motion capture

It is well-known that motion capture technologies have been employed to record human movements.



(a) front side (b) back side

Figure 4 participant attached motion capture system



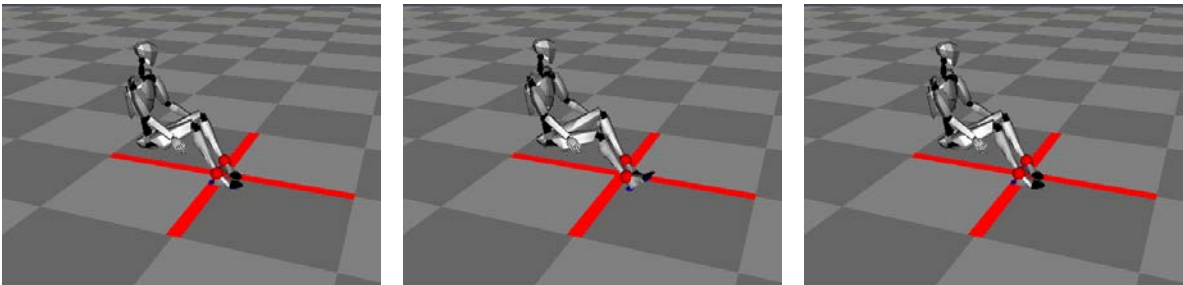
(a) bench (b) driving simulator

Figure 5 Experimental environment for trial with motion capture

The motion capture systems can be classified into two types; optical system and non-optical system. In the optical system, two or more cameras must be installed in the experimental field, and special markers must be equipped to participants. This type of system requires a high initial cost. Moreover, we are concerned about fixing cameras in the small space of the cockpit. Thus, we eliminated the optical motion capture system from our consideration.

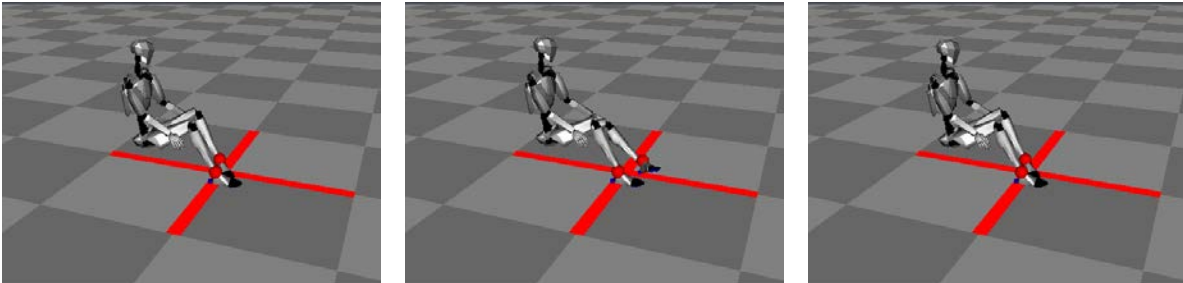
On the other hand, the system combined magnetic sensor and inertial sensor represents the non-optical motion capture system. Since there was our concern about the influence of electromagnetic interference when we utilized in the driving simulator, we performed two types of test; bench test and driving simulator test.

Figure 4 shows the participant who wore the motion capture system (Perception Neuron, Noitom Ltd., China). This system employs 18 pieces of INU, which is composed of a gyroscope, accelerometer,



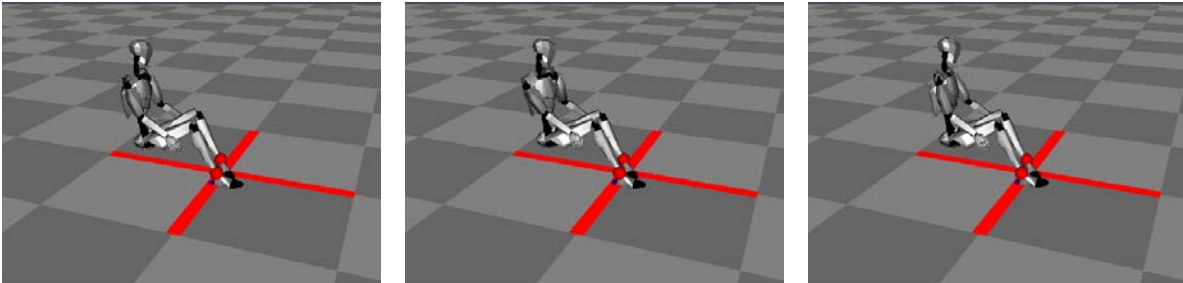
(a) before movement (b) during movement (c) after movement

Figure 6 Motion capture data of right leg movement at bench



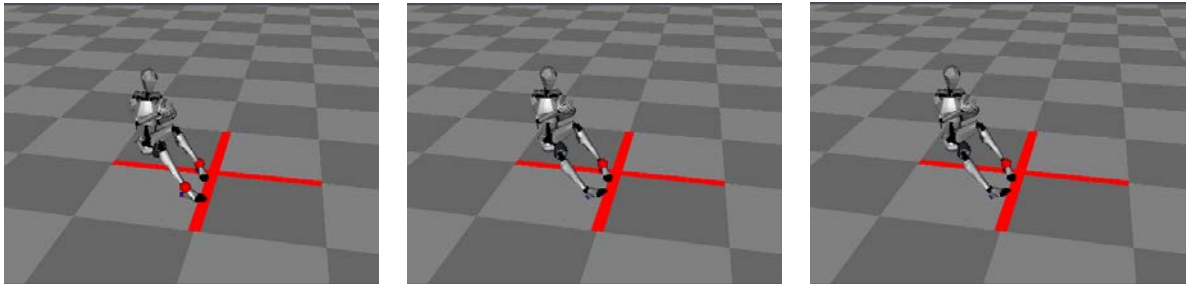
(a) before movement (b) during movement (c) after movement

Figure 7 Motion capture data of left leg movement at bench



(a) before movement (b) during movement (c) after movement

Figure 8 Motion capture data of torso movement at bench

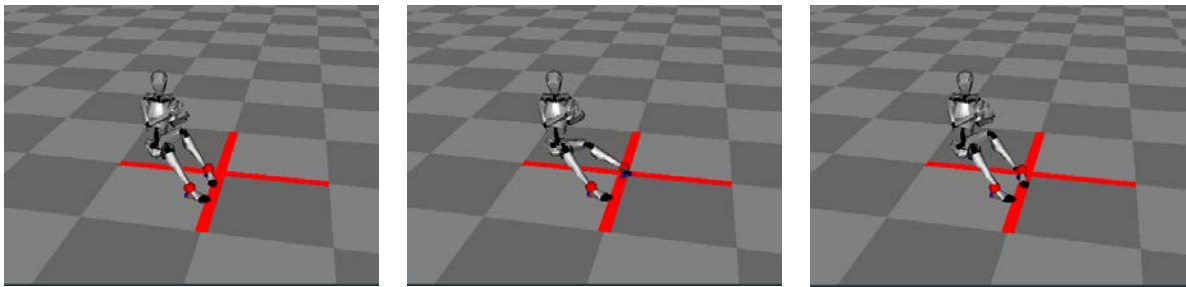


(a) before movement

(b) during movement

(c) after movement

Figure 9 Motion capture data when participant move right leg in driving simulator

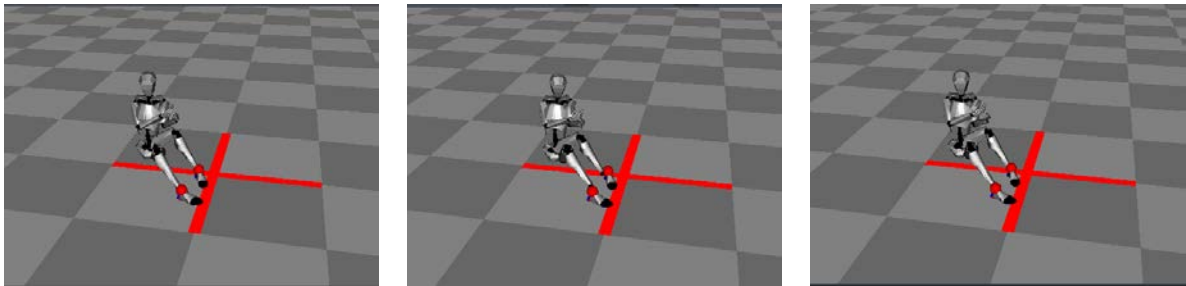


(a) before movement

(b) during movement

(c) after movement

Figure 10 Motion capture data when participant move left leg in driving simulator



(a) before movement

(b) during movement

(c) after movement

Figure 11 Motion capture data when participant move left leg in driving simulator

and magnetometer. As shown in Figure 5 we prepared two types of test environment; bench test and driving simulator test. Under the driving simulator test, we exposed the moderate magnitude of whole-body vibration to the participant by creating the bumpy section in the test course.

We asked the participant to perform three kinds of movement such as right leg, left leg, and torso under both environments. At that time, we recorded his movement by using the dedicated software. Figure 6, 7 and eight show three frames extracted from animation movie generated with measurement data in the bench test. We recognized that the measurement had enough accuracy when we watched the animation movies of all movement. Conversely, the animation movies of the driving simulator experiment brought us a feeling of strangeness. In other words, there were differences between the actual movements of the participant and the movements of the mannequin. It was easy for us to understand that measurements had errors due to electromagnetic interference generated by electrical equipment like as DC motor. Consequently, the motion capture system is not applicable for the detection of the SFMs in the driving simulator as our expected.

3.2 Body pressure measurement system

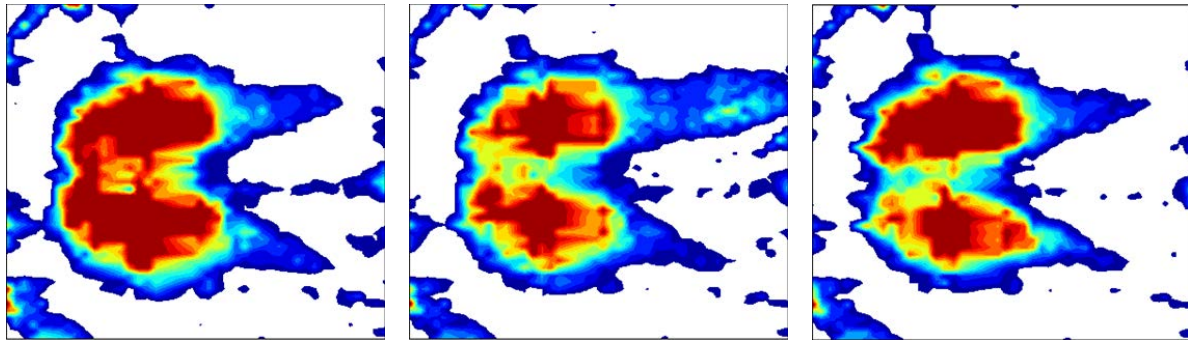
As mentioned before, the study of the SFMs is inspired by the ICM study. In the previous study on the ICM, Fenety et al. utilized an interface pressure mat [4]. Similarly, pressure distribution measurement has been applied to automotive seat evaluation [8]. Thus, in this paper, we investigated a possibility of the SFMs detection with a body pressure measurement system.

Figure 12 shows the experimental environment where we placed a body pressure measurement mat on the seat of the driving simulator. In the previous research on the vehicle seat evaluation, they set two mats on the seat surface and the seat back. We utilized a sensor sheet (BPMS, Nitta Co., Japan) on the surface to investigate a possibility to detect the SFMs with more simply apparatus. By using this measurement, we can obtain the pressure distribution of 44 columns and 48 rows.



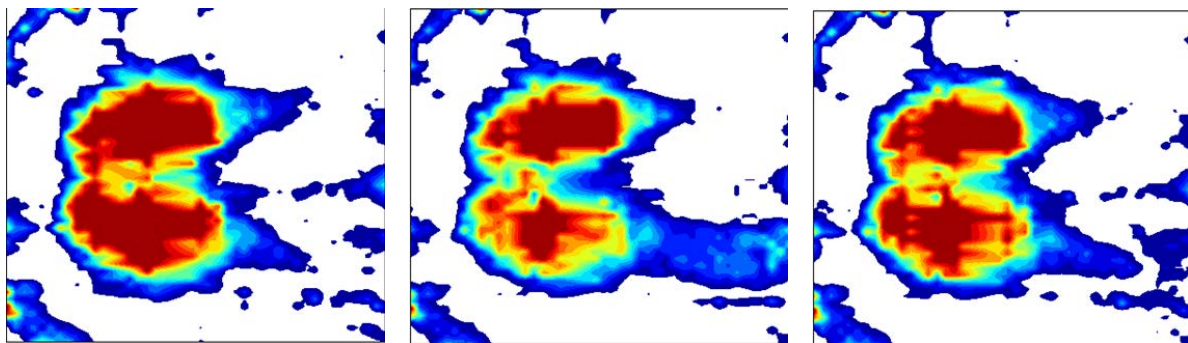
Figure 12 Body pressure mat on the seat of driving simulator

When we asked the participant to perform three kinds of movement, we recorded the pressure distribution at the sampling rate of 2 Hz. Figure 13, 14 and 15 show the body pressure distributions at sampling time before each movement, during each movement, and after each movement. From the distribution change shown in Figure 13, we could understand the load acted on the left leg when he moved his right leg. Likewise, the result of Figure 14 indicates the load acted on the right leg increased during the participant moved his left leg. Meanwhile, it was not easy to find any signature from the distribution change in Figure 15, when the participants moved his torso. Thus, we calculated the trajectories of the gravity center from the time series distribution data. From the trajectories of the gravity center as shown in Figure 16, when the participant makes the SFMs like as movement of his right or left leg, the gravity centers moved to the lateral direction. Meanwhile, when the participant moved his torso, the gravity center moved longitudinally. Although we cannot significantly state that it can detect the SFMs with the body pressure measurement because we have not much sample data, we think that there is a



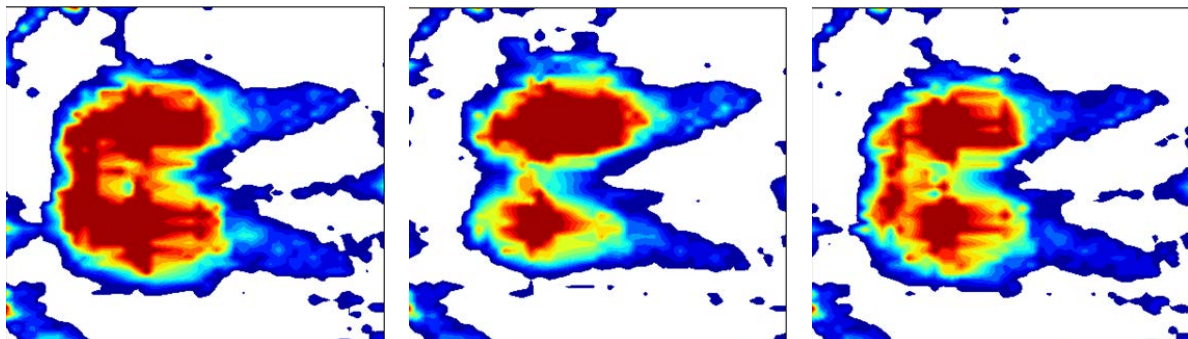
(a) before movement (b) during movement (c) after movement

Figure 13: Body pressure distribution in participant movement of right leg



(a) before movement (b) during movement (c) after movement

Figure 14: Body pressure distribution in participant movement of left leg



(a) before movement (b) during movement (c) after movement

Figure 15: Body pressure distribution in participant movement of torso

possibility to apply to the SFMs detection. However, the method with the body pressure measurement has the following weak point. Using the body pressure measurement requires to cover seat surface with the sheet of the measurement system. In case of evaluating automotive seats, the existence of the sheet might influence participant discomfort.

3.3 Flex sensor

Most seriously, these commercial systems need high initial cost. Profanely, we may obtain precise data more than necessary if we adjust such commercial products. But we recognize that millimeter-sized spatial resolution is not necessary for detecting participant SFMs. In other words, it is enough for us to

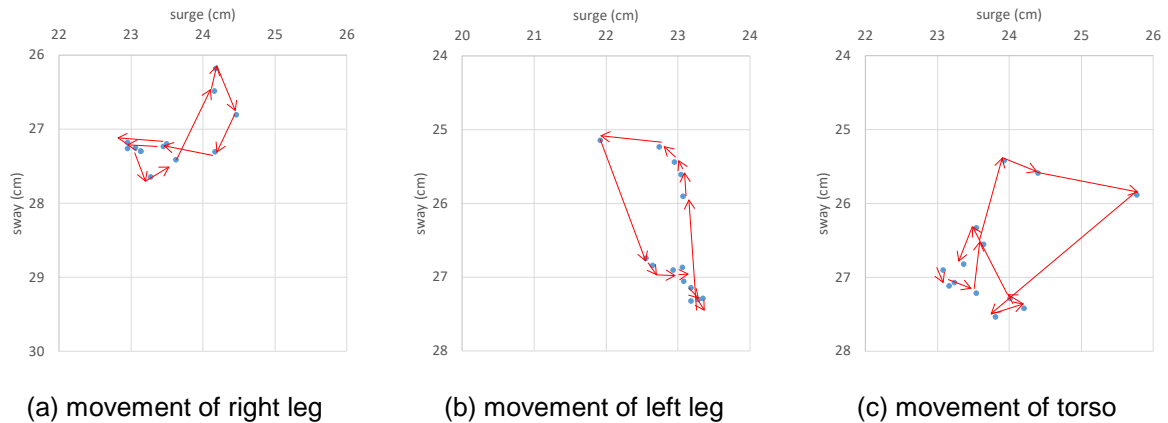


Figure 16: Trajectory of gravity center

obtain rough information that which part of the body moved. From this viewpoint, we proposed a simple detection of participant movement with flex sensors [7, 9]. In this section, we mentioned our progress on the SFMs detection with flex sensors.

As the first step of this research, we tried to detect a participant's leg movement with flex sensors (Spectrasymbol, USA, FS-L-0095-103-ST). Since we can get a flex sensor for 2,000 JPY, the initial cost for installation of the system must be very lower than other methods. As shown in Figure 17, we attached four flex sensors to four joints with packing tapes; right knee, right hip, left knee and left hip. We could measure output voltage by connecting the voltage divider because this sensor is a kind of variable resistor. In addition, it may take less than 10 minutes to attach sensors to participant body, and calibration processes are not necessary because it is enough for us to obtain rough information that which part of the body moved for SFMs evaluation. Through this trial, we found that the proposed method could be applied to measure the SFMs [9]. Meanwhile, we recognized that it was difficult to fix the flex sensor when they wear loose fit cloth.

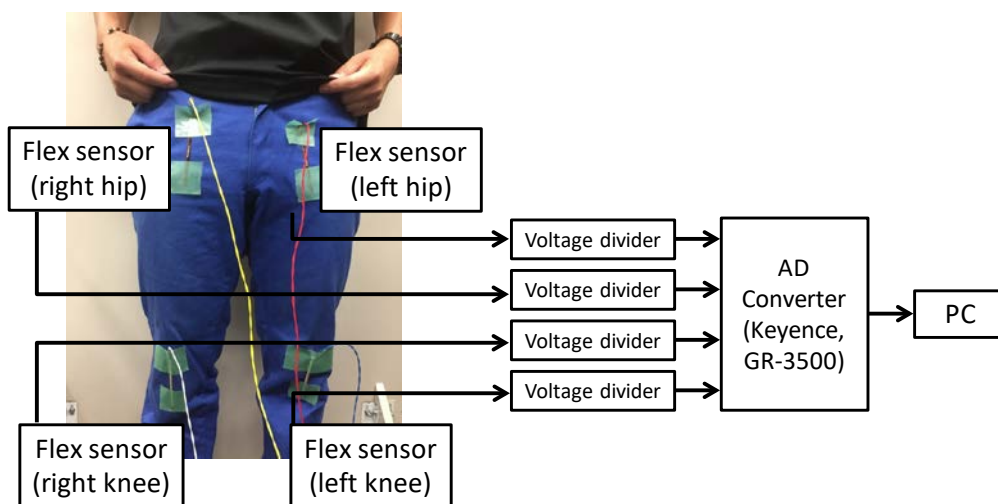
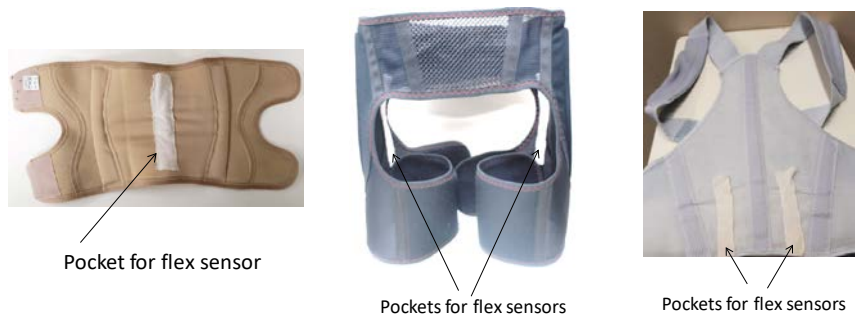


Figure 17: SFMs detection with flex sensors

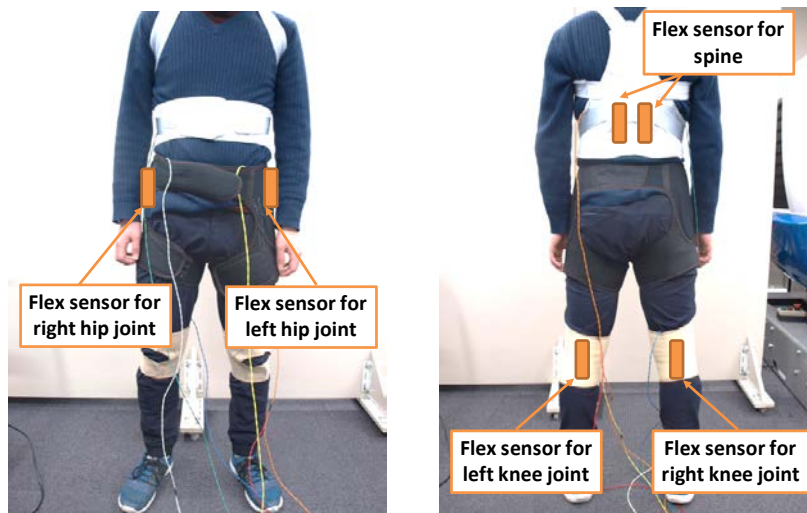
As the second step of this research, we prepared three parts of commercial supporters; knee joint, hip joint, and back (Figure 18). And we sewed pockets to put sensors. At the beginning of the experiments, we ask participants to wear the supporters. At that time, we loosely attached supporters so that they

cannot feel extreme restraining. As shown in Figure 19, we used six flex sensors to evaluate participants' SFMs.



(a) knee joint supporter (b) hip joint supporter (c) back supporter

Figure. 18 Supporters on which pockets for flex sensors were sewed.



(a) front side

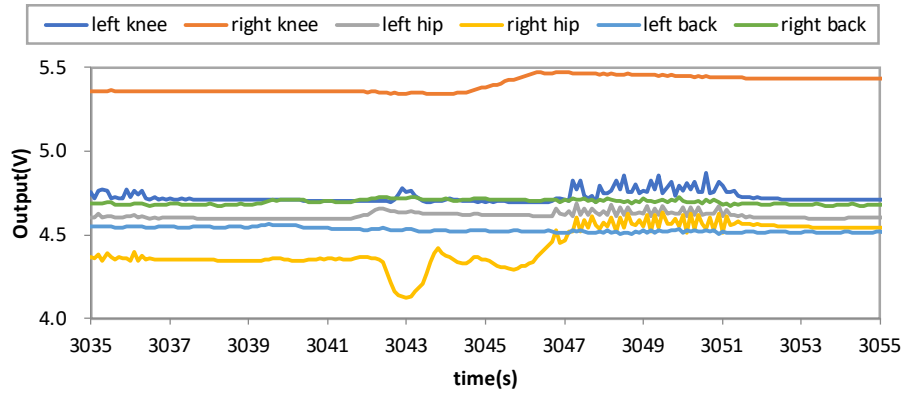
(b) back side

Figure 19 Participant with the supporters.

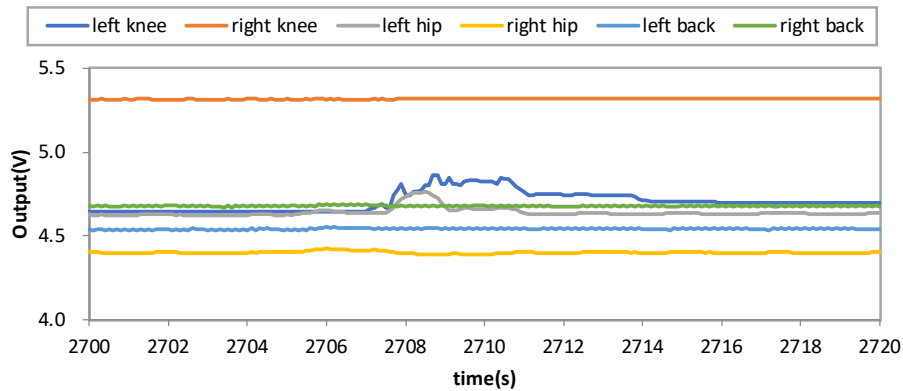
Figure 20 shows the output voltages of all flex sensors. The data as shown in Figure 6(a) implies that the participant moved his right leg significantly. Here, it was found that some signal waves vibrated in the latter half because the driving simulator passed a bumpy section. As mentioned above, we had to carefully observe the movie as shown in Figure 2 to recognize the movement of the participant left leg. However, we can easily understand that the participant moved his left leg from the result in Figure 20(b). This fact means that the flex sensor may be robust over occlusion that becomes a problem when we use the video system. From the result in Figure 20(c), we found that after the participant stretched the back while bending the left knee, he bent the right knee afterward. Consequently, we showed that the affordable system with the flex sensors could extract the participants' SFMs. However, we are concerned that supporter may impair participant movement. Besides, to mitigate our workload, we have to develop software that can automatically classify and enumerate the SFMs with the time-series signals.

4. Conclusion

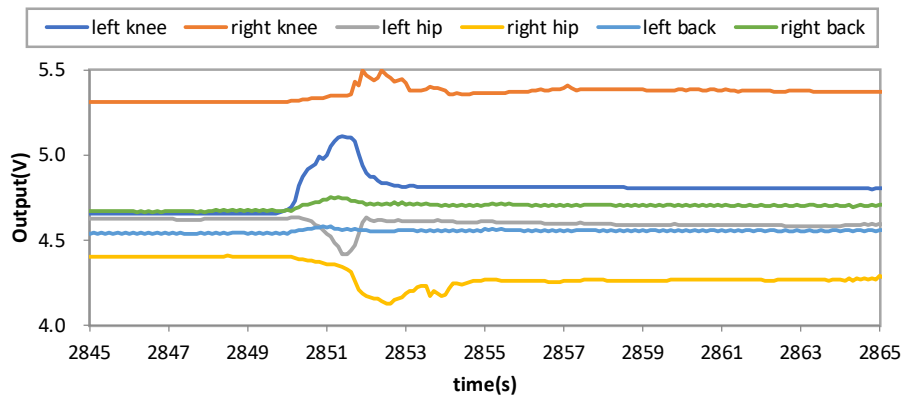
Since we recognized that it was too heavy for us to detect the SFMs of participants with the visual



(a) Movement of right leg



(b) Movement of left leg



(c) Movement of torso

Figure 20 Output voltage of electrical circuit with flex sensors

judgment of video-recorded movie in our previous research, we discussed applicability to SFMs detection with other methods. First, we tried to investigate the applicability of inertial motion capture system. As a result, the inertial motion capture system is not applicable for the detection of the SFMs in the driving simulator because measurements errors were observed due to electromagnetic interference generated by electrical equipment like as DC motor. Second, we tested the body pressure measurement system. We recognized that there is a possibility to apply to the SFMs detection by using not only body pressure distribution but also gravity center change. However, the problem remains that the sensor

sheet might have an influence on participant discomfort. Third, from the viewpoint that it's enough to obtain rough information that which part of the body moved for detecting SFMs, we tried to utilize the affordable flex sensor. In this paper, we introduced a method in which a participant wears three supporters with flex sensor. From the experimental results, it was suggested that the proposed method could be applied to measure the SFMs. However, we are concerned that supporter may impair participant movement, and we have to develop software that can automatically classify and enumerate the SFMs to mitigate our workload.

References

- [1] Huang, Y., and Griffin M. J., (2014) Comparison of absolute magnitude estimation and relative magnitude estimation for judging the subjective intensity of noise and vibration, *Applied Acoustics* 77, 82-88.
- [2] Li, Z., Zhang, M., Li, J., Zin, Q., Chen, G., Li, J., Liu, F., (2012) Spectral analysis of cerebral oxygenation responses to seated whole-body vibration in healthy men, *International Journal of Industrial Ergonomics*, 42(4), 341-346.
- [3] Sammonds, G. M., Fray, M., Mansfield, N. J., (2017) Effect of long term driving on driver discomfort and its relationship with seat fidgets and movements (SFMs), *Applied Ergonomics*, 58, 119-127.
- [4] Fenety, P.A., Putnam, C., Walker, J.M., (2000) In-chair movement: validity, reliability and implications for measuring sitting discomfort, *Applied Ergonomics*, 31 (4), 383-393.
- [5] Tatsuno, J., Maeda, S., Sammonds, G., Mansfield, N., (2017) Possibility of Automobile Seat Evaluation with Seat Fidgets and Movements, *Proceedings of the AHFE 2017 International Conference on Human Factors in Transportation*, 474-483.
- [6] Tatsuno, J., Maeda, S., (2016) Driving Simulator Experiment on Ride Comfort Improvement and Low Back Pain Prevention of Autonomous Car Occupants, *Proceedings of the AHFE 2016 International Conference on Human Factors in Transportation*, pp.511-523.
- [7] Tatsuno, J., Maeda, S., (2018) Development of Simple Detection Method of Involuntary Movements to Evaluate Human Discomfort in Vehicle Seat, *Proceedings of the AHFE 2018 International Conference on Human Factors in Transportation*, 857-865.
- [8] Inagaki, H., Taguchi T., Yasuda, Iizuka, Y., (2000) Evaluation of Riding Comfort: From the Viewpoint of Interaction of Human Body and Seat for Static, Dynamic, Long Time Driving, *SAE Transactions*, Vol. 109, Section 6, 960-964
- [9] Tatsuno, J., Maeda, S.,(2017) Study of Simple Detection of Seat Fidgets and Movements to Evaluate Human Discomfort, *Proceedings of 25th Japan Conference on Human Response to Vibration (JCHRV2017)*, pp.121-126

The 26th Japan Conference on Human Response to Vibration (JCHRV2018)

Kindai University, Osaka, Japan

August 22-24, 2018

**Modeling the effect of building shaking caused by earthquakes
on human body**

Mutsuhiro Yoshizawa¹, Harumi Yoneda² and Masashi Yamamoto³

¹ Research and Development Institute, Takenaka Corporation
yoshizawa.mutsuhiro@takenaka.co.jp
Inzai, Chiba, 270-1395, Japan

² Research and Development Institute, Takenaka Corporation
nishimura.harumi@takenaka.co.jp
Inzai, Chiba, 270-1395, Japan

³ Research and Development Institute, Takenaka Corporation
yamamoto.masashia@takenaka.co.jp
Inzai, Chiba, 270-1395, Japan

Abstract

Social needs for the building seismic performance are changing not only to the life safety but also to the maintenance of functionality after the earthquake. So the human condition during building shaking by earthquakes is also beginning to be considered as a part of the functionality of the building. In order to evaluate this human condition, we continue to conduct surveys by questionnaires for residents of buildings with seismographs installed.

In order to maintain the functionality of the residents of buildings during the earthquake, it is important to ensure safety from indoor damages. Recently, as educational materials of the indoor damage during an earthquake, falling simulations of furniture fixtures are often performed using physical engines. Although simulation results are provided with enhanced immersive feeling such as VR technology, these results are out of consideration of the human condition in the room. Therefore, from the results of the questionnaire survey, we created some VR images considering the human condition in the room.

Through these investigations, we considered the modelling the effect of building shaking caused by earthquakes on human body.

1. Introduction

The social demand for earthquake resistance of buildings is changing from secure the safety of human life to maintaining the functionality of the building. On March 11, 2011, Japan was shaken by the 2011 Great East Japan Earthquake. During the 2011 Great East Japan earthquake, even though structural members of buildings were very little damage, damage of sprinkler-heads, fall of ceiling boards on upper floors, movement of furniture on casters such as a photocopy machine, and fall of books occurred. These damages led to the function loss of the building and had an influence on recovery after the earthquake greatly. And the human condition during building shaking by earthquakes is also beginning to be considered as a part of the functionality of the building.

During the 2011 Great East Japan earthquake, Japan Meteorological Agency(JMA) Seismic Intensity 6 lower or more was observed in a large area throughout Tohoku and Kanto region, and the long-time strong shaking and the long-period ground motion were widely observed. In addition, a large number of aftershocks were occurred. These aftershocks caused outbreaks of dizziness over a large area (M. Honma et al., 2012). And the high-rise buildings in urban area, which have long natural period, were easy to sway by the long-period ground motions, and this long shaking of the high-rise building caused long-term fear and anxiety to people (JMA, 2012). These findings were found from the questionnaire survey result after the earthquake. The questionnaire survey after the earthquake is very useful, because it is possible to reflect the situation in the real building. But time lag between the time when the object person felt shaking and the time when the object person answered the questionnaire might be big. There is a possibility that a correct answer cannot be obtained if this time lag is big. So, using the information of the seismometer installed in the building, a quasi-real-time questionnaire system for the shaking of the building was developed (M.Yoshizawa et al., 2015). The questionnaire result was evaluated based on the observed floor response acceleration using an index such as ISO 2631-1 or JMA seismic intensity.

In order to maintain the functionality of the residents of buildings during the earthquake, it is important to ensure safety from indoor damages. Recently, as educational materials of the indoor damage during an earthquake, falling simulations of furniture fixtures are often performed using physical engines. Although the simulation results are provided with enhanced immersive feeling such as VR technology, these results are out of consideration of the human condition in the room. Based on the results of the questionnaire survey, in order to conduct a more effective indoor simulation, we thought that there is a necessity to consider the viewpoint of human subject during the earthquake.

Yamamoto conducted shaking table tests on human subjects to obtain dynamic response data and produce dynamic human models(M.Yamamoto, 2011). So, we created some VR images considering the human condition in the room using this dynamic human model.

Through these investigations, we examined the necessity of the modelling the effect of building shaking caused by earthquakes on human body.

2. Study on human vibration characteristics by questionnaire survey

2.1 Overview of the questionnaire system

The building as a target of the questionnaire system is seven, Miyagi, Chiba, Tokyo, Kanagawa, Aichi, Osaka, and Fukuoka (as shown in Figure 1). Figure 2 shows the flow of the questionnaire system processing. The seismographs in these seven buildings are connected for 24 hours on the intranet. So, if the intranet can be used after the earthquake, a questionnaire survey is possible in almost real time immediately after the earthquake.

The UC building is the only high-rise building in the questionnaire conducted this study. The UC building is not connected to the intranet, but long term observation of the seismograph is conducted in the UC building.

Table 1 shows the contents of the questionnaire. The questionnaire items are set in reference to the items in the former study of the questionnaire survey carried out for the resident of the high-rise building in the case of the Great East Japan Earthquake (K. Tamura et al. 2012).

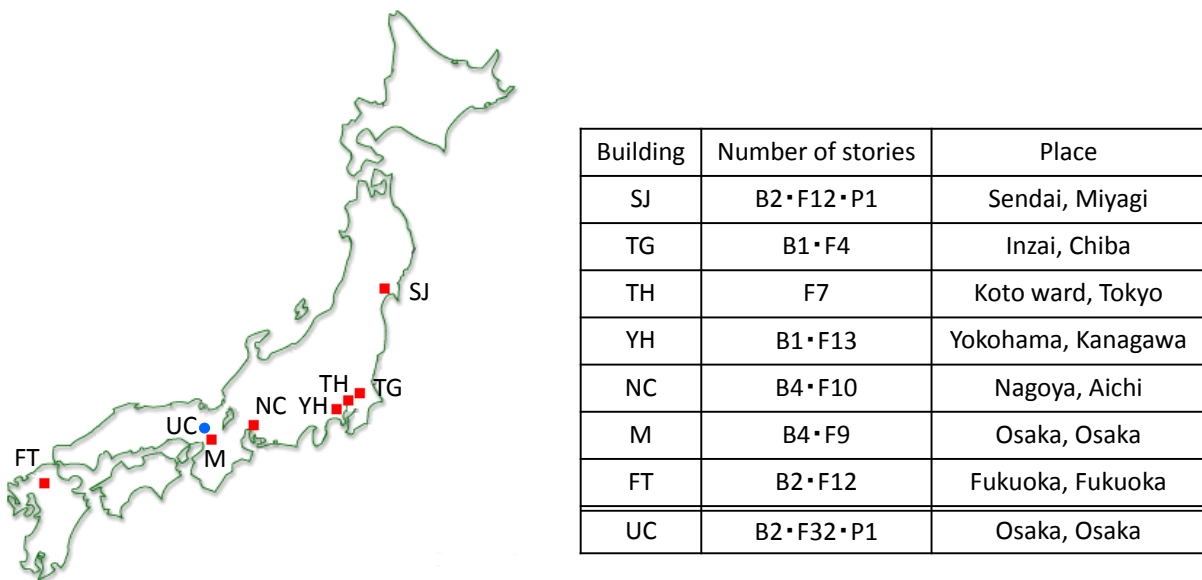


Figure 1 Buildings that conducts the questionnaire system

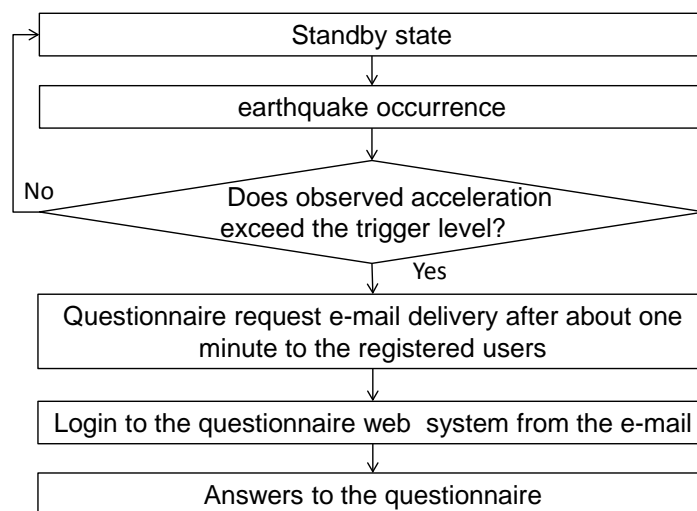


Figure 2 The flow of the questionnaire processing

Table 1 Contents of the questionnaire

Q1 Where did you feel the earthquake?

B1F 1F 2F 3F 4F absence in the registered building do not remember

(If you did not feel the earthquake, please chose the place that was in the time of the earthquake detection time)

Q2 If you select "Absence in the registered building", enter the location where you were.

Q3 Please choose the situation when you feel the earthquake.

sitting position standing position walking sleeping position other, do not remember

Q4 When you felt the earthquake, did you take the evacuation actions?

I did not feel shaking I did nothing I sank under the desk

I protected a body from falling objects (helmet wearing etc.)

I opened the door for immediate evacuation other, do not remember

Q5 How much was the size of the earthquake that you felt?

I did not feel shaking I slightly felt shaking

I felt a clear shook, but there was no trouble in the action

There was a little trouble for walking or moving, It was not possible to standing

I could not act anything, other, do not remember

Q6 What kind of shaking did you feel? Multiple answers are possible.

I did not feel shaking Long-period tremors with slow repetition

Shaking which goes around around in north, south, east and west

Shaking which moves in left and right small tremblingly

Shaking which pushes up and down

Shaking that its amplitude increases suddenly other, do not remember

Q7 How long did you feel the shaking? Please choose the closest match.

I did not feel shaking Less than 10 seconds About 30 seconds About 1 minute

About 2 minutes More than 2 minutes other, do not remember

Q8 While the earthquake shook, did you feel anxious?

I did not feel shaking Not anxious Anxious a little Anxious Anxious very much

other, do not remember

Q9 After the earthquake, did you come to feel sick?

I did not feel shaking No problem with physical condition

Such as feeling dizzy, I came to feel sick slightly Quite feel bad in dizziness and nausea

Such as vomiting, I came to feel sick very much I fell asleep other, do not remember

Q10 How much shaking did you feel it with in the scale of seismic intensity?

I did not feel shaking Less than seismic intensity 1 1 2 3 4 5 Lower

5 upper More than seismic intensity of 6 Lower other, do not remember

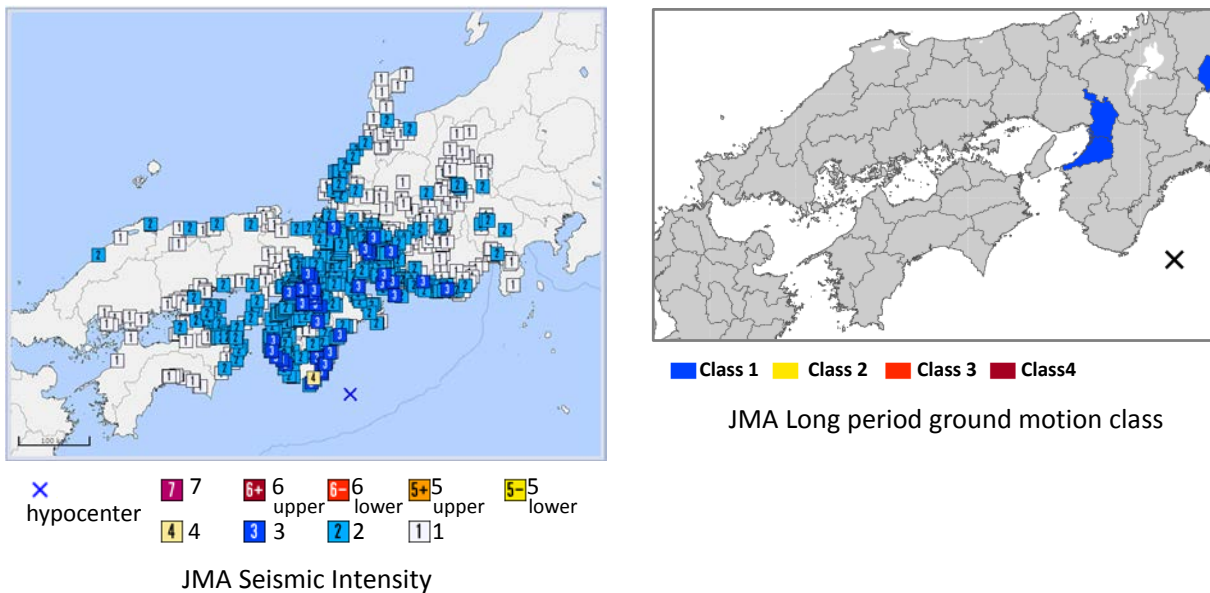
Q11 In addition, please describe impressions about the shaking freely.

2.2 Example of the result with the questionnaire system

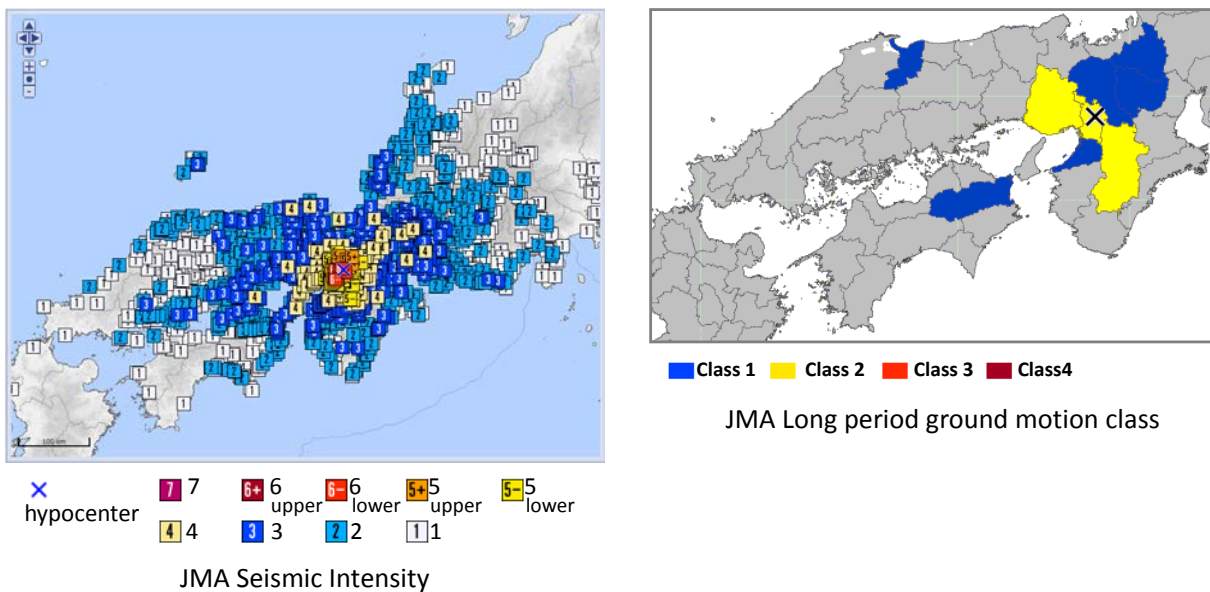
This questionnaire survey started from 2015, but here we will introduce cases where the building shake was relatively large. Figure 3 shows the outline of the target earthquakes.

One is the earthquake occurred at the southeastern part of Mie Prefecture (M=6.5, Depth=29km). In Osaka city, seismic intensity 2 to 3 was observed. The observation seismic intensity was small, but the long period ground motion class 1 was observed in Osaka Prefecture, and newspapers covered the elevator stop damage etc in the high-rise buildings.

The other is the earthquake occurred at the northern part of Osaka Prefecture (M=6.1, Depth=13km). This earthquake occurred directly under the big city, maximum seismic intensity 6 lower was observed. Although the long period ground motion class 2 was observed in Osaka Prefecture, long period ground motion did not excite too much.



(1) Earthquake No.1 Southeastern part of Mie pref. 2016/4/1, M6.5



(2) Earthquake No.2 Northern Osaka pref. 2018/6/18, M6.1

Figure 3 Outline of the target earthquake of the questionnaire

(Map images quoted from the Japan Meteorological Agency website)

(1) UC building (2016/4/1)

In this section, the results of questionnaire survey in the UC building against Earthquake No.1 will be introduced. Table 2 shows the calculated values from the floor response of the UC building. At Table 2, MSDV was calculated by the square root of the integral of the square of the z-axis acceleration after it has been frequency-weighted:

$$MSDV_z = \left(\int_0^T a_{wz}(t)^2 dt \right)^{1/2} \quad (1)$$

where $a_{wz}(t)$ is the frequency-weighted acceleration of the z direction defined in ISO 2631-1. In general, the earthquake shaking in the horizontal direction is larger than the vertical direction. So following the precedent study (Kouhei M. 2005), combining vibrations in three directions is adopted as follows.

$$MSDV_{xyz} = \left(\int_0^T a_w(t)^2 dt \right)^{1/2} \quad (2)$$

$$a_w(t) = \left(a_{wx}(t)^2 + a_{wy}(t)^2 + a_{wz}(t)^2 \right)^{1/2} \quad (3)$$

where $a_{wx}(t)$, $a_{wy}(t)$ and $a_{wz}(t)$ were the frequency-weighted acceleration in direction X, Y and Z.

Table 2 Calculated values from the floor response of the UC building

(1) Seismic intensity, maximum acceleration and long-period ground motion class

Floor	S.I.*	Scale of S.I.	Max. Acc. (cm/s ²)	Long-period ground motion class
31	3.1	3	14.6	No rank (4.5cm/s)
15	2.9	3	11.7	
B2	2.3	2	5.4	

* S.I. : Instrumental seismic intensity

(2) Motion sickness does value

Calculation result floor	Z direction		XYZ direction	
	MSDVz	vomiting ratio	MSDVxyz	vomiting ratio
31F	1.715E-02	0.01%	4.441E-01	0.15%
15F	1.527E-02	0.01%	2.124E-01	0.07%
B2F	1.530E-02	0.01%	4.266E-02	0.01%

Figure 4 shows the results of the questionnaire against Earthquake No.1 at the UC building. In this questionnaire results, the respondents who were above the 16th floor were analyzed as upper floors. About half of the respondents on the lower floors chose "I did not feel shaking", some respondents on the upper floors chose "Such as feeling dizzy, I came to feel sick slightly". Although the vomiting ratio by MSDV_{xyz} on the upper floor was calculated as small as 0.15%, it seems to be consistent with the questionnaire difference between upper floors and lower floors.

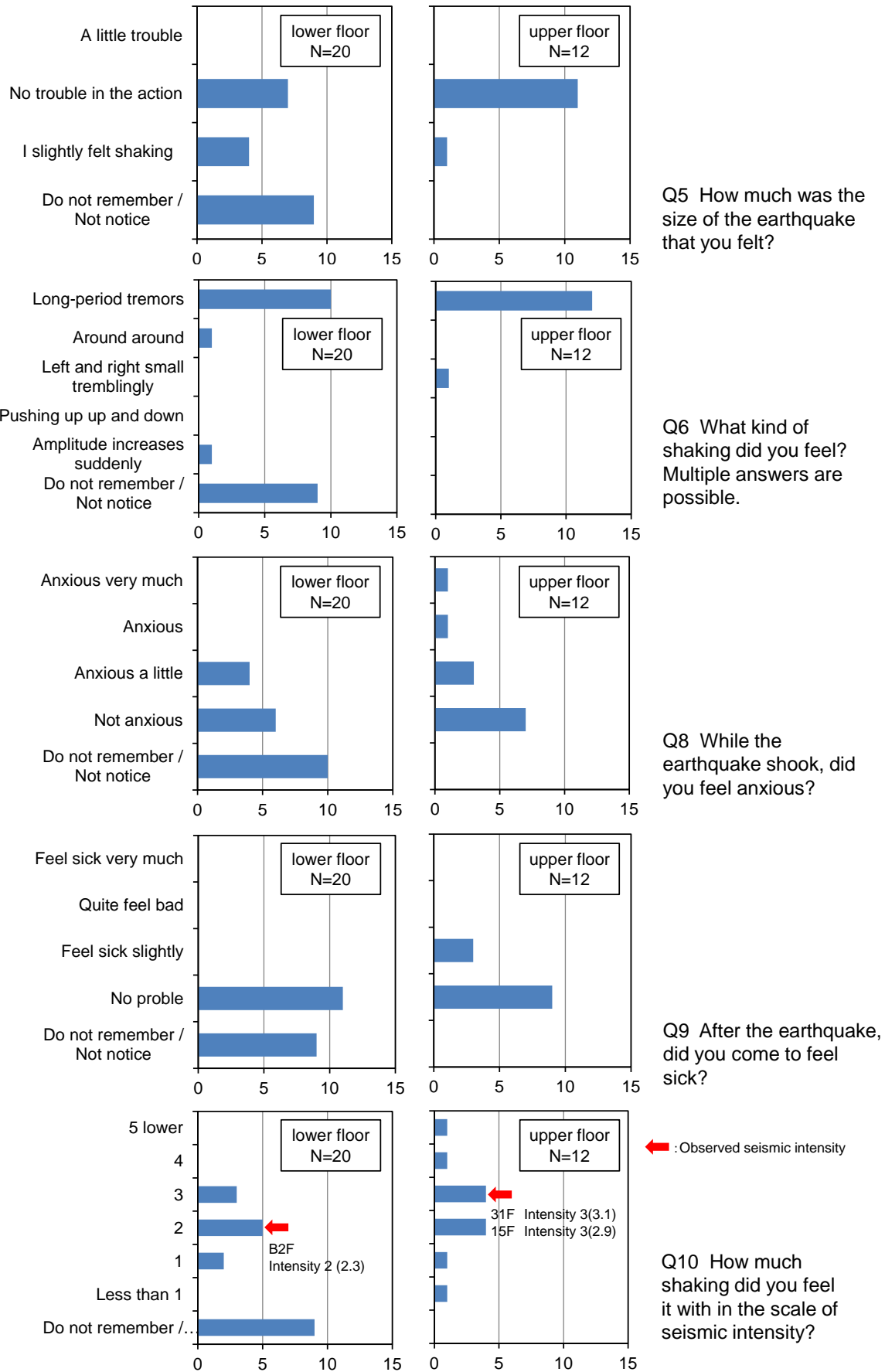


Figure 4 Results of the questionnaire against Earthquake No.1

(2) M building (2018/6/18)

In this section, the results of questionnaire survey in the M building against Earthquake No.2 will be introduced. Table 3 shows the calculated values from the floor response of the M building, Table 4 shows the distribution of questionnaire respondents, and Figure 5 shows the results of the questionnaire against Earthquake No.2 at the M building.

In this questionnaire survey, since there were few users registered in the system at the time of earthquake occurrence, individual surveys were separately conducted in parallel.

Table 3 Calculated values from the floor response of the M building

(1) Seismic intensity, maximum acceleration and long-period ground motion class

Floor	S.I.*	Scale of S.I.	Max. Acc. (cm/s ²)	Long-period ground motion class
9	5.2	5+	269.9	Rank 1 (14.7cm/s)
B4	4.5	5-	169.8	

※ S.I. : Instrumental seismic intensity

(2) Motion sickness does value

Calculation result floor	Z direction		XYZ direction	
	MSDVz	vomiting ratio	MSDVxyz	vomiting ratio
9F	3.520E-02	0.01%	1.021E-01	0.03%
B4F	3.486E-02	0.01%	8.663E-02	0.03%

Table 4 Distribution of questionnaire respondents in the M building at Earthquake No.2

floor	Male	Female	Each total	
8	2	5	7	upper floor
6	7	3	10	middle floor
5	18	3	21	
4	9	0	9	
3	1	0	1	lower floor
1	2	0	2	
B	2	2	4	
total	41	13	54	

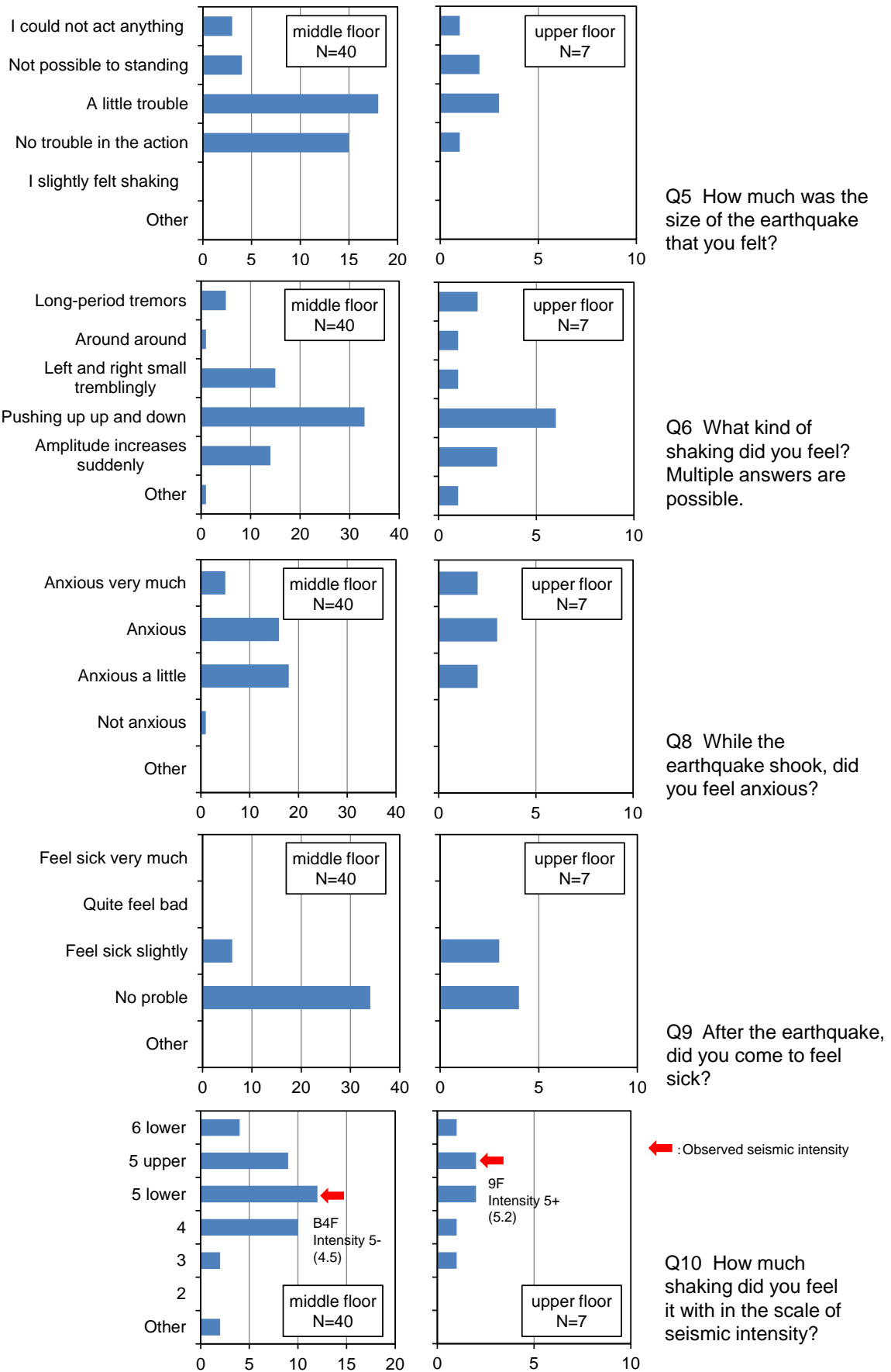


Figure 5 Results of the questionnaire against Earthquake No.2

(3) Consideration on questionnaire results

Quantitative evaluation is difficult because the feeling of fear of the earthquake caused by the earthquake is promoted by the imagination of how the environment it is due to the earthquake. Table 5 shows the results about the sick feeling which was the change in the physiological function against the building shaking. In both buildings, there is a tendency that upper floor people felt sicker than the lower floor people. And especially on the upper floors of UC buildings, there is a tendency that people standing on the upper floor tend to feel worse than those sitting. Although the number of responses was small, the shaking of the building that resonated with the long period ground motion may possibly increase the sensitivity of the standing to the tremor of the person.

Table 5 Answers about the sick feeling

Q9 After the earthquake, did you come to feel sick?

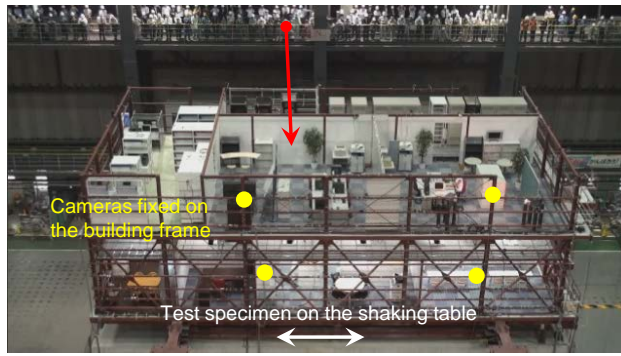
Building	N	Answer					
		no problem	feel sick slightly		Situation who felt sick slightly		
					sitting	standing	
UC building / upper floor	12	9	3	25%	1	2	67%
UC building / lower floor	20	20	0	0%	—	—	—
M building / upper floor	8	5	3	38%	2	1	33%
M building / middle floor	40	34	6	15%	5	1	17%

3. Study on human vibration characteristics by simulation of interior space damages

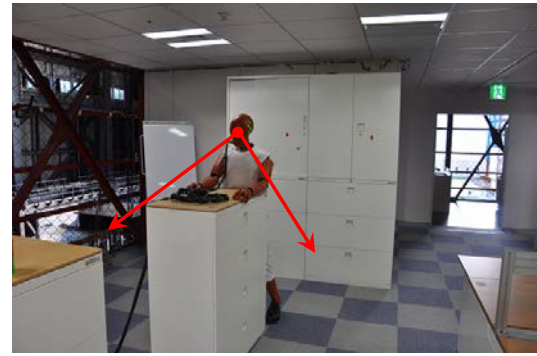
Conventionally, the seismic performance of buildings was generally thought centered on the safety of structures. In addition, since the Great East Japan Earthquake, not only the safety of the structure but also the interest in reducing seismic interior space damages is increasing more. In order to respond to these needs, simulations have been developed to visually understand how the building shakes during an earthquake by visualizing the indoor situation at the time of the earthquake.

Numerous seismic interior space damage simulations using physical engines are performed. Three-dimensional simulation has the advantage of being able to take into account the mutual influence of the furniture group and to visualize the situation at the time of the earthquake by visualization. As a technology to experience earthquake shaking, it is common to require a large-scale experimental facility such as a shaking table, but 3D simulation is possible to feel a fake simulation anywhere in 3D CG video, and as a disaster prevention enlightenment material Use is expected. In recent years, CG video of 3D simulation has advanced to VR, and the realism is increasing more. However, in the VR image, the reproduction of the viewpoint of the person shaking by the earthquake is not considered. In the questionnaire survey results shown in the previous chapter, the possibility that the human's response due to the shake of the building has an influence on the physical condition was shown. Figure 6 shows the pattern of the viewpoint of indoor damage at the time of earthquake, taking video images of shaking table test on E-Defense as an example.

So, in this chapter, we introduce a proposed dynamic human model and reconstruct the viewpoint to examine human's sense of earthquake shaking considering human viewpoint.



Aerial view point image
(Image of the camera shot from the outside of the specimen)



Human head view point image
(Viewpoint of a person standing in the specimen)



Floor fixed view point image
(Images of the cameras fixed on the building frame of the specimen)

Figure 6 Pattern of the viewpoint of indoor damage at the time of earthquake

3.1 Proposed human dynamic model

Yamamoto conducted shaking table tests on human subjects to obtain dynamic response data and produce dynamic human models. The test results showed that under the standing conditions resonant frequencies are around 0.5Hz for lateral reactions, and less than 0.25Hz for front-back reactions. Figure 6 shows the outline of dynamic human model. The model is composed of one mass point pin-supported on the floor and a rotating spring with rotational stiffness (K_R) and rotational damping coefficient (C_R). K_R and C_R are as follows.

$$K_R = \{M \times (0.562H)^2 + 0.0524MH^2\}\omega^2 = 0.368MH^2\omega^2 \quad (3)$$

$$C_R = 2 \times h \times 0.368MH^2\omega = 0.736MH^2h\omega \quad (4)$$

Where H is the height and M is the mass of the whole body, and ω is the natural circular frequency and h is the damping ratio. Here, H = 1.7 m, the natural period in each direction was set to 5 seconds in the front and back direction (Pitch), 2 seconds in the left and right direction (Yaw), and the damping ratio h was 30% in both directions.

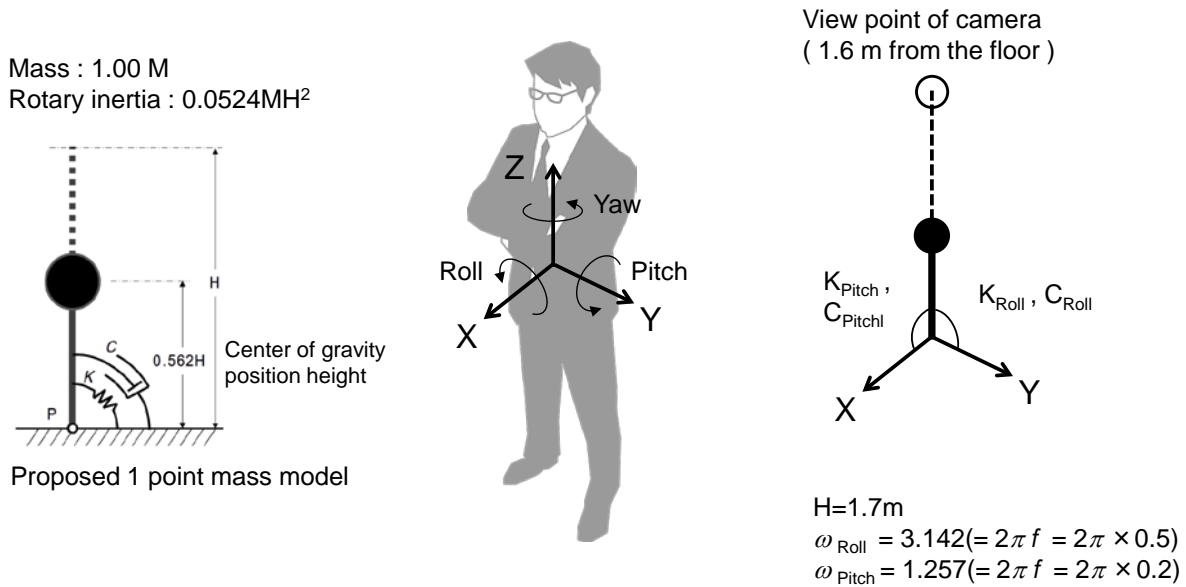


Figure 7 Outline of dynamic human model

3.1 Outline of indoor damage simulation

Yamamoto et al. built an indoor simulation system based on a library called ODE (Open Dynamics Engine) which is an open source rigid body analysis physical engine. They examined the applicability (analysis accuracy, analysis speed) of the simulation system by comparing with the results of past shaking table experiment (Yamamoto et al., 2013). The developed system has been released so that anyone can use it on the web as a tool for understanding the seismic performance of the building in an easy-to-understand manner (Takenaka Corporation, 2014).

Utilizing knowledge on the already constructed system, we used Unity in this study. Unity is a cross-platform game engine developed by Unity Technologies, and it has an advantage that it is easy to extend to VR conversion and human viewpoint. In modeling in Unity's physical engine, we simulated with a pin-supported spring and a damper in two directions at the floor position. We installed a camera restricting rotational displacement at a height of 1.6 m from the floor and reproduced the viewpoint of a human seismic response.

Figure 8 shows the Input floor response acceleration by 1/3 octave band analysis, comparing to overturning limit curve derived from proposed human dynamic model. JMA Kobe is an input motion excited by short-period ground motion components, and NSJ Main (Nishi Shinjyuku observation point, main shock of the Great East Japan Earthquake) is an input motion excited by long-period ground motion components. These input motions were used in the shaking table tests to reproduce the actual large-scale indoor damage done in E-defense (M.Yoshizawa and et al., 2012).

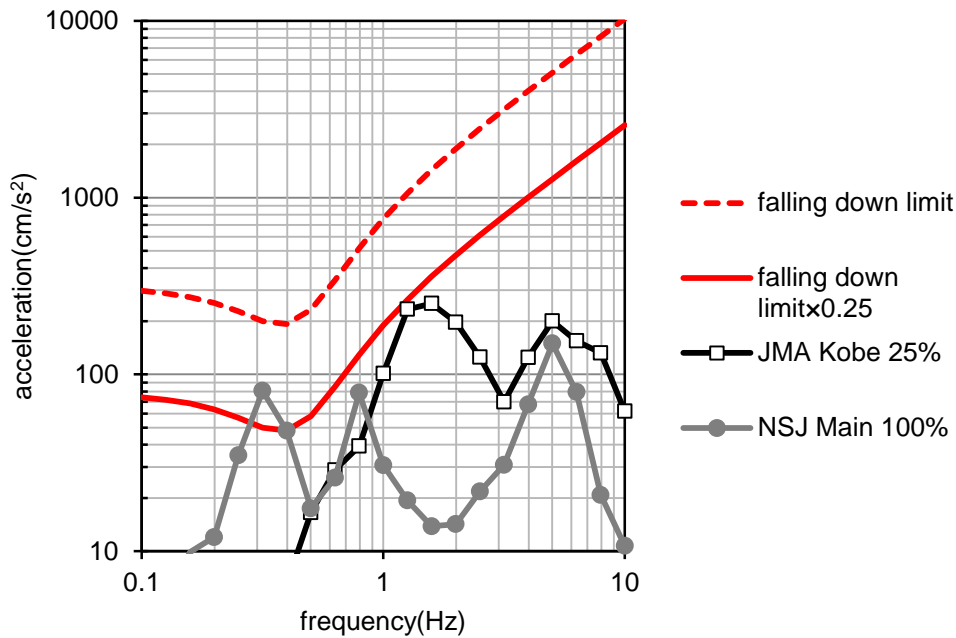


Figure 8 Input floor response acceleration

3.2 Study of human sense to earthquake shaking considering human view point

We made three video images of indoor damage simulation from the following three viewpoints.

- | | |
|------------------------|--|
| Aerial view point | H=1.6m, a point of not moving, not affected at all of the floor response |
| Floor fixed view point | H=1.6m, moving the same as floor response |
| Human head view point | H=1.6m, moving the same as a human being response to the floor response |

Using these three video images, we conducted a hearing survey on subjects for anxiety, ill effect, and possibility to fall. The subjects were not informed of the information on which viewpoint the images were created, then compared three video images and selected the answer choices as shown in Table 6. Finally, the subjects selected most realistic viewpoint among the three video images.

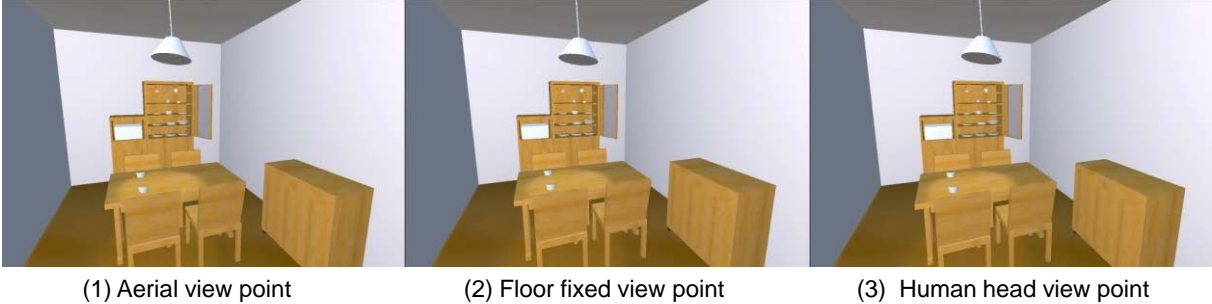
Figure 9 shows the comparison of indoor simulation images due to different viewpoint. In this simulation, no large indoor damage has occurred. In the case of the short-period ground motion, the dish shelves somewhat tilted. And in the case of the long-period ground motion, the furniture situation was almost unchanged.

The subjects were 6 (5 males and 1 female), and the age at hearing was 20 to 50 years. Figure 10 shows the hearing results of anxiety, ill effect and possibility to fall. The values of Figure 10 are the average of the rating scale against each answer choices. As a general trend, the floor fixed viewpoint was hard to feel the earthquake shaking, and the human head viewpoint and the aerial viewpoint were close to each other. This trend seems to be influenced by the fact that the change in indoor situation was small, and the fact that the simulation did not model the one that felt the relative displacement, such as the scenery outside the window. In the case of short period ground motion, there is a tendency that the aerial viewpoint tended to feel that the anxiety and the possibility to fall was higher than the human head viewpoint. In the case of long-period ground motion, the tendency of responses was reversed. But the impression did not differ much.

Figure 11 shows the results of the most realistic viewpoint among the three video images. Regardless of the type of earthquake ground motion, no one chose the result of the floor fixed viewpoint. In the case of the short-period ground motion, the human head viewpoint was the most realistic. And in the case of the long-period ground motion, the aerial viewpoint was the most realistic. Referring to the comments of the hearing results, it is considered that in the case of short- period ground motion, the influence of up-and-down motion might have given different impressions visually.

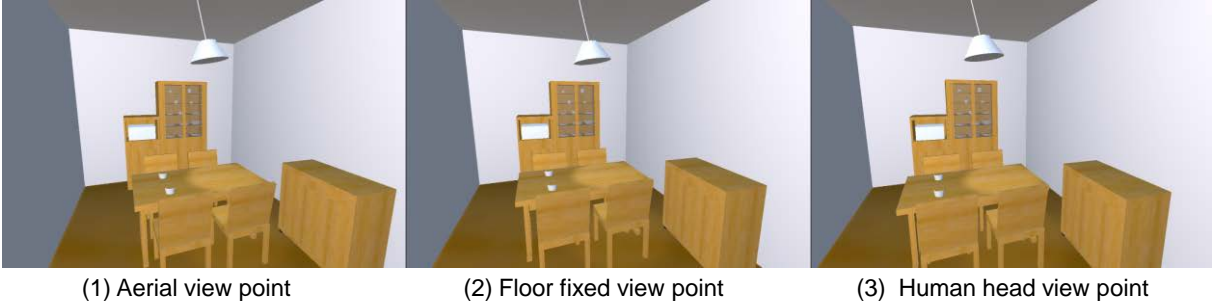
Table 6 Hearing item and answer choices and their rating scale

Hearing item	Answer choices and their rating scale				
	1	2	3	4	5
Anxiety	not anxious at all	not anxious	anxious a little	anxious	anxious very much
ill effect	nothing at all	nothing	slightly feel sick	quite feel sick	feel very sick
possibility to fall	It seems nothing	no trouble in the action	a little trouble in the action	not possible to standing	not act anything



(1) Aerial view point (2) Floor fixed view point (3) Human head view point

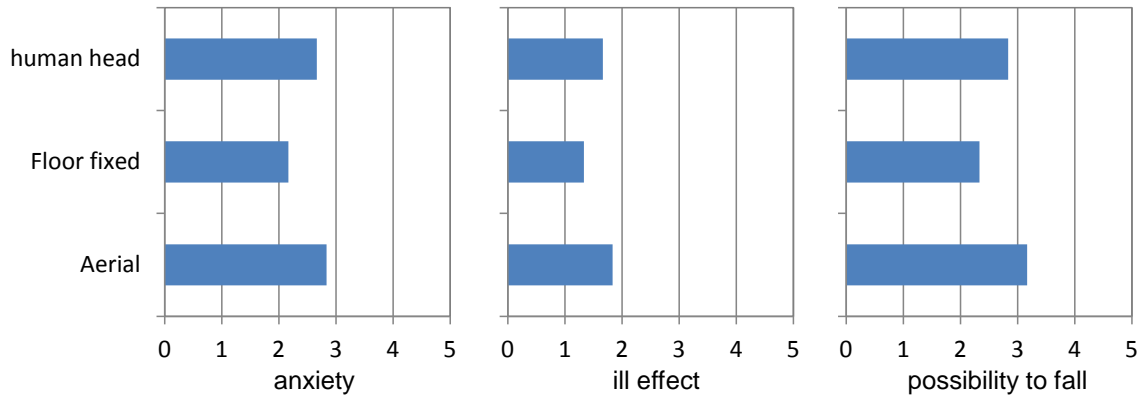
(a) JMA Kobe 25% (short period ground motion)



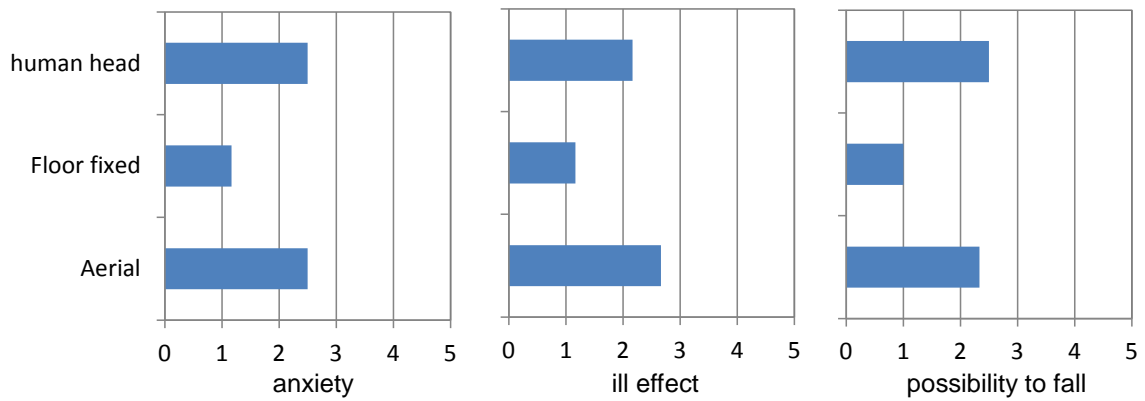
(1) Aerial view point (2) Floor fixed view point (3) Human head view point

(b) NSJ Main 100% (long period ground motion)

Figure 9 Comparison of indoor simulation due to different viewpoint



(a) JMA Kobe 25% (short period ground motion)



(b) NSJ Main 100% (long period ground motion)

Figure 10 Hearing results of anxiety, ill effect and possibility to fall

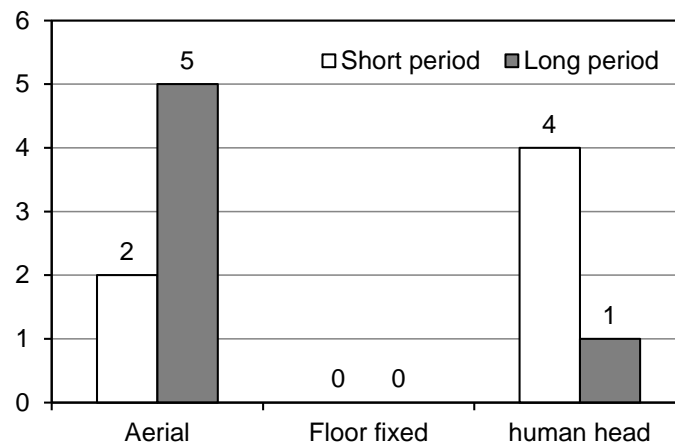


Figure 11 Hearing results of most realistic viewpoint

5. Conclusions

In order to model the effect of building shaking caused by earthquakes on human body, we continue the survey of the quasi-real-time questionnaire system for shaking of buildings caused by earthquakes. The developed system has been operated about 3 years, and the questionnaires for relatively large

earthquakes have also been obtained. These results pointed out that there is a possibility that the influence of the posture of a person at the time of shaking may be great. Therefore, we investigated the influence of considering human viewpoint on the simulation of indoor damage at the time of earthquake caused by physical engine, which is often done in recent years. In this case study, because of the limitations on the model used in modeling the human head viewpoint, we did not study with a big earthquake shake. So, we will proceed experimentally verifying the falling limit of the human vibration model, and would like to build a more realistic indoor damage simulation method at the time of earthquakes. Then we would like to present the building seismic performance considering the human loss estimation, and also consider more effective disaster prevention support system when the big earthquake actually occurs.

6. References

- [1] M. Honma, N. Endo, Y. Osada, Y. Kim and K. Kuriyama(2012). Disturbances in equilibrium function after major earthquake, *Scientific Reports* 2:749, pp1-8
- [2] Seismology and Volcanology Department, Japan Meteorological Agency (2012). Report of a way of information about long-period ground motion (in Japanese),
<http://www.jma.go.jp/jma/press/1204/26a/siryou.pdf>
- [3] M.Yoshizawa and M.Yamamoto(2015). Development of questionnaire system for shaking of buildings caused by earthquakes, *Proceedings of the 23rd Japan Conference of Human response to vibration*, Kinki University, Hiroshima, Japan, August 24 -26, 2015.
- [4] M.Yamamoto(2011). Human Body Dynamics under Horizontal Ground Motions: Shaking-Table Tests and Simplified Modeling under Standing Conditions, *J. Struct. Constr. Eng., AIJ*, Vol. 76 No. 667, 1631-1637, Sep., 2011
- [5] K. Tamura, M. Kaneko, H. Kitamura and T. Saito(2012). A Questionnaire on Seismic Indoor Damage and Occupant's Behavior of Tall Residential Buildings in Tokyo, *AIJ J. Technol. Des.* Vol.18, No.39, pp.453-458, Jun., 2012
- [6] International Organization for Standardization (1997). Mechanical vibration and shock - Evaluation of human exposure to whole-body vibration -. International Standard, ISO 2631-1.
- [7] Kouhei M. and Kousuke O.(2005). Study on Method of Measurement and Analysis for Motion Sickness Evaluation, *JSME annual meeting*, 239-240.(in Japanese)
- [8] M.Yoshizawa, T.Nagae, K. Kajiwara, (2012). A study on human body sensitivity for building response subjected to long-period ground motions, *Proceedings of the 20th Japan Conference of Human response to vibration*, Kinki University, Osaka, Japan, September 4 - 6, 2012.
- [9] M.Yamamoto, H.Hamaguchi, M.Higashino(2012). A proposal of an index to evaluate human sense utilizing an analytical model of human body dynamics.
- [10] M.Yamamoto, H.Yoneda, H.Hamaguchi(2013). A study on the situation of furniture in a room during earthquakes Part 1 : 3D simulation by using a physics engine,
- [11]Open Dynamics Engine. <http://www.ode.org/>
- [12]Takenaka Corporation(2014). TAFT® Takenaka Furniture Teller, <http://www.taft.takenaka.co.jp/taft>
- [13] Unity web page. <https://unity3d.com/>

The 26th Japan Conference on Human Response to Vibration (JCHRV2018)

Kindai University, Osaka, Japan

August 22-24, 2018

**New Strategies to Prevent Hand-Arm Vibration Syndrome with
Work Practice Management****Kazuhisa Miyashita* [1, 2], Shigeki Takemura [2]**

[1] President, Wakayama Medical University

[2] Department of Hygiene, School of Medicine, Wakayama Medical University
811-1, Kimiidera, Wakayama City, Wakayama Prefecture, 641-8509, JAPAN

(* miyaka@wakayama-med.ac.jp)

Abstract

While governments require employers to regulate hand-arm vibration exposure among workers operating vibrating tools, it is not clear how to assess the vibration magnitude at the worksite workers are exposed to. To monitor occupational hand-arm vibration exposure, we developed a simple assessment system. In this system, the vibration magnitude of tools is measured at the worksite, the magnitude is sent to the server with a personal device, and then the allowable operating time is reported to the worker at the worksite from the server. Measured vibration magnitude data are stored on the server and available at the base station. This system was tested at the forestry worksite in the mountain and worked successfully, which will help improve work practice management by monitoring and reducing the hand-arm vibration exposure.

1. Introduction

According to the national statistics on occupational compensation regarding hand-arm vibration exposure, the number of cases due to hand-arm vibration syndrome (HAVS) has decreased year by year, but is ceasing to fall in recent years [1]. This shows the countermeasures against HAVS are not sufficient, that is, work practice management should be improved. A new guideline was dispatched from the Ministry of Health, Labour and Welfare of Japan on July 10, 2009 [2-4]. This guideline is based on ISO (the International Organization for Standardization) or EU (the European Union) standards, in which the work practice management of operating vibrating tools should be regulated based on the vibration magnitude and the operating time of the tool. In details, the EU Directive 2002/44/EC of the Physical Agent Directive (Vibration) [5] demands that employers should take the following measures to prevent HAVS among their employees: ① choose appropriate working equipment producing the least possible vibration, ② assess probable magnitude of the vibration, based on the daily exposure magnitude normalized to an eight-hour reference period A(8) [6], and ③ if possible, measure the magnitude of mechanical vibration to which workers are exposed at the worksite, to assess whether the health and safety of each worker is ensured. Among them, ① and ② are demanded by the above-mentioned guideline of the Ministry of Health, Labour and Welfare of Japan on July 10, 2009. However, ③ has not been introduced to this guideline at this moment.

In Japan, it is required that employers appoint vibrating tool managers to measure and assess the vibration magnitude of the tools at the worksite every day. As existing devices for vibration measurement are complex and expensive and require highly skilled operators, a simple measurement device is needed. Then an inexpensive and easy-to-operate measurement device has been developed by Mae et al [3]. This developed device was designed for use by vibrating tool managers [4] to assess the vibration condition of tools before and after work at the worksite. In practice, they need to measure the vibration magnitude of each worker's tool used at the worksite. However, at the worksite where workers are located in different places separate to one another, it is unfeasible for a single tool manager to go around all these places and measure the vibration magnitude of each worker's tool even with the above-mentioned measurement device [3]. It is desirable to have a system with which workers self-measure the vibration magnitude of their own tools at the worksite and self-monitor their own daily allowable operating time.

Under these circumstances, we tried to develop an assessment system on hand-arm vibration exposure at the worksite. The purpose of this study is to develop a new assessment system to monitor the vibration magnitude of each worker at the worksite to meet the demand of the EU Directive 2002.

2. Development of assessment system on hand-arm vibration exposure at the worksite

We propose an assessment system on hand-arm vibration exposure at the worksite as shown in Figure 1.

For developing the system in Figure 1, research and development was carried out under the four following steps (Figure 2).

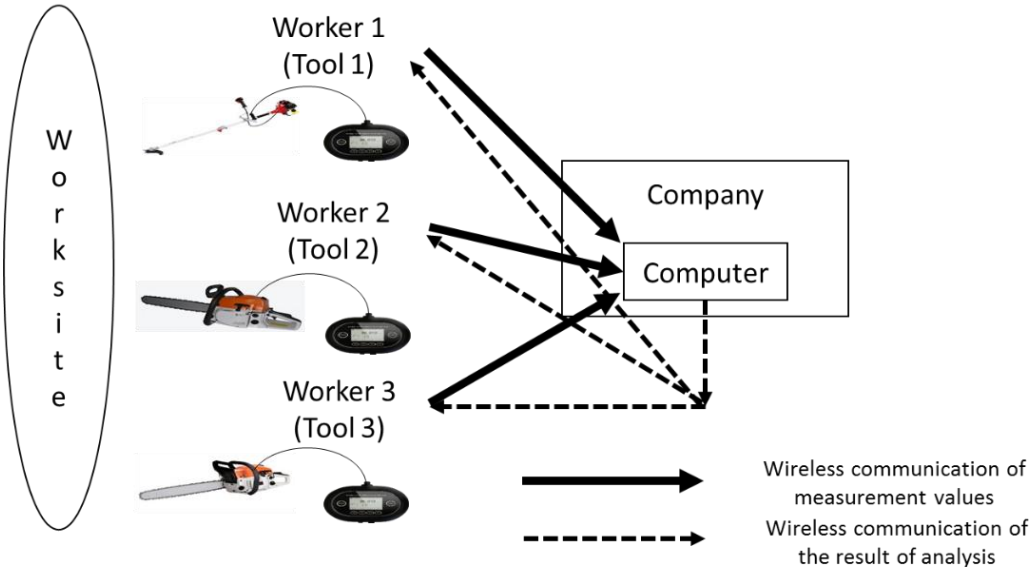


Figure 1 – Assessment system on hand-arm vibration exposure at the worksite

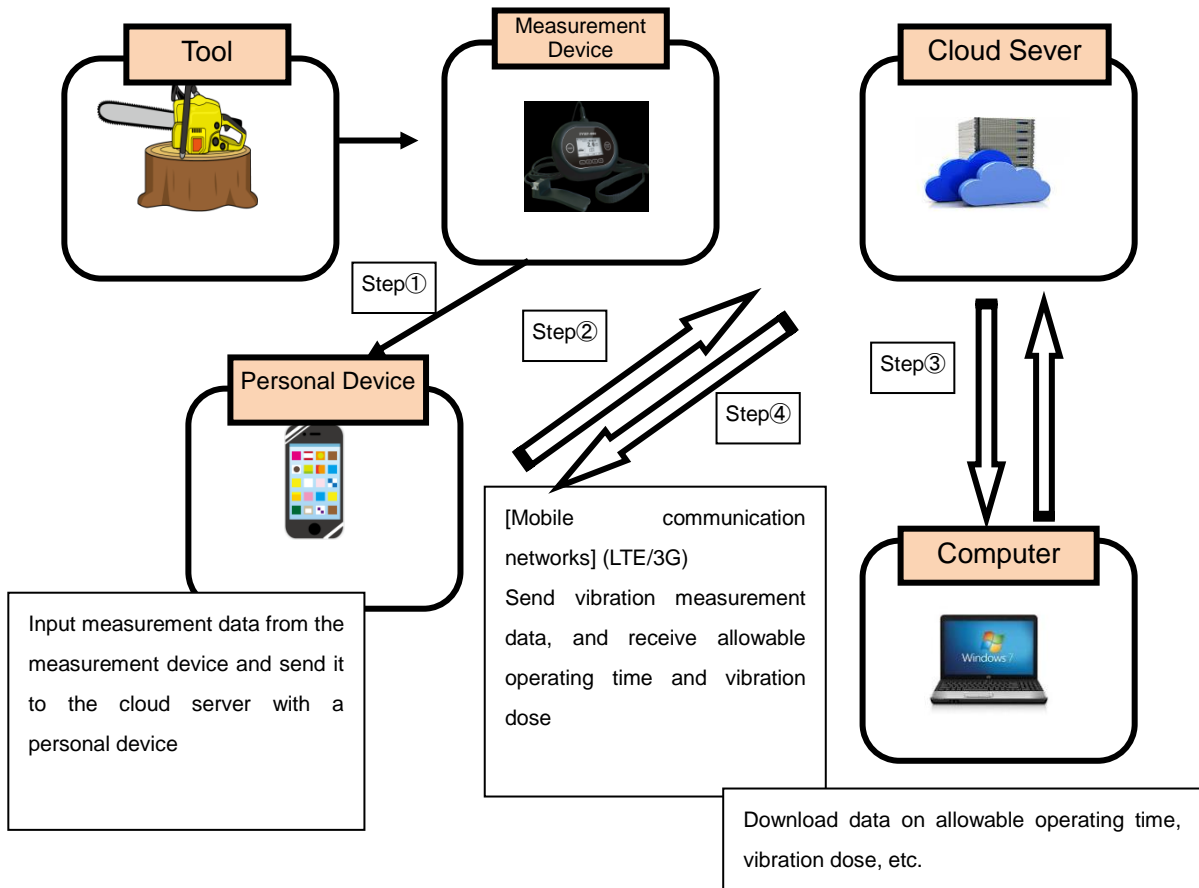


Figure 2 – Assessment system on hand-arm vibration exposure developed under four steps

- Step ①. Developing and improving a simplified measurement device with which operators of vibrating tools can measure vibration magnitudes easily by themselves.
- Step ②. Building a cloud server system which enables operators of vibrating tools to send vibration magnitude data obtained from the vibration tool and receive a data receipt report with their personal device (feature phone or smartphone) (Figure 3).

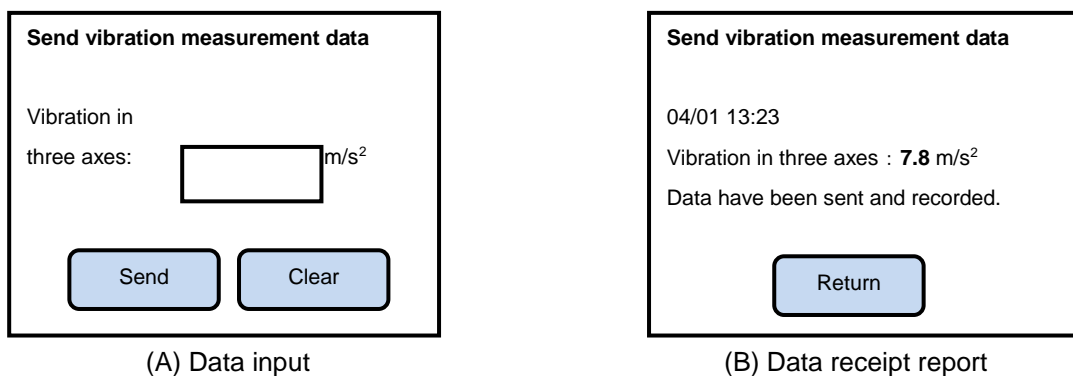


Figure 3 – An example of the screen to send vibration measurement data

Step ③. Designing a user interface and developing software for the personal device to send the measured data easily from the personal device (feature phone or smartphone) through the above-mentioned cloud server system.

Step ④. Designing a user interface and developing software for the personal device to calculate allowable operating time by using the measured value of the vibrating tool received from the personal device, and then transfer the calculation result back to the personal device (these data are available in a laptop computer located at the base station connected to the above-mentioned system).

Through these steps, this assessment system gives each operator their allowable operating time at the worksite (Figure 4). This system also provides the cumulative vibration dose for a certain period of each worker (Figure 5).

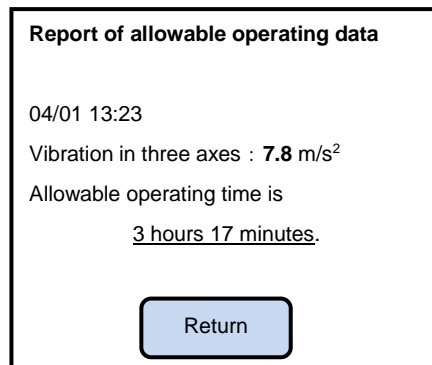


Figure 4 – An example of the screen of allowable operating time report

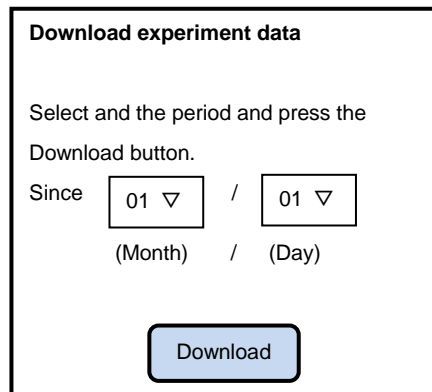


Figure 5 – An example of the screen to download data for a certain period

Daily vibration exposure value $A(8)$ is calculated as follows:

$$A(8) = a \times \sqrt{\frac{T}{8}} [m/s^2]$$

where $a [m/s^2]$ is the vibration total value of frequency-weighted root mean square (r.m.s.) acceleration; and $T [hours]$ is the daily vibration exposure time.

If a worker operates more than one vibrating tool on the same day, the vibration total value $a_{hv(rms)}$ is calculated as follows, considering the frequency-weighted r.m.s. acceleration from each tool and its operating time:

$$a_{hv(rms)} = \sqrt{\sum_{i=1}^n (a_{hv(rms)i}^2 T_i)} \text{ [m/s}^2\text{]}$$

and then the daily vibration exposure $A(8)$ is calculated as follows:

$$A(8) = a_{hv(rms)} \times \sqrt{\frac{T_v}{8}} \text{ [m/s}^2\text{]}$$

where $a_{hv(rms)i}$ [m/s²] is the vibration total value of frequency-weighted r.m.s. acceleration of vibrating tool no. i ; T_i [hours] is the operating time (vibration exposure time) of vibrating tool no. i ; n is the number of vibrating tools; and T_v [hours] is the total operating time (total vibration exposure time from all vibrating tools operated).

A nomogram [7] and a Microsoft Excel spreadsheet file [8] to calculate $A(8)$ are available online.

If $A(8)$ exceeds 5.0 [m/s²] (above the exposure limit value), employers need to reduce vibration exposure time and choose tools with lower vibration values. If $A(8)$ exceeds 2.5 [m/s²] but does not exceed 5.0 [m/s²] (above the exposure action value, but not above the exposure limit value), they need to make their efforts to reduce vibration exposure time and choose tools with lower vibration values. If $A(8)$ does not exceed 2.5 [m/s²] (the exposure action value), they do not need to take further countermeasures.

If vibration exposure time exceeds 2 hours assuming that $A(8)$ is set at 5.0 [m/s²], employers need to reduce the time to 2 hours daily. If vibrating tools are maintained according to manufacturers' or importers' instructions, their vibration magnitudes are measured and calculated before and after the maintenance, and operated within the maximal limit of allowable operating time corresponding their vibration magnitudes, this 2-hour restriction does not apply (nevertheless, it is recommended to reduce the operating time to 4 hours daily). If vibration magnitudes are not available, apply the vibration magnitude of similar tools instead to calculate the maximal limit of allowable operating time. If the maximal limit exceeds 2 hours daily, they need to reduce the operating time to 2 hours daily, hopefully as short as possible.

3. Testing the assessment system in the worksite

This system was tested in two different sites in the mountain (Figure 6), where forestry workers operating their vibrating tools are dispatched to different logging sites separate to one another.

Vibration magnitudes were measured in the handle of the chainsaw at the logging site (two units of Shindaiwa E1480S, Yamabiko Corporation, Oume City, Tokyo, Japan) and in the handle of the bush clearer on the logging road (one unit of Shindaiwa 234 and one unit of Shindaiwa 250, Yamabiko Corporation). They were 6.5 m/s² in Shindaiwa E1480S, 3.1 m/s² in Shindaiwa 234 and 3.8 m/s² in Shindaiwa 250. Measured values were successfully transmitted via mobile communication networks, and allowable operating time was obtained in the worksite from the server. These data were available

in a laptop computer located at forestry workers' office connected to the above-mentioned system.

Assuming $A(8)$ was set at 5.0 m/s^2 , the daily allowable operating time in was 4.73 hours in Shindaiwa E1480S, 20.81 hours in Shindaiwa 234 and 13.85 hours in Shindaiwa 250. These vibrating tools cleared the recommendation to reduce the operating time to 4 hours daily under measurement of vibration magnitudes.

In our study, three out of four industrial vibrating tool operators engaged mainly in forestry reported their daily operating time was 4.0 hours or longer [9]. These workers may benefit from work practice management by monitoring and reducing their $A(8)$.



(A) Tree felling at the logging site



(B) Bush clearing on the logging road

Figure 6 – Testing the assessment system in the worksite

In these pictures, the measurement device for hand-arm vibration was operated by an operator behind the forestry worker in tree felling or bush clearing. This device was designed so simple that these forestry workers could operate it alone while operating their vibrating tools.

Recently, Maeda et al. have been developing a wearable personal vibration exposure monitor measuring each worker's exposure to hand-arm vibration in the wrist continuously, calculating the cumulative vibration dose in a working day from the vibration level in the wrist and its duration, and showing how long the worker is allowed to operate vibrating tools in that day [10].

4. Conclusions

In this study, a new assessment system to monitor the vibration magnitude of each worker at the worksite has been developed. Its effectiveness was confirmed in the real worksite.

5. Acknowledgements

This study was supported by Japan Society for the Promotion of Science Grant-in-Aid for Scientific Research (C) [JSPS KAKENHI] (Grant Number 26460808).

6. References

[1] Miyashita K, Maeda S, Takemura S, Tsuno K, Yoshimasu K (2014) Recent international trends in researches on hand-arm vibration syndrome. *Occupational Health Review*, 27(3), 189-218 (in Japanese).

- [2] Maeda S (2013) Development status of equipment for vibrating tool managers. *Industrial Safety & Health*, 64(3): 270-272 (in Japanese).
- [3] Mae T, Fujimoto K, Yoshida S, Shimizu K, Miyashita K, Maeda S (2012) Development of hand-arm vibration measurement device. *Proceedings of the 20th Japan Conference on Human Response to Vibration (JCHRV2012)*; 4-6 September 2012; Osaka, Japan, p. 30-37.
- [4] Mae T, Yoshida S, Shimizu K, Miyashita K, Maeda S (2013) Development of hand-arm vibration measurement device. *Proceedings of the 21th Japan Conference on Human Response to Vibration (JCHRV2013)*; 27-29 August 2013; Tokyo, Japan, p. 30-37.
- [5] European Commission (2002) Directive 2002/44/EC of the European Parliament and of the Council of 25 June 2002 on the minimum health and safety requirements regarding the exposure of workers to the risks arising from physical agents (vibration) (sixteenth individual Directive within the meaning of Article 16(1) of Directive 89/391/EEC). *Official Journal of the European Communities*. 2002 July 6; L 177/13.
- [6] International Organization of Standardization (2001) Mechanical vibration — Measurement and evaluation of human exposure to hand-transmitted vibration — Part 1: General requirements. *International Standard, ISO 5349-1:2001*.
- [7] The Ministry of Health, Labour and Welfare, Prefectural Labour Bureaus, and Labour Standards Inspection Offices of Japan. For prevention of hand-arm vibration syndrome: an overview of new countermeasures to prevent hand-arm vibration syndrome. The Ministry.
URL: <https://www.mhlw.go.jp/file/06-Seisakujouhou-11200000-Roudoukijunkyouku/0000180362.pdf> (Browsed on July 18, 2018.) (In Japanese.)
- [8] Japan Advanced Information Center of Safety and Health (JAISH). Calculation table for A(8). JAISH.
URL: http://www.jaish.gr.jp/information/mhlw/nichishindo_bakuroryo.xls (Browsed on July 18, 2018.) (In Japanese.)
- [9] Takemura S, Yoshimasu K, Tsuno K, Fukumoto J, Kuroda M, Miyashita K (2016) Association between anthropometric factors and peripheral neuropathy defined by vibrotactile perception threshold among industrial vibrating tool operators in Japan. *J Occup Health*, 58(2), 145-154.
- [10] Maeda S, McLaughlin J, Anderson L, Buckingham M-P (2017) Necessity of wearable personal vibration exposure meters for preventing hand-arm vibration syndrome. *Proceedings of the 25th Japan Conference on Human Response to Vibration (JCHRV2017)*; 13-15 September 2017; Tokyo, Japan, p. 45-58.

The 26th Japan Conference on Human Response to Vibration (JCHRV2018)

Kindai University, Osaka, Japan August 22-24, 2018

Shock and Vibration Issues in Professional Sports

Thomas Jetzer MD MPH FACOEM

Occupational Medicine Consultants

Minnesota Twins

Douglas Reynolds Ph. D.

Department of Sound and Vibration

University of Nevada, Las Vegas

Introduction

While shock and vibration has long been recognized as a workplace hazard, ergonomic intervention over the years has made significant strides in ameliorating these issues in many jobs. However more recently, the effects of shock and vibration has become to be appreciated as a significant risk factor in various professional sports including soccer, football, baseball as well as other sports activities. This is led to the appreciation of resulting pathology to the head, whole body and extremities depending on the insult. The implication of this has included significant disability, impairment of function and careers, financial cost and post career disease including even death. While the major attention has been focused on professional sports, similar injury and impairment has also been identified in the amateur arena of the same sports. It is recommended, that like the endeavors to control whole body and hand-arm vibration in the workplace by the scientific community, that a similar multidisciplinary endeavor be instituted to address and resolve this risk.

Methods

Analysis of injuries in contact sports such as football and hockey indicate significant incident of head trauma leading to concussions, brain trauma and long-term brain damage. Analysis of hand intensive supports such as baseball and other ball related sports leads to shock damage to hands and as well as causing other upper extremity pathology. Sports that require prolonged gripping vibration such as mountain biking can lead the same pathological medical conditions seen in industries that have vibration exposure. Exploration of these sports indicate that the incidence and severity of these conditions may be increasing. Attempts to remedy these issues have often been hindered by sport rules, technological limitations and reluctance of players to accept uncomfortable or unfashionable solutions.

Review the literature indicates that specific sports events are more prone to the effects of shock and vibration and others. In particular, of current interest is the game of American football. The diagnosis of chronic encephalopathy brain injury, otherwise known as CTE, has exploded into a disastrous epidemic of pathology in many of the individuals who have played the game of football. The pathogenesis of this is the repetitive shocks to the head that occurs despite the use of helmets. The mechanism this injury is suspected to be repetitive inflammation in the brain. Concussions are still common, despite the use of helmets, the nature of the game causes repetitive shocks that occur with every play with the crashing of two lines of players together that also can contribute to the progressive chronic inflammation of the brain.

Recent studies have shown that there is new understanding of the immune systems effect on the brain which has the ability to have inherent adaptive immunity for trauma, whose mechanism is one of inflammation is one of his main mechanisms of dealing with trauma the brain.¹ While some temporary injuries or one-time injuries can often be cleared by the now discovered lymphatic drainage of the brain, repetitive shocks leave the factors such as cytokines perpetuated chronic inflammation in the brain itself. Current helmet design is primarily focused on preventing skull fractures and is not necessarily designed to prevent the repetitive or one-time shocks that are transmitted to the brain from blows that may not result in any skull trauma. Both these repetitive shocks and concussions are responsible for chronic brain inflammation. Effects of chronic CTE include early dementia, abnormal behavior, cognitive impairment and often early death. The effects on the brain as noted both an autopsy and MRI scanning can be seen in image 1. Results of this epidemic is resulted in billion-dollar lawsuits by the players, the marked diminution in the number of individuals who want to participate in the sport at both amateur and professional levels. It is not uncommon to hear that many families do not want their child to participate in the sport anymore for the fear of these type of injuries that occur even in the high school or college level. An example of type of injuries that occur typically is seen in images 2 and 3. The number of claims in football has reached class-action status with hundreds of claims ranging into the billions of dollars of liability is now served to extend into the amateur level.

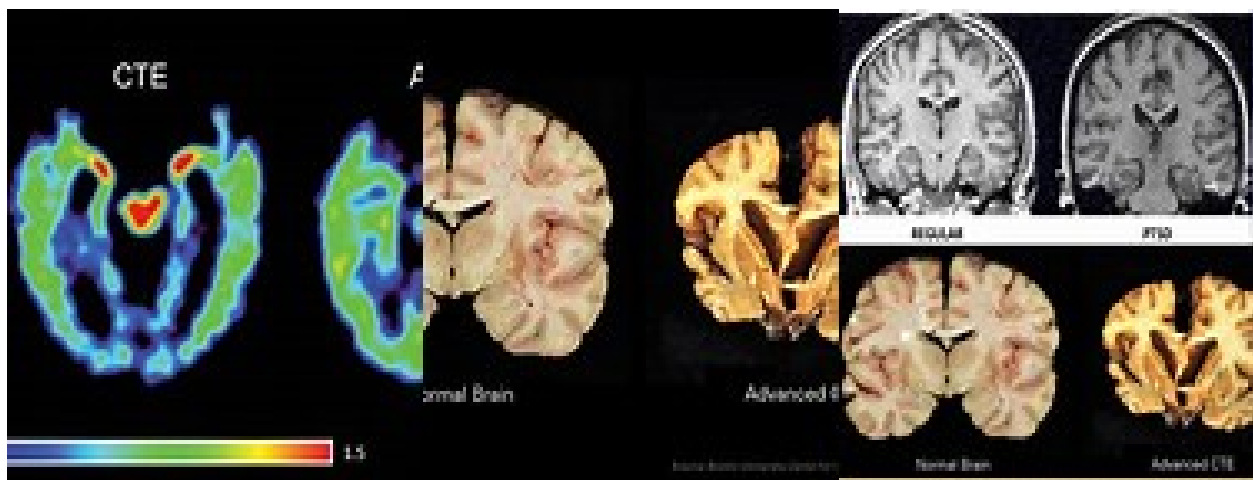


Image 1



Image 2



Image 3

A similar but somewhat more brutal game without as much protection is rugby, where no helmets for the most part is worn. The brutality of the sport as well as the mediocre attempt at protection is illustrated in images 4 and 5. Another high-risk sport is ice hockey, which is essentially another field sport played on slippery ice. Head trauma from concussions is also supplemented in the sport by falls on the ice, crashes into the walls, and fistfights. While heavy protective gear is provided, including helmets with

protection from being hit by in the puck, insufficient protection from concussion and chronic brain inflammation is not necessarily provided in this sport as well.



Image 4



Image 5

Baseball has been played for over 100 years and is not immune from this issue as well. Although less common than other sports, head trauma can occur from collisions with players, against outfield walls and simply being hit by the baseball. The batter, pitcher or umpire could easily be hit by baseball traveling at hundred miles an hour with only a hard-plastic helmet for the batter with no significant

protection for the pitcher or the umpire. Attempts to provide protection has been rudimentary with no significant improvement in batter helmets and only rigid improvement in the soft caps on the pictures. Unfortunately, due to the comfort and cosmetic factors even these improvements are rarely used by the players. Players can also be subject to hands and upper extremity trauma from batting in the shock involved of hitting a baseball. It is not uncommon to see wrist injuries to occur such as hook of the hamate fractures, navicular pathology, wrist tendinitis, and elbow inflammation despite the use of batting gloves with minimal vibration protection. It is interesting to note that the people with the greatest protection from trauma are the fans sitting behind home plate area where screens are provided and recently extended to prevent trauma from the baseball itself no.

Other sports that include shock and vibration trauma to the upper extremities include mountain biking tennis is that, tennis and even golf. Not only can vibration associated with the sports that injury but may impede competitiveness by inducing early fatigue in the upper extremities.

One must consider the risk factors in both collegiate and amateur sports as well. The estimated concussion rate is actually higher in high school athletics it an 8.9% overall versus 5.8% in collegiate sports of all types. 2011 to 12 season statistics indicate there were 1485 concussions in 1410 athletes in collegiate level. At the amateur level, in high school level 30 to 46% of adolescents participate in some sports at risk with 7 million students in high school sports. Some of this population stay active throughout their life at a decreasing rate. It is indicated that sports injuries in the amateur group represent 25% of all injuries presenting to emergency rooms and 8% of these are concussions. The United States Center for Disease Control estimates that 20% of the annual 1.7 million concussions are related to sports. Overall statistics show that the CI risk factors for the following sports are: rugby 4.28, hockey 1.2, American football .53 and overall amateur sports it .23.²

While war is not a sport, head trauma has become even more common in the military and various operations where IEDs and subsequent concussion traumas have become just as common as trauma from bullets and other projectiles. It is being noted that the blast shock waves can cause brain trauma even without direct contact that can result in chronic headaches, vertigo, cognitive deficits and possible increased incidence of CTE as this population ages. Is also been speculated that this can contributes to the perpetuation of PTSD and impairs soldier recovery possibly related complications in the brain structure itself. The US government presently spends \$60 billion per year in veteran disability benefits with a substantial proportion being for brain related trauma.

Research in this area is a difficult the past due to lack of biological markers, adequate imaging and the difficulty of doing control studies. Whatever newer imaging studies capabilities, chemical valuation for brain markers and neurological and cognitive testing modalities should allow for better assessments of both the nature of these injuries and the effects of various intervention modalities, particularly for studying the brain. The techniques for assessing upper extremity problems has well been established by the methods used for controlling vibration shock induced trauma to the upper extremity in industry and simply needs to be employed in the sports venue. Redressing the current standards for helmets and

other protective gear need to be addressed as well as establishing or modifying standards that may exist that affect the sports equipment. Lastly some modifications the game mechanics and rules has already started in may need to be further addressed in the future as well.

Results

While there have been considerable investigations to define the level of pathology as result of these shock and vibration hazards in sports, no definitive solution has been found for all or individual supports. Efforts from a combination of engineering, medical and ergonomic resources need to be marshalled to find acceptable solutions. If these solutions are not found, one can only expect an ongoing list of injured athletes, legal and financial challenges and possible threat to the nature of the sport themselves. It is recommended that the expertise that applied to dealing to shock and vibration in the industrial setting now be also directed to the sports venue.

1. Kipnis, Jonathan, Multifaceted Interactions between Adaptive Immunity and the Central Nervous System, Science, Vol 353, 766-771 August 2016
2. Center for Disease Control, Atlanta, Georgia

The 26th Japan Conference on Human Response to Vibration (JCHRV2018)

Kindai University, Osaka, Japan

August 22-24, 2018

**Vibration Isolation performance of Glove under Tri-axial Hand-arm
Vibration****Nobuyuki Shibata**National Institute of Occupational Safety and Health
Nagao 6-21-1, Tama-ku, Kawasaki, 2148585, Japan**Abstract**

Vibration-reducing (VR) glove is one of the effective personal protective equipment (PPE) that has been often used in real workplaces to reduce vibration transmitted from hand-held power tools to the hand. Although the test protocol of vibration attenuation performance of VR gloves has been specified in ISO 10819 (2013), vibration-isolating performance of VR gloves for real tool vibration is not clear for power tool operators in real workplaces. Although the evaluation method of glove performance specified in ISO 10819 (2013) intend to measure single-axis vibration, vibration transmitted through real hand-held power tools to the hand is tri-axial. In this study, the vibration-isolating performance of VR gloves was measured along three orthogonal axes to elucidate the vibration attenuation characteristics of VR gloves for real tri-axial tool vibrations.

1. Introduction

Vibration-reducing (VR) gloves have been widely used to reduce vibration transmitted from hand-held power tools to the hand. Although the measurement and evaluation method of vibration attenuation performance of gloves has been specified in the international standard ISO 10819 (2013) [1], vibration-isolating performance of VR gloves for real tool vibration is not clear for power tool operators in real workplaces. This is because the evaluation method of glove performance specified in ISO 10819 (2013) cannot be easily introduced into real workplace evaluation of human exposure to hand-arm vibration (HAV) specified in ISO 5349-1 (2001) [2].

The current standard specifies only one-axis vibration measurement perpendicular to the glove palm surface. However, vibration transmitted in real workplaces from hand-held tools to the hand is 3D vibration. As vibration attenuation materials used in VR gloves are polymer materials, their mechanical characteristics are nonlinear and hyper-elastic. The mechanical characteristics of glove resilient materials under single axis vibration normal to the material surface are different from those under tri-axial vibration. Thus vibration transmissibility of VR gloves has to be examined for 3D vibration in order to evaluate the vibration attenuation performance of VR gloves for real tool vibration.

The aims of this study were to measure the vibration transmissibility of VR gloves in three orthogonal directions and to elucidate the vibration attenuation characteristics of VR gloves for 3D real tool vibrations.

2. Subjects and Methods

2.1 Subjects

The experiments were performed with four healthy male subjects. None of the subjects have been exposed to high levels or long periods of HAV occupationally or in their leisure time activities. The hand sizes of the subjects belonged to the size category of 8 defined in the European Standard of EN 420 [3]. The dominant hand of each subject was the right hand.

The experiments were approved by the Research Ethics Committee of Japan National Institute of Occupational Safety and Health. All the subjects underwent an explanation of the test procedure and gave their written informed consent to participate in this study.

2.2 Experimental apparatus

A tri-axial hand-arm vibration test system was used in this study. Three electro-dynamic shakers were orthogonally oriented to one another on separated stages to realize tri-axial vibration. Each shaker was connected by using a stinger with a rigid frame that supports an experimental handle.

The instrumented handle, cylindrical with a diameter of 40 mm and an effective grip length of 150 mm, was secured to the rigid frame so that the centreline axis of the handle is vertically oriented. This handle consists of the handle base and measuring cap, between which two piezoelectric three-components force sensors (9017B; Kistler Inc., Winterthur, Switzerland) were sandwiched along the handle centreline to measure the grip force of subjects. Signals coming out from these two force sensors were passed through a high-pass filter with a cutting frequency of 0.7 Hz and were then summed up to obtain the total force acting on the measuring cap. Also a tri-axial accelerometer (356A12; PCB Piezotronics, Inc., New York, USA) was secured at the centre of the measuring cap to measure the vibratory acceleration at the handle in the X_h , Y_h , and Z_h direction.

Another tri-axial accelerometer (356A01; PCB Piezotronics, Inc., New York, USA) was embedded in a palm adaptor, which was used to measure the three-dimensional vibration transmitted through glove samples to the palm. The palm adaptor whose dimension was based on the design requirements specified in ISO 10819 (2013) was fabricated with PLA by using a 3D printer. A line marker was drawn at the longitudinal centreline of the palm adaptor.

2.3 Preparation of test signals

Vibration spectra of five different power tools obtained from a previous field study were prepared in this study. The power tools selected in this study were a random sander, a hammer drill, a coil nailer, a tipping hammer, and an impact drill. Magnitudes of frequency-weighted vibration acceleration (r.m.s) components of these five hand-held tools were shown in Table 1. These tool vibration spectra were resampled at 4.096 kHz to obtain tool vibration test spectra. The tool vibration spectra, the duration of which was arranged to 30 seconds, were reproduced in the tri-axial hand-arm vibration test system.

Table 1: Magnitudes of frequency-weighted vibration acceleration (r.m.s) components of hand-held power tools selected in this study. (unit: m/s²)

Hand-held tool	a_{hwx}	a_{hwy}	a_{hwz}	a_{hw}
Random sander	3.76	5.96	4.52	8.37
Hammer drill	9.60	4.05	8.30	13.3
Coil nailer	3.53	2.38	6.12	7.46
Tipping hammer	4.32	15.1	8.60	17.9
Impact drill	2.81	6.45	4.96	8.61

2.4 Procedure of experiments

2.4.1 Glove samples

Three types of VR gloves were prepared in this study. Among these three types, Gloves 1 and 2 were certified as anti-vibration gloves that were satisfied with the ISO 10819 (2013) and JIS T8114 (2007) [4] test requirement. JIS T8114 (2007) is the domestic standard of the anti-vibration test protocol in Japan, which is identical to a previous version of ISO 10819 (1996) [5].

The main characteristics of the glove samples were summarized in Table 2. These glove samples use different types of vibration attenuation material. Each glove sample was slit at the grip-end positions of the palm section to view and adjust the alignment of the adaptor inside the glove.

Table 2: Glove samples used in this study

	Glove 1	Glove 2	Glove 3
Vibration attenuation material	Chloroprene rubber	Synthetic rubber with carbon fibers embedded	Gel foam
Outer surface material	Nitrile rubber	Cow skin	Nitrile rubber
ISO 10819 test requirement	TR _M	OK	OK
	TR _H	OK	OK

* According to the manufacturer's statement, Glove 3 is satisfied with the vibration transmissibility requirement specified in ISO 10819. However the measurement result in author's previous study did not support the statement.

2.4.2 Posture condition

Subject's posture was based on the ISO 10819 (2013) test protocol. Each subject grasped the experimental handle with the adaptor inserted between a test glove and the palm in the dominant hand. Each subject adjusted the palm adaptor with help of the line marker on the adaptor to the appropriate position through the slit on a glove sample.

The subjects were asked to stand upright on the force plate. In grasping the handle, the subjects were

advised to keep the forearm horizontally and to bend their elbows with an angle of 90 ± 15 degrees, not to touch the arm to their body during the measurement. At this posture the subjects were exposed to three dimensional hand-arm vibration. In addition, the subjects were advised to control the gripping and feed forces to 30 ± 5 N and 50 ± 8 N, respectively through a monitor that displays the real-time magnitudes of these forces.

2.4.3 Vibration transmissibility

The vibration transmissibility of the bare adaptor T_b and the vibration transmissibility of glove T_g in each direction are given as follows:

$$T_b = \frac{\sqrt{\sum_i [a_{h(Pb)}(f_i)w(f_i)]^2}}{\sqrt{\sum_i [a_R(f_i)w(f_i)]^2}} \quad (4)$$

$$T_g = \frac{\sqrt{\sum_i [a_{h(Pg)}(f_i)w(f_i)]^2}}{\sqrt{\sum_i [a_R(f_i)w(f_i)]^2}} \quad (5)$$

where $a_R(f_i)$ denotes the unweighted acceleration measured at the handle in the i th $1/3$ octave band, $a_{h(Pb)}(f_i)$ the unweighted acceleration measured on the palm adaptor in the i th $1/3$ octave band, and $a_{h(Pg)}(f_i)$ the unweighted acceleration measured on the palm adaptor of the gloved hand in the i th $1/3$ octave band.

Thus the vibration transmissibility of glove at a certain measurement position along one direction can be calculated using eqs. (4) and (5).

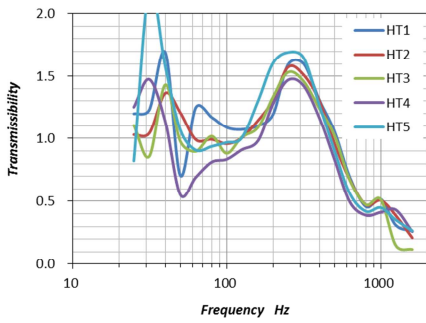
$$TR = \frac{T_g}{T_b} \quad (6)$$

3. Results

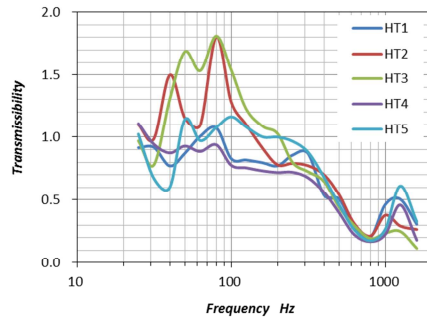
Vibration transmissibility curves of Gloves 1, 2 and 3 for five tool vibration spectra are shown as a function of vibration frequency in Figures 1, 2 and 3, respectively. Vibration transmissibility was affected by tool vibration spectra particularly at frequencies less than 200 Hz in x (vertical) and y (lateral) direction.

In z (fore-aft) direction, vibration transmissibility values due to a few hand tools were more than 1.0 at peaks appearing at frequencies of 30, 100, and 300 Hz. In y (lateral) direction, vibration transmissibility values due to HT2 (hammer drill) and HT3 (coil nailer) overwhelmingly exceeded 1.0 at frequencies ranging from 35 Hz to 160 Hz. In x (vertical) direction, vibration transmissibility values overwhelmingly exceeded 1.0 at peaks appearing at frequencies of 40 and 250 Hz. Vibration transmissibility in z (fore-aft) direction was not affected by differences in tool vibration spectra compared to those in x (vertical) and y (lateral) direction.

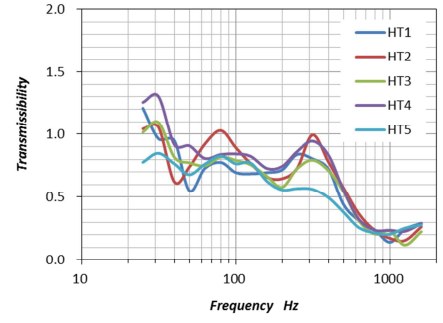
Figure 4 shows vibration transmissibility curves obtained from vibration total values due to five tool vibration spectra. Regardless of glove types, differences in vibration transmissibility values based on vibration total values obtained from different tool vibration spectra were small compared to those in individual component.



(a) x (vertical) direction

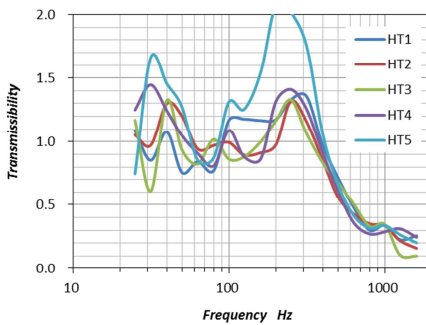


(b) y (lateral) direction

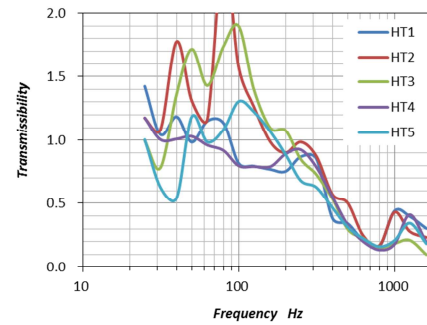


(c) z (fore-aft) direction

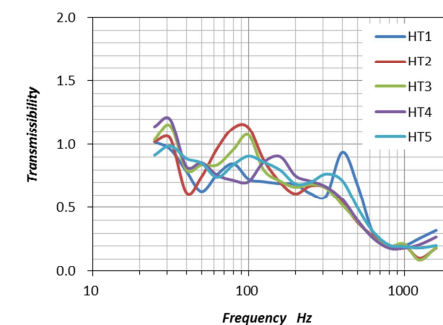
Figure 1 Vibration transmissibility of *Glove 1* measured for five tool vibration spectra. HT1: random sander, HT2: hammer drill, HT3: coil nailer, HT4: tipping hammer, HT4: impact drill.



(a) x (vertical) direction

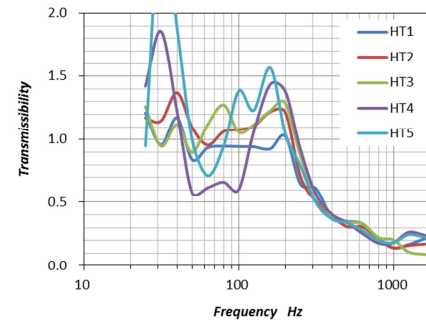


(b) y (lateral) direction

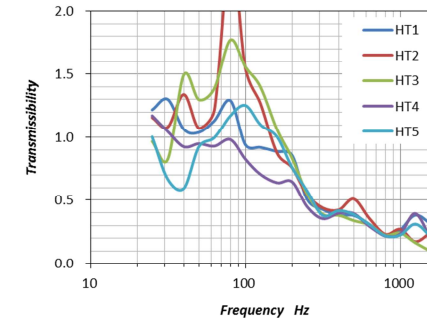


(c) z (fore-aft) direction

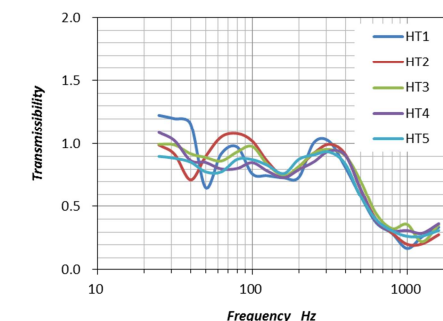
Figure 2 Vibration transmissibility of *Glove 2* measured for five tool vibration spectra. HT1: random sander, HT2: hammer drill, HT3: coil nailer, HT4: tipping hammer, HT4: impact drill.



(a) x (vertical) direction

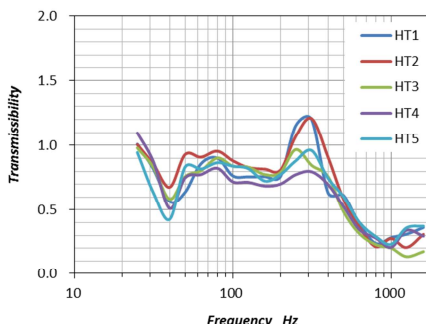


(b) y (lateral) direction

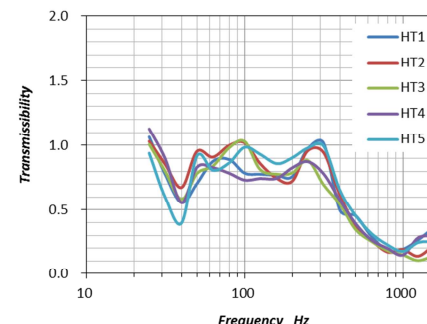


(c) z (fore-aft) direction

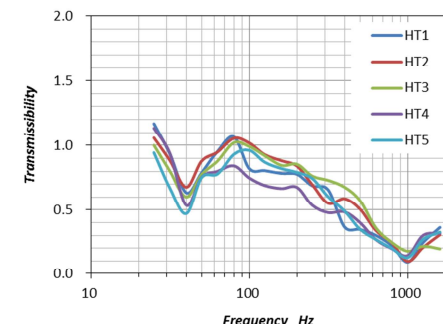
Figure 3 Vibration transmissibility of *Glove 3* measured for five tool vibration spectra. HT1: random sander, HT2: hammer drill, HT3: coil nailer, HT4: tipping hammer, HT4: impact drill.



(a) Glove 1



(b) Glove 2



(c) Glove 3

Figure 4 Vibration transmissibility obtained from vibration total values due to five tool vibration spectra. HT1: random sander, HT2: hammer drill, HT3: coil nailer, HT4: tipping hammer, HT4: impact drill.

Based on the evaluation method of glove vibration transmissibility specified in ISO 10819 (2013), vibration total values were calculated by using eqs.(4)-(6) in three frequency ranges: in the middle frequency range of 25-200 Hz denoted by M, in the high frequency range of 200-1,250 Hz denoted by H, and in the overall frequency range of 25-1,250 Hz denoted by “overall” (see Tables 3, 4, and 5).

Table 3 Vibration transmissibility values at frequency range M (25–200 Hz).

Glove		HT1	HT2	HT3	HT4	HT5
Glove 1	x (vertical)	1.126	1.225	1.054	0.672	1.287
	y (lateral)	0.817	1.371	1.325	0.887	0.837
	z (fore-aft)	0.711	0.832	0.822	0.883	0.741
	total	0.848	1.115	0.949	0.875	0.865
Glove 2	x (vertical)	1.197	1.161	0.960	1.042	1.341
	y (lateral)	0.790	1.637	1.362	0.976	0.824
	z (fore-aft)	0.710	0.898	0.899	0.833	0.857
	total	0.861	1.126	0.981	0.956	0.893
Glove 3	x (vertical)	0.951	1.268	1.139	0.718	1.376
	y (lateral)	0.912	1.464	1.310	0.911	0.826
	z (fore-aft)	0.750	0.890	0.908	0.833	0.870
	total	0.878	1.163	1.015	0.885	0.900

HT1: Random sander, HT2: Hammer drill, HT3: Coil nailer, HT4: Tipping hammer, HT4: Impact drill

Table 4 Vibration transmissibility values at frequency range H (200-1,250 Hz).

		HT1	HT2	HT3	HT4	HT5
Glove 1	x (vertical)	1.590	1.451	1.329	1.123	1.441
	y (lateral)	0.718	0.755	0.684	0.702	0.883
	z (fore-aft)	0.798	0.724	0.609	0.759	0.563
	total	1.239	1.108	0.787	0.789	0.913
Glove 2	x (vertical)	1.336	1.096	1.073	1.044	1.656
	y (lateral)	0.661	0.834	0.683	0.866	0.686
	z (fore-aft)	0.617	0.547	0.536	0.650	0.707
	total	1.048	0.875	0.684	0.867	0.996
Glove 3	x (vertical)	0.609	0.611	0.860	0.827	0.698
	y (lateral)	0.445	0.546	0.504	0.557	0.576
	z (fore-aft)	0.998	0.830	0.786	0.797	0.901
	total	0.692	0.696	0.757	0.647	0.780

HT1: Random sander, HT2: Hammer drill, HT3: Coil nailer, HT4: Tipping hammer, HT4: Impact drill

Table 5 Vibration transmissibility values at overall frequency range (25-1,250 Hz).

		HT1	HT2	HT3	HT4	HT5
Glove 1	x (vertical)	1.281	1.253	1.093	0.698	1.328
	y (lateral)	0.812	1.270	1.167	0.884	0.837
	z (fore-aft)	0.722	0.820	0.788	0.882	0.702
	total	0.902	1.118	0.916	0.873	0.876
Glove 2	x (vertical)	1.241	1.154	0.970	1.034	1.425
	y (lateral)	0.784	1.500	1.195	0.974	0.804
	z (fore-aft)	0.705	0.854	0.838	0.829	0.826
	total	0.885	1.097	0.924	0.953	0.910
Glove 3	x (vertical)	0.862	1.215	1.084	0.711	1.154
	y (lateral)	0.892	1.335	1.144	0.906	0.803
	z (fore-aft)	0.782	0.883	0.886	0.833	0.878
	total	0.862	1.117	0.966	0.881	0.874

HT1: Random sander, HT2: Hammer drill, HT3: Coil nailer, HT4: Tipping hammer, HT5: Impact drill

Vibration transmissibility values at frequency range M and H in z (fore-aft) direction correspond to the vibration transmissibility values specified in ISO 10819 (2013). Almost of the vibration transmissibility values at frequency range M in z (fore-aft) direction were less than 0.9, which satisfied the threshold of vibration transmissibility value at frequency range M specified in ISO 10819 (2013).

In contrast, the vibration transmissibility values of Glove 1 at frequency range H in z (fore-aft) direction except for HT5 were larger than 0.6. For Glove 2, the vibration transmissibility values at frequency range H in z (fore-aft) direction were more than 0.6 for HT1, HT4, and HT5 tool vibration spectra. For Glove 3 all the vibration transmissibility values at frequency range H in z (fore-aft) direction were more than 0.6.

According to the vibration transmissibility values at overall frequency range obtained in this study, only the vibration transmissibility values for HT2 (hammer drill) exceeded 1.0, which suggests that the use of Gloves 1, 2, and 3 for operating hammer drill results in amplification of vibration transmitted to the hand. The vibration transmissibility values at overall frequency range for HT1, HT3, HT4, and HT5 ranged from 0.862 to 0.966. Also the vibration transmissibility total values at overall frequency range were larger than the vibration transmissibility values in z (fore-aft) direction regardless of glove types or tool vibration spectra.

4. Discussion

According to the results obtained in this study, the vibration transmissibility total values at overall frequency range were larger than the vibration transmissibility values in z (fore-aft) direction regardless of glove types or tool vibration spectra, which suggests that the current single axis vibration test of gloves defined in ISO 10819 (2013) might overestimate the vibration attenuation performance of gloves. The current version of ISO 10819 (2013) still has difficulty in its application to real workplace evaluation of human exposure to hand-arm vibration specified in ISO 5349-1 (2001). The vibration transmissibility values of VR gloves are influenced by various factors; vibration frequency components, vibration magnitude, VR materials, and biodynamic response of the hand of glove users. To make evaluation of the glove use effectiveness possible in real workplaces, 3D test protocol on vibration attenuation

performance of gloves has to be established as well as the consistency of frequency range of interest in between ISO 10819 (2013) and ISO 5349-1 (2001).

5. Conclusion

This study measured vibration transmissibility spectra of VR gloves in three orthogonal directions and elucidated the 3D vibration attenuation characteristics of VR gloves at three positions: at the tip of fingers, the bottom of fingers, and the palm of the hand. The results obtained this study shows that the current single axis vibration test of gloves defined in ISO 10819 (2013) might overestimate the vibration attenuation performance of gloves.

6. References

- [1] International Organization for Standardization (2013) Mechanical vibration and shock – Hand-arm vibration – Measurement and evaluation of the vibration transmissibility of gloves at the palm of the hand. International Standard, ISO 10819.
- [2] International Organization for Standardization (2001) Mechanical vibration – Measurement and evaluation of human exposure to hand-transmitted vibration – Part 1: General requirements. International Standard, ISO 5349-1.
- [3] European Committee for Standardization (2003) Protective gloves – General requirements and test methods, EN420.
- [4] Japanese Standards Association (2007) Anti-vibration glove. Japan Industrial Standard, JIS T8114.
- [5] International Organization for Standardization (1996) Mechanical vibration and shock – Hand-arm vibration – Measurement and evaluation of the vibration transmissibility of gloves at the palm of the hand. International Standard, ISO 10819.

The 26th Japan Conference on Human Response to Vibration (JCHRV2018)

Kindai University, Osaka, Japan

August 22-24, 2018

**How Much Does Cold-Water Immersion Contribute to
Detecting Peripheral Neuropathy and Vasculopathy among
Industrial Vibrating Tool Operators?**

**Shigeki Takemura* [1], Kouichi Yoshimasu [1],
Kanami Tsuno [1], Jin Fukumoto [1, 2], Mototsugu Kuroda [1],
Setsuo Maeda [3], Kazuhisa Miyashita [1, 4]**

[1] Department of Hygiene, School of Medicine, Wakayama Medical University

[2] National Hospital Organization Hizen Psychiatric Center

[3] Department of Applied Sociology, Faculty of Applied Sociology, Kindai University

[4] President, Wakayama Medical University

[1, 4] 811-1, Kimiidera, Wakayama City, Wakayama Prefecture, 641-8509, JAPAN

(* steakmmi@wakayama-med.ac.jp)

[2] 160, Mitsu, Yoshinogari Town, Kanzaki District, Saga Prefecture, 842-0192, JAPAN

[3] 3-4-1, Kowakae, Higashiosaka City, Osaka Prefecture, 577-8502, JAPAN

Abstract

Cold-water immersion (CWI) in hand-arm vibration syndrome (HAVS) screening is conducted to detect peripheral neuropathy and vasculopathy among industrial vibrating tool operators (IVTOs). However, it is unclear how much CWI contributes to provoke these findings.

We included 325 male Japanese IVTOs without history of diabetes predominantly engaged in forestry (average [standard deviation] of age, 47.8 [11.9] years) who received HAVS screening. The prevalence of neuropathy (vibrotactile perception threshold (VPT)) and vasculopathy (finger skin temperature (FST) and capillary nail refill test (CNRT)) were compared between data before CWI only and data both before and after CWI (10 minutes at 10°C).

The prevalence of neuropathy and vasculopathy increased (abnormal findings from data both before and after CWI vs. data before CWI only): VPT, 40.3% vs. 17.5% ($p=0.000$, chi-square test); FST, 73.8% vs. 66.8% ($p=0.048$); CNRT, 58.2% vs. 11.4% ($p=0.000$).

CWI significantly contributed to detecting neuropathy and vasculopathy among IVTOs. CWI may be considered to detect HAVS cases proactively.

1. Introduction

Hand-arm vibration syndrome (HAVS) is an occupational disease among industrial vibrating tool operators (IVTOs), characterized by peripheral vasculopathy (finger blanching and coldness), neuropathy (dysesthesia, paresthesia, tingling and numbness) and musculo-osteo-arthropathy (osteoarthritis, grip force loss, pinch force loss, etc.) in upper extremities [1]. To detect this occupational disease and improve the occupational environment, special examinations have been conducted, based on a notice from the Ministry of Labour (presently the Ministry of Health, Labour and Welfare) in Japan [2]. This notice shows two steps of special examinations. In the first step, some screening tests are conducted to detect workers likely to have HAVS. In the second step, some further examinations are conducted including cold-water immersion (CWI) tests for those with positive findings in the first step. CWI tests are conducted to provoke peripheral neuropathy and vasculopathy including Raynaud's phenomenon (vibration-induced whiter fingers) among IVTOs. CWI simulates exposure to the cold occupational environment such as high-altitude working sites in the mountain. Actually, we encountered an IVTO engaged in forestry with Raynaud's phenomenon which was confirmed with CWI [3]. On the other hand, there may be HAVS cases with neuropathy and vasculopathy who are left undetected with negative findings in the first-step examinations without CWI tests. However, it is not well known how much CWI contributes to detecting peripheral neuropathy and vasculopathy among IVTOs.

We have been participating in special examination for IVTOs where the above-mentioned two steps of health examinations are merged into a one-stop examination for HAVS, where tests including CWI tests are given assuming all IVTOs examined are at risk of HAVS. We evaluated the effectiveness of CWI to detect HAVS in this population of IVTOs.

2. Methods

2-1. Study subjects

This analysis was a cross-sectional study. For this analysis, we recruited study participants from workers predominantly engaged in forestry, who were exposed to hand-arm vibration through hand-held vibrating tools, mainly chain saws (n=336, all males). These workers received medical examinations to evaluate HAVS. The examinations were conducted annually as a part of occupational health management, pursuant to a circular from the Ministry of Health, Labour and Welfare (formerly the Ministry of Labour), Government of Japan [2]. We have been providing annual medical examinations for the abovementioned workers. We included these workers to evaluate how much CWI contributed to detection of HAVS-related peripheral neuropathy and vasculopathy. Medical examinations that included the assessment of neuropathy (vibrotactile perception threshold (VPT)) and vasculopathy (finger skin temperature (FST) and capillary nail refill test (CNRT)) were performed from November to December 2013.

A total of 331 workers (98.5%) gave written consent to have their data from the medical examinations included in this study. This study was approved by the Institutional Review Board of Wakayama Medical University.

2-2. Procedure

Workers were asked to complete a self-administered questionnaire about their conditions, including years engaged in operating industrial vibrating tools, days per year operating such tools, hours per day operating them, lifestyle factors (smoking, alcohol consumption, etc.), medical history (including occupational traumas), HAVS-related symptoms (tingling, numbness, dysesthesia, pain, white finger,

etc.), and other symptoms and complaints. Total operating time (TOT) (hours) was defined as daily operating time (hours/day)×number of days exposed to vibration (days/year)×years exposed to vibration (years).

Medical examinations were conducted in a quiet room, with the temperature set at 20-23°C. Workers were asked to abstain from smoking and drinking beverages with caffeine and alcohol for at least two hours beforehand.

After acclimatization to the room temperature for at least 30 minutes, VPTs at 125 Hz, FST and CNRT were measured in four fingertips (except thumbs) of both hands. VPTs were measured in a sitting position with a vibrometer [AU-02 or AU-02B, Rion Co., Ltd., Kokubunji City, Tokyo, Japan (reference value: 0 dB=308 mm/s²)]. During measurement, the ascending threshold was observed; vibration began at a low level (-10.0 dB in general) and then gradually intensified at an interval of 2.5 dB until the worker perceived it, which was taken as the VPT. FST was measured with a laser thermometer (IT-550S, Horiba, Ltd., Kyoto City, Kyoto Prefecture, Japan) before the CWI test. CNRT was measured after pressing IVTO's nail with examiner's fingers for 10 seconds in four fingers (thumbs not included) of each hand.

Afterwards, the workers were given a CWI test. After staying in a sitting position, they immersed their dominant hand or the hand with HAVS-related symptoms (tingling, numbness, dysesthesia, pain, white finger, etc.), if any, in cold water to the wrist for a designated time period (10 minutes at 10°C. The 10°C, 10-min method is a conventional test condition for evaluating HAVS in Japan [4, 5] and adopted in ISO 14835-1 [6].

During the CWI test, VPT in the index finger and CNRT in the ring finger were measured in the same way as measured before CWI, but FST in the middle finger was measured with a thermistor thermometer (D922, Takara Thermistor, Ichinoseki City, Iwate Prefecture, Japan [as of July 31, 2018, this product is supported by Tateyama Kagaku Module Technology Co., Ltd., Toyama City, Toyama Prefecture, Japan]), at a total of three time points (0, 5 and 10 minutes after finishing the 10-minute immersion).

After finishing the CWI test, the subjects received physical and neurological examinations from a physician.

2-3. Statistical analysis

After excluding (a) workers with history of diabetes ($n=1$) and (b) workers who did not participate in the CWI test ($n=5$), 325 male workers were included for the statistical analysis.

Cut-off points of FST-based vasculopathy and CNRT-based vasculopathy were defined at each time point as shown in Table 1, based on a review about the diagnostic cut-off line of HAVS under CWI by Miyashita [7].

VPT, FST and CNRT were compared among four time points (before CWI, and 0, 5 and 10 min after CWI) with analysis of variance (ANOVA), then post-hoc Dunnett test was conducted to compare the average before CWI and that each of the three time points after CWI.

The prevalence of VPT-based neuropathy, FST-based vasculopathy and CNRT-based vasculopathy was calculated in the four time points as well as the prevalence of these findings (a) in at least one time point among the three time points after CWI, and (b) in at least one time point among all the four time points. The prevalence before CWI was compared with those at the three time points after CWI, then with those (a) in at least one time point among the three time points after CWI, and (b) in at least one time point among all the four time points, using chi-square test. The concordance of the prevalence

between pre-CWI evaluation and post-CWI evaluation in the three time points, chi-square test was conducted.

Assuming that pre-CWI tests are screening tests for HAVS and that post-CWI positive findings indicates the prevalence of the corresponding HAVS-related neuropathy or vasculopathy, the sensitivity and specificity were calculated in each test.

All comparisons were two-tailed. A value of $p < 0.05$ was considered significant, and a value of $0.05 \leq p < 0.10$ was considered marginally significant. All analyses were conducted using the SAS 9.4 software (SAS Institute, Inc., Cary, NC, USA).

Table 1. Cut-off points of neuropathy and vasculopathy

	VPT-based neuropathy (dB)	FST-based vasculopathy ($^{\circ}$ C)	CNRT-based vasculopathy (sec)
Before CWI	≥ 15.0	< 32.5	≥ 2.0
0 min after CWI	≥ 30.0	< 11.5	≥ 3.0
5 min after CWI	≥ 20.0	< 15.0	≥ 2.0
10 min after CWI	≥ 17.5	< 18.0	≥ 2.0

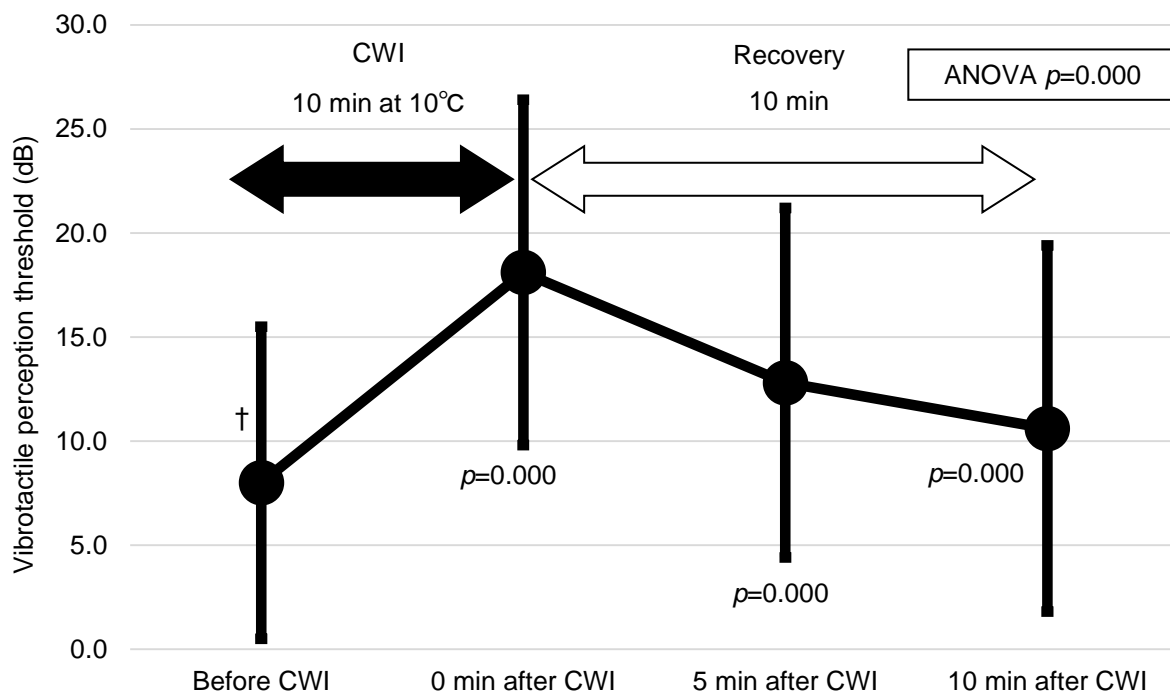
CWI, cold-water immersion test; VPT, vibrotactile perception threshold; FST, finger skin temperature; CNRT, capillary nail refill test.

3. Results

A total of 325 workers (average and standard deviation of age, 47.8 years and 11.9 years, respectively) were eligible for analysis.

Figure 1 shows the average and standard deviation of VPT, FST and CNRT during the examination. CWI significantly increased VPT and CWI and decreased FST, which lasted until 10 min after CWI.

(1-a)



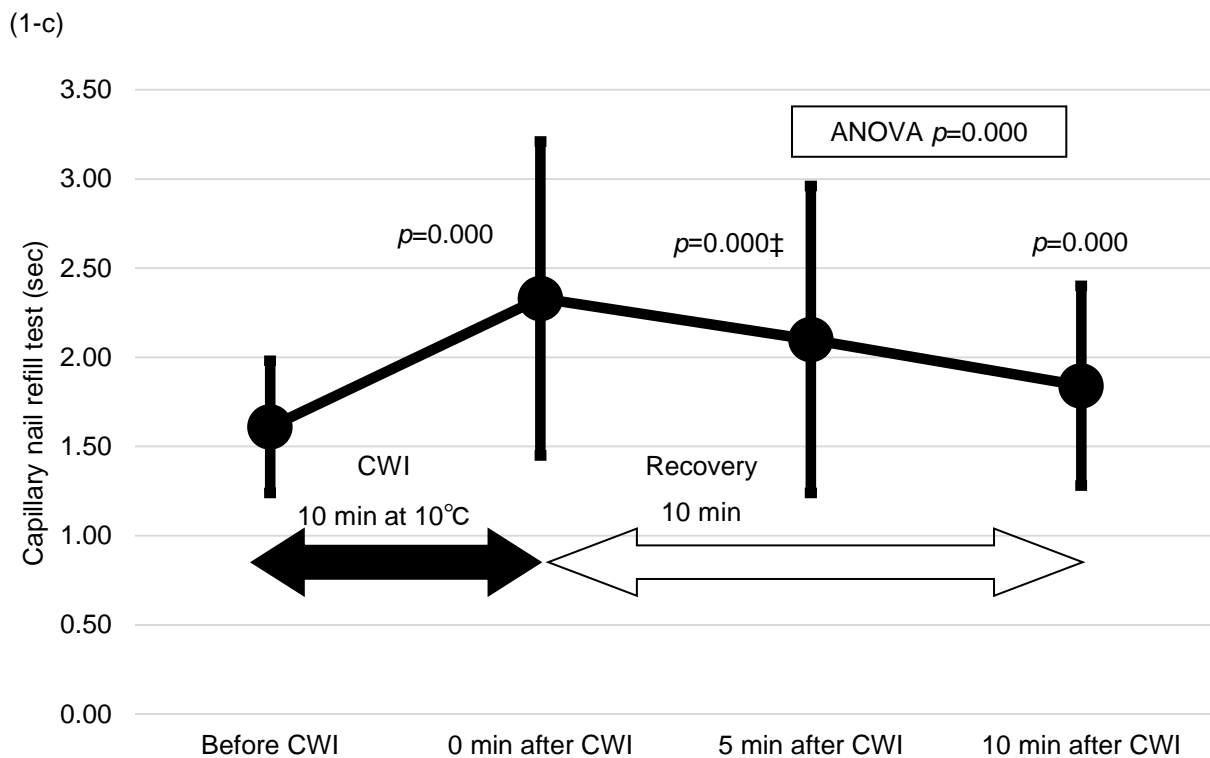
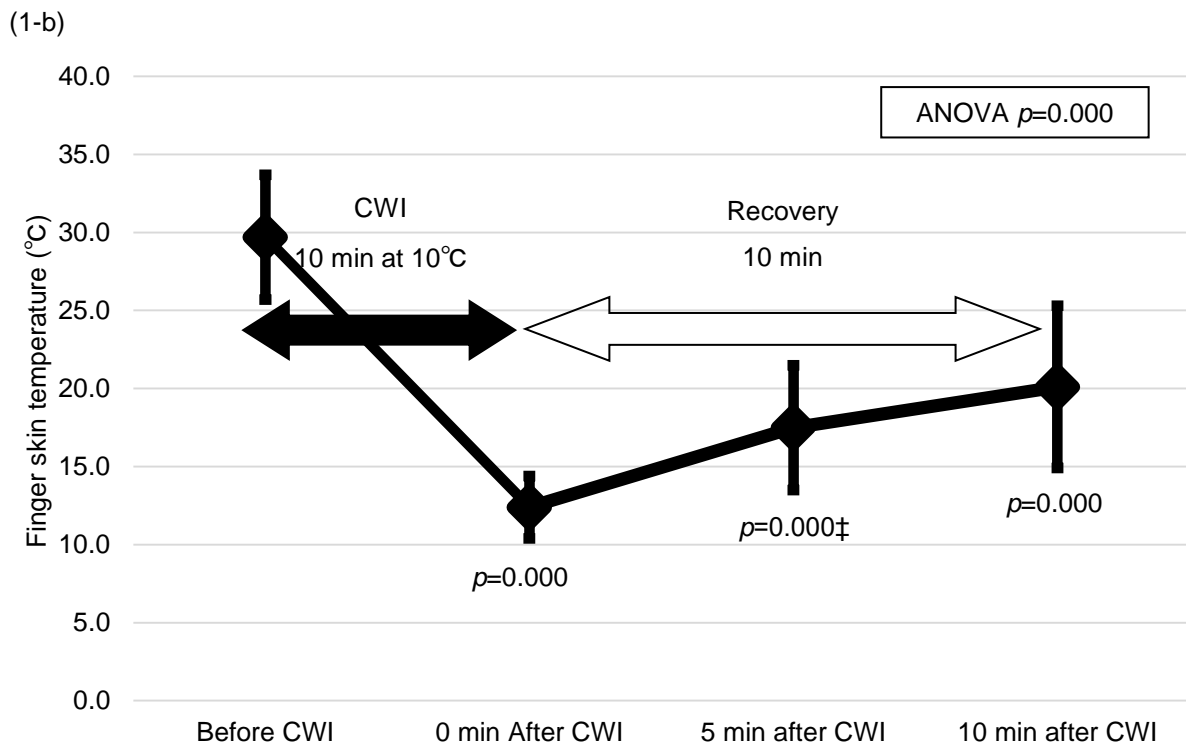


Figure 1. Change in the average and standard deviation: (1-a) Vibrotactile perception threshold (dB), (1-b) Finger skin temperature (°C), and (1-c) Capillary nail refill test (sec).

The line chart shows the average at each time point. The vertical line denotes one unit of standard deviation. Analysis of variance (ANOVA) was conducted to compare the average of measured values among four time points, then post-hoc Dunnett test was conducted to compare the average before CWI and that each of the three time points after CWI. † $n=323$; ‡ $n=324$. CWI, cold-water immersion test.

Figure 2 shows the prevalence of VPT-based neuropathy, FST-based vasculopathy and CNRT-based vasculopathy before CWI, and 0, 5 and 10 min after CWI. The prevalence before CWI, and 0, 5, and 10 min after CWI was 17.6%, 9.5%, 23.1% and 24.3% for VPT-based neuropathy, 66.8%, 30.5%, 24.7% and 47.1% for VPT-based neuropathy, and 11.4%, 11.7%, 45.7% and 30.5% for VPT-based neuropathy, respectively. The prevalence of VPT-based neuropathy decreased at 0 min after CWI, which gradually increased and reached significance at 10 min after CWI. On the other hand, the prevalence of FST-based vasculopathy after CWI was consistently lower than that before CWI. The prevalence of CNRT-based vasculopathy became significantly higher at 5 and 10 min after CWI.

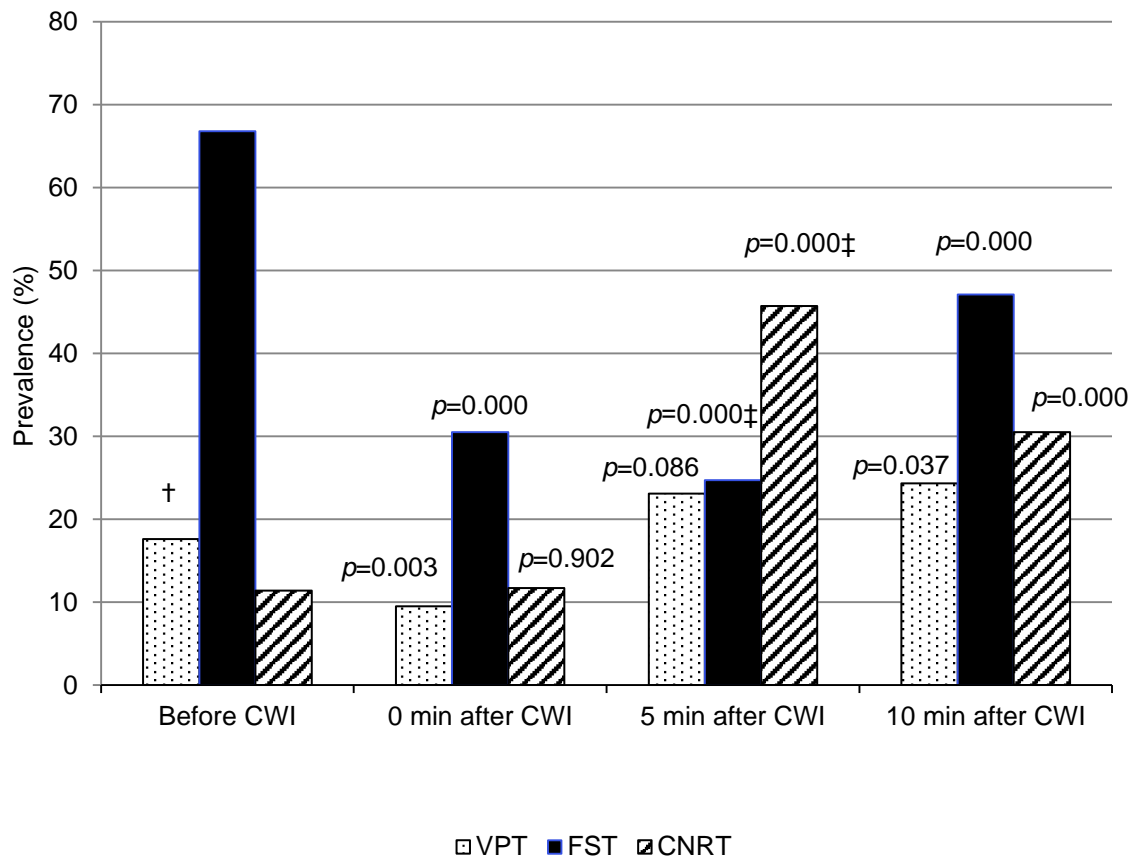


Figure 2. The prevalence of neuropathy and vasculopathy in the time course of CWI.

Bar charts show the prevalence (%) of neuropathy and vasculopathy among industrial vibrating tool operators in the time course of CWI ($n=325$; $\dagger n=323$; $\ddagger n=324$). CWI, cold-water immersion; VPT, neuropathy evaluated with vibrotactile perception threshold; FST, vasculopathy evaluated with finger skin temperature; CNRT, vasculopathy evaluated with capillary nail refill test.

Figure 3 shows the prevalence between the prevalence calculated from findings before CWI (17.5% for VPT-based neuropathy, 66.8% for FST-based vasculopathy and 11.4% for CNRT-based vasculopathy) and the prevalence calculated from findings after CWI only (31.4% for VPT-based neuropathy, 59.1% for FST-based vasculopathy and 53.8% for CNRT-based vasculopathy) as well as findings both before and after CWI (40.3% for VPT-based neuropathy, 73.8% for FST-based vasculopathy and 58.2% for CNRT-based vasculopathy). VPT-based neuropathy and CNRT-based vasculopathy increased their prevalence in findings after CWI only and findings both before and after CWI. FST decreased when considering post-CWI data only but increased taking both pre-CWI and post-CWI data into account.

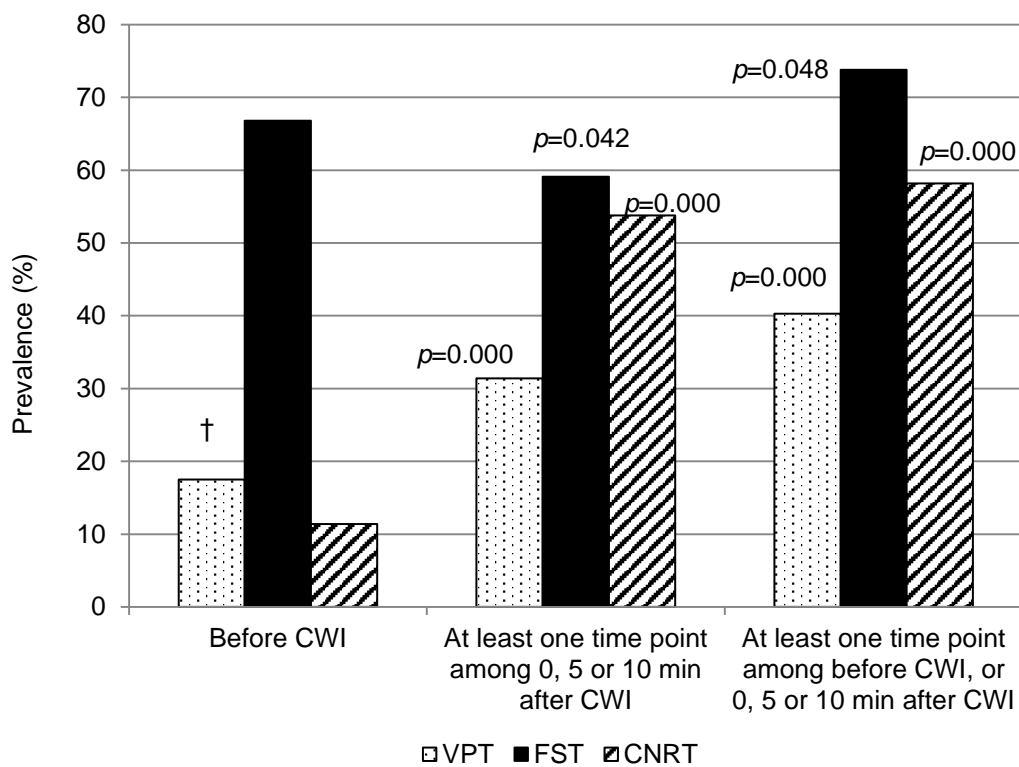


Figure 3. The prevalence of neuropathy and vasculopathy: findings from data with post-CWI findings *versus* data without post-CWI findings.

Bar charts show the prevalence (%) of neuropathy and vasculopathy among industrial vibrating tool operators ($n=325$; † $n=323$). Chi-square test was conducted to compare the prevalence between (1) before CWI and (2) at least one time point among 0, 5 or 10 min after CWI, then (1) and (3) at least one time point among before CWI, or 0, 5 or 10 min after CWI. CWI, cold-water immersion; VPT, neuropathy evaluated with vibrotactile perception threshold; FST, vasculopathy evaluated with finger skin temperature; CNRT, vasculopathy evaluated with capillary nail refill test.

Table 2 demonstrates the association between findings before CWI and those after CWI. The prevalence was significantly different in VPT-based neuropathy and FST-based vasculopathy but not in CNRT-based vasculopathy.

Assuming that pre-CWI tests are screening tests for HAVS and that post-CWI positive findings indicate the prevalence of the corresponding HAVS-related neuropathy or vasculopathy, the sensitivity and specificity were 28.0% (28/100) and 87.0% (194/223) in VPT, 88.0% (169/192) and 63.9% (85/133) in FST, 13.1% (23/175) and 90.7% (136/150) in CNRT, respectively.

Table 2. The prevalence of neuropathy and vasculopathy before and after CWI.

Outcome	Before CWI	After CWI		p value*
		Negative	Positive at least one time point among 0, 5 or 10 min after CWI	
Vibrotactile perception threshold (VPT)-based neuropathy	Negative	194 (72.9%)	72 (27.1%)	0.001
	Positive	29 (50.9%)	28 (49.1%)	
Finger skin temperature (FST)-based vasculopathy	Negative	85 (78.7%)	23 (21.3%)	0.000
	Positive	48 (22.1%)	169 (77.9%)	
Capillary nail refill test (CNRT)-based vasculopathy	Negative	136 (47.2%)	152 (52.8%)	0.281
	Positive	14 (37.8%)	23 (62.2%)	

Figures denote the number of industrial vibrating tool operators unless otherwise specified.

* Chi-square test. CWI, cold-water immersion test.

4. Discussions

In this cross-sectional study, CWI significantly increased the prevalence of VPT-based neuropathy, FST-vasculopathy and CNRT-based vasculopathy among IVTOs, when comparing data before CWI. Using data after CWI only detected a significantly higher prevalence of VPT-based neuropathy and CNRT-based vasculopathy was detected but FST-based vasculopathy was not. Using data both before and after CWI significantly increased the prevalence of all three abnormal findings.

Forestry workers are exposed to the cold occupational environment in winter, especially in the high altitude of mountains. The significant increase in the prevalence of neuropathy and vasculopathy showed the importance of CWI to provoke neuropathy and vasculopathy in the cold environment which could be missed in health examinations without CWI.

The sensitivity was high in FST but low in VPT and CNRT. On the other hand, the specificity was high in VPT and CNRT but low in FST. VPT is a quick and non-invasive method in the assessment of HAVS-related neuropathy and other conditions [9]. The prevalence of VPT-based neuropathy before CWI was low in this analysis. Patients with neuropathy might be underestimated in the first-step

examinations. To evaluate neuropathy in the first-step examinations and assess whether the second-step examinations to workers, it may help to assess them comprehensively not only from VPT data but also from other findings. We previously reported CWI increased the sensitivity and specificity in the VPT measurement in accordance with ISO 13091 [10]. FST assessment is also a conventional method in the assessment of HAVS-related vasculopathy. Its sensitivity and specificity have been reported [4, 5], but it was not evaluated how much adding CWI increases positive findings of FST-based vasculopathy in health examinations for HAVS. Giving the second-step examinations of HAVS including CWI tests for confirmation should be considered among workers with lower FST in the first-step examinations without CWI tests [2]. CNRT is simple and inexpensive, but it is difficult to standardize the nail-pressing force and the evaluation of the time for the nail to regain its color. Therefore, its usefulness to detect vibration-induced white finger is limited [8]. This limitation might be complemented with CWI.

The advantage of this study is that CWI helped to detect a significant number of cases with abnormal findings in neuropathy and vasculopathy. To screen cases with possible HAVS more proactively, CWI tests may be considered. In some subjects, however, disease symptoms can be affected by cold provocation, which could intensify the subject's adverse reaction to cold-stress [6]. Therefore, it is important to conduct CWI tests after assessing subjects' health condition and obtaining informed consent from them, under examiner's supervision and physician's approval.

The limitation of this study should be also mentioned. Firstly, this study was a cross-sectional study conducted in a single occupational group consisting of forestry workers mainly. Other occupational groups with a different prevalence of HAVS-related abnormalities may not benefit from adding CWI to health examinations for HAVS. Secondly, workers' exposure to occupational vibration was not taken into account in this analysis. Further analysis considering operating years and other potential risk factors may help to detect groups CWI is helpful to detect HAVS cases. Thirdly, this analysis was based on mass-screening health examinations for HAVS in some different examination sites in Wakayama, not in the same, strictly temperature-controlled laboratory equipped with automatically regulated water baths. Due to logistic constraints, we had to regulate room and water temperature in the examination site manually, although we controlled test conditions as much as possible according to conventional test conditions including ISO 14835-1 [6].

5. Conclusions

CWI significantly contributed to detecting neuropathy and vasculopathy among IVTOs. CWI may be considered to detect these findings proactively in health examinations for HAVS.

6. References

- [1] Kákosy T (1989) Vibration disease. *Baillière's Clin Rheum*, 3(1), 25-50.
- [2] Labour Standards Bureau, Ministry of Labour, Government of Japan (1975) Circular Notice 609—The enforcement procedure of the special health examination concerning the duties of the hand-held vibrating tools—. Tokyo (Japan): Ministry of Labour (in Japanese).
- [3] Takemura S, Yoshimasu K, Tsuno K, Fukumoto J, Maeda S, Miyashita K (2017) Raynaud's phenomenon in a forestry worker provoked with cold-water immersion test (10 min at 10°C): a case report. Paper presented at: The 57th Annual Meeting in Kinki Region, the Japanese Society of Occupational Health; November 18; Nara Prefectural Cultural Hall, Nara, Japan (in Japanese).
- [4] Hand-Arm Vibration Syndrome Research Committee, Japanese Society of Occupational Health (2013) Guideline for diagnosis of hand-arm vibration syndrome 2013. *Sangyo Eiseigaku Zasshi*; 55(6),

A105-A122 (in Japanese).

[5] Hand-Arm Vibration Syndrome Research Committee, Japanese Society of Occupational Health (2008) Reports on the standard for measurement and evaluation of finger skin temperature under cold-water immersion (10°C, 10-min method) in hand-arm vibration syndrome. Sangyo Eiseigaku Zasshi, 50(5), A57-A66 (in Japanese).

[6] International Organization for Standardization (2016) Mechanical vibration and shock---Cold provocation tests for the assessment of peripheral vascular function, Part 1: Measurement and evaluation of finger skin temperature. Second Edition. International Standard, ISO 14835-1.

[7] Miyashita K (1990) Evaluation standards in the cold provocation test of 10°C. In: Compensation Division, Labour Standards Bureau, Ministry of Labour, Government of Japan, editor. Confirmation of Occupational Diseases: References. ISBN 4-89764-209-4. Tokyo (Japan): Rodo Horei Kyokai; p.155-192 (in Japanese).

[8] Olsen N (2002) Diagnostic aspects of vibration-induced white finger. Int Arch Occup Environ Health, 75(1-2), 6-13.

[9] Gandhi MS, Sesek R, Tuckett R, Bamberg SJ (2011) Progress in vibrotactile threshold evaluation techniques: a review. J Hand Ther, 24(3), 240-55; quiz 256.

[10] Takemura S, Yoshimasu K, Tsuno K, Maeda S, Miyashita K (2017) Vibrotactile perception thresholds among industrial vibrating tool operators measured in accordance with ISO 13091. Paper presented at: The 25th Japan Conference on Human Response to Vibration (JCHRV2017); September 13-15; Nagoya University Daiko Campus, Nagoya, Aichi, Japan.

The 26th Japan Conference on Human Responses to Vibration (JCHRV2018)
Kindai University, Osaka, Japan
August 22-24, 2018

**ASSESSING THE RELATIONSHIP BETWEEN THE HUMAN RESPONSE TO
VIBRATION IN THE VIBROTACTILE THRESHOLD SHIFT WITH HAV EXPOSURE
DETERMINED ON THE SUBJECT**

Leif Anderson³, Mark D. Taylor², Setsuo Maeda¹, and Jacqui Mclaughlin³

¹Department of Applied Sociology, Faculty of Applied Sociology, Kindai University
3-4-1, Kowakae, Higashiosaka, Osaka, 577-8502, Japan, E: maeda@socio.kindai.ac.jp

²School of Engineering and The Built Environment, Edinburgh Napier University, 10 Colinton Road,
Edinburgh, EH10 5DT, UK, E: m.taylor@napier.ac.uk

³Reactec Ltd., Vantage Point, 3 Cultins Road, Edinburgh EH11 4DF, UK,
E: LeifAnderson@reactec.com

Abstract

Existing risk assessment methodologies are based on fixed tool vibration magnitude emission data (such as tool declaration data or a point in time (typically annually) tool measurement to ISO5349) and tool usage time. The research evaluates the relationship between vibration dose assessment on subjects using wearable sensors with temporary threshold shift (TTS) in vibrotactile perception threshold and examine if this real use data would be beneficial for workplace risk assessment compared to the traditional approach of using a fixed vibration level. Human response to vibration, using TTS perception response, in male subjects (n = 12) exposed to hazardous vibration was undertaken. Simultaneous vibration measurements were undertaken on the subject and conventional measurements at the tool hand-grip interface in accordance with ISO 5349-2. Two modes of tool operation (drill and impact) and two postures (horizontal and vertically downwards) of tool use were considered. This choice of experiment was aimed at examining a range of vibration exposure from a controlled set of test conditions where conventionally a single vibration magnitude data point would be used in a risk assessment. The results demonstrate a more linear relationship between the hand transmitted vibration determined by the wearable sensor on the subjects and the human response to the vibration over the conventional measurement on the tool. It could be further hypothesised that control measures derived from in-use tool data would be more effective in reducing the underlying risk to operatives.

1. Introduction

Hand-arm vibration syndrome (HAVS) is a recognised industrial disease induced by excessive exposure to vibration through occupational tasks involving vibrating machinery (Bovenzi, 1998). HAVS

comprises a range of disorders affecting the peripheral circulatory system, peripheral nervous system and muscular skeletal system of the hand and arm. As a progressive and irreversible condition, the ability to predict a rate of progression and take timely preventative action through exposure reduction or complete elimination of hazardous exposure is highly desirable. However, reliable dose response relationships have proved elusive. This is in part due to the difficulties in acquiring sufficiently reliable exposure and epidemiological evidence and in part due to the fundamental shortcomings in the existing exposure assessment methodologies (Bovenzi 1998).

The established method for assessing exposure has been standardised in the form of ISO 5349 (BSI, 2001a) with employers being required to control exposure levels to predetermined limits within their respective territorial legislation. Despite the existence of international standards concerning exposure assessment and regional legislation regarding working practices, reported cases of HAVS remain significant as indicated by disability benefit claims in the UK (HSE, 2018). It should be noted that this data does not reflect all diagnosed cases of the conditions, only those sufferers choosing to claim disability benefit from the UK Government. Since the condition typically takes many years to become symptomatic there is significant variation in the reported rate of progression relative to exposure. Defining an accurate response relationship is a significant challenge. The standards provide clear guidance on vibration magnitude measurements to be taken on the tool within the work place. However, compliant measurements are seldom undertaken frequently enough to adequately reflect the range of tool deployment in the work place. In research laboratory work it is common to determine exposure from a fixed vibration magnitude which has not been taken from the *in-situ* use of the tool (Bovenzi, 2010, Tominaga, 2005, Mahmood et al., 2017, Su et al., 2011, Su et al., 2016, Griffin et al., 2003). The standard method for calculating exposure based on vibration measurements taken on the tool requires skilled technicians to execute a repeatable assessment. In practise, this is unlikely to capture the effects of different posture, coupling force, operator physiology and the variability in day-to-day tasks undertaken by tool operators within different industry sectors. The CEN technical report CEN/TR 15350 (BSI, 2013) identifies the difficulties in capturing all the factors affecting the vibration level of a tool and recognises the expense in doing so. CEN/TR 15350 advises that the exposure to vibration does not only depend on the machine used but also to a large extent on the quality of inserted tools, the work situation and operator behaviour. It concludes that these factors must be considered to make an ideal assessment of vibration exposure.

In numerous industrial sectors, there are difficulties associated with obtaining a conventional vibration measurement on the tool at the workplace. This results in a common approach to HAV risk management being the use of tool manufacturer's declared vibration emission values. Guidance from the HSE illustrates the risk of using declared emission data for risk management and the likelihood of under estimating materially an individual's exposure (HSE, 2005 Page 64, section 216). CEN/TR 15350 identifies that uncertainty of the vibration value has more influence on the uncertainty of the daily vibration exposure than that of the duration and that the uncertainty of the vibration value in real use is normally much greater than the uncertainty factor declared by the manufacturer.

The effect of hand coupling action on vibration transmission through to the hand arm system has been undertaken in historical studies.. Maeda et al. (2007) investigated the effect of hand coupling actions on the TTS of vibrotactile perception, illustrating that hand coupling actions affect the human response. Maeda and Shibata (2008) also provided evidence of the effect of operative posture on TTS results. Further research to examine operator physiology and biodynamics is required to fully understand the response of structures within the hand and arm to mechanical vibration.

The sensitivity of mechanoreceptors can be significantly reduced by long-term exposure to hand-transmitted vibration (Brammer et al., 1987). For this reason, the measurement of finger vibration perception threshold (VPT) has been viewed as an important approach and has been widely used to diagnose and investigate hand-arm vibration syndrome (HAVS). The method has been standardized by the International Organization for Standardization (BSI, 2001b). Previous studies (Bjerker et al., 1972, Hahn, 1966, Lundström and Johansson, 1986) have also shown that after a person is exposed to hand-transmitted vibration, the vibration perception threshold could be temporarily increased and it could take some time (usually greater than 10 minutes) for the VPT to come back to its normal value, which is conventionally termed as temporary VPT shift (TTS). Lidström et al. (1982) found that the magnitude of the TTS was higher for workers exposed to long-term hand-transmitted vibration than for age-matched controls. Radzyukevich (1969) suggested that the temporary threshold shift (TTS) in vibrotactile perception threshold at the end of a working day correlated with the permanent threshold shift (PTS). Malinskaya et al. (1964) found that the mean TTS of workers after a day of work that included vibration exposure corresponded to the PTS of vibratory sensation that occurred in the group after 10 years of exposure. These observations suggest that the TTS after daily exposure may be used as a measure to indicate the PTS after prolonged exposure to vibration. Therefore, TTS may be used as a convenient and relevant index to investigate the effects of the vibration exposure and influencing factors on the development of finger nerve disorders.

Experiments were performed to examine the relationship between the human response to vibration determined by the TTS of subjects, and the in-use hand transmitted vibration as determined by a wearable sensor. Conventional measurements of vibration emission on the tool grip were performed concurrently as a control reference. From this experiment the suitability of a wearable technology for determining HAV exposure risk is considered relative to in-use testing on the tool and fixed data, such as declared vibration magnitude.

2. Experiment

2.1. Human test subjects

Tool vibration data was obtained from a series of controlled tests performed using a standard industrial power tool in a laboratory setting. Twelve healthy male subjects between 18 and 24 years of age with no previous history of vibration exposure were selected as subjects. Alcohol, nicotine and caffeine intake were prohibited prior to and for the duration of the test protocol in accordance with ISO 13091-1 (BSI, 2001b). Screening was undertaken to ensure that all participants were clear of medical conditions that would have an impact upon the research. The experimental method was approved by

the Edinburgh Napier University research ethics committee, all subjects were willing volunteers and individual consent was obtained prior to commencing the experiments.

2.2. Tools and in-use postures

A single mechanized hand tool was used during the course of the experiments with variable speeds and action settings. Tool specification and operating descriptions are provided in Table 1.

Table 1 Tool specification.

	Setting 1	Setting 2
Tool description	Drill	Hammer drill
Mechanical action	Rotary	Impact
No Load Speed	400 rpm	6000 blows / min
Mass (kg)	1.7	1.7

To assess the role different postures and subjects have on the human response relative to the two respective dose assessment methods, two postures were considered. These were horizontal and vertically downwards. A reaction frame was constructed to allow a 450 x 450 mm x 50 mm concrete test panel to be mounted in the two configurations. The reaction frame ensured that the correct posture was attained and that structural resonance from the substrate were minimized. Figure 1 shows the general arrangement of the reaction frame, the two posture configurations and the location of a force plate.

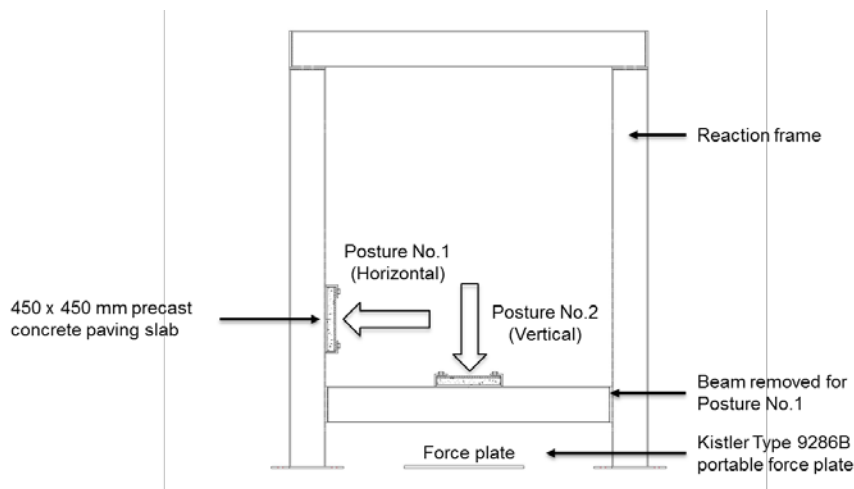


Figure 1 Reaction frame configuration showing postures and force plate location.

The postures illustrated in Figure 1 were considered for the investigation as those commonly employed when operating a hand-held drill. Figure 2 further illustrates the positions of use and the position of the human subject and the force plate.



Figure 2 Test postures (i) horizontal (ii) vertical downwards and (iii) force plate location.

Push force for each of the tool tests was controlled through the use of a force plate (Kistler 9286B) mounted on concrete and a digital display to ensure a steady 50 N force was applied against the work test panel. Figure 2 (iii) shows a test subject standing on the force plate while applying the tool to the substrate affixed to the reaction frame in posture 1. Subjects applied the tool to the substrate continuously, only removing it when required to start a fresh hole in the concrete substrate.

2.3. Experimental conditions

All subjects were given induction training on how to operate and grip each tool. However, subjects were not experienced tool operators and demonstrated a degree of variability in tool operation performance. Grip force was not monitored. Prior research examining the effects of grip force for vibration transmission (Maeda et al., 2007) concluded that grip force was not considered to be significant providing a grip force of at least 30 N was attained. Tool vibration

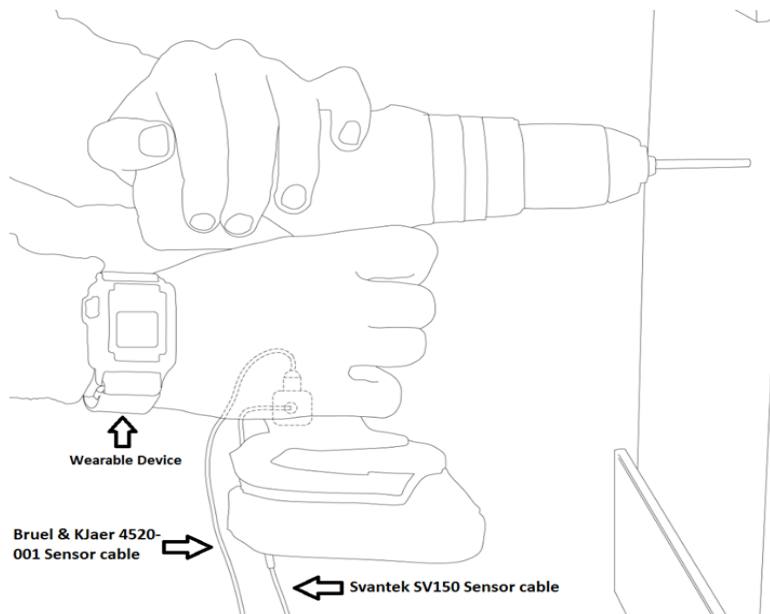


Figure 3 Wearable Device and reference instrument sensor locations

emission data during two minutes was measured using two ISO 8041 compliant reference instruments; a Svantek SV106 and a Brüel & Kjær Photon+ with RT Pro software. The devices were configured to obtain a continuous two-minute duration measurement. Two accelerometers were attached to the tool hand grip as illustrated in Figure 5. A Svantek SV150 and Brüel & Kjær 4520-001 were used.

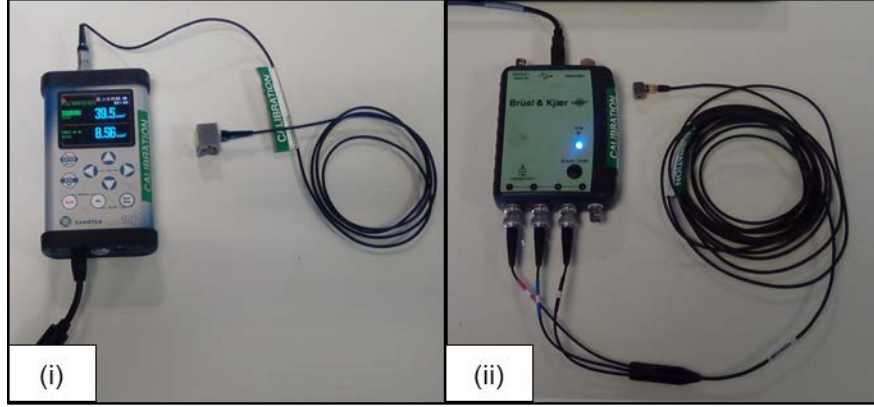


Figure 4 Tool emission instrumentation (i) Svantek SV106 & SV 150 accelerometer (ii) Brüel & Kjær Photon+ 4520-001 accelerometer.

2.4. Vibration dose measurement on tool

Tool vibration emission data measurement equipment is defined by the standard ISO 8041 (BSI, 2017). In working environments, the hand-arm vibration dose from the tool handle to the operative follows the ISO 5349-2 (BSI, 2015) standard by using the measurement equipment compliant with ISO 8041. In accordance with ISO 8041 the frequency-weighted root-mean-square (r.m.s.) vibration acceleration value in a specified axis, a_{hw} , is defined by the following expression:

$$a_{hw} = \left(\frac{1}{T} \int_0^T a_{hw}(t)^2 dt \right)^{1/2} \quad \text{Equation 1}$$

Where $a_{hw}(t)$ is the frequency-weighted vibration acceleration in a specified axis as a function of the instantaneous time, t , in meters per second squared (m/s^2). T is the duration of the measurement.

The combined vibration from the three axes x , y and z is defined by the following expression:

$$a_{hv} = \sqrt{a_{hwx}^2 + a_{hwy}^2 + a_{hwz}^2} \quad \text{Equation 2}$$

Where a_{hwx} , a_{hwy} and a_{hwz} are the weighted vibration values in the three orthogonal axes x , y and z .

2.5. Wearable sensor dose measurement on subject

Annex D of the ISO 5349-1 standard identifies a number of factors which will impact the hand transmitted vibration magnitude. This could be represented mathematically such that when the tool handle vibration magnitude is 'a', the hand-transmitted vibration magnitude may be defined by the following equations:

$$a_{HTVx} = a_x H_{FW} H_{a_x} H_{b_x} H_{c_x} H_{d_x} H_{e_x} H_{f_x} H_{g_x} H_{h_x} H_{i_x} H_{j_x} H_{k_x} H_{l_x} \quad \text{Equation 3}$$

$$a_{HTVy} = a_y H_{FW} H_{a_y} H_{b_y} H_{c_y} H_{d_y} H_{e_y} H_{f_y} H_{g_y} H_{h_y} H_{i_y} H_{j_y} H_{k_y} H_{l_y} \quad \text{Equation 4}$$

$$a_{HTVz} = a_z H_{FW} H_{a_z} H_{b_z} H_{c_z} H_{d_z} H_{e_z} H_{f_z} H_{g_z} H_{h_z} H_{i_z} H_{j_z} H_{k_z} H_{l_z} \quad \text{Equation 5}$$

Where Ha_x is the transfer function of factor a in the x-axis and so on. H_{FW} is the frequency weighting defined by ISO 5349-1. These equations take all affecting factors into the tool handle vibration magnitude 'a'.

The effect of an individual factor on vibration magnitude may be studied experimentally in isolation. For example, the transmission factor of He of coupling force was examined by Pan et al. (2018) and Kaulbars (1996) in laboratory conditions. Also, Pan et al. (2018) established that the coupling action influenced the vibration transmission to the wrist from the tool handle emitted vibration but did not model this as an He weighting coefficient.

If the individual factors or some combination of factors from Annex D of ISO 5349 are not modelled, then a properly conducted measurement of the emitted vibration from the tool handle will carry remaining uncertainties as to the vibration magnitude transmitted to the hand. In moving the measurement point to the recipient of the vibration it is believed that the effects of at least some of the factors influencing equations 3, 4 and 5 above can be considered in the determination of the hand transmitted vibration.

Vibration on the subject was measured using a wrist mounted industrial wearable device (HVW-001, Reactec Ltd.). The device is mounted to the wrist by way of an adjustable nylon webbing strap, adjusted and fastened by way of velcro loop arrangement. The device features a three axis MEMS accelerometer sampling at 1.6kHz for 0.66 seconds every 1.5 seconds. A frequency range from 3Hz to 650Hz is captured. Acceleration data from each axis is converted independently from time domain to frequency domain through a Fourier analysis incorporating a Hanning window function to generate discrete magnitude values for each axis (Maeda et al., 2017). Acceleration a_{rhv} is calculated using the following formula.

Transformed vibration magnitude for x - axis during iteration n :

$$a_{rhx}(n) = \sqrt{\sum_i w_{rhx}(i)^2 \cdot a_{hx}(n, i)^2} \quad \text{Equation 5}$$

$w_{rhx}(i)$ is the i^{th} frequency dependent transfer function for the x – axis.

Similar definitions are derived for axis y and z axes:

$$a_{rhy}(n) = \sqrt{\sum_i w_{rhy}(i)^2 \cdot a_{hy}(n, i)^2} \quad \text{Equation 6}$$

$$a_{rhz}(n) = \sqrt{\sum_i w_{rhz}(i)^2 \cdot a_{hz}(n, i)^2} \quad \text{Equation 7}$$

Running average (r.m.s.) 3 - axes vibration magnitude formula after iteration n :

$$a_{rhz} = \sqrt{\frac{\sum_n a_{rx}(n)^2}{n}} \quad \text{Equation 8}$$

$$a_{rhv} = \sqrt{a_{rhx}^2 + a_{rhy}^2 + a_{rhz}^2}$$

Equation 9

Where, $w_{rhx}(i)$, $w_{rhy}(i)$ and $w_{rhz}(i)$ are the transfer functions from the tool handle to the wrist calculated as below from a characterized transmissibility for each axis between a grip point incident vibration to a measured point on a human wrist. The idealized transfer function $w_{rhx}(i)$, $w_{rhy}(i)$ and $w_{rhz}(i)$ are derived by the calculations:

$$w_{rhx}(i) = (\text{ISO 5349-1 frequency weighting}) / (\text{x-axis of measured transmissibility on the Wrist})$$

$$w_{rhy}(i) = (\text{ISO 5349-1 frequency weighting}) / (\text{y-axis of measured transmissibility on the Wrist})$$

$$w_{rhz}(i) = (\text{ISO 5349-1 frequency weighting}) / (\text{z-axis of measured transmissibility on the Wrist})$$

The transmissibility between the tool user interface and the accelerometer within the wearable sensor was determined by the device manufacturer by assessing the transmission of input vibration energy across a defined frequency spectrum in the three orthogonal axes. Three-dimensional input vibration energy was generated utilising three 1-D shakers (MB Dynamics) arranged along the three orthogonal axis. A random broad band signal was employed across a frequency range of 10-500Hz. Vibration amplitude was maintained throughout the duration of the characterisation process by means of a closed loop control system at a 1G level. The vibration was delivered to the human hand through an instrumented handle coupled with each shaker using a flexible linkage system. The control system utilised vibration data from the instrumented handle to ensure correct vibration magnitude was maintain in each axis throughout the test cycle. The instrumented handle was equipped with a tri-axial accelerometer (Endevco, 65-100) and a pair of force sensors (Interface, SML-50) for measuring the acceleration at the user interface and applied grip force. A force plate (Kistler, 9286AA) was used to measure the push force applied to the handle. The applied and target grip and push forces were displayed on two virtual dial gauges on a computer monitor in front of the subject. The subjects were instructed to control the grip force and push force to 30N and 50N respectively. An additional accelerometer (Endveco, M35A) was attached to the subjects' skin using I.V. needle adhesive tape adjacent to the wearable sensor to provide additional reference data.

Applying the protocol described above a series of 6 characterisations were conducted on each test subject. Each characterisation was conducted continuously for a duration of 1 minute. For the purposes of this initial detailed characterisation subjects were limited to N=3. Normative data from the above series of characterisation was used to derive a mean transmissibility for each axis. Transmissibility was seen to reach an effective minimum in all axis above 500Hz therefore characterization beyond this frequency was not seemed necessary.

By way of demonstrating the effectiveness of the wearable sensor to determine the vibration required to assess HAV exposure through transformation of a measurement taken on the subject's wrist, figures 5 and 6 illustrate the frequency spectrum of vibration magnitude for a measurement taken on the tool in compliance with ISO5349 and that determined by the wearable sensor for each of the two tool settings used in the experiment of this paper.

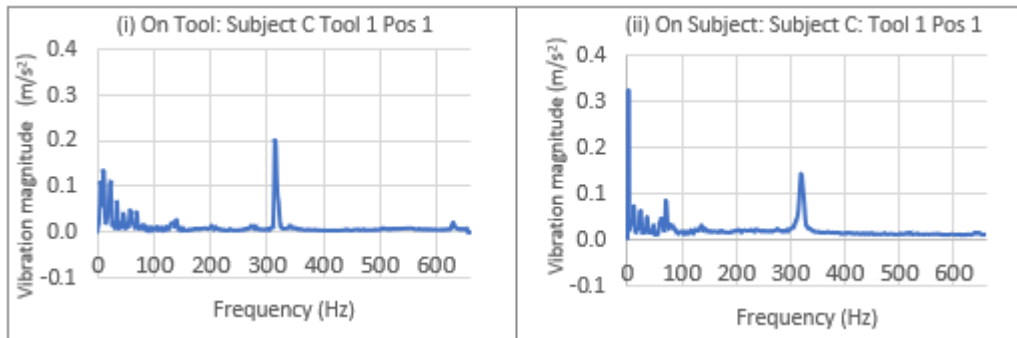


Figure 5 Tool setting No.1 (drill), posture 1 – (i) frequency response on tool and (ii) frequency response on subject.

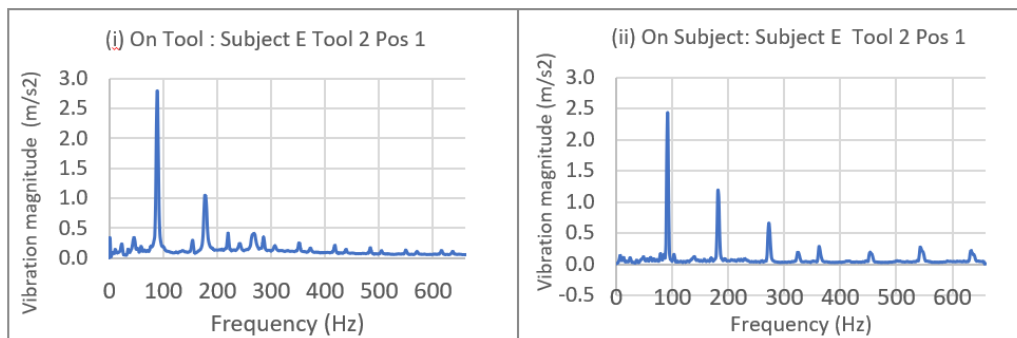


Figure 6 Tool setting No.2 (impact drill) – (i) frequency response on tool and (ii) frequency response on subject.

While there is an intention to further refine the transfer function to address more of the factors identified in equations 3, 4 and 5, at this stage, the transfer function developed from the average transmissibility to the wrist of the three male subjects was used for demonstrating the effectiveness of the wearable sensor’s dose measurement in the presented study. An experiment was designed to indicate whether the wearable sensor, while mounted at the wrist, is effective in measuring the hand-transmitted vibration.

2.6. Assessment of vibrotactile temporary threshold shift (TTS)

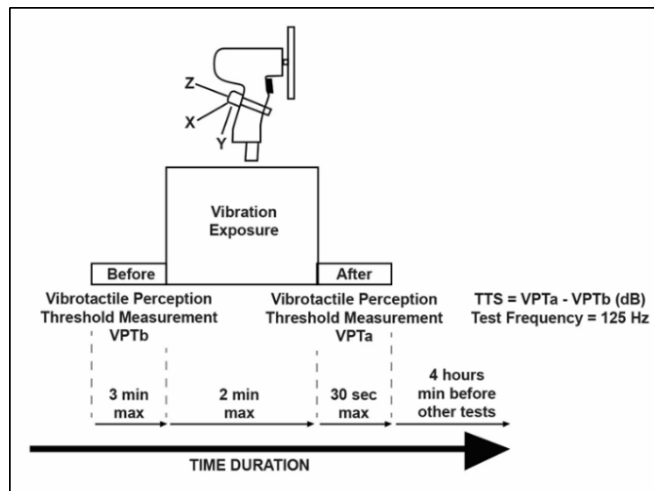
VPT was assessed on each individual subject for each tool test. A VPT test was undertaken three minutes prior to commencing the tool activity test and within thirty seconds of completing the two minute tool activity test. The VPT of 125 Hz was measured at the tip of the index finger of the right hand. A vertical force was maintained by mounting the vibration exciter on digital scales. The subjects were asked to maintain 0.20 kg by monitoring the value on the digital display. Vibration thresholds were determined using a RION type AU-02A vibrotactile sensation meter by means of gradually increasing and decreasing vibration source noting the level at which it becomes perceptible by the subject. Thresholds were calculated by the mean values of three measurements obtained over a period not exceeding thirty seconds. The TTS was defined as the difference (dB) of the vibrotactile thresholds before and after vibration exposure (Yonekawa et al., 1998). Subjects were limited to two vibration test sessions per day with a minimum of four hours rest between each test.

The TTS was calculated by the following equation.

$$TTS \text{ (dB)} = VPT_A - VPT_B \quad \text{Equation 10}$$

where, VPT_A (dB) is the vibrotactile perception threshold after tool vibration exposure and VPT_B (dB) is the vibrotactile perception threshold before tool vibration exposure. The experiment protocol timeline is summarised in figure 7.

Figure 7 Test protocol timeline.



Ambient temperature within the test laboratory was maintained at 20°C +/- 4°C for the duration of all tests and subject fingertip temperature was measured and recorded during each TTS assessment. This was undertaken using a thermocouple attached to a digital display (RS 206-3738). A Grant 2020 Series Squirrel data logger with four thermocouples was used to monitor ambient air temperature throughout the duration of the tests. An industrial electric fan heater was used to maintain the ambient air temperature at approximately 20°C. VPT test apparatus is shown in figure 8.

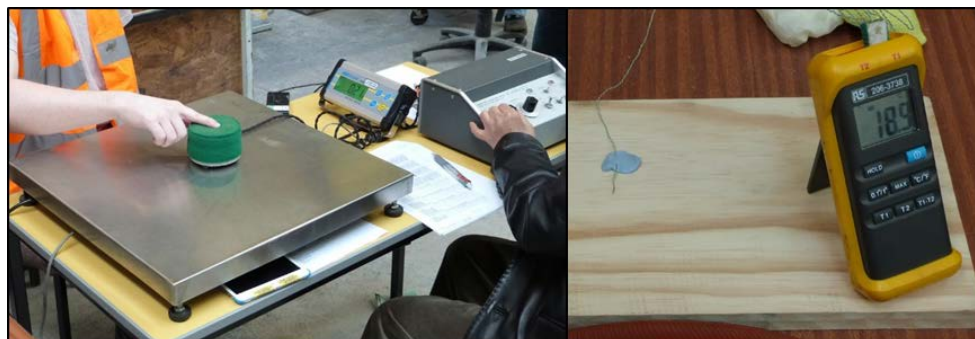


Figure 8 VPT assessment using vibratory sensation meter (Rion Company Ltd. Model AU-02A) and skin temperature thermocouple sensor (RS 206-3738).

Fingertip temperature was checked before and after VPT measurement. If the subject's fingertip temperature was lower than 23°C, the subject was instructed to warm their finger. During this experiment, all subject's fingertip temperature was over 25°C.

3. Results

Each test subject, a tool setting and a tool posture was conducted once in this experiment. All test results are included in the presented data with the exception of four results where there was inadequate triggering of the wearable sensor for tool setting No.1 (drill). Figure 9 (i) shows the relationship of TTS and the vibration magnitude on the tool handle. Figure 9 (ii) shows the relationship of TTS and the

wearable sensor vibration magnitude, all for tool setting No.1 (drill) and in the horizontal posture (Posture No.1).

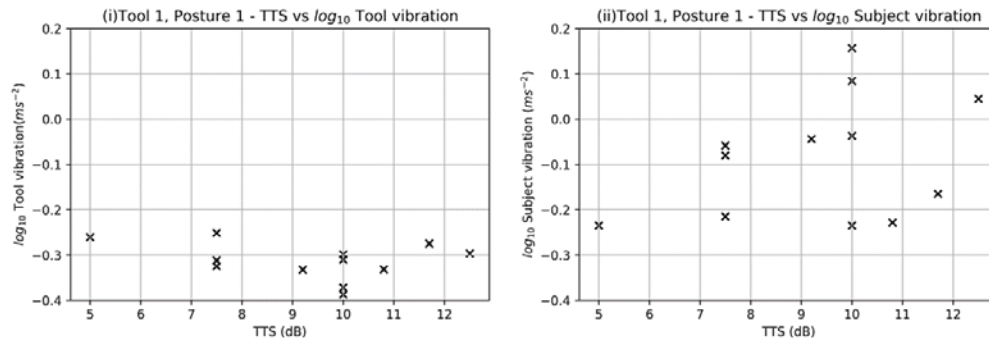


Figure 9 TTS results (i) tool vibration and (ii) subject vibration (Tool setting 1, Posture 1).

Figures 10 (i) shows the relationship for each subject between TTS and the vibration magnitude on the tool handle. Figure 10 (ii) shows the relationship for each subject between TTS and the wearable sensor vibration magnitude, for tool setting No.2 (impact drill) and in the horizontal posture.

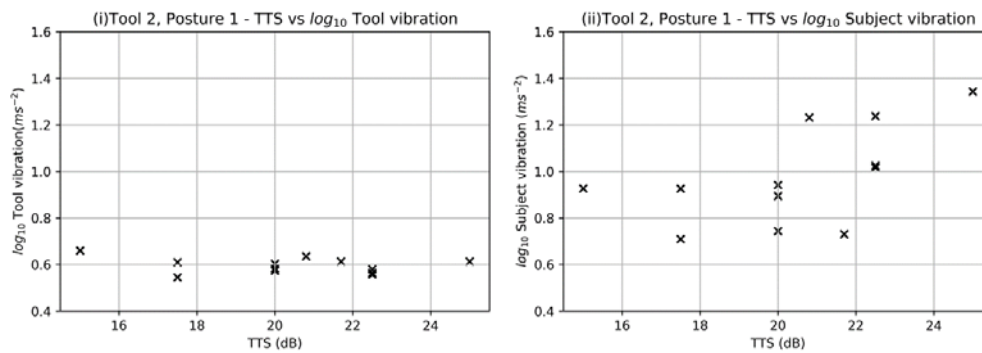


Figure 10 TTS results (i) tool vibration and (ii) subject vibration (Tool setting 2, Posture 1).

For both tool settings there is variation in the human response to vibration across the subjects while the measured vibration on the tool remains relatively constant. In contrast, the vibration transmitted to the subject determined by the wearable sensor trends more distinctly with the increased level of human response to vibration. Figures 11 provides TTS results for an individual subjects illustrating the human response to the tools' vibration for the two different tool settings and two postures used for the tool.

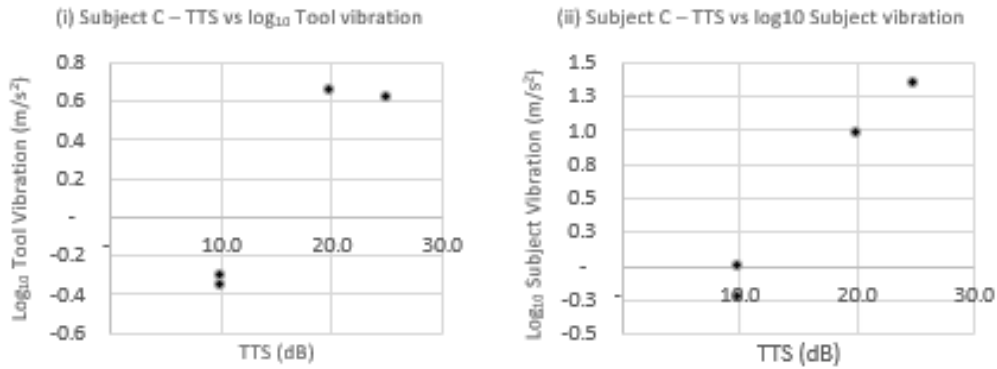


Figure 11 TTS results (i) tool vibration and (ii) subject vibration Subject C (Tool settings 1 and 2, Posture 1 and 2).

Figure 12 provides a summary of the all tests showing tool and subject vibration measurements.

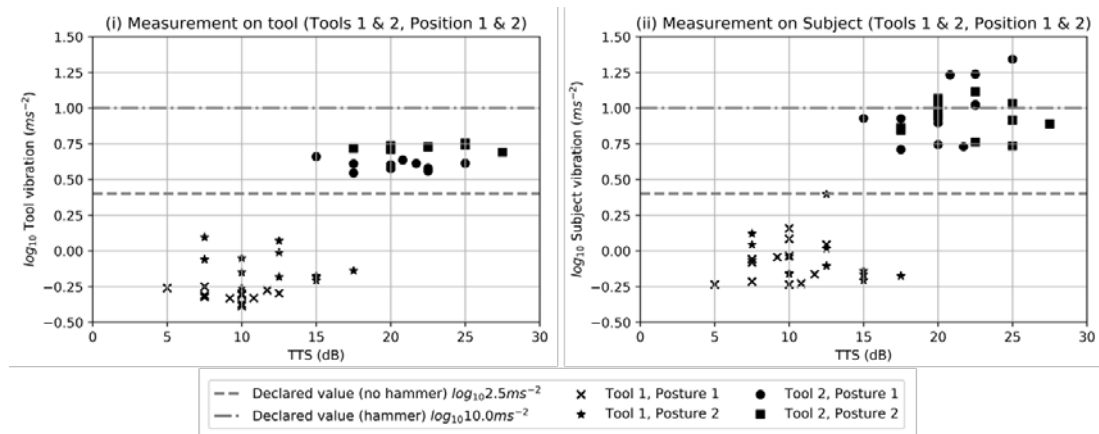


Figure 12 TTS vs (i) tool and (ii) subject vibration measurements for all tests. Manufacturers declared emission values of 2.5 ms⁻² and 10.0 ms⁻² provided for reference purposes

The measurement of vibration on the tool has two distinct clusters between the two tool settings. While the range of human response to the vibration is distinctive between the two tool settings, within each tool setting the vibration magnitude measured on the tool remains essentially constant relative to the human response. A more proportional relationship of increasing human response with increasing magnitude is apparent in the determined vibration from the wearable sensor on the subject.

The tool used for the experiments has in total four settings based on two speeds and engagement of a hammer setting for impact mode. In accordance with the ISO 28927-5 standard, the manufacturer declares two vibration magnitudes for the tool depending on whether the hammer action is activated or not and was not prepared to advise on which speed setting was used for the declaration.

4. Discussion

Figure 12(i) shows that the tool vibration magnitude was relatively constant for the two different settings across the two postures and subjects. Experimental results showed the TTS of the subjects varied significantly for each of the two tool settings across subjects and postures of tool use. However, the

vibration magnitude measured on the tool handle, in compliance to ISO 5349, was essentially fixed for each tool setting. The measurement on the handle was therefore not able to reflect some of the factors which resulted in a different human response to the vibration. Figure 12 (ii) shows a positive relationship between the human response to vibration of the subjects as determined by their TTS and the hand transmitted vibration magnitude determined by the wearable sensor. This may imply the wearable sensor on the wrist can measure the hand-transmitted vibration considering the affecting factors of Annex D of ISO 5349-1 standard. Further research is required to validate such measurement in industrial working environments. A specific test subject's results provided evidence of the wearable device vibration measurements correlating with the range of TTS results in comparison with the tool grip vibration measurements. The results presented show that there is a significant relationship between TTS results and the measurement of vibration exposure using a wearable monitoring device.

The results shown in figure 12 (i) support the issues highlighted in CEN/TR 15350 (2013) in that the exposure to vibration depends on things like the work situation and operator behaviour. These factors need to be taken into account to make an ideal assessment of vibration exposure.

The difficulties outlined in CEN/TR 15350 (2013) in measuring vibration in the work place has resulted in CEN/TR 15350 (2013) and other research (Brocal 2017) advising on ways to estimate vibration exposure from fixed declared vibration magnitudes of tool manufacturers. The HSE "The Control of Vibration at Work Regulations 2005 Guidance on Regulations, Page 64, section 216" illustrate the difficulties in understanding how to interpret the declared emission from tool manufacturers. Figure 12(ii) suggests that a wearable sensor can distinguish between tool performance and operator behaviour in determining the hand transmitted vibration.

The results of this study show a distinct variability at an individual level on the human response to vibration and the potential for a wearable sensor to be able to distinguish more readily the vibration transmitted to the user and resulting risk. Consideration of the human response to vibration as measured with wearable measurement devices may help identify potential hazards and provide more satisfactory assessment of risk when compared to general tool emission assessments.

5. Conclusions

The research findings contribute to the development of wearable vibration exposure monitoring devices as a means of capturing authentic *in-situ* work environment operative exposure. The results presented demonstrate that the assessment of vibration transmitted to the operator using wearable technology is positively correlated with the human response as measured using TTS of vibrotactile response. Therefore, use of vibration exposure assessment on the body represents a useful assessment of vibration exposure hazards and in sight to the working scenarios which contribute to the development of hand-arm vibration over exposure symptoms. The results show that tool vibration emission is potentially an unreliable method of assessing in-use tool vibration exposure as it fails to capture the effects of different operative posture and operative skill have on the human response. The practice of work environment controls based upon static laboratory tool emission test data does not capture the possible range of work-face variables that contribute to operative vibration exposure. This may

contribute to uncertainty relating to the assessment of risk based upon tool vibration emission magnitudes. Such uncertainty is likely to contribute to the continuing reporting of injury and illness associated with excessive and uncontrolled vibration exposure.

6. References

- BJERKER, N., KYLIN, B. & LIDSTRÖM, I.-M. 1972. Changes in the Vibratory Sensation Threshold after Exposure to Powerful Vibration. *Ergonomics*, 15, 399-406.
- F. BROCALA, C. GONZALEZB, M.A. SEBASTIAN Practical methodology for estimating occupational exposure to hand-arm vibrations according to CEN/TR 15350:2013. *Safety Science* 103 (2018) 197–206 Dec 2017.
- BOVENZI, M. 1998. Exposure-response relationship in the hand-arm vibration syndrome: an overview of current epidemiology research. *International Archives of Occupational and Environmental Health*, 71, 509-519.
- BOVENZI, M. 2010. A prospective cohort study of exposure-response relationship for vibration-induced white finger. *Occupational and Environmental Medicine*, 67, 38.
- BRAMMER, A. J., PIERCY, J. E. & AUGER, P. L. 1987. Assessment of impaired tactile sensation. A pilot study. *Scandinavian Journal of Work, Environment & Health*, 380-384.
- BSI 2001a. BS EN ISO 5349-1:2001 Mechanical vibration - Measurement and evaluation of human exposure to hand-transmitted vibration - Part 1: General requirements. British Standards Institution.
- BSI 2001b. BS ISO 13091-1:2001 Mechanical vibrations. Vibrotactile perception thresholds for the assessment of nerve dysfunction. Methods of measurement at the fingertips. BSI Standards Ltd.
- BSI 2013. PD CEN/TR 15350:2013 Mechanical vibration - Guideline for the assessment of exposure to hand-transmitted vibration using available information including that provided by manufacturers of machinery. BSI Standards Ltd.
- BSI 2015. BS EN ISO 5349-2:2001+A1:2015 Mechanical vibration - Measurement and evaluation of human exposure to hand-transmitted vibration - Part 2: Practical guidance for measurement at the workplace.: British Standards Institution.
- BSI 2017. BS EN ISO 8041-1:2017 Human response to vibration. Measuring instrumentation. General purpose vibration meters.
- HSE. 2018. Hand arm vibration in Great Britain. [ONLINE] Available at: <http://www.hse.gov.uk/statistics/causdis/vibration/index.htm>
- GRIFFIN, M. J., BOVENZI, M. & NELSON, C. M. 2003. Dose-response patterns for vibration-induced white finger. *Occupational and Environmental Medicine*, 60, 16.
- HAHN, J. F. 1966. Vibrotactile adaptation and recovery measured by two methods. *Journal of Experimental Psychology*, 71, 655-658.
- HSE. 2005. *The Control of Vibration at Work Regulations 2005 Guidance on Regulations (L140)* [Online]. Health and Safety Executive.
- KAULBARS, U. 1996. Measurement and evaluation of coupling forces when using hand-held power tools. *Central European Journal of Public Health*, 4, 57-58.
- LIDSTRÖM, I. M., HAGELTHORN, G. & BJERKER, N. 1982. *Vibration perception in persons not previously exposed to local vibration and in industry.*, New York, John Wiley & Sons.
- LUNDSTRÖM, R. & JOHANSSON, R. S. 1986. Acute impairment of the sensitivity of skin mechanoreceptive units caused by vibration exposure of the hand. *Ergonomics*, 29, 687-698.
- MAEDA, S., MCLAUGHLIN, J., ANDERSON, L. & BUCKINGHAM, M.-P. 2017. Necessity of wearable personal vibration exposure meters for preventing hand-arm vibration syndrome. *The 25th Japan Conference on Human Response to Vibration*. Nagoya, Japan: Nagoya University Daiko.
- MAEDA, S. & SHIBATA, N. 2008. Temporary threshold shifts (TTS) of fingertip vibrotactile perception thresholds from hand-held tool vibration exposures at working surface. *International Journal of Industrial Ergonomics*, 38, 693-696.
- MAEDA, S., SHIBATA, N., WELCOME, D. E. & DONG, R. G. 2007. Effect of coupling action on temporary threshold shift (TTS) of vibrotactile perception. *11th International Conference on Hand-Arm-Vibration*. Bologna, Italy.
- MAHMOOD, F., FERGUSON, K. B., CLARKE, J., HILL, K., MACDONALD, E. B. & MACDONALD, D. J. M. 2017. Hand-arm vibration in orthopaedic surgery: a neglected risk.

- MALINSKAYA, N. N., FILIN, A. P. & SHKARINOV, L. N. 1964. Problem of occupational hygiene in operating mechanized tools. *Vestnik Akademii Meditsinskikh*, 19, 31-36.
- PAN, D., XU, X. S., WELCOME, D. E., MCDOWELL, T. W., WARREN, C., WU, J. & DONG, R. G. 2018. The relationships between hand coupling force and vibration biodynamic responses of the hand-arm system. *Ergonomics*, 61, 818-830.
- RADZYUKEVICH, T. M. 1969. Interrelation of temporary and permanent shifts of vibration and pain sensitivity threshold under the effect of local vibration. *Gigiena Truda i Professional'nye Zabollevanija*, 14, 20-23.
- SU, A., MAEDA, S., FUKUMOTO, J., MIYAI, N., TAKEMURA, S., YOSHIMASU, K. & MIYASHITA, K. 2016. A Proposal on Neurological Dose-Response Relationship for Inclusion in ISO 5349-1 Documentation to be Used in Tropical Environment. *Acoustics Australia*, 44, 379-382.
- SU, T. A., HOE, V. C. W., MASILAMANI, R. & AWANG MAHMUD, A. B. 2011. Hand-arm vibration syndrome among a group of construction workers in Malaysia. *Occupational and Environmental Medicine*, 68, 58.
- TOMINAGA, Y. 2005. New Frequency Weighting of Hand-Arm Vibration. *Industrial Health*, 43, 509-515.
- YONEKAWA, Y., MAEDA, S., MORIOKA, M., KANADA, K. & TAKAHASHI, Y. 1998. Prediction of TTS for Hand Intermittent Vibration. *INDUSTRIAL HEALTH*, 36, 191-196.

The 26th Japan Conference on Human Response to Vibration (JCHRV2018)
Kindai University, Osaka, Japan
August 22-24, 2018

Is it effective to prevent HAVS by using tool vibration declaration values?

*Setsuo Maeda¹, Mark D. Taylor², Leif Anderson³ Jacqueline McLaughlin³

¹Department of Applied Sociology, Faculty of Applied Sociology, Kindai University
3-4-1, Kowakae, Higashiosaka, Osaka, 577-8502, Japan, E: maeda@socio.kindai.ac.jp

²School of Engineering and The Built Environment, Edinburgh Napier University, 10 Colinton Road,
Edinburgh, EH10 5DT, UK,

³Reactec Ltd., Vantage Point, 3 Cultins Road, Edinburgh EH11 4DF, UK,

Abstract

This study reports the results of an investigation into A(8) based on tool vibration declaration values evaluation effects of hand-transmitted vibration on temporary threshold shifts of vibratory sensation on the finger. The hand-transmitted vibration was applied with an electric tool to the right hand of twelve male subjects with three different working postures. The threshold of 125 Hz vibratory sensation was measured at the tip of the right forefinger before and after vibration exposure. As a result, the TTS following vibration exposure did not have the same values after vibration exposure with three different working postures, even though the A(8) value was the same. The results suggest that the A(8) method based tool vibration declaration values of vibration evaluation in ISO 5349-1 is inappropriate for the prediction of the TTS after hand-transmitted vibration exposure with different working postures.

1. Introduction

In July 2002 the European Union published the Directive 2002/44/EC the Physical Agents (Vibration) Directive (PA(V)D) [1]. It outlines new guidelines for exposure to vibration in the workplace. It sets action and limit values for vibration exposure and it describes the employer's obligations to manage the risk from exposure to vibration. This directive is intended as a guide for the employer who has employees using vibrating hand-held power tools, and also give practical tips regarding what can be done to reduce vibration exposure from hand-held power tools. The Physical Agents (Vibration) Directive was developed from an original proposal made by the European Commission in 1993. This proposal was revised, amended and eventually agreed by Member States and the European Parliament and came into force on 6 July 2002. The Directive lays down the minimum standards for the health and safety of workers exposed to hand-arm vibration and supports the general requirements for improving health and safety that are outlined in

the Framework Directive (89/391 /EEC) [2]. For preventing HAVS, the consideration of A(8) is introducing to the risk assessment. The A(8) is consisting of the vibration total value of frequency-weighted r.m.s. acceleration and the daily Exposure Times. In the work places, the managers of the vibration tool users must consider the risk of the tool works to the employers before real works according to the consideration of A(8). So, the managers need the vibration total value of frequency-weighted r.m.s. acceleration of the individual tool. On the EU Directive, the manufacturers have to declare the magnitude of the individual tool according to the test protocols or to the field measurements for preventing the HAVS in the workplace.

Therefore, in the present study, the experiment performed for clarifying whether the Tool Vibration Declaration Values according to the tool vibration test protocols can assess the risk from the real tool work vibration exposure.

2. Vibration Magnitude of Tools (The responsibility of the manufacturers)

The responsibility of the manufacturers is regulated according to Machinery Directive (98/37/EC) or after December 2009 (2006/42/EC). All manufacturers have to declare the vibration total value of frequency-weighted r.m.s. acceleration of the individual tool. The manufacturers also have to follow the two methods of deriving the vibration total value of frequency-weighted r.m.s. acceleration of the individual tool:

(1) The vibration total value of frequency-weighted r.m.s. acceleration by test protocol;

The hand-held vibration tool manufacturer specifically uses it, and the measurement of the tool vibration value based on the test protocol is performing by International Standards as shown in Table 1, and the manufacturer must give to the users as the declaration value of the vibration value from the hand-held vibration tool before sales of the tool. As for this declaration value, it is necessary to obtain a value comparable even if it measures it in which country of the world by a comparable all over the world a vibration value and the vibration of the hand-held vibration tool should be able to be evaluated all nations and together in a similar way.

(2) The vibration total value of frequency-weighted r.m.s. acceleration by measurement on workplace;

The vibration total value of frequency-weighted r.m.s. acceleration from the hand-held vibration tool cannot be specified according to the vibration value obtained by the test protocol such as International Standards, it is necessary to evaluate the physical value of the vibration tool in the workplace according to the ISO 5349-2 standard [3].

2.1 Manufacturer's declared vibration value by Test Protocol

In order for these measures to be adopted by business entities in which workers use vibratory tools, vibratory tool manufacturers need to measure and declare the " the vibration total value of frequency-weighted r.m.s. acceleration " of such tools.

With regard to vibratory tools, the "the vibration total value of frequency-weighted r.m.s. acceleration" shall be measured and calculated as follows:

Vibration acceleration shall be measured (hereinafter referred to as "vibration measurement") and declared with the following notes in mind after applicable measuring standards are considered in the order of ISO 8662 or ISO 28927-series, ISO 22867, EN 60745, and EN 50144.

3. Procedure of Work Management for Preventing Hand-Arm Vibration Syndrome (The responsibility of the employers and the workers)

The potential hazard or the hazardous property of the office is specified, and it is defined with the working management by a new indicator as devising the method for the removal, and decreasing this. Thus, the working management for the hand-transmitted vibration trouble prevention is an idea of the approach of the precaution-based approach (advance type) for the industrial accident prevention.

The potential hazard or the hazardous property of the office is specified, and it is defined with the working management by a new indicator as devising the method for the removal, and decreasing this. Thus, the working management for preventing the hand-arm vibration syndrome is an idea of the approach of the precaution-based approach (advance type) for the industrial accident prevention. Figure 1 shows the management method for preventing the hand-arm vibration syndrome based on the Daily Personal Vibration Exposure quantity $A(8)$ [4,5,6,7].

Procedure 1:

Understand of the vibration total value of frequency-weighted r.m.s. acceleration of the individual tool

The employers must find out the hazard of the vibration from the usage of the vibration tool in the workplace, and specify the hazardous (the vibration total value of frequency-weighted r.m.s. acceleration of the individual tool) of vibration tool.

Procedure 2:

Calculation of Daily Personal Vibration Exposure ($A(8)$)

The employers have to calculate the $A(8)$ from the vibration total value of frequency-weighted r.m.s. acceleration from Procedure 1 and the Daily Exposure Times.

Procedure 3:

Judgment of the necessity of the Vibration reduction treatment according to the Daily Personal Vibration Exposure Value ($A(8)$)

① Case of $A(8) > 5.0$ (Above exposure limit value)

Take immediate action to bring exposure below the exposure limit value and also perform the control of vibration exposure time and the selection of low vibration tools.

② Case of $2.5 < A(8) \leq 5.0$ (Above exposure action value, but exposure limit value not exceeded)

Implement a program of measures to reduce exposure and risks to a Minimum and also perform the control of vibration exposure time and the selection of low vibration tools.

Procedure 4:

Consideration and Execution of Concrete Vibration reduction treatment according to Daily Personal Vibration Exposure Value ($A(8)$)

The decrease measures of this day amount $A(8)$ of the vibration exposure is examined and executed concretely.

Figure 1 Procedures of Work Management for Preventing the Hand-Arm Vibration Syndrome

3.1 Procedure 1. Understand of the vibration total value of frequency-weighted r.m.s. acceleration of the individual tool

Employers must obtain the vibration total value of frequency-weighted r.m.s. acceleration of the individual tool.

3.2 Procedure 2: Calculation method of Daily Personal Vibration Exposure (A(8))

It is a Procedure 2 to calculate Daily Personal Vibration Exposure quantity A (8) based on the way of thinking about the equivalent vibration acceleration value (Daily Personal Vibration Exposure quantity A (8)) from "the vibration total value of frequency-weighted r.m.s. acceleration" of the vibration tool which employers obtained with a Procedure 1 and "the exposure time (the tool usage time)".

How to calculate daily vibration exposure quantity A (8)

Daily vibration exposure quantity A (8) is calculated from "the vibration total value of frequency-weighted r.m.s. acceleration" that manufacture, import employers declared value, and the exposure time. Daily vibration exposure quantity A (8) is found by the Equation (3) and a 8-hour energy equivalent frequency-weighted r.m.s. acceleration value A (8) is make an easy comparison with the different daily vibration exposure time.

The daily vibration exposure quantity $A(8) = a_{hv} \times (T/8)^{1/2} \quad [m/s^2] \quad (3)$

Where, $a_{hv} [m/s^2]$ is the vibration total value of frequency-weighted r.m.s. acceleration.
 T [time] is the daily vibration exposure time.

And, when the same worker uses more than one vibration tool on the same day, employers have to find the daily vibration exposure quantity A (8) of worker concerned by the Equation (4) from " The vibration total value of frequency-weighted r.m.s. acceleration" of each every tool and so on.

$$a_{hv(rms)} = \sqrt{\frac{1}{T_v} \sum_{i=1}^n (a_{hv(rms)i}^2 T_i)} \quad [m/s^2]$$

The daily vibration exposure quantity

$$A(8) = a_{hv(rms)} \sqrt{\frac{T_v}{8}} \quad [m/s^2] \quad \dots \quad (4)$$

Where, $a_{hv(rms)i}$ is The vibration total value of frequency-weighted r.m.s. acceleration of the work of the i turn; T_i is the tool usage time (vibration exposure time) of the work of the i turn; n is the number of totals of work, T_v is the total vibration exposure time of the work of the n individual.

3.3 Procedure 3: Judgment of the necessity of the Vibration reduction treatment according to the Daily Personal Vibration Exposure Value (A(8))

The employers have to judge the necessity of the decrease the vibration exposure to the

worker from the daily vibration exposure quantity A (8) obtained with a Procedure 2 when daily vibration exposure quantity A (8) exceeds the vibration exposure limit value 5.0 (m/s²).

The employers have to judge the necessity of the decrease the vibration exposure to the worker when it exceeds 2.5 (m/s²) even if the daily vibration exposure quantity A (8) are less than 5.0 (m/s²).

3.4 Procedure 4: Consideration and Execution of Concrete Vibration reduction treatment according to Daily Personal Vibration Exposure Value (A(8))

(1) When daily vibration exposure quantity A (8) exceeds 5.0 (m/s²):

When Daily vibration exposure quantity A (8) exceeds 5.0 (m/s²), the employers have to examine the cause, and furthermore, based on that cause, and the repression of the exposure time, the selection of the vibration tool of the low vibration, have to be done.

(2) When daily vibration exposure quantity A (8) exceeds 2.5 (m/s²):

When Daily vibration exposure quantity A (8) exceeds 2.5 (m/s²), even if it is less than 5.0 (m/s²), the employers have to examine the cause, and furthermore, based on that cause, and the repression of the exposure time, the selection of the vibration tool of the low vibration, have to be done.

4. Validation Experiment of Tool Vibration Declaration Value for preventing HAVS

4.1 Subject

Tool vibration data was obtained from a series of controlled tests performed using standard industrial power tools in a laboratory setting. Twelve healthy male subjects between 18 and 24 years of age with no previous history of vibration exposure were selected as subjects. Alcohol, nicotine and caffeine intake were prohibited prior to and for the duration of the test protocol in accordance with ISO 13091-1.

4.2 Procedures

In order to study the TTS in fingertip vibratory sensation, the vibratory sensation threshold was measured before and after subjects were exposed to hand-transmitted vibration. The experiment was carried out in a sound-proof room. The room temperature was held at about 22°C. Vibration was applied to the right hand through a handle of the electric tool. The subjects were instructed to clasp the handle tightly and constantly with part of the palm and fingers with a real grip force in the appointed posture. The exposure time was 2 minutes. The threshold of 125 Hz vibratory sensation was measured at the index finger of the right hand. Vibration thresholds were determined with the vibrotactile sensation meter (RION type AU-02A). Vibrotactile thresholds were determined by the method of adjustment. In this method, the measurement was performed three times. Thresholds were calculated by the mean values of three measurements obtained less than 30 seconds after the end of the vibration exposure. The TTS was defined as the difference (in decibels) of the vibrotactile thresholds before and after vibration exposure. The experiment was performed on 12 different days.

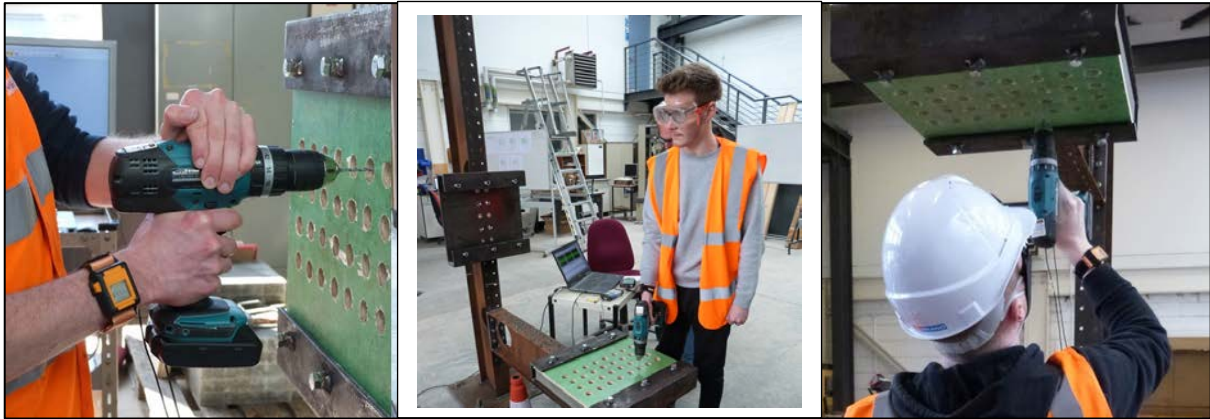


Figure 1 Test postures (i) horizontal, (ii) vertical downwards and (iii) vertical overhead.

The TTS was calculated by the following equation.

$$TTS \text{ (dB)} = VPT_A - VPT_B$$

where, VPT_A (dB) is the Vibrotactile Perception Threshold After tool vibration exposure:

VPT_B (dB) is the Vibrotactile Perception Threshold before tool vibration exposure:

5. Results

The Figure 3 shows the results the relationship between TTS and the vibration magnitude on the tool handle of each subject. This horizontal tool vibration magnitude is usually getting the tool test protocol such as ISO 28927-5 (Impact Drill) standard. From this Figure 3, although the TTS value of each subject is changing, the vibration magnitude of individual subject is almost same number. From the former researcher's results, when the TTS value is increasing, it was clarify that the tool vibration magnitude is increasing. From these evidences, on the Figure 3, when the TTS value is increasing, the tool vibration magnitude might be increasing. But, the tool vibration magnitude is almost the steady tool vibration magnitude. So, from these results, although the tool vibration magnitude is the same, the TTS is increasing. This means that the hand transmitted vibration magnitude is increasing. So, the tool vibration declaration value cannot use the risk assessment for the workers.

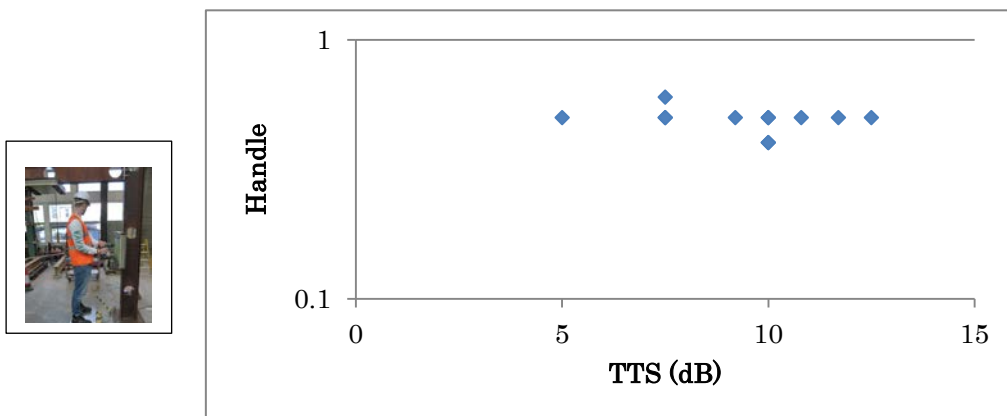


Figure 3 Results the relationship between TTS and the vibration magnitude on the tool handle of each subject at horizontal posture.

Figure 4 shows the results of the relationship between TTS and the vibration magnitude on the tool handle of each subject at vertical downwards posture. The tendency is almost the same with Figure 3. But, the tool vibration magnitude was different with the horizontal posture. So, this means the vibration declaration value from the ISO 28927-5 standard can't apply to the different posture.

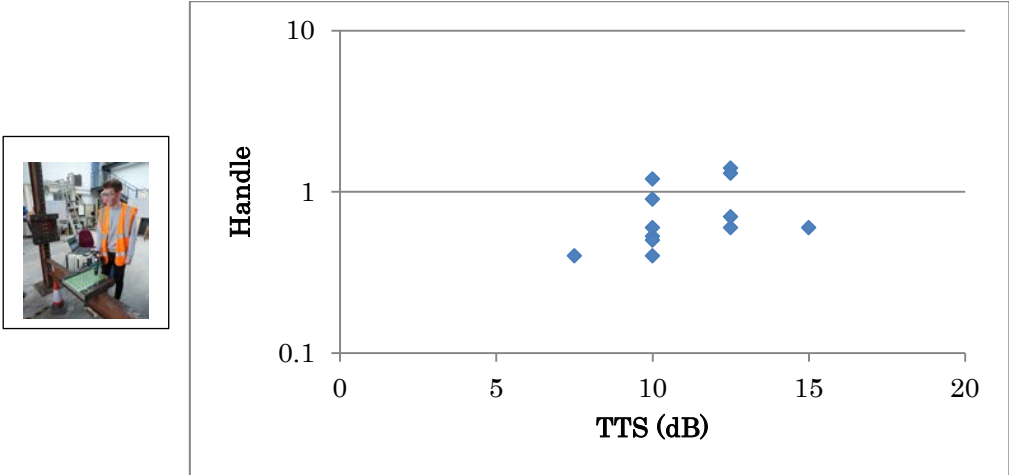


Figure 4 Results the relationship between TTS and the vibration magnitude on the tool handle of each subject at vertical downwards posture.

Figure 5 show the results of the relationship between TTS and the vibration magnitude on the tool handle of each subject at vertical overhead posture. The tendency is almost the same with Figure 3 and 4. But, the tool vibration magnitude was different with the horizontal and vertical downwards postures. So, this means the vibration declaration value from the ISO 28927-5 standard can't apply to the different posture too.

Now days, although many countries are using the tool vibration declaration values by assessing the ISO 28927 series for preventing HAVS, the values from the test protocol can't apply to the all postures such as the real work conditions. So, from these results, the new evaluation method or equipment need to develop for preventing HAVS.

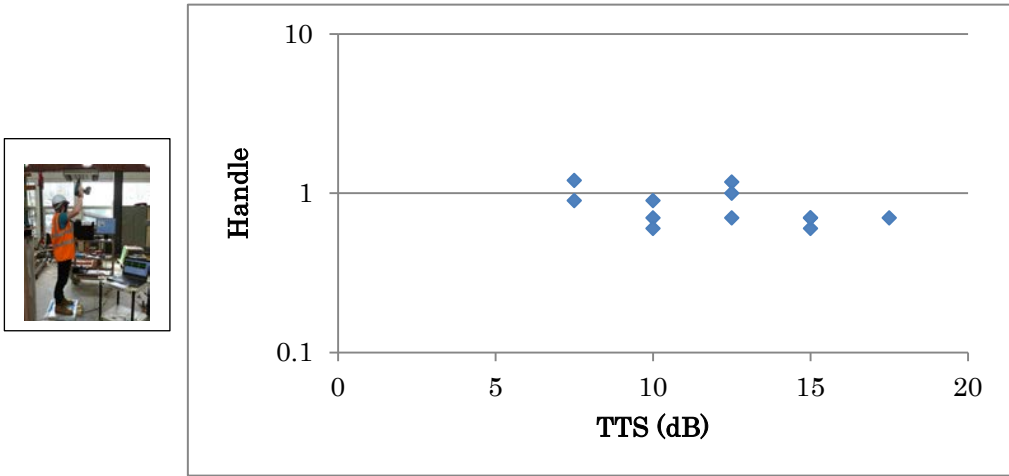


Figure 5 Results the relationship between TTS and the vibration magnitude on the tool handle of each subject at vertical overhead posture.

6. Discussion

From this experiment, although many countries are using the tool vibration declaration values by assessing the ISO 28927 series for preventing HAVS, it is cleared that the values from the test protocol can't apply to the all postures such as the real work conditions.

Former consideration of the Tool Vibration Declaration Value is showing the following Equation.

$$TTS = f(a_{hv}, t)$$

Also, TTS of physiological effect is the same effect from the Tool Declaration Value with the different posture or the any kind of tool use. From these current results, the following is considering.

$$TTS = f(a_{hv} (\text{Posture}), t)$$

At present employers seek to follow guidance within the ISO5349-1 standard for preventing HAVS. Within clause 4.3 of this standard, it is stated that the characterization of the vibration exposure is assessed from the acceleration of the surface in contact with the hand as the primary quantity. Therefore, ISO 5349-1 is assuming that the hand-transmitted vibration exposure magnitude is the tool handle vibration measurement, although the hand-transmitted vibration is affecting by the many factors of Annex D of ISO 5349-1 standard [9] as shown in Figure 6.

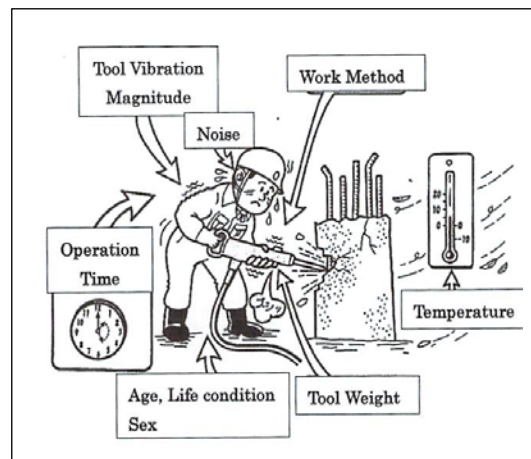


Figure 6 Factors likely to influence the effects of human exposure the hand-transmitted vibration in the working conditions of Annex D of the ISO 5349-1 standard.

In the real work conditions, as shown in Figure 6, many factors of Annex D of ISO5349-1 standard. If we take all affecting factors into the hand-transmitted vibration, the TTS equation might be showing the following equation.

$$TTS = f(a_{hv}(\text{Posture, Coupling force, Direction, Age, Gender, Handle Dimension, Climatic conditions, Disease, Nicotine, Noise, and so on}), t)$$

Many affecting factors individually are investigating by many researchers. From these results, although it is clear that the vibration transmission is changing by the Posture, Coupling force, Direction, Handle Diameter, and so on, they can't show how to take all affecting factors into the

vibration magnitude from the tool handle to human hand, such as hand-transmitted vibration magnitude.

So, from these results, the new evaluation method or equipment need to develop for preventing HAVS to evaluate the hand-transmitted vibration magnitude.

And, in the consideration of real work, when the worker is using the tool continuous using the different posturers, such as (i) horizontal, (ii) vertical downwards and (iii) vertical overhead **as** shown Figure 7(a), as show to Figure 3, 4, and 5, the effects from vibration exposure are changing Figure 7(b).

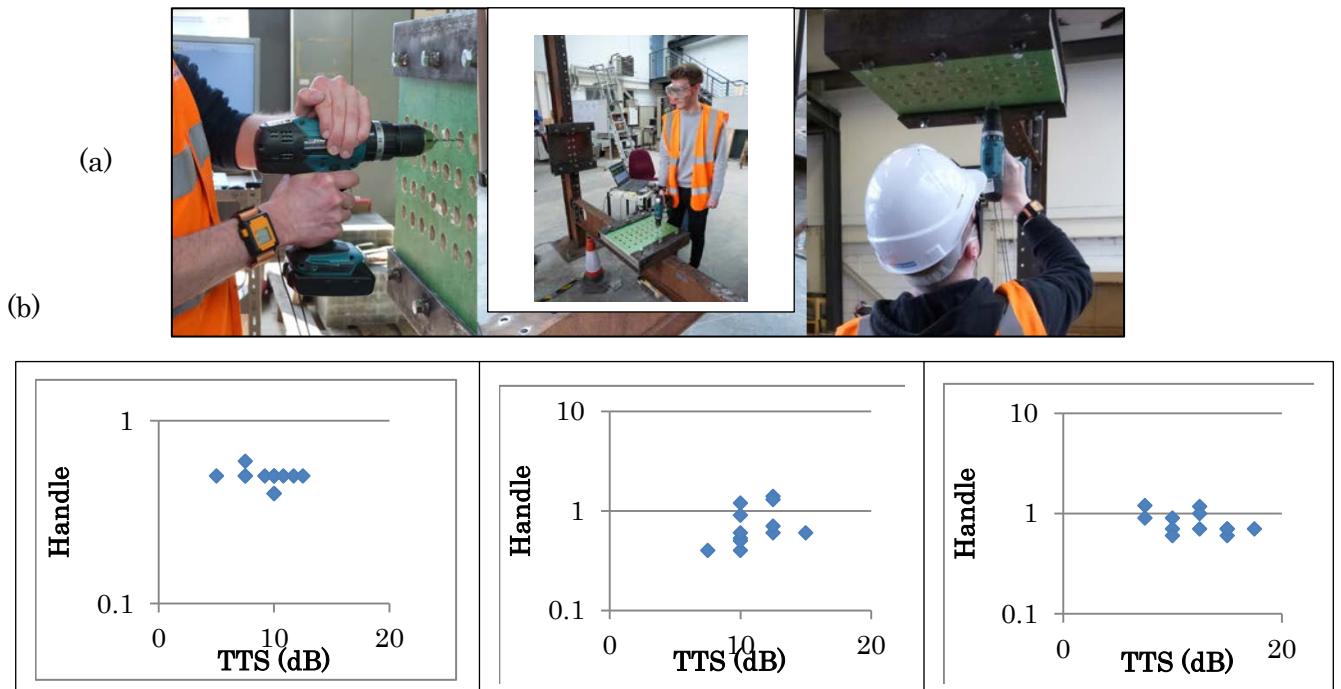


Figure 7 Continuous tool using at work site, such as (i) horizontal, (ii) vertical downwards and (iii) vertical overhead posture.

As shown in Figure 7 (a) and (b), when the worker is using the tool with different postures continuously, the hand-transmitted vibration is supposed to expose in time-variant. In this situation, the tool declaration value can't use for preventing the HAVS. In this real work situation, the continuous monitoring the vibration magnitudes for reducing the risk from the vibration tools in the work site.

Therefore, it is very urgent that the development of the continuous monitoring devices and the hand-transmitted vibration measurement equipment and the relationship between the results of this device measurement values and the physiological data in the world.

7. Conclusions

In the current study, the experiment performed for clarifying whether the Tool Vibration Declaration Values can assess the risk from the real tool work vibration exposure. From these experiments, it was cleared the following things:

- (1) although many countries are using the tool vibration declaration values by assessing the ISO 28927 series for preventing HAVS, it is cleared that the values from the test protocol can't apply to the all postures such as the real work conditions. So, from these results, the new evaluation method or equipment need to develop for preventing HAVS.
- (2) when the worker is using the tool with different postures continuously, the hand-transmitted vibration is supposed to expose in time-variant. In this situation, the tool declaration value can't use for preventing the HAVS. In this real work situation, the continuous monitoring of the vibration magnitudes for reducing the risk from the vibration tools needs for all workers in the work site.
- (3) it is very urgent to develop the continuous monitoring devices and the hand-transmitted vibration equipment and the relationship between the results of this device measurement values and the physiological data in the world.
- (4) For many years, the factors outlined within Annex D of ISO 5349-1 have not been adequately captured when making an assessment of hand-transmitted vibration exposure for the purposes of prevention of HAVS in real work environments. A desire by employers to adhere strictly to the ISO 5349-1 standard may be contributing to inaccurate dose assessments and inferior outcomes for the worker. Although researchers have shown the effects of many of these factors on the vibration magnitude, their results cannot apply directly to evaluate the hand-transmitted vibration magnitude in the real work site.

8. References

[1] Directive 2002/44/EC of the European parliament and of the council of 25 June 2002 on the minimum health and safety requirements regarding the exposure of workers to the risks arising from physical agents (vibration)

[2] Directive 98/37/EC of the European Parliament and of the council of 22 June 1998 on the approximation of the laws of Member States relating to machinery. (Machinery Safety Directive)

[3] International Organization for Standardization (2001) Mechanical vibration — Measurement and evaluation of human exposure to hand transmitted vibration —Part 2:Practical guidance for measurement at the workplace ISO 5349-2.

[4] LSB (Labour Standards Bureau) Issue No.0710-1(2009)

Guidelines for Handling Chain Saws

<http://www.jaish.gr.jp/anzen/hor/hombun/hor1-50/hor1-50-26-1-0.htm>

[5] LSB (Labour Standards Bureau) Issue No.0710-2(2009)

Guidelines for Preventive Measures against Vibration Hazards in Work with Vibratory Tools other than Chain Saws

<http://www.jaish.gr.jp/anzen/hor/hombun/hor1-50/hor1-50-27-1-0.htm>

[6] LSB (Labour Standards Bureau) Issue No.0710-3(2009)

Management and Indication of Vibration Total Value of Frequency-Weighted r.m.s. Acceleration” of the individual tools

<http://www.jaish.gr.jp/anzen/hor/hombun/hor1-50/hor1-50-28-1-0.htm>

[7] LSB (Labour Standards Bureau) Issue No.0710-5(2009)

Promotion of Comprehensive Measures against Vibration Hazards

<http://www.jaish.gr.jp/anzen/hor/hombun/hor1-50/hor1-50-29-1-0.htm>

[8] International Organization for Standardization (2001) Mechanical vibration — Vibrotactile perception thresholds for the assessment of nerve dysfunction —Part 1:Methods of measurement at the fingertips. ISO 13091-1.

[9] International Organization for Standardization (2001) Mechanical vibration measurement and evaluation of human exposure to hand-transmitted vibration - Part 1: General requirements. ISO 5349-1.

The 26th Japan Conference on Human Response to Vibration (JCHRV2018)

Kindai University, Osaka, Japan

August 22-24, 2018

Effects of Whole-Body Vibrations on Lane Keeping Performance**Amzar Azizan, Husna Padil**

Universiti Kuala Lumpur-Malaysian Institute of Aviation Technology

Sepang, 43900, Malaysia

Abstract

Despite the fact that a lot of research has been carried out at the characterization of the effects of whole-body vibration on seated occupants' comfort, there's very little scientific knowledge of drowsiness caused by vibration. There also are much less verified measurement methods available to quantify whole body vibration-induced drowsiness in vehicle occupants. This study, therefore, set out to evaluate the effect of vibration on drowsiness. Here, twenty male volunteers had been recruited for this experiment. Data for this study have been gathered from 10-minutes simulated driving sessions under no-vibration conditions and with a vibration that had been randomly organized. Gaussian random vibration, with 1-15 Hz frequency bandwidth at 0.2 ms^{-2} r.m.s. for 30-minutes was used. During the driving session, volunteers have been required to obey the speed limit of a 100 kph and keep a consistent position in the left-hand lane. A deviation in the lateral position has been recorded and analyzed. Additionally, volunteers also rated their subjective drowsiness by means of the Karolinska Sleepiness Scale (KSS) scores every five-mins. The evidence from this study indicates that the role of vibration in promoting drowsiness that can be observed from driving impairment following 30-mins of exposure to vibration.

1. Introduction

One of the most prominent causes of accidents on main roads and highways is drowsy driving, and it was reported that 1 in 5 traffic-related injuries is caused by drowsy driving [1]. In response, the EU has introduced a new regulation on sleepiness during driving, specifically among drivers suffering from sleep apnoea. According to this new regulation, candidates for driving license and drivers that suffer from moderate to severe obstructive sleep apnoea will need medical recommendations from medical practitioners prior to applying or renewing their driving license [2]. This shows that the authority is considering the severity of drowsy/sleepy driving and equates it to drunk driving. Meanwhile, there is still a limited investigation of drowsiness caused by vehicular vibration even though there are some studies that have shown a probable relationship between exposure to vibration and reduction of the level of wakefulness [3]–[5]. As a result, there is still no requirement for the automotive industry to limit vibration induced drowsiness.

Past studies have shown the drowsiness could significantly affect a driver's concentration and his/her overall performance which eventually, can compromise road safety [6]–[8]. Such drowsiness could be caused by a range of reasons, including monotonous driving, nighttime driving or influences of drugs or alcohol. However, there is still a limited description of the components of drowsiness that is caused by exposure to vibration.

There are limited studies that have tested the assumption on the link between vibration amplitude and vibration frequency of vehicle occupant and drowsiness. One of these reasons is that there is little quantitative information on drowsiness since it is a multifactorial phenomenon. Meanwhile, there are studies that have shown the correlation between vibration with different physiological reactions of the human body including coronary heart rate and lower back pain [9], [10]. Vibration could act as a stressor and affect muscle and neurological features, [11], [12]. In the context of the automotive industry, vibration can occur on a car seat structure due to various reasons, including road surface and vehicle powertrain. For a seat structure in a vehicle, the vibration modes transmitted to the seat structure, comprising of correspondence mode shapes and resonant frequency, occur at a frequency below 60 Hz [13] while for the human frame, the basic resonance occurs at a frequency less than 15 Hz [14]. It is widely known that the transmitted vibration affects the human perception and ride comfort [14]–[16]. The ISO 2631-1 (1997) international standard has been used efficaciously to assess human exposure to whole-body vibration. The “Equivalent Comfort Contour,” international standard has been developed to assess human body discomfort. On the other hand, the “Equivalent Drowsiness Contour” has still not developed yet [17].

As a result, there is a broad scope to outline how drivers' drowsiness levels are affected by the vehicle, particularly seat vibration. There have been no particularly working that has ranked the significance of the factors that cause co-driving force drowsiness. Thus, this study will only focus on drowsiness caused by vibration. According to past study, sleepiness or drowsiness refers to the state between being awake and asleep [18]. Many past studies have claimed that one's ability to drive effectively could be affected by drowsy driving [19], and in line with past examinations on car control and drowsiness, there is a close link between lane position variability and drowsiness. Here, the standard deviation of lateral position (SDLP) is considered as the common lateral role standard deviation as it reflects on how many times a vehicle weaves and the increase in lane variability could cause lane crossing into the next traffic lane.

As discussed above, there is still no simulated driving experiment that has tested the drowsiness caused by vehicle vibration despite the various studies that showed the links between driving performance and drowsiness. In this regard, it is imperative to analyze the possibility of applying simulated driving to detect drowsiness caused by vibration. Consequently, the primary aim of this study in to examine the effects of vibration on human drowsiness level using both objective (Simulated driving test) and subjective (Karolinska Sleepiness Scale) measurement methods.

2. Experiment setup

2.1 Volunteers

This study involved twenty young males ($n=20$) who have a mean age of 23.0 ± 1.3 . These volunteers were selected randomly from students of a university college. The volunteers need to have a regular or corrected-to-everyday vision and no history of low back pain (LBP). Their demographic information was recorded at enrolment. Their height was 168.2 ± 4.0 cm, and weight was 64.2 ± 12.2 kg with the average of BMI 22.6 ± 2.54 kg/m². The Pittsburgh Sleep Quality Index (PSQI) was used to screen the volunteers based on their sleep excellence. Those with poor sleep pleasant index (PSQI > 5) were excluded from the study.

2.2 Ethical considerations

The volunteers were given verbal and written explanations on the contents and aims of the experiment before starting. The volunteers were also told that they have the right to choose not to participate in the experiment and that their input during the experiment will remain confidential. In this regard, after they were briefed on the experimental procedure and the laboratory facilities have been introduced to them, each volunteer was required to fill in an informed written consent form. Meanwhile, the experimental protocol was sent to the RMIT college Human Research Ethics Committee for review and accreditation. It was approved with the Approval number: EC 00237.

2.3 Test setup

This study has developed an experimental setup for drowsiness assessment. Here, is a mid-sized sedan car seat with adjustable headrest was used for the experiments. The seat was established on a cast aluminium table (2 m x 1.2 m x 1.2 m), and the table was set up on 4 air mountings (regulated to 20 psi). The angle of the seat's inclination was set at 15° to the vertical axis. A servo-managed hydraulic actuator (5 kN), fixed vertically on the corner of the desk provided the table's excitation input force. The off-centre excitation will provide multi-axial input power in specific orientations as well as supply usual vibration similar to those generated by the vehicle seat mountings. Furthermore, we have designed the vibration table to be dynamically rigid at frequencies below one hundred Hz to prevent any interaction with automobile seat structural dynamics. In this regard, the total transmitted vibration to each volunteer has been conducted based on ISO 2631-1 (1997) before the drowsiness was measured. [17].

The measurement was done to modify each volunteer's desired hydraulic input force to be 0.2 ms⁻²r.m.s. We have used two tri-axial accelerometer pads (SVANTEK SV-38V version) to measure the vibration transmitted to the body of a human volunteer t the seat cushion and the seatback [20] while to get the complete frequency weighted transmitted vibration to the seated human body, we used the SV 106 Human Vibration exposure (HVE) meter (analyzer), which was connected to the accelerometer pads. In the meantime, the total frequency-weighted transmitted vibration to the seated human frame calculated by the HVE analyser through the HVE analyzer uses the weighting factors (ω_k , ω_d , ω_c) and multiplication factors.

2.4 Objective measurements

The York driving simulator software (York pc technology, Kingston, Ontario, Canada) was used to examine the Volunteers. A past study [21] has determined the stimulator as an ecologically valid study tool to measure psychomotor performance. The simulator comprises of a personal computer, a 40-inch screen and peripheral guidance wheel, accelerator and brake accessories. During the experiment, the volunteers were shown a customized advanced driving scenario ahead view from the driver's seat. The driving simulation contains a cross-country motorway, with two lanes in each path. The volunteers were instructed to maintain a steady position in the left traffic lane at some point of the test and to maintain a steady constant velocity of 100 km/hour. The outcome variables which were measured using the simulator present the deviation from the centre of the lane (SDLP). The varying results show whether the volunteers were able to conduct the test accurately based on the instruction given.

2.5 Subjective measurements

The Karolinska Sleepiness Scale (KSS) was used to assess the subjective drowsiness level [22]. At each 5-mins interval during the simulated driving mission, the researcher had prompted the volunteers to use the word “KSS” to provide a subjective score based on the scales that are visible to them subsequent to the reveal screen. In this regard, the volunteers were given the practice to use of the scale prior to the experiment. The scale comprises of the following ratings: 1 = extremely alert, 2 = very alert, 3 = alert, 4 = instead alert, 5 = neither alert or sleepy, 6 = some signal of sleepiness, 7 = sleepy, however no effort to live wide awake, eight = sleepy, some attempt to stay wide awake, nine = very sleepy, splendid attempt to stay unsleeping [22].

2.6 Experiment protocols

The site of the experiment is a laboratory with temperature and light control (21°C - 23°C, < 70 lux) with a noise level of below 60 dB. For the experiment, the volunteers arrived at the laboratory at 0800 hrs. They had a normal sleep on the previous night and had eaten a light breakfast. It is imperative for the volunteers to not drink any caffeinated or alcoholic drinks. An initial screening session was conducted to assess the volunteers' to determine whether they are fit to join the study. They were also screened using the Epworth Sleepiness Scale (ESS) to detect any sleep abnormalities. Those with score > 10 were excluded as this suggests excessive daylight hours sleepiness.

The experiment began at 0830 hrs. The experiments were conducted in two weeks, wherein each week, the volunteers completed either one of the separate test condition [baseline (no-vibration condition) and with-vibration condition] in a randomized cross-over design. Each test was conducted one week apart and to prevent order-related influences, the condition orders were randomly ordered. Moreover, to decrease the learning effect, each volunteer went through 10-mins exercise session prior baseline and with-vibration situations to acquaint themselves with the simulator interface. The experiments were conducted on all volunteers at the similar time of the day. In the with-vibration condition, volunteers were required to drive with no vibration for 10-minutes as well as sitting for 30-minutes with exposure to vibration. They were exposed to a Gaussian random vibration with the bandwidth frequency of 1-15 Hz. A steady total acceleration of at 0.2 ms⁻² r.m.s was transmitted to the human body. Subsequently, the subjective sleepiness of volunteers was rated using the KSS prior to the vibration exposure, at each five-min of vibration and after vibration exposure. The score was initiated through the “KSS” pronounced by the check chief. The volunteers went through a 30-mins sitting with the same process and sitting arrangement as the with-vibration condition. However, at this time, there was no vibration exposure. Afterwards, the volunteers were required to drive for another 10-minutes right after a 30-minutes sitting. In this regard, the whole length of every condition (no-vibration and with-vibration) is 50-minutes.

3. Results

In total, 20 volunteers had completed the experiment. The Epworth Sleepiness Scale (ESS) between baseline (no-vibration situation) and with-vibration condition at the start of the test found no significant difference in alertness level. This section presents the results of the assessment that used the objective performance index (SDLP) and subjective sleepiness scale (KSS) between no-vibration and with-vibration condition. Figure 1 presents the results of Standard Deviation of Lane position (SDLP) where each panel in the figure presents the SLDP average and standard error of the mean (SE) prior and after 30-minutes of exposure to vibration and sitting (no-vibration). As shown by the figure, there

was no significant difference in SDLP between before no-vibration condition and before with-vibration condition ($P > 0.05$). Meanwhile, compared to the baseline (no-vibration condition), the SDLP measure between before exposure within the first 10 minutes of driving, as well as after exposure to vibration indicated that being exposed to vibration for 30-minutes had significantly impacted the volunteers' lane maintaining performance. After being exposed to vibration for 30-minutes, there was an extensive acceleration of lane variability or the deviation from a lateral function from (mean \pm SE: 23.6 ± 0.02 to 26.2 ± 0.01 ; $P < 0.05$). In this regard, the 2.6 cm increase of the variability showed poor lane control among volunteers. Based on the analysis of lane variability, the volunteers found it hard to maintain the vehicle in the middle of the left-hand lane when their alertness was low in response to being exposed to vibration. On the other hand, for the baseline (no-vibration condition) where lane position variability was decreased from (mean \pm SE: 23.5 ± 0.01 to 22.8 ± 0.01 ; $P > 0.05$), there was no significant difference. From both conditions (no vibration and with-vibration) repeated-measures evaluation, we could observe that there is a considerable difference among group variations ($P < 0.05$). This shows that vibration has a significant influence on drowsiness level as measured by SDLP.

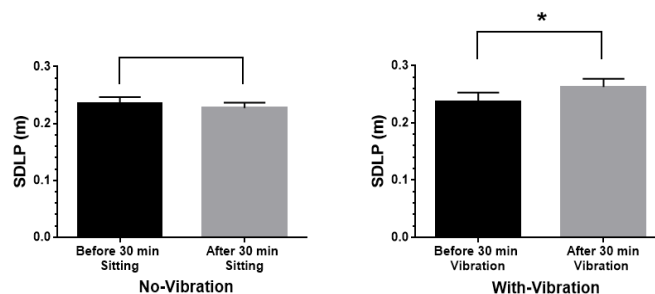


Fig.1. The bar graph presents the mean (\pm SE) of SDLP for twenty volunteers in no-vibration condition and with-vibration condition. The measurement was obtained 10 minutes driving before and 10 minutes driving after 30 minutes sitting in no-vibration and 30 minutes sitting with-vibration. We have observed that there is a significant increase in lane position variability (SDLP) ($P < 0.05$) in the with-vibration condition. These differences, in relation to the legal limits for driving, were +2.4 cm (BAC 0.05%) [23]. These changes showed that after being subjected to vibration for 30 minutes of vibration, * $P < 0.05$, the volunteers were unable to maintain a straight position.

For the first 10 minutes, there was no significant distinction found in both conditions with KSS score (mean \pm SE: 3.58 ± 0.29 in with-vibration condition and 3.16 ± 0.19 in no-vibration circumstance). Figure 2 shows that there is an apparent decrease in the degree of alertness as demonstrated by the gradual increase in the rating of subjective sleepiness throughout the path of exposure to vibration. After being exposed to vibration after 15-mins, the onset of drowsiness faster with KSS value of (mean \pm SE: 6.11 ± 0.32) while the most effective KSS value (mean \pm SE: 4.84 ± 0.32) was shown by the no-vibration condition. KSS value accelerated significantly following 30-minutes, exposure to vibration than without vibration (mean \pm SE: 7.26 ± 0.40 one and 5.16 ± 0.29 respectively; $P < 0.05$).

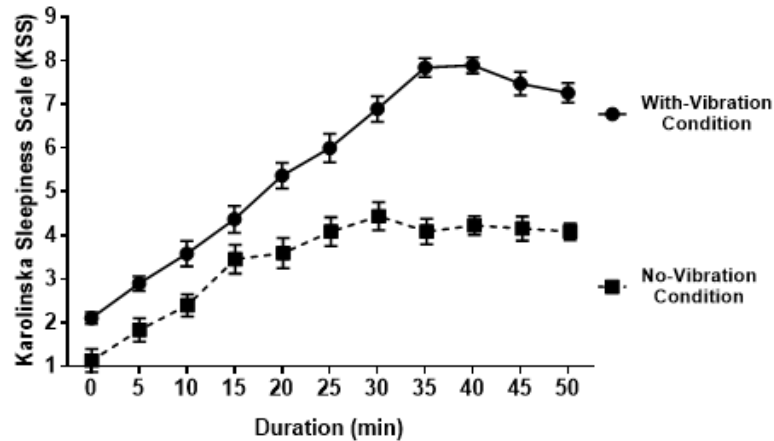


Fig.2. The figure presents the average score of subjective sleepiness scale (KSS) plotted against time for twenty volunteers in no-vibration condition and with-vibration condition. There were no significant changes observed for both states ($P > 0.05$) prior to the experiment. On the other hand, the subjective sleepiness scales for all volunteers have shown there was a significant increase after exposure to vibration ($P < 0.05$). This shows that the level of alertness was reduced after vibration exposure.

4. Conclusion

This study has characterized that vibration is a critical source of driver drowsiness. This study supports that the exposure to vibration could significantly influence the subjective sleepiness levels, as well as human psychomotor and lapse of attention. In this regard, the lane keeping the performance of the driver (SDLP) is affected by the exposure to vibration. Based on the result, the low excitation vibration at $0.2 \text{ ms}^{-2} \text{ r.m.s}$ increased SDLP by 11%. This is similar to the SDLP of drivers under the influence of alcohol (BAC .05%) [23]. This supports that SDLP is a highly reliable, steady approach to measure riding performance. Moreover, KSS measures the formulation of drowsiness which shows that the reduction in the alertness level as a result of vibration is more apparent in vibration comparison compared to the no-vibration situation. Additionally, the high correlation can be located among KSS and SDLP. Hence, this research can help the development of realistic and applicable guidelines to prevent vibration exposure in the automobile industry to decrease road injuries. This will complement the present ISO 2631-1 to extend these recommendations to evaluation and establish the thresholds and safe limits for drowsiness-inducing vibration.

5. References

- [1] Horne J A and Reyner L A (1995), Sleep-related vehicle accidents. *Br. Med. Journal* 310, 565–567.
- [2] Commission. EU Commission Directives. *Off. J. Eur. Union* 2012, 4, 2012–2015.
- [3] Satou Y, Ando H, Nakiri M, Nagatomi K, Yamaguchi Y, Hoshino M, Tsuji Y, Muramoto J, Mori M, Hara K and Ishitake T (2007), Effects of short-term exposure to whole-body vibration on wakefulness level. *Ind. Health* 45, 217–223.
- [4] Satou Y, Ishitake T, Ando H, Nagatomi K, Hoshiko M, Tsuji Y, Tamaki H, Shigemoto A, Kusano M, Mori M and Hara K (2009), Effect of short-term exposure to whole-body vibration in humans: the relationship between wakefulness level and vibration frequencies. *Kurume Med. J* 56, 17–23.

- [5] Azizan A, Fard M, Azari M F, Benediktsdottir B, Arnardottir E S, Jazar R, and Maeda S (2016), The influence of vibration on seated human drowsiness. *Ind. Health* 54, 296–307.
- [6] Kamdar B B, Kaplan K A, Kezirian E J, and Dement W C (2004), The impact of extended sleep on daytime alertness, vigilance, and mood. *Sleep Med* 5, 441–448.
- [7] Larue G S. Predicting effects of monotony on driver's vigilance (2010) Thesis-queensl. Univ. Technology.
- [8] Akerstedt T, Peters B, Anund A, and Kecklund G (2005), Impaired alertness and performance driving home from the night shift: a driving simulator study. *J. Sleep Res* 4, 7–20.
- [9] Callaghan J P and McGill S M (2001) Low back joint loading and kinematics during standing and unsupported sitting. *Ergonomics* 44, 280–294.
- [10] Vicente J, Laguna P, Bartra A, and Bailón R (2011), Detection of Driver's Drowsiness by Means of HRV Analysis. *Comput. Cardiol* 38, 89–92.
- [11] Oliveira C G D and Nadal J (2004), Back muscle EMG of helicopter pilots in flight: effects of fatigue, vibration, and posture. *Aviat. Space. Environ. Med* 75, 317–322.
- [12] Giminiani R. Di, Masedu F, Tihanyi J, Scrimaglio R and Valenti M (2013), The interaction between body position and vibration frequency on acute response to whole body vibration. *J. Electromyogr. Kinesiol* 23, 245–521.
- [13] Fard M (2011) Structural dynamics characterization of the vehicle seat for NVH performance analysis. SAE Tech. Paper, 1–12.
- [14] Griffin M J (1990) Handbook of Human Vibration. Academic Press Limited, London.
- [15] Kitazaki S and Griffin M J (1997), A modal analysis of whole-body vertical vibration, using a finite element model of the human body. *J. Sound Vib.* 200, 83–103.
- [16] Baik S (2004) A study on the characteristics of vibration in seat system. *KSCE J. Civ. Eng* 8, 135–139.
- [17] International Standard (1997), ISO 2631-1 Mechanical vibration and shock - Evaluation of human exposure to whole-body vibration.
- [18] Lal S K and Craig A (2001), A critical review of the psychophysiology of driver fatigue. *Biol. Psychol* 55, 173–194.
- [19] Gander P H, Nguyen D, Rosekind M R and Connell L J (1993), Age, circadian rhythms, and sleep loss in flight crews. *Aviat. Sp. Environ. Med* 64, 189–195.
- [20] Azizan M A and Fard M (2013), Effects of vehicle seat dynamics on ride comfort assessment in International Congress on Noise and Vibration.
- [21] Chung F, Kayumov L, Sinclair D R and Edward R (2005). What is the driving performance of ambulatory surgical patients after general anesthesia?. *Anesthesiology* 103, 951–956.
- [22] Gillberg M, Kecklund G and Akerstedt T (1994), Relations between performance and subjective ratings of sleepiness during a night awake. *Sleep* 17, 236–241.
- [23] Verster J C and Roth T (2011), Standard operation procedures for conducting the on-the-road driving test, and measurement of the standard deviation of lateral position (SDLP). *Int. J. Gen. Med* 4, 359–371.

The 26th Japan Conference on Human Response to Vibration (JCHRV2018)

Kindai University, Osaka, Japan

August 22-24, 2018

Effect of magnitude of vibration on driver drowsiness by HRV measures**M.H.U. Bhuiyan^{*a}, M. Fard^a and S. R. Robinson^b**^a School of Engineering, RMIT University, Bundoora, Australia;^b School of Health and Biomedical Sciences, RMIT University, Melbourne, Australia**Abstract**

This study focused on the influence of vibration magnitudes on driver drowsiness. In this experimental study, the vibration levels (rms acceleration) were adjusted in low level (0.1 ms^{-2}) and medium level (0.2 ms^{-2}) at 4-7 Hz frequency range. Both physiological (Heart Rate Variability, HRV) measurement and subjective assessment (Karolinska Sleepiness Scale, KSS) conducted to evaluate the effect of vibration on driver drowsiness. The statistical significance estimated among the groups of different vibration level and control condition (no vibration). The result of this study showed that a significant increase of KSS score ($P=0.0001$) and LF/HF ratio ($P=0.0191$) in the medium level vibration compared with no vibration. The growth of LF/HF ratio, the balance of sympathetic and parasympathetic nervous activity of autonomic nervous system, indicates the enhancement of drowsiness. The outcome of this study is a preliminary sign on the effect of vibration magnitude on driver drowsiness.

1. Introduction

The economic growth in any country is governed by the development of transportation systems. Motor vehicle crashes owing to driver drowsiness is one of the most important safety problems in the automobile industry. Drowsiness, a state of somnolence can effect on regular activity as well as physical and mental condition of human body [1]. Human requires sustained cognitive effort and attention during driving a vehicle. Because, drowsiness compromises a change of cognitive status, it will effect on driver alertness and vehicle control [2]. According to the Transport Accident Commission, fatigue (including drowsiness), is responsible for 16-20% of all motor vehicle crashes in Victoria, Australia. A Federal Government inquiry reported that fatigue-related road accidents also cost around \$3 billion every year in Australia [3]. In US, approximately 56,000 traffic accidents are caused by driver drowsiness every year (The National Highway Traffic Safety Administration (NHTSA)). A study

of AAA foundation pointed out that 21% of fatal crashes were involved by a drowsy driver from 2009 to 2013 in US [4]. The drowsy driving expenditures around \$16.4 billion per year in terms of property damage, health claims, and productivity lost in the North America [5]. Moreover, driver drowsiness is as dangerous as blood alcohol concentration (BAC) level. If a person awake for 17 hours, his drowsiness level is equivalent to BAC level of 0.05% and it rises to 0.1% in 28 hours [6]. The preceding statistics may not justify the vulnerability of drowsiness, the accidents attributed by driver drowsiness might be more devastating than the statistics revealed. Therefore, it is essential to figure out the inducing factor of drowsiness to develop the countermeasures to reduce fatal accidents.

Fatigue and drowsiness are denotes to the physical state of tiredness or weariness, lack of consciousness and drop of cognitive and mental state caused by exertion. In addition, human exhibits physical, psychological and physiological responses when exposed to vibration [7]. The transmission of vehicle vibration to the occupants has a large impact on human comfort, performance, and health [8]. The engine, vehicle condition, environment and the interaction with the road surface are the main source of generating vehicle vibration. It excited the chassis structure, seat, steering and transmitted into the driver body. The sensation of vibration can be evaluated by assessing the human sensitivity to vibration in terms of different magnitudes, frequencies, directions, and durations of vibration [9]. When human exposed to whole body vibration (WVB), his performance has been found to be most severe in the frequency range of 1 to 2 Hz in the x and y direction and 4 to 8 Hz in the z direction [10]. The European Health and Safety Institutes noticed that frequency-weighted rms acceleration varies from 0.4 ms^{-2} to 1.2 ms^{-2} for trucks in the z direction [11]. The ISO 2631-1 (1997) suggested that frequency weighted rms accelerations above 0.50 ms^{-2} (approximately) for 8 hour period can be effects on human health. Moreover, Howarth et al. observed that the magnitude of human sensation increases approximately linearly with acceleration magnitude for WBV [12]. It has been proven that an increase in vibration magnitude will lead to increased human discomfort level [13]. As the drivers are frequently exposed to vibration for a long time, the researcher have shown interest to evaluates the effect of vibration characteristics on the driving performance[14]. Satou et al.[15, 16] revealed that short-term exposure to vibration reduces the wakefulness level of the occupants. Newell et al.[17] exhibited that participants are more fatigued and reduced their performance after exposed to WBV. Nonetheless, the vibration acceleration, frequency, duration with fatigue and drowsiness has been considered without adequate research. This study aims to identify the effects of vehicle vibration magnitude on driver drowsiness.

In order to assess the level of drowsiness, researchers have been used a diverse range of physiological, behavioral, vehicular controls and subjective methods. It has been reported that vibration influences human physiological reactions such as heart rate, blood pressure and respiration [18]. Electroencephalography (EEG) is the most reliable and commonly used method to measure human brain activity. It has been classified in various frequency bands: delta band corresponding to deep sleep, theta band related to light sleep or drowsiness, whereas alpha and beta band represents alertness [19]. However, this method is challenging in a real-world driving conditions due to the complexity of the EEG measurement system. In contrast, Heart Rate Variability (HRV) is an extensively used non-invasive technique to evaluate driver drowsiness [20, 21]. It measures the variations of beat-to-beat interval of the heartbeats. It regulates the interactions between sympathetic and the parasympathetic nervous systems, two opposing arms of the autonomic nervous system (ANS) [22]. Typically, sympathetic activity tends to increase heart rate, while parasympathetic activity decreases the heart rate [23]. The RR intervals have been analyzed mostly in time-domain and frequency-domain to identify drowsiness. In the time domain, the change of mean RR, SDNN, RMSSD, NN50 and pNN50 are the most common indicators of driver drowsiness [20, 24, 25],

whereas frequency domain comprises mostly LF, HF and LF/HF ratio [26]. The low-frequency (LF), and high-frequency (HF) represents the sympathetic and parasympathetic activities respectively and LF:HF ratio denotes the sympathovagal balance of ANS. The effect of vibration on driver fatigue investigated by Jiao et al. [27]. They observed that 6 Hz vibration influenced by both the sympathetic and parasympathetic activities; nevertheless, 1.8 Hz vibration dominated by only parasympathetic activity. Recently, Zhang et al.[28] reported that low frequency vibration (4-7 Hz) significantly increases driver drowsiness. They found higher values of LF/HF ratio, lower values of RMSSD (ms) and pNN50 (%) in vibration condition compared with no vibration. On the contrary, a significant decrease of LF/HF ratio, LF and increases in HF detected when subject is in drowsy state during monotonous driving [29]. Therefore, the authors investigated combined physiological & subjective measurement to detect driver drowsiness. LF, HF, LF/HF ratio and KSS score were used to estimate drowsiness and compared between all the groups (low, medium and control conditions).

2. Experimental Method

2.1 Participants

The participants are primarily selected from healthy university students (males/ females) with mean age: 23.0 ± 2.5 years. Participants were scrutinized based on good physical and mental health conditions, no muscular and cardiovascular related problems. Particularly, they had to maintain a normal sleep pattern at least 7 h regular sleeps. They had to refrain from consuming any type of alcoholic, caffeinated beverages and medications that induce sleepiness within last 24 hours. Ten (10) healthy participants were participated voluntarily to conduct the experiment between 9 PM to 1 AM. However, three participant's data were excluded from this study due to disturbance during data recording.

2.2 Ethical consideration

In this study, the participants were participated in a voluntary basis. The purpose of the study, experimental procedure, their responsibilities and tasks were explained to the participants. They were committed to keep the outcomes of the study confidential and a written consent form collected accordingly. Nevertheless, they had the right to withdraw their participation at any time during the experiment. The protocol of this study was reviewed and approved by RMIT University Human Research Ethics Committee (Approval Number: EC 00237).

2.3 Vibration level adjustment

Before commencing the experiment, the total transmitted vibration (seat pan and backrest) measurement have done according to ISO 2631-1 (1997) [30] for each participants by using the method reported by Fard et al. [31]. Two tri-axial accelerometer pads (SVANTEK SV-38Vmodel) were used to measure the transmitted vibration to participants at both the seat cushion and seatback. The measurements were carried out to adjust the hydraulic input force for the participant based on required vibration magnitudes (rms acceleration).

2.3 Experimental procedure

This experimental set-up is similar to real car driving, where vibration can transform from the vehicle body to the human body. The participants were selected for the experiment at the time of their regular bed time. A wireless Polar H7 heart rate monitoring sensor made by Finland was attached firmly to the participant's chest according to the instruction of the device manual. After that, they were instructed to lounge comfortably in a vehicle seat that mounted with a vibration platform. They were asked to rate their present sleepiness state according to KSS scale (1=extremely alert to 10=extremely sleepy) [32]. They put on an earmuff to eliminate the surrounding noise. They were instructed to maintain left lane, focused and carried out the driving task for next 45 minutes by York Driving Simulator, Canada. The driving simulator displayed a scenic two-way highway road view considered a countryside environment with widely spaced trees, few roadside objects like traffic signs, lamp post and a constant high speed (130 Km/h) to create a monotonous highway driving. The laboratory room temperature was controlled at 24°C with low lighting environment. After 45 minutes experiment, they were again asked to rate their present KSS level.

2.4 Experimental set up

A schematic diagram of the experimental setup in the laboratory is shown in Figure1. A mid-sized sedan car seat was mounted on a cast aluminium platform (2.0 m×1.2 m×0.3m) along with four air mountings (regulated to 20 psi). The steering wheel and the vehicle control systems were coupled with the platform and controlled by the driving simulator. The platform was controlled by a vertical hydraulic actuator located under the platform and away from the center. It can generate similar type of vibration that an occupant experienced in regular vehicles in x, y and z-direction. A 32-inch monitor was located in front of the participant to display the driving scenario.

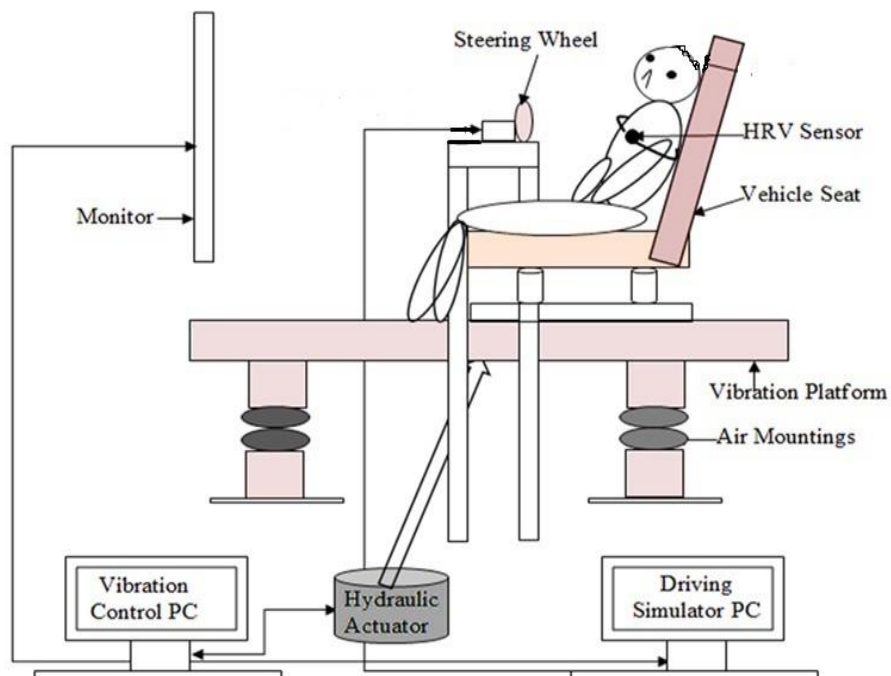


Figure1: Schematic diagram of the experimental set up.

2.5 HRV recording and signal analyses

Heart rate variability (HRV) is the physiological sensations that measured the deviation in the beat-to-beat interval called RR Interval (RRI), The values of RRI were recorded in a smart phone app through the Bluetooth technology of the HRV monitor. The date were computed using Kubios HRV software[33]. RR spectrum is estimated in the Welch's periodogram method. In this method, the spectrum is segmented into 300s window with 50% overlapping to decrease the leakage effect. The spectrum is obtained by averaging the FFT spectra of these segments and detrended using the smooth-ness prior method ($\lambda=500$) for removing any disturbance in low frequency components. An automatic artifact correction used to eliminate any artifacts from RR spectrum. For frequency-domain analysis, the data were segmented into 15 samples using three minutes successive segmentation. The frequency bands were calculated using the range 0 to 0.04 Hz for very low frequency band (VLF), 0.04 to 0.15 Hz for low frequency band (LF), and 0.15 to 0.4 Hz for high frequency band (HF).

2.6 Statistical significance analyses

The repeated measures one way ANOVA was used to test the significance level of LF, HF and LF/HF ratio. The Tukey's multiple comparison tests were performed to compare all the experimental conditions (low level vibration, medium level vibration and (no vibration)).95% confidence interval ($P<0.05$) was considered to observe the statistical significance. The repeated measure two-way ANOVA was used to test the significance level of KSS scores. The Bonferroni's multiple comparisons test were executed to compare the KSS values of two conditions (before and after the experiment) for three different groups (low, medium and control).

3. Results

3.1 Subjective Assessment

Karolinska Sleepiness Scale, KSS is the most commonly used self-reporting assessment method to detect the level of drowsiness [32]. In this method, the participants reported their instant level of drowsiness, which were recorded before and after the experiment. In Figure-2 and table-1, the mean value of seven participant's data showed a significant change of KSS score between before and after the experiment when exposed to the medium level of vibration. The highest significance level ($P=0.0001$) observed in medium level vibration compared with low level ($P=0.1329$) and no vibration ($P=0.002$) condition.

Table 1: Statistical analysis of KSS for before and after the experiment (Two way ANOVA, Bonferroni's multiple comparisons test)

Comparisons	Mean Differences	95.00% CI of differences	Significant Summary	Adjusted P Values
Control (0)	-1.9	-3.4 to -0.27	*	0.0211
Low level (0.1 ms^{-2})	-1.3	-2.9 to 0.31	ns	0.1329
Medium level (0.2 ms^{-2})	-3.6	-5.2 to -2	***	0.0001

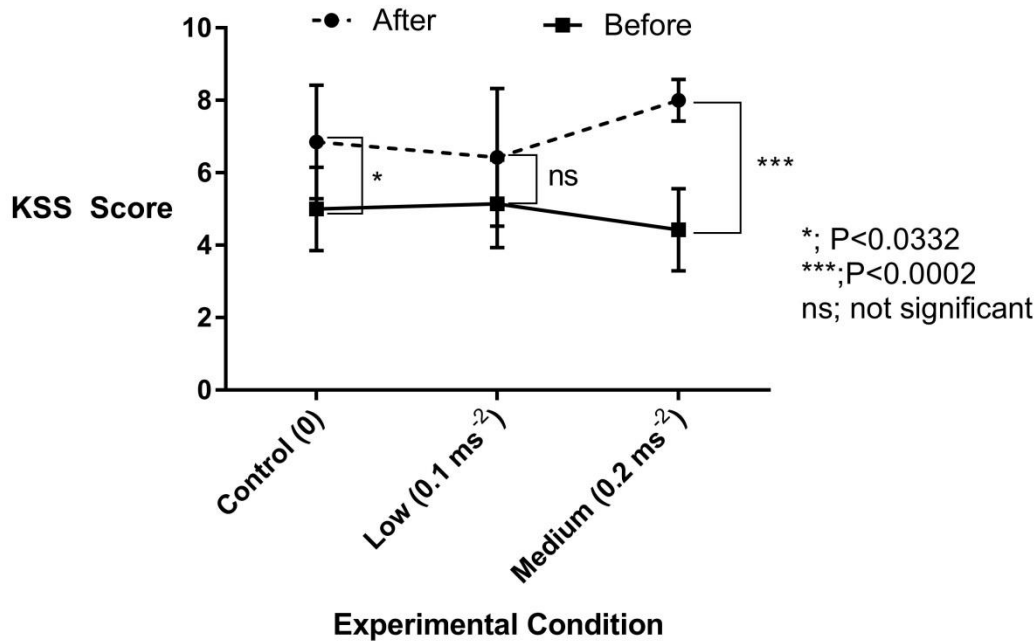


Figure 2: The mean value of KSS score between before and after 45 minutes of experiment for all groups (control, low and medium).

3.2 Physiological Assessment

HRV is a continuous, sensitive, and non-invasive physiological measure to monitor driver drowsiness. The mean value of LF/HF ratio, LF and HF of HRV measured to evaluate the level of drowsiness for the participant. The statistical significance of all HRV indices has been reported in the Table-2 between all three groups (control, low and medium). In Figure-3, the mean value of LF/HF ratio (balance of sympathetic and parasympathetic activity of ANS) showed a significant increase when participants exposed to the medium level of vibration compared to low level vibration and the control condition (no vibration). The significant increase of LF/HF ratio ($P=0.01$) observed when compared control (no vibration) to medium level and low to medium level vibration ($P=0.02$). The results indicated that the sympathovagal balance of the participant's increases under medium vibration condition compared to low and no vibration conditions in the same period of experiment session.

Apart from LF/HF ratio, there is no significant differences ($P<0.05$) were observed in the sympathetic activity (LF) and parasympathetic activity (HF) of HRV indices while compared with three groups of experimental conditions (Figure-3 and Table-2). Nonetheless, the results showed that sympathetic activity (LF) increased ($P=0.0788$) while parasympathetic activity (HF) inclined to decrease ($P=0.0767$) in control vs. medium level vibration compared with other conditions.

In a nutshell, the results of this study reported that LF/HF ratio and LF showed towards increases while HF decreases in medium level vibration compared with low level and control condition (no vibration). It indicates that sympathetic nervous activity of ANS system more dominated in the medium level vibration. However, the sample size of this study is small and more study is in progress to conclude the effect of vibration magnitudes on driver drowsiness.

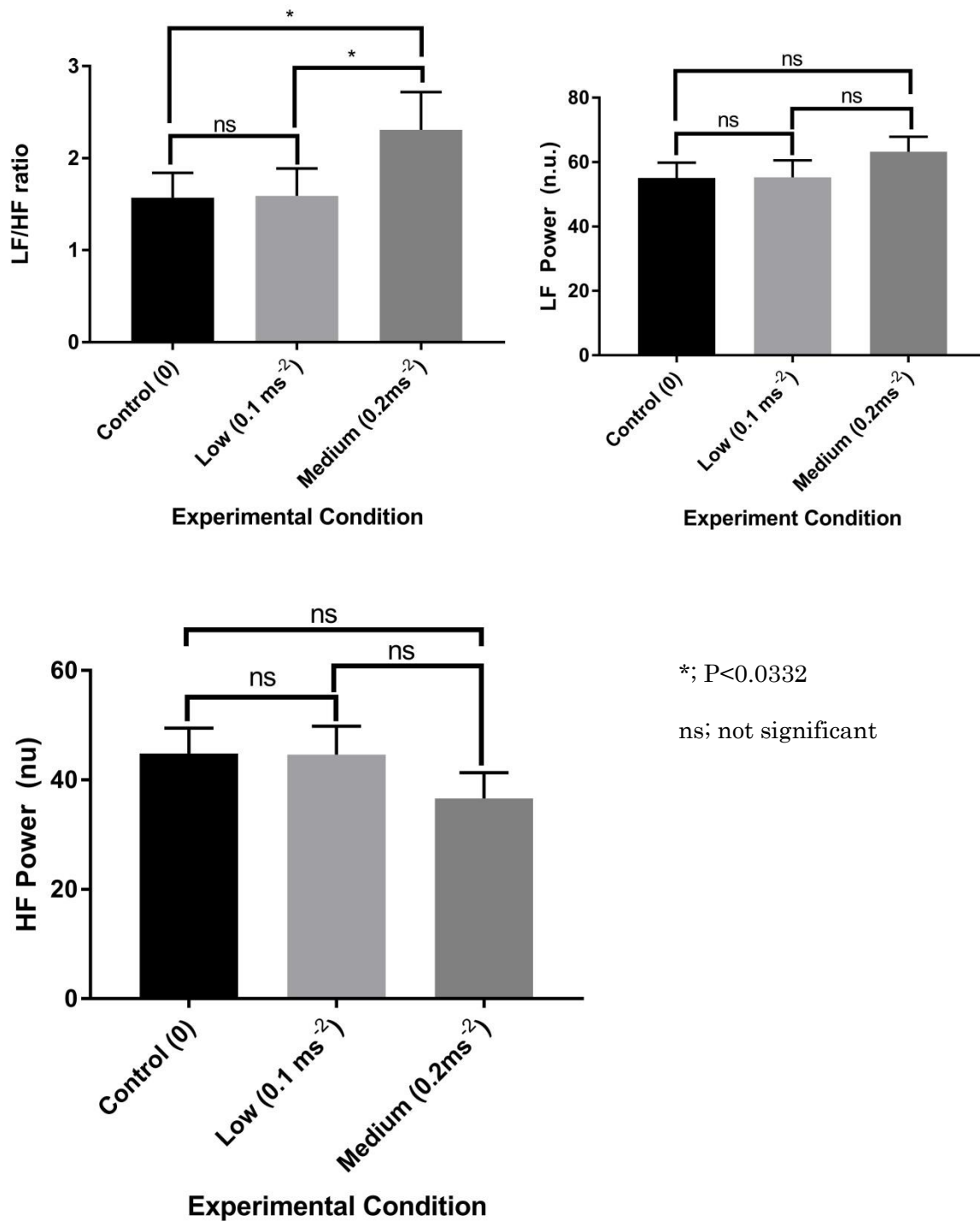


Figure 3 : The mean value of frequency domain HRV indices (LF, HF and Lf/HF ratio) for for all groups (control, low and medium) over 45 minutes experiment.

Table 2: Statistical analysis of HRV indices (One way ANOVA, Tukey's multiple comparisons test)

HRV Indices	Comparisons	Mean Differences	95.00% CI of Differences	Significant summary	Adjusted P Values
LF/HF Ratio	Control vs. Low	-0.02012	-0.634 to 0.5937	ns	0.9958
	Control vs. Medium	-0.7382	-1.352 to -0.1243	*	0.0191
	Low vs. Medium	-0.7181	-1.332 to -0.1042	*	0.0223
LF	Control vs. Low	-0.1912	-6.057 to 5.675	ns	0.9945
	Control vs. Medium	-8.122	-17.34 to 1.094	ns	0.0788
	Low vs. Medium	-7.931	-17.7 to 1.833	ns	0.1031
HF	Control vs. Low	0.1926	-5.676 to 6.061	ns	0.9944
	Control vs. Medium	8.174	-1.027 to 17.38	ns	0.0767
	Low vs. Medium	7.981	-1.761 to 17.72	ns	0.1003

4.0. Discussion

The subjective assessment KSS scale is a sensitive measure that reflects the psycho-physical state of the subject. Several studies reported that KSS scores rise with increasing the level of driver drowsiness [34, 35]. The results of KSS study indicated that participant's drowsiness increases significantly in the medium level of vibration. After experiment, the participant also reported that they were more sleepy, tired and fatigue than before the experiment commence in vibration than control condition. Because of, when participants exposed to vibration, they required to be more, active, attentive, conscious to control the vehicle and conducting the driving task than before, which increases their mental workload demand and hence, induces fatigue and drowsiness [28]. Furthermore, exposure to vibration increases physical and mental fatigue of the participants that impact on driver vigilance and develops discomfort [36]. It has been noted that vibration stimulus also influences the autonomic and central nervous systems of the human during monotonous activity [37].

The autonomic nervous system is regulated by heart rate variability (HRV). Heart rate (HR) is as an indicator of mental workload that could be increase due to vibration [38]. On the other hand, it is well known that, HRV decrease when increase in cognitive strain and workload. Typically, HRV controlled by two branches of autonomic nervous system (ANS): parasympathetic and sympathetic nervous activities. Heart rate could be increased by decreasing parasympathetic activity or by increasing sympathetic activity, or by a combination of the two systems. In this study, a significant increase of sympathovagal balance (LF/HF ratio) observed under vibration compared with no vibration in the same time session. As we know that, there is a strong relationship between the LF/HF ratio and the driver's drowsiness. The findings of LF/HF ratio are consistent with the result of Zhang et al.[28], Jiao et al. [27]. Their results also concluded that driver drowsiness increases with increase in LF/HF ratio under vibration compared with no vibration. The results also pointed out that sympathetic activity are more dominated than parasympathetic activity in the medium level vibration compared to low level and no vibration. The outcomes of this study are similar to several studies [27, 28, 39].

5. Conclusion

Drowsiness contributes driving related accidents and fatalities. It has been proven that vibration influences driver drowsiness and fatigue. Although there is a great knowledge about the effect vibration magnitude on human discomfort, its impact on drowsiness is not well investigated yet. This study aimed to address the influence of vibration magnitude on driver drowsiness by investigating physiological behaviors of the driver. The statistical significance has been evaluated between the different groups of vibration exposure level and control condition (no vibration). The results of this

study indicated that notable driver drowsiness observed in the medium level vibration compared with low level and control (no vibration). However, the outcomes of this study are primitive to evaluate the effect of vibration magnitudes. More study is in progress for different magnitudes to understand the effect of vibration magnitudes on driver drowsiness.

5. References

1. Brinkel, J., M. Khan, and A. Kraemer, A Systematic Review of Arsenic Exposure and Its Social and Mental Health Effects with Special Reference to Bangladesh. *International Journal of Environmental Research and Public Health*, 2009. **6**(5): p. 1609.
2. Dong, Y., et al., Driver Inattention Monitoring System for Intelligent Vehicles: A Review. *IEEE Transactions on Intelligent Transportation Systems*, 2011. **12**(2): p. 596-614.
3. Transport Accident Commission. Available from: <https://www.tac.vic.gov.au/road-safety/tac-campaigns/drowsy-driving>.
4. Tefft, B.C., Prevalence of motor vehicle crashes involving drowsy drivers, United States, 2009–2013. AAA Foundation for Traffic Safety, 2014.
5. Sayed, R.A., A. Eskandarian, and A. Mortazavi, Drowsy and Fatigued Driver Warning, Counter Measures, and Assistance, in *Handbook of Intelligent Vehicles*, A. Eskandarian, Editor. 2012, Springer London: London. p. 975-996.
6. Williamson, A.M., et al., Developing measures of fatigue using an alcohol comparison to validate the effects of fatigue on performance. *Accident Analysis & Prevention*, 2001. **33**(3): p. 313-326.
7. Troxel, W.M., et al., Evaluating the Impact of Whole-body Vibration (wbv) on Fatigue and the Implications for Driver Safety, 2015, Rand Corporation.
8. Griffin, M.J., *Handbook of human vibration*. 1990, London: Academic Press Limited.
9. Griffin, M.J., Discomfort from feeling vehicle vibration. *Vehicle System Dynamics*, 2007. **45**(7-8): p. 679-698.
10. Sagberg, F., et al., Fatigue, sleepiness and reduced alertness as risk factors in driving. 2004: Institute of Transport Economics Oslo.
11. Cann, A.P., A.W. Salmoni, and T.R. Eger, Predictors of whole-body vibration exposure experienced by highway transport truck operators. *Ergonomics*, 2004. **47**(13): p. 1432-1453.
12. Howarth, H.V. and M.J. Griffin, The frequency dependence of subjective reaction to vertical and horizontal whole-body vibration at low magnitudes. *The Journal of the Acoustical Society of America*, 1988. **83**(4): p. 1406-1413.
13. Basri, B. and M.J. Griffin, Equivalent comfort contours for vertical seat vibration: effect of vibration magnitude and backrest inclination. *Ergonomics*, 2012. **55**(8): p. 909-922.
14. Aziz, S.A.A., M.Z. Nuawi, and M.J. Mohd Nor, Predicting whole-body vibration (WBV) exposure of Malaysian Army three-tonne truck drivers using Integrated Kurtosis-Based Algorithm for Z-Notch Filter Technique 3D (I-kaz 3D). *International Journal of Industrial Ergonomics*, 2016. **52**: p. 59-68.
15. Satou, Y., et al., Effect of Short-term Exposure to Whole Body Vibration in Humans: Relationship between Wakefulness Level and Vibration Frequencies. *The Kurume Medical Journal*, 2009. **56**(1+2): p. 17-23.

16. Satou, Y., et al., Effects of Short-Term Exposure to Whole-Body Vibration on Wakefulness Level. *Industrial Health*, 2007. **45**(2): p. 217-223.
17. Newell, G.S. and N.J. Mansfield, Evaluation of reaction time performance and subjective workload during whole-body vibration exposure while seated in upright and twisted postures with and without armrests. *Int J Ind Ergonom*, 2008. **38**.
18. Kubo, M., et al., An investigation into a synthetic vibration model for humans:: An investigation into a mechanical vibration human model constructed according to the relations between the physical, psychological and physiological reactions of humans exposed to vibration. *International Journal of Industrial Ergonomics*, 2001. **27**(4): p. 219-232.
19. Kar, S., M. Bhagat, and A. Routray, EEG signal analysis for the assessment and quantification of driver's fatigue. *Transportation Research Part F: Traffic Psychology and Behaviour*, 2010. **13**(5): p. 297-306.
20. Choi, U.-S., et al., A Simple Fatigue Condition Detection Method by using Heart Rate Variability Analysis, in *Advances in Parallel and Distributed Computing and Ubiquitous Services: UCAWSN & PDCAT 2015*, H.J.J. Park, et al., Editors. 2016, Springer Singapore: Singapore. p. 203-208.
21. Vicente, J., et al., Drowsiness detection using heart rate variability. *Medical & Biological Engineering & Computing*, 2016. **54**(6): p. 927-937.
22. Malik, M., Heart Rate Variability. *Annals of Noninvasive Electrocardiology*, 1996. **1**(2): p. 151-181.
23. Berntson, G.G., et al., Heart rate variability: Origins, methods, and interpretive caveats. *Psychophysiology*, 1997. **34**(6): p. 623-648.
24. Mahachandra, M., et al. Sensitivity of heart rate variability as indicator of driver sleepiness. in *Network of Ergonomics Societies Conference (SEANES), 2012 Southeast Asian*. 2012.
25. Al-Libawy, H., et al. HRV-based operator fatigue analysis and classification using wearable sensors. in *2016 13th International Multi-Conference on Systems, Signals & Devices (SSD)*. 2016.
26. Patel, M., et al., Applying neural network analysis on heart rate variability data to assess driver fatigue. *Expert Systems with Applications*, 2011. **38**(6): p. 7235-7242.
27. Jiao, K., et al., Effect of different vibration frequencies on heart rate variability and driving fatigue in healthy drivers. *International Archives of Occupational and Environmental Health*, 2004. **77**(3): p. 205-212.
28. Zhang, N., et al., The Effects of Physical Vibration on Heart Rate Variability as a Measure of Drowsiness. *Ergonomics*, 2018(just-accepted): p. 1-19.
29. Awais, M., N. Badruddin, and M. Drieberg. A non-invasive approach to detect drowsiness in a monotonous driving environment. in *TENCON 2014 - 2014 IEEE Region 10 Conference*. 2014.
30. ISO2631-1, Mechanical vibration and shock--Evaluation of human exposure to whole-body vibration--Part1: General requirements., 1997, International organization for standardization.
31. Fard, M., et al., Effects of seat structural dynamics on current ride comfort criteria. *Ergonomics*, 2014. **57**(10): p. 1549-1561.

32. Shahid, A., et al., Karolinska Sleepiness Scale (KSS), in STOP, THAT and One Hundred Other Sleep Scales, A. Shahid, et al., Editors. 2012, Springer New York: New York, NY. p. 209-210.
33. Tarvainen, M.P., et al., Kubios HRV – Heart rate variability analysis software. *Computer Methods and Programs in Biomedicine*, 2014. **113**(1): p. 210-220.
34. Liu, C.C., S.G. Hosking, and M.G. Lenné, Predicting driver drowsiness using vehicle measures: Recent insights and future challenges. *Journal of Safety Research*, 2009. **40**(4): p. 239-245.
35. Åkerstedt, T. and M. Gillberg, Subjective and objective sleepiness in the active individual. *International Journal of Neuroscience*, 1990. **52**(1-2): p. 29-37.
36. Du, B.B., et al., The impact of different seats and whole-body vibration exposures on truck driver vigilance and discomfort. *Ergonomics*, 2018. **61**(4): p. 528-537.
37. Konishi, K. and H. Hagiwara. Influence of monotonous work and body sensory vibration stimulus on physiological responses. in 2015 IEEE 15th International Conference on Bioinformatics and Bioengineering (BIBE). 2015.
38. Egelund, N., Spectral analysis of heart rate variability as an indicator of driver fatigue. *Ergonomics*, 1982. **25**(7): p. 663-672.
39. Rodriguez-Ibañez, N., et al. Changes in heart rate variability indexes due to drowsiness in professional drivers measured in a real environment. in 2012 Computing in Cardiology. 2012.

Experimental examination for vibration masking on human perception

**Koki SUGIMOTO [1], Gen TAMAOKI [1], Takuya YOSHIMURA [1],
Naoyuki SARUWATARI [2]**

[1] Tokyo Metropolitan University

1-1 Minami-osawa, Hachioji, Tokyo 192-0397, Japan

[2] Honda R&D Co., Ltd. Automobile R&D Center

4630 Shimotakanezawa, Haga-machi, Haga-gun, Tochigi, 321-3393, Japan

Abstract

In the field of psychoacoustics, the masking effect on acoustic perception is widely known. For the masking on the perception of whole-body vibration, there is only study on the fore-and-aft vibration by Morioka et al., although there are some studies of the effect on the perception of hand-transmitted vibration. In this study, we examined an appropriate measurement method in order to investigate the influence of the masking on the perception threshold for vertical vibration. We used the method of adjustment and the up-down transformed response method (UDTR method). UDTR method had less variation in data between subjects compared to the adjustment method. In addition, UDTR method produced the higher reliable data because the number of trials to determine the thresholds was more in UDTR method than in the adjustment method. From the above, it was concluded that UDTR method was the appropriate experimental method to obtain the masked threshold.

1. Introduction

Vibration reduction is one of the important factors when a comfortable automobile is designed. In order to reduce the vibration of the automobile, it is very important not only to reduce the vibration generated from the automobile, but also to understand how humans perceive the vibration received from the automobiles and to choose frequency band which must be reduced based on the human perception. In ISO2631-1, frequency weighting curves are shown as regulations of the evaluation for whole-body vibration exposure[1]. The frequency weighting curves have inverse characteristics of equivalent comfort contours which are curves connected accelerations that humans perceive equivalently at each frequency. Amplitude of the vibration that humans are exposed is converted into index values based on the human sensory by using the frequency weighting curves, and the health and comfort are evaluated by the index values. However, it is pointed out that the index values do not match with the sensation of occupants of the automobiles. Reasons of the gap are considered that the frequency weighting curves don't take level dependency of the vibration acceleration into consideration and underestimate the high

frequency vibration. We have been studying to review the frequency weighting curves. Another reason is masking effect. The occupants are exposed to vibration including the resonances of engine, seat, sprung mass and unsprung mass. In particular, the resonance of the unsprung mass existing from 10 to 15 Hz has large amplitude. It is conceivable that the resonance of the unsprung mass acts as masker and the masking makes the difference between the index values and the human sensory. For the masking on the perception of the whole-body vibration, there is only study on the fore-and-aft vibration by Morioka et al.[2], although there are some studies of the masking on the perception of hand-arm vibration[3],[4]. In this study, we compare two methods to measure the masked perception threshold and examine an appropriate method in order to investigate the influence of the masking on the perception threshold for vertical vibration.

2. Masking effect

The masking includes spectrum masking, which occurs on the frequency domain, and temporal masking, which occurs on the time domain. The spectrum masking effect is a phenomenon in which one vibration is affected by the presence of another vibration and is hardly to be felt or not to be felt when humans are exposed to multiple vibrations. In this study, the spectrum masking is dealt with and is called the masking. The vibration that masks another vibration is called masker.

3. Experimental method

For the determination of the masked threshold at each frequency under the masker, two experimental methods shown in section 3.1 and 3.2 were used. They are method of adjustment and UDTR method. And then, we examined an appropriate measurement method by comparing experimental results of the two methods. A subject sat on a rigid seat fixed on a shaking table and was vibrated in the vertical direction. The rigid seat did not have a backrest, a footrest and an armrest. There was the footrest that was independent of the seat and did not vibrate. A subject placed its feet on the footrest and was exposed to the vibration only from the seat surface. Masked threshold of sine vibration was measured at each frequency under the masker, as shown in table 1. The frequencies of the sine vibration were 5, 10, 15, 20, 31.5, 40, 50, 63, 80 and 100 Hz which were selected in center frequencies of one-third octave bands. The masker was the narrow-band random vibration from 10 to 15 Hz. And amplitudes of the masker were 0.1 and 0.6 m/s² r.m.s.. The subjects are three healthy males. Their average height are 173 cm and their average weight was 60 kg. Prior to the experiment, informed consent to participate in the experiment was given by all subjects. All subjects participated in the experiment after consenting to their understanding that they can cancel the experiment immediately at any time by their own will. This experiment was approved by the ethics committee at Tokyo Metropolitan University.

Table 1 Experimental condition

Vibration direction	Vertical direction (Z-axis)
	Masker
Type of vibration	Random
Frequency	10-15 Hz
Amplitude	0.1, 0.6 m/s ² r.m.s.
	Sine vibration
Frequency	5, 10, 15, 20, 31.5, 40, 50, 63, 80, 100 Hz

3.1 Method of adjustment

The method of adjustment is the way that the subjects themselves increase or decrease a level of a stimulus until they barely perceive the presence of the stimulus. In this study, the stimulus is the sine vibration. As shown in figure 1, the subjects switched between a reference vibration, which was only the masker, and a comparative vibration, which contained the masker and the sine vibration, freely with a controller and adjusted the level of the sine vibration. The level of the masker and the frequency of the sine vibration were changed as shown in table 1, and the threshold at each frequency for certain level of the masker was measured, and the threshold curve was obtained by connecting the thresholds. Moreover, the threshold curve for each level of the masker was obtained by changing the level of the masker and repeating the same experiment.

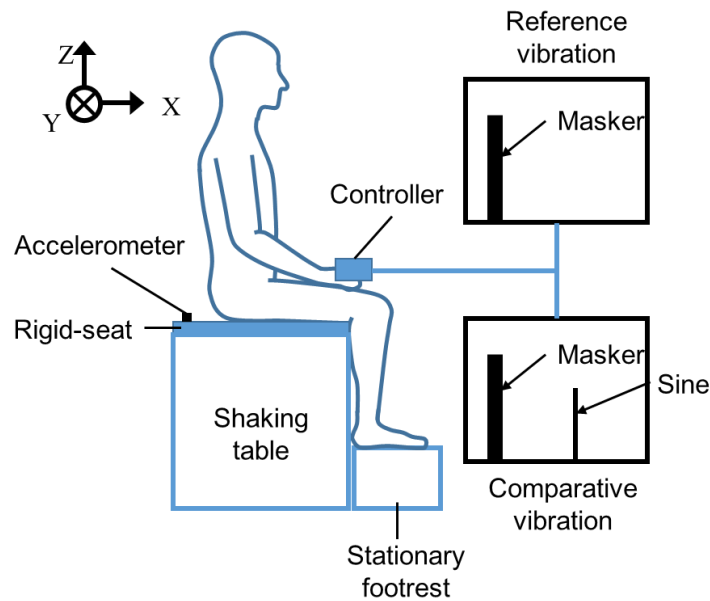


Figure 1 Experiment schematic

3.2 UDTR method

The up-down transformed response method (UDTR method) proposed by Wetherill and Levitt (1965) [5] is a method of repeating rising and descending sequences with taking reaction for a stimulus of several previous trials into consideration. Unlike the method of adjustment, an intensity of the stimulus is controlled by the experimenter. In this study, the stimulus was the sine vibration and the masker was the narrow-band random vibration. The subjects were vibrated for ten seconds. The time-series waveform was shown in figure 2. As shown in figure 2, the subjects were exposed to three vibrations. First vibration is set to be recognized as target vibration which is sine vibration by the subjects. The other two vibrations were the masker only and the sine vibration with the masker. The order of last two vibrations was at random. The subjects observed the second and third vibrations, of which periods were called observation 1 and observation 2, respectively. The subjects judge the vibration whether contained a sine wave in second or third vibration. Three-down one-up rule was utilized to determine the thresholds. The rule is, as shown in figure 3, that the magnitude of the sine vibration is increased by 1 step (2 dB) after one incorrect judgement and decreased by 1 step after three consecutive correct judgements. And then, the threshold was calculated from the mean of the last two peaks (p_2, p_3) and the last two troughs (t_2, t_3) omitting the first peak and the first trough (p_1, t_1). Initial value of the magnitude of the sine vibration was the mean threshold of the subjects obtained with the method of adjustment, and was used as a reference value for decibel value.

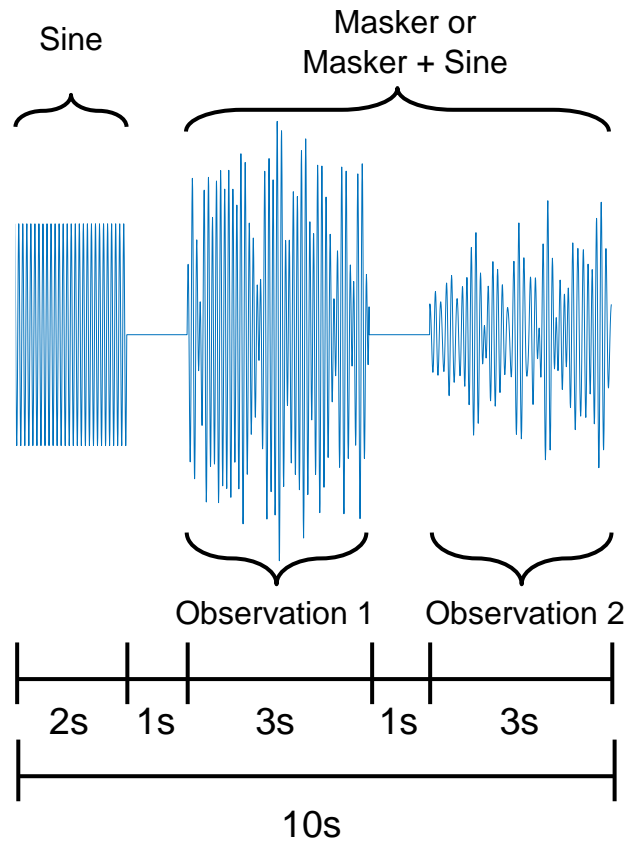


Figure 2 Time-series waveform (UDTR method)

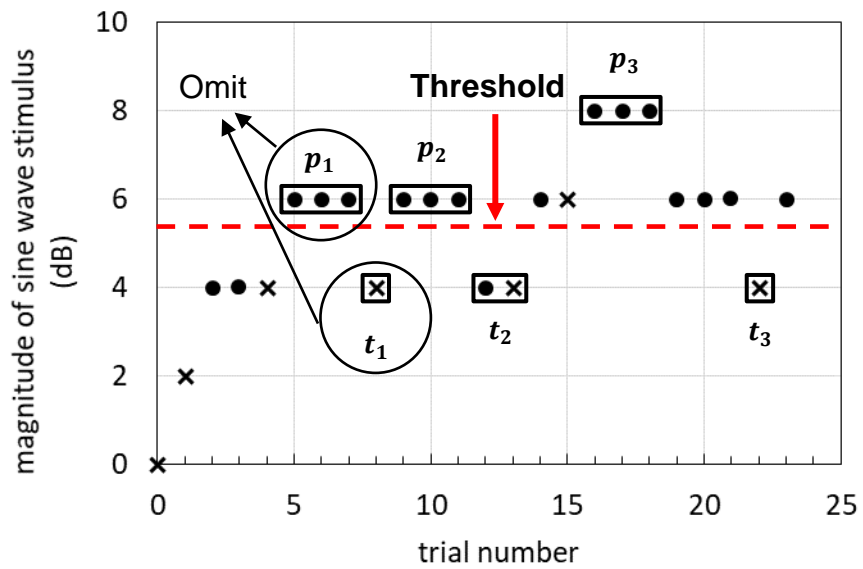


Figure3 Detail of UDTR procedure

4. Results of human vibration experiment

Figure 4 shows the threshold curves for each measurement method for three subjects. Firstly, the variations in the threshold obtained with UDTR method among the subjects were smaller than ones obtained with the method of adjustment. The thresholds around the frequency band of the masker were clearly larger than ones in the other frequencies in UDTR method, which was considered as the masking effect. This was also observed with all subjects in UDTR method. However this was not clearly observed in the method of adjustment. Especially when the amplitude of the masker was small (0.1 m/s²), this was observed for all subjects in UDTR method. However one of the subjects responds that the threshold in every frequency was similar in the method of adjustment. Secondly, the thresholds obtained with UDTR method were lower than ones obtained with the method of adjustment in the high frequency range over about 31.5 Hz. It was considered that one reason of the differences of the above experimental results were the burden on the subjects. In the method of adjustment, the subjects repeated to perceive the sine vibration under they exposed to both the sine vibration and the masker together until they obtained the threshold and therefore the method of adjustment forced the subjects to concentrate for a long time. In UDTR method, meanwhile, the subjects repeated the judge that was short and simple, and were easy to keep their concentration. In addition, it was considered that UDTR method produced the higher reliable data because the threshold was estimated by a lot of judgements in UDTR method and was determined by a last judgement after many judgements in the method of adjustment. From the above, UDTR method was more appropriate than the method of adjustment to measure the threshold of the sine vibration under the narrow-band random vibration as masker.

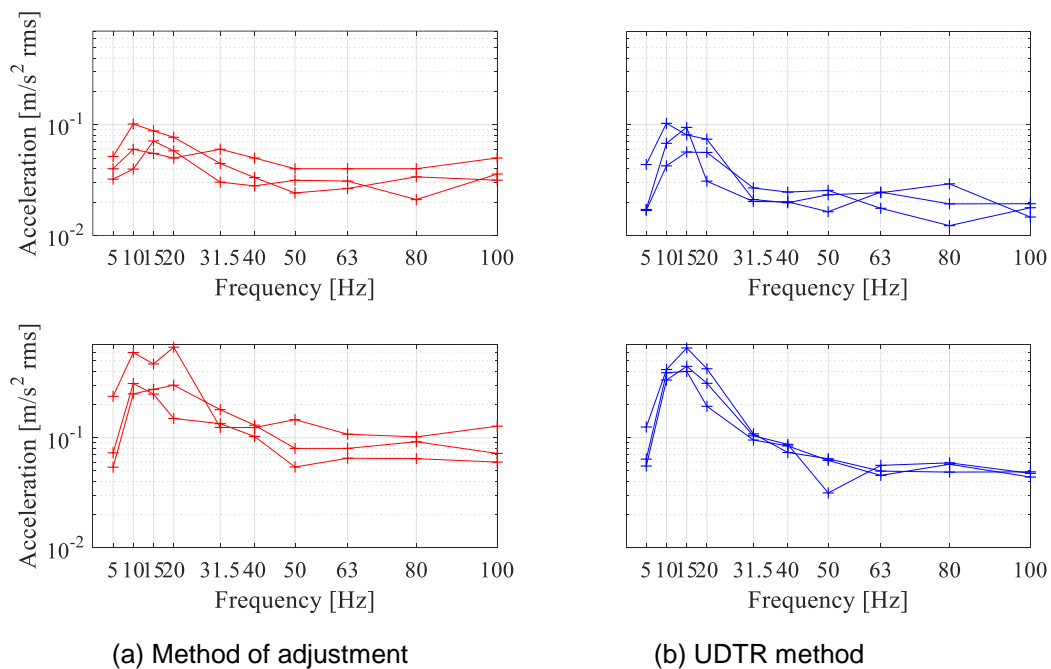


Figure 4 Threshold curve for each subject on method of adjustment and UDTR method
 Upper stage: Threshold curve for masker level 0.1 m/s²
 Lower stage: Threshold curve for masker level 0.6 m/s²

5. Conclusions

This study investigated the appropriate method for measuring the perception threshold of the sine vibration in the presence of the narrow-band random vibration from 10 to 15 Hz as a masker. Two methods to measure the masked perception threshold were compared. The following characteristics of the difference between two methods were obtained and it was found that UDTR method was more suitable than the method of adjustment.

- 1) The variations in the threshold obtained with UDTR method among the subjects were smaller than ones obtained with the method of adjustment.
- 2) The thresholds obtained with UDTR method were lower than ones obtained with the method of adjustment in the high frequency range over about 31.5 Hz.

6. References

- [1] International Organization for Standardization, Mechanical vibration and shock -Evaluation of human exposure to whole-body vibration -Part1:General requirements, Second edition (1997), ISO2631-1.
- [2] Miyuki Morioka, Michael J. Griffin (2015), Masking of thresholds for the perception of fore-and-aft vibration of seat backrests. *Applied Ergonomics*, 50, 200-206.
- [3] George A. Gescheider, Martin J. O'Malley and Ronald T. Verrillo (1983), Vibrotactile forward masking : Evidence for channel independence. *The Journal of the Acoustical Society of America*, 74, 474-485.
- [4] Miyuki Morioka, Michael J. Griffin (2005), Independent responses of pacinian and Non-Pacinian systems with hand-transmitted vibration detected from masked thresholds. *Somatosensory and Motor Research*, 22(1-2), 69-84.
- [5] G.B.Wetherill, H.Levitt (1965), Sequential estimation of points on a psychometric function. *British Journal of Mathematical and Statistical Psychology*, 18(1), 1-10.

P16

The 26th Japan Conference on Human Response to Vibration (JCHRV2018)

Kindai University, Osaka, Japan

August 22-24, 2018

A New Paradigm for Evaluating and Designing Seat Suspensions

Peter W. Johnson, University of Washington

Professor of Environmental and Occupational Health Sciences

4225 Roosevelt Way NE, Suite 100

Seattle, WA 98105, USA

petej@u.washington.edu

Vibration Characteristics of Human Body on a Rigid Seat

**Mitsuaki KANO [1], Gen TAMAOKI [1], Takuya YOSHIMURA [1],
Yoichiro KITAHARA [2]**

[1] Tokyo METROPOLITAN University

1-1 Minami-osawa, Hachioji, Tokyo 192-0397, Japan

[2] Mazda Motor Corporation

3-1 Shinchi, Fuchu-cho, Aki-gun, Hiroshima, 730-8670, Japan

Abstract

In order to improve ride comfort of an automobile, it is necessary to clarify the vibration characteristics of a seated human body. The vibration characteristics of human body have been dealt with for the frequency range below about 20 Hz in many previous studies because the main resonance frequencies of human body exist in the range. However, with the recent development in vibration reduction technologies in automobile design, countermeasures against a higher frequency vibration have been becoming one of important topics. The purpose of this study is to examine the vibration characteristics of the seated human body on a rigid seat with a tilted backrest in the frequency range from 2 to 50 Hz including the higher frequencies. For this purpose, the vibration experiments are carried out to measure the acceleration transmissibilities from the seat surface to the head and several locations on the spine. Then, the natural frequencies and the mode shapes are obtained by conducting curve fit to the measured transmissibility.

1. Introduction

When people ride in cars, they are exposed to vibrations of various frequencies, and their vibrations have a great influence on ride comfort. In past studies, many experiments were carried for low frequency vibrations, e.g. less than 15 Hz because the fundamental resonance frequencies of human body exist in the range and the vibration exposure level is relatively large. On the other hand, even though the vibration amplitude is small in the high frequency range (e.g. > 15 Hz) it is known that the magnitude of the perception is also small. Furthermore, the demand for improving ride comfort grows in automotive industries. Therefore, the needs to grasp human vibration characteristics in the high frequency range arise. It is noted that there have been limited number of previous studies including the higher frequency range. In the previous study by our research group including Sugimoto et al., they examined the measurement method of human response in the high frequency range (from 2 to 100 Hz)[1]. They showed that light weight accelerometers such as 1.0 g can be used to measure human response attached on the skin, which do not seriously suffer from the influence of the skin and tissue

vibration. Another previous research by Osaka et al. showed how human body vibration characteristics change depending on the seated posture. It revealed that the relationship among three postures; the upright posture, the relaxed posture and the intermediate posture without a backrest[2]. However, since the seat of an actual car is equipped with a backrest and it likely affects human body vibration characteristics greatly, human body vibration characteristics with backrest are focused in this paper.

Therefore, the purpose of this study is to understand the vibration properties of seated human body in the wider frequency range (from 2 to 50 Hz) considering the effect of backrest. In this study the subject is seated on a rigid seat which does not have dominant resonance in the frequency range of interest. The vibration properties are extracted from the transmissibilities that are from the floor to the head and spine.

2. Theory

2.1 Transmissibility

In this study, transmissibilities of human body are measured experimentally and vibration characteristics are evaluated through the data. Input is the vertical acceleration on the seating surface. In this research, the accelerations both in the fore-and-aft and the vertical direction are measured as the output. The transmissibility, T is estimated by the following where a_{in} and a_{out} are the frequency spectra of accelerations of input and output, respectively.

$$T = a_{out}/a_{in} \quad (1)$$

2.2 Modal parameter estimation

Modal parameters are extracted by conducting curve fit to the measured transmissibilities. Natural frequencies and mode shapes are obtained as modal parameters, by which we understand what kinds of vibration behavior human body has as its natural modes. In the curve fit, non-linear least square algorithm is applied to obtain modal parameters, which seeks several natural modes simultaneously by using all the transmissibilities. The FRF (transmissibility) expressed in n natural modes is expressed by the Eq. (2).

$$G(\omega) = -\omega^2 \left[\sum_{r=1}^n \left\{ \frac{U_r + jV_r}{\sigma_r + j(\omega - \omega_{dr})} + \frac{U_r - jV_r}{\sigma_r + j(\omega + \omega_{dr})} \right\} - \frac{C}{\omega^2} + D \right] \quad (2)$$

Here, $-C/\omega^2$ and D represent the residual mode effect outside the frequency band of analysis; the former compensates the residual mass effect (lower frequency modes) and the latter does the residual stiffness effect (higher frequency modes), respectively. Note that ω_{dr} is damped natural frequency and σ_r is modal decay rate; those are global parameters independent from the response locations and these are nonlinear term as is apparent from Eq. (2). On the other hand, U_r , V_r , C and D are linear terms, and they are local parameters depending on the response locations. Since modal parameters contain nonlinear parameters, we need to solve the nonlinear least squares problem, which require initial set of parameter for iteration; initial values of natural frequencies and modal damping ratios need to be prepared. By conducting iterative calculation, all the parameters are determined such that the errors are converged to a minimal value.

3. Human vibration experiment

The experiment schematic is shown in Fig.1. In this study, we use the coordinate system defined in ISO 2631 (X: front and aft, Y: lateral, Z: vertical). The subject sat on a rigid seat fixed on a shaking table and was vibrated in the Z direction. The examination of the vibration characteristics of a rigid seat used in

this experiment showed that there are no resonance frequencies in the target frequency range (from 2 to 50 Hz). Therefore, vibration behavior of the seat can be assumed to be rigid. The measurement positions were a forehead, a neck (C7), a thoracic spine (T3 and T7), a lumbar (L1 and L5), sacral bone (greater trochanter and anterior superior iliac spine). In order to measure the acceleration response of each human body, an accelerometer (PCB, 356A03) with a mass of 1.0 g was used and the acceleration on the seat surface was measured using an accelerometer (PCB, 356A32) with a mass of 5.4 g. The accelerometer was attached to the cardboard using a double-sided tape and the cardboard was affixed to the skin. The excitation frequency was in the frequency range below 50 Hz and the excitation signal is a random wave with magnitude of 1.0 m/s^2 . Subjects were four healthy men; average height was 173 cm, average weight was 71 kg. Prior to the experiment informed consent to participate in the experiment was given by all subjects. All subjects participated in the experiment after consenting to their understanding that they can cancel the experiment immediately at any time by their own will. This experiment was approved by the Tokyo Ethics Committee of the Tokyo Metropolitan University.

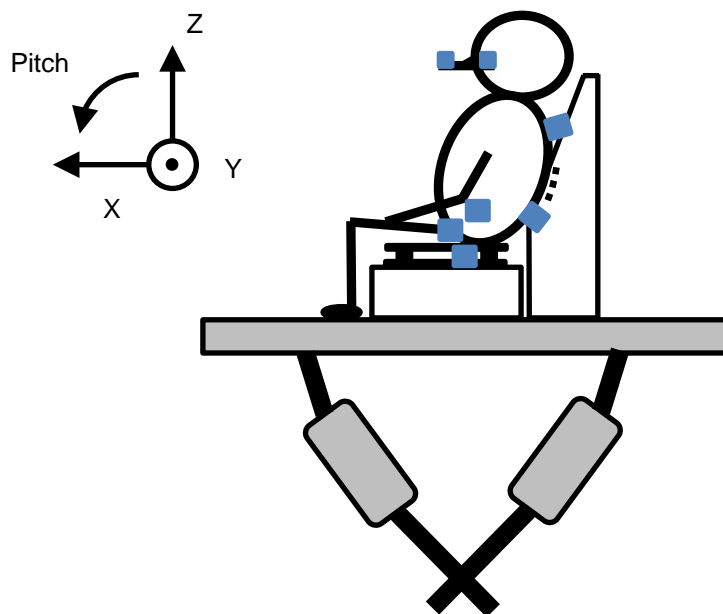


Fig.1 Experiment schematic

4. Results of human vibration experiment

4.1 Comparison of experimental data

The results of the modal parameter identification (curve fit) on the transmissibility of the subject 4 are shown in Fig.2. The transmissibilities in the fore-and-aft direction and the vertical direction of C7 and L5 are used as a typical example. It can be seen that there are two resonance peaks in the low frequency range in C7 and L5 in the vertical direction. The transmissibilities by this study are compared with those which are measured w/o backrest obtained in the previous study by Osaka et al. It can be confirmed that the response magnitude in the low frequency range ($< 15 \text{ Hz}$) by this study is larger than the previous study. It can be inferred that the amplitude is magnified due to the influence by the backrest. For transmissibility at L5, a mild resonance peak can be confirmed around 30 Hz in the vertical direction around 20 Hz in the fore-and-aft direction. These resonant frequencies in the higher frequency

range (> 15 Hz) are commonly observed among four subjects.

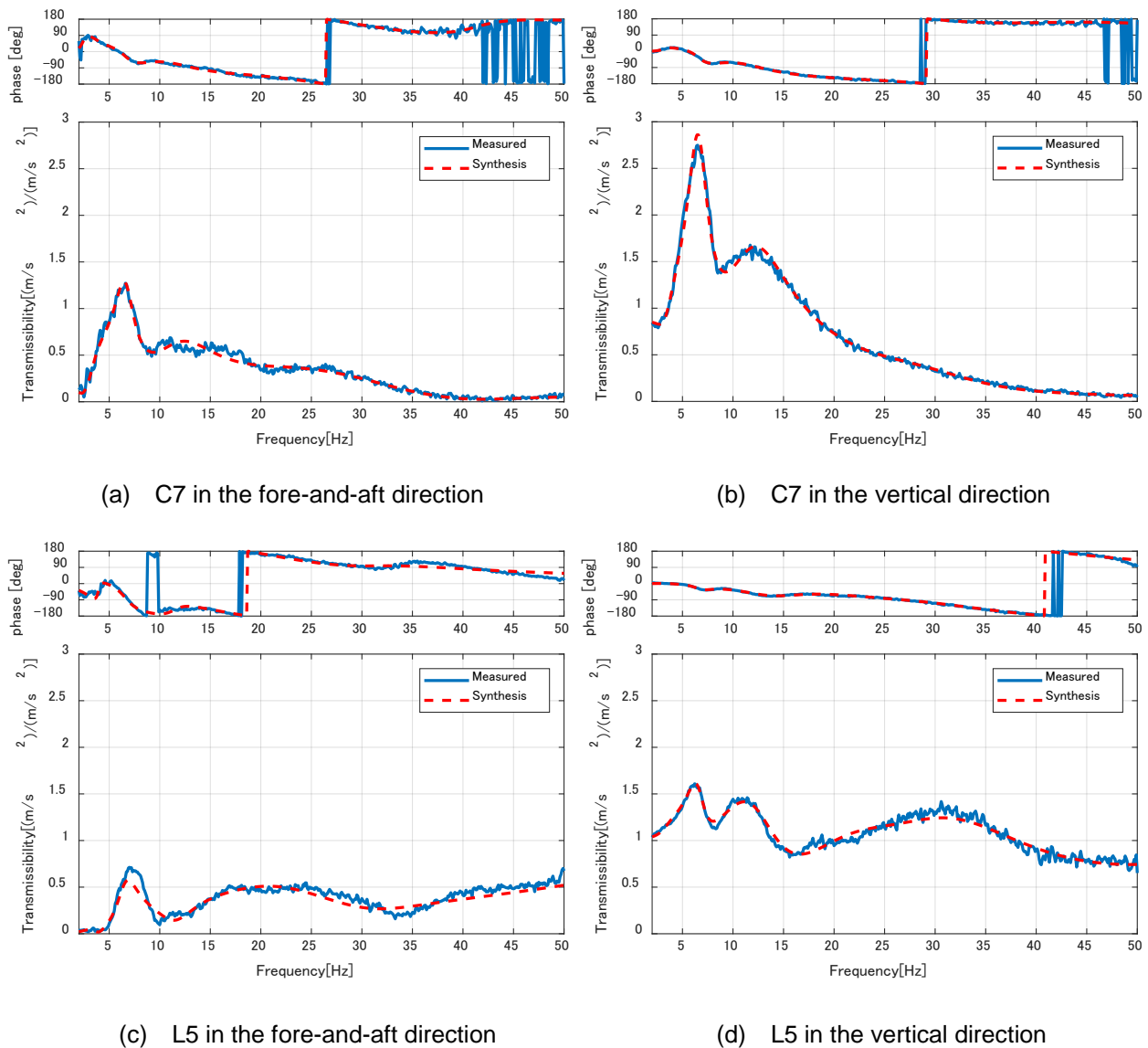


Fig.2 Comparison of Transmissibilities (subject 4)

4.2 Mode shape

In order to represent the mode shape, a seated human body is described on the sagittal plane as shown in Fig.3.2. In all subjects, five modes are identified: three modes in the lower frequency range (< 15 Hz) and two in the higher range (> 15 Hz). Table1 shows the natural frequency and mode damping ratio of each subject. In the 1st mode at 3.36 Hz, the vertebra vibrates in the fore-and-aft direction. C7 in the upper part of the spine and L3 in the lower part of the spine are vibrating in opposite phases in the fore-and-aft direction with the vicinity of T7. Depending on the behavior, the head can rotate in pitch rotation direction. In the 2nd mode at 6.60 Hz, all parts of the spine are vibrating in the same phase in the fore-and-aft direction. C7 vibrated greatly in the anteroposterior direction. So the head rotates largely in the pitch direction. In the 3rd mode at 12.0 Hz, all the parts of the spine vibrates in the same phase in the vertical direction, the head vibrates vertically, and it rotates slightly also in the pitch

direction. In the low frequency range, the same vibration behavior is confirmed as compared with the previous research (w/o backrest), but the natural frequency is lower than the condition seated on a rigid seat w/o backrest. In this time we will refer to the mode shapes in the higher frequency range (from 15 to 50 Hz). Mode shape of the 4th mode and that of the 5th mode are shown in Fig.3.2 (a) and (b), respectively. In the 4th mode, it is confirmed that T7 and L5 are mainly vibrating in an oblique direction(x-z direction). In the 5th mode, the entire thoracic vertebrae (dominantly T7) vibrates in the vertical direction and the whole lumbar vertebrae (dominantly L5) vibrates in the fore-and-aft direction. It is considered that the behavior of L5 in the vertical direction is associated with the vibration of the anterior superior iliac spine in the vertical direction.

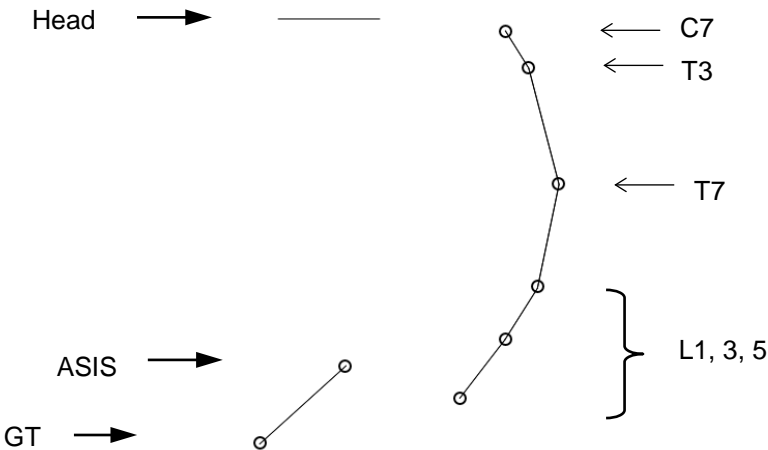
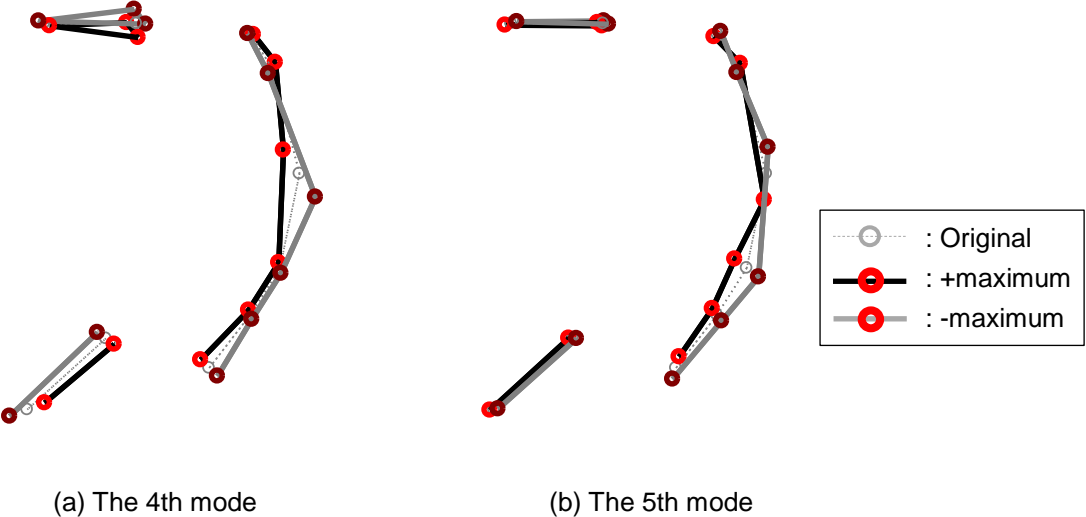


Fig.3.1 Seated human body in original posture



(a) The 4th mode

(b) The 5th mode

Fig.3.2 Seated human body in the 4th and 5th mode

Sub.	Natural frequency (Hz)					Mode damping ration (%)				
	1st	2nd	3rd	4th	5th	1st	2nd	3rd	4th	5th
1	3.76	6.67	11.6	15.0	31.8	24.4	21.3	25.4	27.1	39.8
2	3.23	6.30	10.3	17.0	28.4	18.9	18.1	27.1	23.0	41.0
3	3.87	6.83	10.7	15.4	31.5	23.3	19.4	28.6	24.8	32.0
4	3.36	6.60	12.0	21.5	30.9	33.2	15.0	27.4	32.7	26.3

Table1 Damped natural frequency and modal damping ratio of each subject

5. Conclusion

In this study, transmissibilities of human body seated on a rigid seat were measured within the wider frequency band (from 2 to 50 Hz) while exposed to vertical vibration. The natural modes of human body are extracted and evaluated on a sagittal plane. Due to the comparison of the result with the previous study w/o backrest, the effect of backrest was examined.

The followings can be concluded:

- It was found that the response magnification at the resonance peak is increased by using the rigid sheet with the backrest.
- In the high frequency range (> 15 Hz), vibration of the spinal column is confirmed. In the 4th and 5th modes, both T7 and L5 vibrated dominantly, but the vibration manners including direction are different.

6. Reference

- [1] Koki Sugimoto, Gen Tamaoki and Takuya Yoshimura (2013), Transmissibility of seated human in high frequency.
- [2] Masao Osaka, Gen Tamaoki and Takuya Yoshimura (2013), Relation between index values for seated posture and vibration characteristics of human body. JSME Symposium:Sports and Human Dynamics, 2013, ROMBUNNO.219.

Investigation on characteristics of Whole Body Vibration exposures of Roller Compactor operators and effect of Waste Rubber on reducing the vibration

¹Subashi De Siva G.H.M.J and ²Madhavi M.K.J

¹Senior Lecturer (subashi@cee.ruh.ac.lk)

²Research student (janimigun@gmail.com)

Department of Civil and Environmental Engineering, Faculty of Engineering,
University of Ruhuna, Sri Lanka

Abstract

Technological developments, especially in construction industry, have caused an increase in occupational exposure to Whole Body Vibration (WBV). The WBV has now been recognized as a health hazard for operators, although the construction industry is not well aware about the risk ahead. Objective of this study is to investigate the characteristics of WBV exposures of roller compactor operators and the effect of waste rubber on reducing the WBV.

WBV exposures of twelve soil roller compactor operators were measured to investigate the characteristics of WBV vibration transmitted to the operators. All the subjects were in the seated position and vibration transmission at the interface between the operator and seat was measured. SVANTEK 106 tri-axial vibration accelerometer together with six channel vibration meter was used for measuring vibration. Eight hour exposure (A (8)) and Vibration Dose Value (VDV) were used to assess operators' exposure levels.

It has been found that, among the study group, 75% of roller compactor operators exceed the limiting WBV exposure values specified in ISO 2631-1, indicating moderate or high potential of health risks. Frequency weighted rms acceleration and vibration dose value in the vertical direction were significantly greater than those in fore and aft direction and lateral direction, which could bring negative health effects for operators

A rubber mat, having 16% damping ratio, 1.76 Hz natural frequency and 76.9 N/m stiffness was able to produce with waste rubber. It was found that the rubber mat with 6 mm thickness and 300 mm x 300 mm area can be used to damp transmitted WBV in all three directions with a significant reduction in vertical direction.

1. Introduction

Operators of the heavy vehicles in construction industry have high level of exposure to Whole Body Vibration (WBV), which transmitted through the driver seats (Zhao and Schindler, 2014). Technological developments, specially in construction industry, has caused an increase in occupational exposure to Whole Body Vibration. For example, it was estimated that over 9 million people in Great Britain are exposed to occupational WBV in each week (Smets. et al., 2010). Many operators of mobile equipment used in different industries are exposed to WBV for long time durations and often become the victims of adverse health consequences associated with cardiovascular, respiratory, digestive, reproduction metabolic and endocrine systems (Wolfgang and Burgess, 2014).

The WBV has now been recognized as a health hazard for operators although the construction industry is not well aware about the risk ahead (Vitharana V, et al., 2015). Long term exposure to WBV cause series of adverse health problems including: spine degeneration and spinal disc disease (Zhao and Schindler, 2014). Subsequently, the damages caused due to continuous exposure to vibrations with higher magnitudes are sever and naturally irreversible (Madhushanka, et al., 2015). By evaluating load-haul dump truck operators, it has been found that 14% of operators experience with

moderate severity neck pain, 14% with upper back pain of mild severity, 29% with lower back pain of moderate severity and 14% with moderate severity knee pain (Smets. et al.,(2010)) Further, operators whom have been exposed to WBV in several years have been suffered with health issues: 50% of operators have back pain and 30% have normal daily tiredness (Madhushanka, et al., 2016)..Exposure to WBV predicts subsequent disability pension retirement (Langer, et al., 2012). However, limited studies were carried out to evaluate the WBV experienced by operators in Heavy Construction Vehicles (HCVs) Zhao and Schindler, (2014), studied about compact wheel loaders, Langer, et al., (2012) evaluated the exposure levels of backhoe loaders and Eger, et al., (2008) investigated WBV exposures of load-haul-dump mining operators. However, no any previous study on investigation and evaluating of WBV exposure characteristic of roller compactor operators, although this knowledge is necessary to protect operators from health risk.

The vibrating roller operators have higher potential of facing health effect than other commonly used construction machine operators like backhoes and excavators (Madhushanka, et al., 2016) Dynamic compaction using vibration is developed and established in present construction world due to the higher efficiency and quality in this technology. Generally these vibrations are generated by rotating eccentric mass, and roller drum therefore moves up and down or else back and forth depending on the type of roller compactor while transmitting vibrations to the compacting terrain. However, as a side effect, low frequency Whole Body Vibration (WBV) induced during the operation directly transmits to the operator via the driver's seat. (Rakheja, et al., 2011), indicating the requirement in reducing whole body vibration exposures of roller compactor operators.

On the other hand, Sri Lanka is the 7th largest exporter in natural rubber and rank among the top ten largest rubber producers in world (Sri Lankan Export Development Board). Sri Lankan rubber industry includes both manufacturing of raw rubber and finished products. Including large foreign direct investments, rubber related industries are well established in industrial zones in Katunayake, Ekala, Biyagama, and Sapugaskanda. Sri Lanka manufacture products like rubber bands, beadings, industrial and household gloves, industrial products like hoses, auto parts, industrial components, tyres, tubes, automotive and aviation tyres and general rubber products like rubber flooring, floor mats, carpets, sports goods, footwear, hot water bottles and related components (Sri Lankan Export Development Board). Simultaneously, these manufacturing processes generate waste rubber in different forms and different compositions. Based on the production procedures and items type, quality and the quantity of waste produced may varies. However, there is no proper usage of this waste rubber. Rubber is commonly used as a damping material and generally possess good damping properties Usually polar structured rubber polymers improve the compatibility between layers. and enhances the damping property, wear property and strength. Nitrile rubber has such polar structure and rich with damping ability (Zang, et al., 2016). In this study, performance of a rubber mat produced by adding waste rubber sludge generated in glove manufacturing is evaluated. Re-use of waste will be a favorable solution in terms of both WBV control and sustainable manufacturing approach. Recycle and reuse of waste generated by another manufacturing process support the Zero Waste Manufacturing (ZWM) strategy, which is an encouraging term for both producers and consumers to reduce their expenditures as well as to help in reaching sustainable world (Singh, et al., 2017). The objectives of this study are to investigate the characteristics of WBV transmitted to roller compactor operators and assess the exposure level according to ISO-2631-1:1997 standards. Further, this study focused on investigating the effect of waste rubber in damping the WBV exposure, to reduce operators WBV exposures and enhance the re-use of waste rubber.

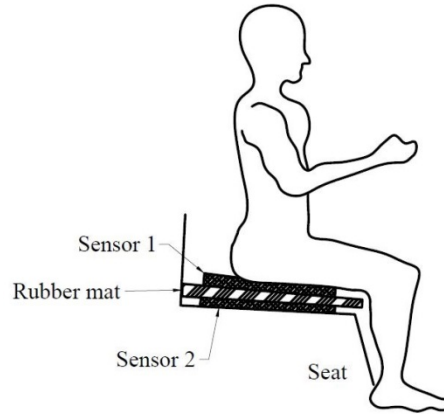


Figure1: Arrangement of sensors and the rubber mat during vibration measurement

2. Methodology

2.1 Study Group

Twelve roller compactor operators, who are trained manpower for construction machine handling, were selected. All the subjects were in a 20-55 yrs age group. Roller compactors with the capacity, varying from 6-15 tons with different brands and service durations were considered. Measurements were taken at construction sites while operators were engaging in their regular occupational tasks (i.e., soil compaction)

2.2 Data Acquisition Instrument

Six channel vibration meters together with two tri-axial seat pad accelerometers (SVANTEK 106) were used. One seat pad accelerometers was placed at the interface between the seat and the rubber mat. The other seat pad accelerometers was placed at the interface between the rubber mat and the operator (Figure 1). Operators exposure was measured with three dimensional; vertical (z axis), lateral (y axis) and for-and-aft (x axis). Instrumental setup was adjusted to meet the ISO-2631-1 standards as guided in SVANTEK 106 user manual. SavnPC++ software together with instrument was later used to analyze the vibration measurements.

2.3 Measurement of Exposure

Seat pad accelerometer was placed to coincide with orthogonal axis system defined for the seated position in ISO-2631-1 standards. Vibration impact to the operator in x, y and z directions were recorded in channel 1, 2 and 3 of the vibration meter, respectively. Measurements were recorded for about 3 minutes time duration to satisfy ISO requirement as well as to include at least one complete working cycle of the machine. These exposure levels were recorded after adjusting the start delay time (5 seconds), weighting factors for each axis (1.4, 1.4 and 1 for x, y and z axes respectively) and data logging time (100 milliseconds) under instrumental setup.

2.4 Evaluation of WBV exposure levels

Root Mean Square acceleration values (RMS), vector sum of frequency weighted rms acceleration (a_w), Vibration Dose Value (VDV) were obtained using Equations (1), (2), (3) respectively

$$RMS = \frac{1}{T} \left[\int_0^T a^2(t) dt \right]^{\frac{1}{2}} \quad (1)$$

$$a_w = \sqrt{(1.4 \times a_{w_x})^2 + (1.4 \times a_{w_y})^2 + (1 \times a_{w_z})^2} \quad (2)$$

$$VDV = \left[\int_0^T a^4(t) dt \right]^{\frac{1}{4}} \quad (3)$$

Where a_{wx} , a_{wy} and a_{wz} are the frequency weighted RMS acceleration in x, y and z axes respectively; $a(t)$ is the running RMS values of frequency weighted acceleration T is the observation time.

Then Crest Factor (CF) was calculated using equation (4) to identify the suitable evaluation method. When CF values not greater than 9 RMS method is sufficient to evaluate the WBV effect [ref]. However, in this evaluation both $A(8)$ and $VDV(8)$ were used. Equations (5)- (7) were used to calculate $A(8)$ and Equation (8) was to obtain $VDV(8)$

$$CF = \frac{\max[a_w(t)]}{RMS a_w} \quad (4)$$

Where, $\max[a_w(t)]$ is the absolute maximum instantaneous peak value of the frequency weighted acceleration signal and $RMS[a_w]$ is the frequency weighted rms acceleration.

$$A_x(8) = 1.4 \times a_{wx} \sqrt{\frac{T_{EXP}}{T_0}} \quad (5)$$

$$A_y(8) = 1.4 \times a_{wy} \sqrt{\frac{T_{EXP}}{T_0}} \quad (6)$$

$$A_z(8) = 1 \times a_{wz} \sqrt{\frac{T_{EXP}}{T_0}} \quad (7)$$

In which, $A_x(8)$, $A_y(8)$, $A_z(8)$ are daily vibration exposure of eight hour equivalent frequency weighted rms acceleration values for x, y, z directions, respectively, T_{EXP} is duration of exposure to vibration and T_0 is the reference duration of eight hours as indicated in ISO-2631-1:1997. Highest value from $A_x(8)$, $A_y(8)$, $A_z(8)$ is considered as the daily vibration exposure, $A(8)$ to compare with ISO-2631-1 exposure limits.

$$VDV_8 = \sqrt[4]{\frac{T_{EXP}}{T}} \times VDV^4 \quad (8)$$

Here VDV_8 is the maximum of VDV_8 calculated for three orthogonal axes.

VDV and RMS values were used to assess the exposure levels as specified in ISO 2631-1 standards (Table 1) .

The negative health effects associated with WBV can be minimized by risk assessment of WBV exposure under standard guidelines. To evaluate the effect of periodic, random and transit vibration on human health the International Organization for Standardization (ISO) published the ISO-2631-1:1997 standards. For the evaluation primary quantity of vibration magnitude shall be acceleration and location of measurement shall be the interface between the human body and the source of it's vibration (ISO-2631-1, 1997).[9].

2.5 Dynamic characteristics of waste rubber mat

Four channel seismograph connected to a tri-axial geophone was used to investigate the dynamic characteristic of the rubber mat. Seismograph has the ability to measure the vibration transmission in three orthogonal directions as transverse (the direction parallel to the source) vertical and longitudinal (the directions perpendicular to the source). Continuous mode and fixed time stop mode of geophone were used to record the vibration transmission. The rubber mat was placed on a rigid and flat concrete floor and a hammer blow was applied on corner of the mat in order to generate an impact wave. Seismograph was placed on the middle of the mat and the magnitude of the vibration transmitted through the rubber mat was measured for a time of 120 seconds. Experimental setup is shown in Figure 2. Using vertical, lateral and longitudinal wave forms dynamic characteristics (i.e, stiffness and damping coefficients) of the rubber mat were determined.

Damping ratio (ξ) was calculated using Equation (9), where j is the number of cycles and U_j is the amplitude of j^{th} cycle.



Figure 2: Experimental setup used to obtain the damping properties of rubber mat

$$\xi = \frac{1}{2\pi J} \ln \left(\frac{U_1}{U_{1+j}} \right) \quad (8)$$

3. Results and Discussion

3.1 Characteristics of WBV exposures

Frequency weighted rms acceleration, crest factors, VDV, A(8) and VDV8 for each operator are summarized in Table 1. It was found that 75% of operators were with dominant frequency weighted rms acceleration and VDV in vertical (z axis) direction. Except OP7-OP9, all other operators showed highest frequency weighted rms and VDV in vertical direction (Figure 3), indicating that operator exposure to WBV dominant in vertical direction. There was a significance difference in rms acceleration recorded in vertical direction when compared to lateral and fore-and- aft directions ($p < 0.001$ Wilcoxon signed rank test). VDV in vertical direction was significantly greater than that in other two directions (i.e., lateral, fore-and-aft) ($p < 0.001$ Wilcoxon signed rank test) Similarly; it has been often reported that vibrational effect on vertical direction is more dominant than the other two directions (Subashi et al., 2009 , Alan G, et al., 2018, Eger, et al., 2008) found that 67% of operators with dominant frequency weighted rms acceleration and VDV in vertical direction by a study on WBV exposure of operators of load-haul-dump mining vehicles. Every operator shows shocks with large magnitudes during operation in all three directions; 55% - 94% greater than the average RMS value of corresponding direction (Figure 4). These extreme values were identified during the change of gears of the machine, turning the machine and switching on and shutting down of the engine. However, shocks received to operators during gear change and turning of the machine can be significantly reduced by switching off the vibration mode in above actions. These shocks were evident in all three directions. For all operators, the Crest factors (Table 1) is found to be greater than 1.

3.2. Assessment of exposure levels.

It was found that 97% of crest factors are below nine (Table 2), indicating that RMS method is sufficient to evaluate the WBV effect (ISO-2631-1, 1997) . However, both A(8) and VDV (8) were used to predict the associated health risk. Considering A(8) value, 17% of operators were found to be above the HGCZ, 75% within the zone and 8% were below the HGCZ. When the same study group compared with VDV_8 limiting values, no one was above HGCZ. Based on VDV, 75% of operators were with moderate level of health risk while 25% were with low level of health risk.

Figure 4 shows the position of operators in predicted health risk zones considering both A(8) and VDV8. In the study, only one operator experience vibration levels below HGCZ limits according to both assessment methods used , indicating that they are at low risk. Eleven operators were identified with a predicted health risk. Among them, 2 operators were with high level of predicted health risk.

Table 1: Frequency weighted rms acceleration, Instantaneous peak acceleration, Crest factors, Vibration dose value, Eight hour exposure and Eight hour equivalent VDV at the rubber mat/seat interface (transmitting WBV to operator) during roller compactor operation

Operator ID	Frequency weighted rms acceleration (m/s ²)				Instantaneous peak acceleration (m/s ²)			Crest factors			Vibration Dose Value (m/s ^{1.75})			A(8) (m/s ²)	VDV8 (m/s ^{1.75})
	a _{wx}	a _{xy}	a _{wz}	a _{wxyz}	Peak a _{wx}	Peak a _{wy}	Peak a _{wz}	CF _x	CF _y	CF _z	VDV _x	VDV _y	VDV _z		
OP1	0.215	0.189	0.492	0.635	0.394	0.7	0.832	4.5	4.7	2.3	1.101	0.905	2.384	0.49	8.5
OP2	0.215	0.185	0.551	0.679	0.55	0.724	0.759	4.5	10.8	2.3	1.162	1.408	2.502	0.55	8.9
OP3	0.207	0.171	0.568	0.681	1.064	1.099	1.067	5.1	6.4	1.9	1.117	1.085	2.535	0.57	9
OP4	0.18	0.143	0.697	0.768	0.724	0.822	0.832	4	5.8	1.5	0.948	0.828	3.134	0.7	11.1
OP5	0.182	0.149	0.655	0.733	0.61	0.977	0.794	3.4	6.3	1.5	0.889	0.835	2.928	0.65	10.4
OP6	0.233	0.282	0.683	0.853	1.23	1.531	0.813	5.2	5.3	1.6	1.274	1.457	3.029	0.68	10.8
OP7	0.129	0.308	0.288	0.549	0.562	1.012	0.417	4.4	3.4	2.1	0.634	1.417	1.27	0.43	7.1
OP8	0.153	0.364	0.308	0.632	0.668	1.496	0.473	4.4	4.2	1.8	0.761	1.755	1.359	0.51	8.7
OP9	0.163	0.381	0.289	0.648	0.575	1.349	0.537	3.2	3.7	1.9	0.813	1.737	1.306	0.53	8.7
OP10	0.168	0.152	0.515	0.605	0.596	1.303	0.724	3.9	8.7	1.9	0.887	1.086	2.172	0.52	7.7
OP11	0.229	0.23	0.917	1.024	1.047	1.109	2.163	4.3	4.6	2.9	1.204	1.353	4.013	0.92	14.3
OP12	0.205	0.212	0.891	0.982	0.484	1.567	1.413	2.6	7.3	1.9	0.962	1.447	3.781	0.89	13.4

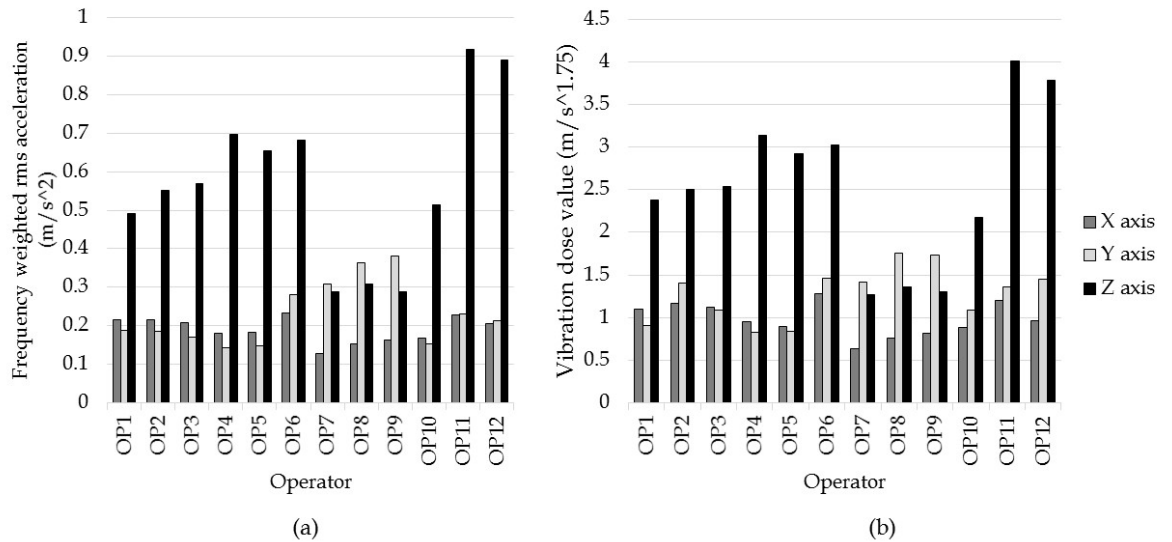


Figure 3: (a) Frequency weighted rms acceleration and (b) vibration dose value resulted for operators in three orthogonal directions; x, y and z

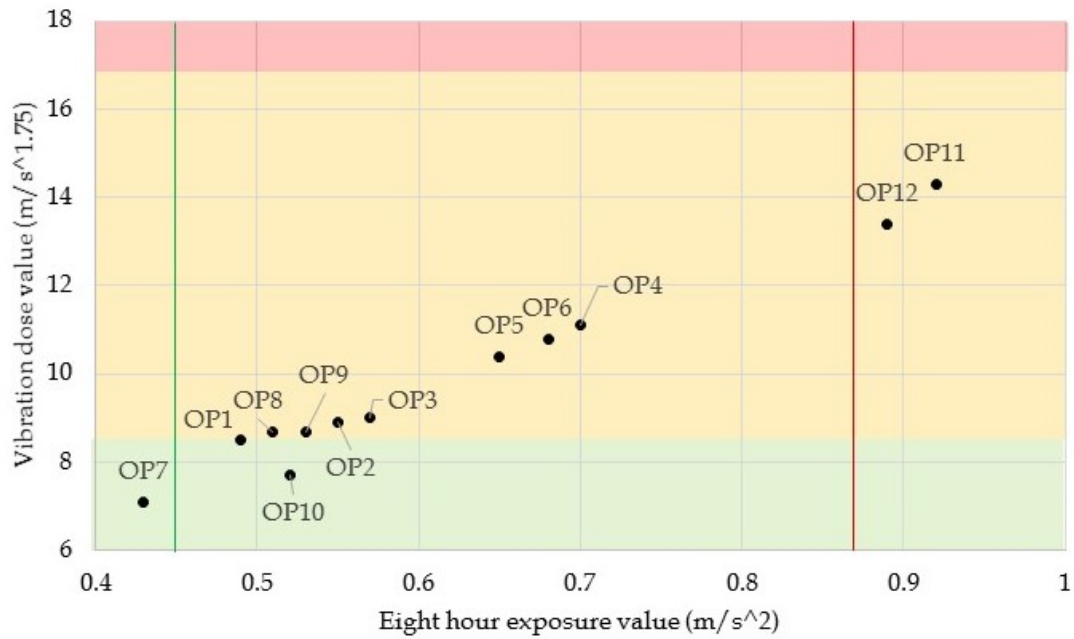


Figure 4: Relationship between health risk predicted by VDV8 vs A(8) for operators. Green coloured area represent the low health risk zone, Yellow shows the moderate health risk zone and Red represent the high health risk zone corresponding to the HGCZ based on VDV₈. Green line shows the upper limit of low health risk zone and red line shows the lower limit of high health risk zone based on A(8) exposure limits

Above results show that majority of roller compactor operators exceed the WBV limiting values, where they are with moderate or high risk of health problems. It was found that 92% of operators, who were engaged in roller compactors are in moderate or high health risks where the exposure levels need to be controlled. Though it is not specified for soil compactors, the studies by Zhao and Schindler, (2014) for operators of compact wheel loaders, Langer, et al., (2012) for operators of backhoe loaders also conclude higher exposure levels of WBV for operators of construction machinery.

3.3. Effect of waste rubber in reducing WBV

3.3.1. Properties of waste rubber mat

Free vibration response has been found in all three directions: transverse, longitudinal and vertical (Figure 5). Damping properties and physical properties obtained for the rubber mat are summarized in Table 2. Rubber mat showed a significant damping of vibration in all three directions within about four seconds. Highest particle velocity was indicated in longitudinal direction with a magnitude of 24m/s. Damping ratio of rubber mat in the vertical direction was found to be 16% and natural frequency of 1.75 Hz. The similar value of damping ratio (i.e., 14%) has been found with 2 mm thick high damping rubber specimen through a study by Burtcher et al (1998).

Table 2: Physical properties and damping properties of rubber mat

Property	Unit	Value
Weight	g	625.25
Area	mm × mm	300 × 300
Thickness	mm	6
Density	kg/m ³	115.8
Damping ratio (vertical)	-	0.16
Natural frequency	Hz	1.76
Stiffness	N/m	76.9

3.3.2 Effect of waste rubber in damping WBV transmission

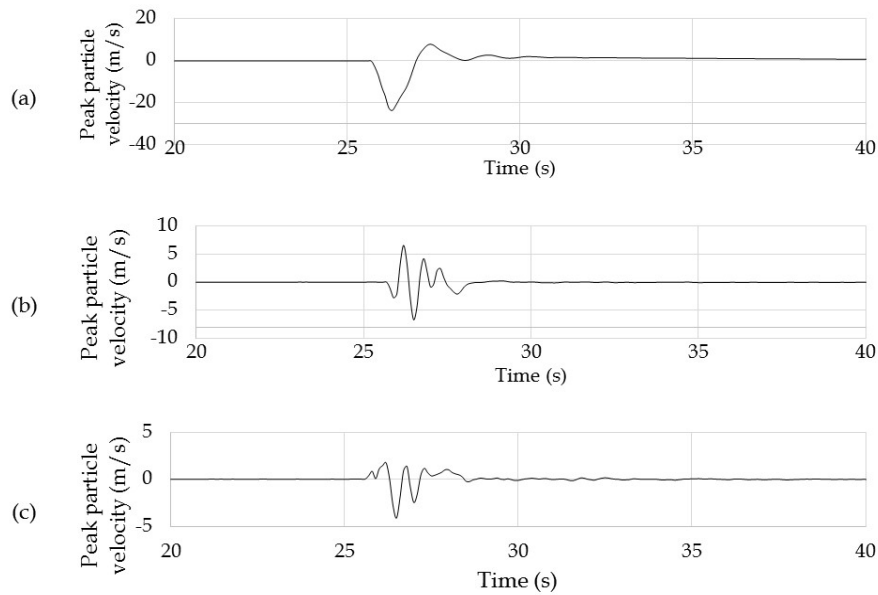


Figure 5: Decay of vibration resulted in (a) Longitudinal direction, (b) Transverse direction and (c) Vertical direction, while in the propagation via the rubber mat produced with waste rubber sludge

With the presence of the rubber mat, WBV exposure of the same operators was reduced. This reduction in WBV is statically significant: for A(8) value ($p=0.008 < 0.05$), for VDV ($p=0.003 < 0.05$) (Wilcoxon signed rank test). Figure 6 shows the resultant frequency weighted rms acceleration of WBV vibration transmitted through the seat and the damped vibration due to the presence of rubber mat. Operators showed damping of 2% in fore-and-aft direction and 5% in lateral direction. Highest damping percentage was found in vertical direction with an average value of 18%.

Rubber mat produced with waste rubber sludge has a capability in damping WBV transmitted to operators more significantly in vertical direction. It showed damping of exposure levels up to 39% and average damping of 12%. Although the applied rubber mat was able to lower the exposure level, damping provided was not enough to lower the associated health risk of all the operators to the safe limits indicated in ISO 2631-1. Therefore further studied are suggested with increase of thickness of the waste rubber mat and modifications of the materials.

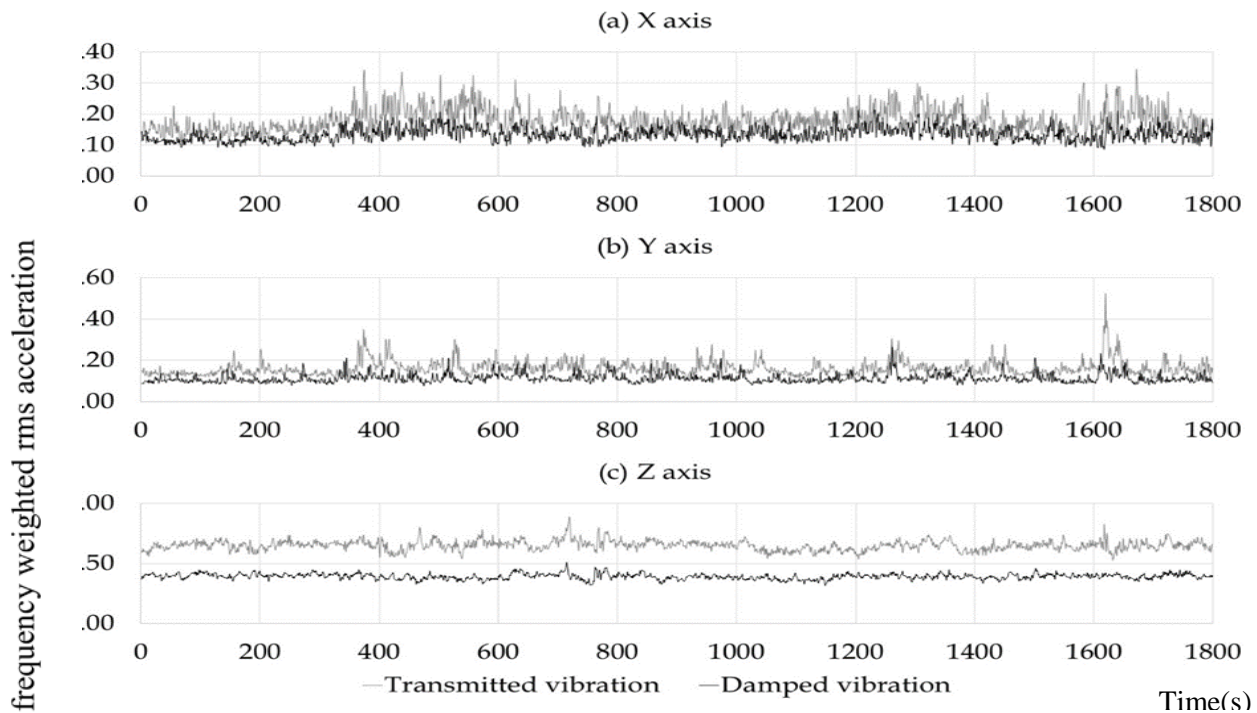


Figure 6: Resultant frequency weighted rms acceleration of WBV transmitted via the operator's seat and resultant damped vibration received to the operator in three orthogonal directions (a) fore-and-aft direction (x axis), (b) lateral direction (y axis) and (c) vertical direction (z axis)

4. Conclusions

Frequency weighted rms acceleration and vibration dose value in the vertical direction were significantly greater than those in fore and aft direction and lateral direction. Vertical axis (Z axis) was found to be the dominant vibrating axis of WBV for roller compactors operators. Operators were identified with shocks with large magnitudes in all three axes which could bring negative health effects for operators.

From the study group, 75% of roller compactor operators exceed the limiting WBV exposure values specified in ISO 2631-1:1997, indicating moderate or high potential of health risks.

Rubber mat, having 16% damping ratio, 1.76 Hz natural frequency and 76.9 N/m stiffness were able to produce with waste rubber. This rubber mat with 6mm thickness can be used to reduce WBV transmission to operators by 39 % in vertical direction, 2% in fore-and aft direction, and 5% in lateral direction, indicating damping of transmitted WBV in all three direction with a significant reduction in vertical direction.

5. References

- Alan G, M. et al., 2018. Investigation of human body vibration exposure on haul trucks operating at U.S. surface mines/quarries relative to haul truck activity. *International Journal of Industrial Ergonomics*, Volume 64, pp. 188-198.
- Burtscher, S., Dorfmann, A. & Bergmeister, K., 1998. *Mechanical aspects of high damping rubber*. Budapest, 2nd International PhD Symposium in Civil Engineering.
- Eger, T. et al., 2008. Predictions of health risks associated with the operation of load-haul-dump mining vehicles: Part 1 1—Analysis of whole-body vibration exposure using ISO 2631-1 and ISO-2631-5 standards. *International Journal of Industrial Ergonomics*, Issue 38, pp. 726-738.

- ISO-2631-1, 1997. *Mechanical Vibration and Shock-Evaluation of Human Exposure to Whole Body Vibration-Part I*, General Requirements: Geneva,Switzerland.
- Kittusamy, N. & Buchholz, B., 2004. Whole Body Vibration and Postural Stress Among Operators of Construction Equipment: a Literature Review.
- Langer, T. H. et al., 2012. Reducing whole-body vibration exposure in backhoe loaders by education. *International Journal of Industrial Ergonomics*, pp. 304-311.
- Madhushanka, J., Subashi De Silva, G. & De Silva, G., 2016. Investigation on Whole Body Vibration Exposures of Operation of Construction Vehicles. pp. 37-44.
- Rakheja, S., Kordestani, A. & Marcotte, P., 2011. *Evaluation of Whole Body Vibration Exposure of Operators of Soil Compactors*, Montreal: IRSST-Communication Division.
- Singh, S., Ramakrishna, S. & Gupta, M., 2017. Towards Zero Waste Management: A Multidisciplinary Review. *Journal of Cleaner Production*, p. doi:10.1016/j.jclepro.2017.09.108.
- Smets.M.P.H, Eger, T. & Grenier, S., 2010. Whole-body vibration experienced by haulage truck operators in surface mining operations: A comparison of various analysis methods utilized in the prediction of health risks. *Applied Ergonomics*, Volume 41, pp. 763-770.
- Vitharana V, H., Subashi De Silva G, H. & De Silva G, S., 2015. Health hazards, Risk and Safety practices in construction sites –A Review Study. *Institution of Engineers, Sri Lanka (IESL)*, 48(3), pp. 35-44.
- Zang, L. et al., 2016. Preparation of Damping Properties of an Organic-Inorganic Hybrid Material Based on Nitrile Rubber. *Composites (Part B)*.
- Zhao, X. & Schindler, C., 2014. *Evaluation of whole body vibration exposure experienced by operators of a compact wheel loader according to ISO 2631-1:1997*, s.l.: <http://dx.doi.org/10.1016/j.ergon.2014.09.006>,

Participants List of JCHRV2018

Name	Affiliation	E-Mail address
Kazuhisa MIYASHITA	Wakayama Medical University	miyaka@wakayama-med.ac.jp
Toshiyuki Hasumi	RION Co.,Ltd.	hasumi@rion.co.jp
Kazuhito Kato	NHK SPRING Co., LTD.	kazuhito.kato@nhkspg.co.jp
Kousuke Suzuki	NHK SPRING Co., LTD.	kou.suzuki@nhkspg.co.jp
Peter Johnson	University of Washington	petej@uw.edu
Leif Anderson	Reactec Ltd	LeifAnderson@reactec.com
Youji TOUDOU	ATOM Corporation	ytoudou@atom-glove.co.jp
Mohd Amzar Azizan	Universiti Kuala Lumpur	mohdamzar@unikl.edu.my
Mohammed Hedayet Ullah Bhuiyan	RMIT	s3577951@student.rmit.edu.au
Tetsuya Ohno	MAX Co.,Ltd	ohno-5-t@uno.max-ltd.co.jp
OKA Shizuto	AISIN SEIKI Co.,Ltd	oka@rd.aisin.co.jp
Thomas Jetzer	Minnesota Twins	Tomjetzer@aol.com
MATOBA, Tsunetaka	Shin-Koga Hospital	matoba.t@icloud.com
Yasuo Higurashi	Yasuo Higurashi	higu@yamaguchi-u.ac.jp
Shigeki Takemura	Wakayama Medical Universit	steakmmi@wakayama-med.ac.jp
Gen TAMAOKI	Tokyo Metropolitan University	tamaoki@tmu.ac.jp
Koki SUGIMOTO	Tokyo Metropolitan University	sugimoto-kouki@ed.tmu.ac.jp
Mitsuaki KANOU	Tokyo Metropolitan University	kano-mitsuaki@ed.tmu.ac.jp
Kenji Kumagai	Bridgestone Corporation	kenji.kumagai@bridgestone.com
Chieko Baba	Bridgestone Corporation	chieko.baba@bridgestone.com
IKEDA Kazuhiro	Hokkaido Health and Safety Research Institute	kikeda@xa.ejnet.ne.jp
Junya Tatsuno	Kindai University	tatsuno@hiro.kindai.ac.jp
Kazuma ISHIMATSU	Graduate School of Health Care Sciences, Jikei Institute	k-ishimatsu@ghsj.ac.jp
Subashi De Siva G.H.M.J	University of Ruhuna	subashi@cee.ruh.ac.lk
Nobuyuki Shibata	National Institute of Occupational Safety and Health	shibata@h.jniosh.johas.go.jp
Keikichi Shimokobe	Auto Technic Japan Co.,Ltd.	keikichi_shimokobe@autotechnic.co.jp
Akira Roppongi	Auto Technic Japan Co.,Ltd.	Akira_Roppongi@autotechnic.co.jp
Masahito Hara	KISTLER Japan	Masahito.hara@kistler.com
Mutsumihiro Yoshizawa	Takenaka Corporation	yoshizawa.mutsumihiro@takenaka.co.jp
Masatomo Komai	Burrtec Co. Ltd.	mkomai@burrtec.co.jp
Ryotaro Takagi	Burrtec Co. Ltd.	rtakagi@burrtec.co.jp
Kazushige Ebe	Bridgestone Corporation	kazushige.ebe@bridgestone.com
Shinichiro OTA	Okayama Prefectural University	ota@ss.oka-pu.ac.jp
Setsuo Maeda	Kindai University	maeda@socio.kindai.ac.jp